Deflections of Reinforced Concrete Flat Slabs

Estée M. Eigelaar

Thesis presented in partial fulfilment of the requirements for the degree of Masters of Science of Engineering at the Stellenbosch University

Supervisor: Professor J.A. Wium

Date of Award: March 2010

5 EXPERIMENTAL TEST SIMULATION

5.1 INTRODUCTION

The empirical approximation of the time-dependent characteristics of flat slabs is relevant in order to suggest a suitable method for acceptable deflection prediction. The previous chapters have discussed the various influences on flat slab deflection; the empirical methods available for deflection prediction; the limits of the empirical methods concerning deflection prediction for lightly reinforced slabs and finally; a finite element model which can potentially simulate the occurrence of cumulative cracking. Chapter 3 also proposed an alternative deflection prediction approach as a product from the discussions in Chapters 2 and 3.

For testing the hypothesis of the proposed finite element model and the alternative deflection prediction method, a series of experimental tests are required with which the calculated deflections may be compared. An experimental study was conducted by Gilbert and Guo (2005) to record flat slab deflections over time. These results were used as the basis for all the deflection comparisons in this chapter.

This chapter thoroughly presents the slab specimens and data obtained from the experimental study, as done by Gilbert and Gou (2005). The experimental data is compared with the calculated deflections obtained from the various design standard methods as well as the deflections obtained from the finite element models. More details are also discussed on the procedure followed to obtain the proposed finite element model. The actual and allowable span/depth ratios (L/d ratios) for each slab specimen is calculated and compared, as it is presented by the various design standards. The chapter concludes by presenting the findings for each slab specimen.

5.2 DISCUSSION ON RECORDED EXPERIMENTAL DATA

5.2.1 Gilbert and Guo's (2005) Experimental Program

The experimental program by Gilbert and Guo (2005), involved the testing of seven large-scale reinforced concrete flat slabs (S1 to S7) under sustained, uniformly distributed, transverse, service loads for periods up to 750 days. The instantaneous and time-dependent deflections were recorded throughout the period of loading, together with the extent and distribution of cracks, concrete surface strains, and the variation with time of the external reaction forces. Numerous companion specimens were also tested to determine the material properties and deformation characteristic of the concrete used in the slabs, including the compressive strength, the flexural strength the elastic modulus, the creep coefficient, and the shrinkage strain.

Each slab had an overall plan dimension of 6.2 x 7.2 m and was continuous over two 3.0 m spans in each orthogonal direction. Each slab was supported on nine 200 x 200 x 1250 mm long columns below the slab. A typical plan view is shown in Figure 5-1.

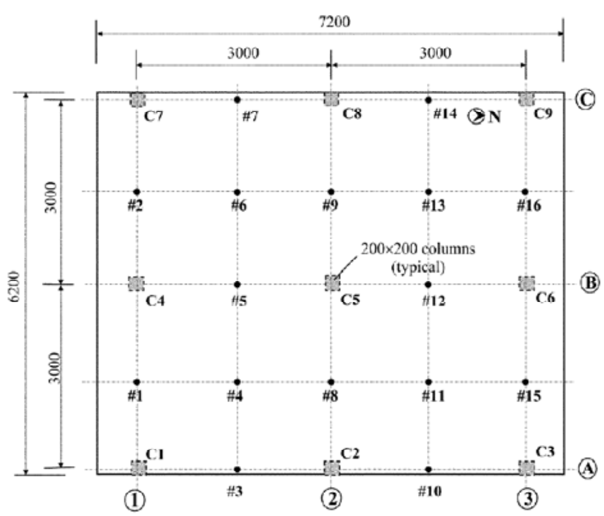

Figure 5-1: Plan of each slab and dial gauge locations (no. 1 to 16) (Gilbert and Guo, 2005).

Each slab cantilevered over the external columns at the northern and southern edges by 600 mm, but at the eastern and western edges there was no overhanging. The supporting columns were either fixed at their base through pad footings connected to the laboratory floor or pinned at their base.

Several parameters were varied from slab to slab to determine their influence on the long-term behaviour. The slab loading history, slab exposure, slab thickness, column support conditions, slab reinforcement layout and test period were varied over the different specimens. A summary of the variables for each specimen is presented in Table 5-1.

Table 5-1: Details for each slab specimen as designated by Gilbert and Guo (2005).

Slab	S1	S2
Slab Exposure and Loading History	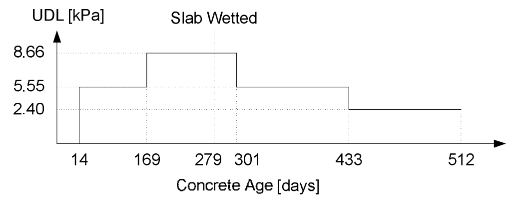	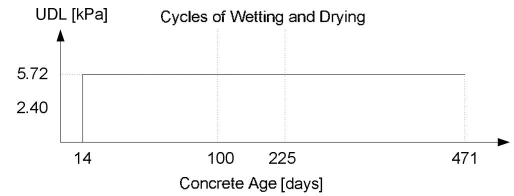
Slab Thickness	100 mm	100 mm
Column Support Conditions	Pinned	Fixed
Reinforcement Layout	I	I
Age at First Loading	14 days	14 days
Test Period	512 days	470 days
Slab	**S3**	**S4**
Slab Exposure and Loading History	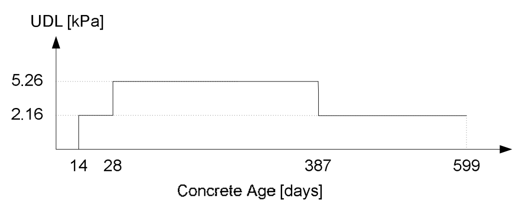	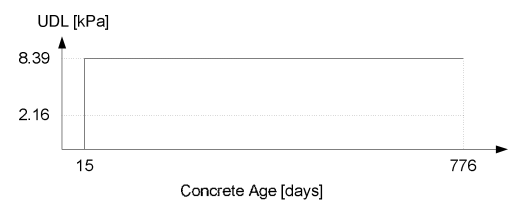
Slab Thickness	90 mm	90 mm
Column Support Conditions	I	I
Reinforcement Layout	Fixed	Fixed
Age at First Loading	14 days	15 days
Test Period	599 days	776 days

Table 5-1: (Continued).

Slab	S5	S6
Slab Exposure and Loading History	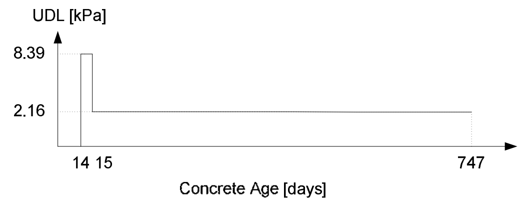	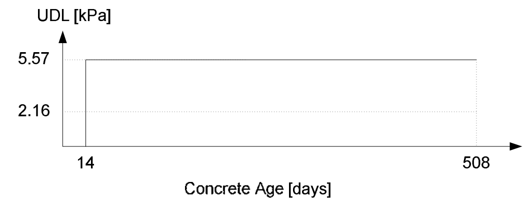
Slab Thickness	90 mm	90 mm
Column Support Conditions	I	II
Reinforcement Layout	Fixed	Pinned
Age at First Loading	14 days	14 days
Test Period	747 days	508 days
Slab	**S7**	
Slab Exposure and Loading History	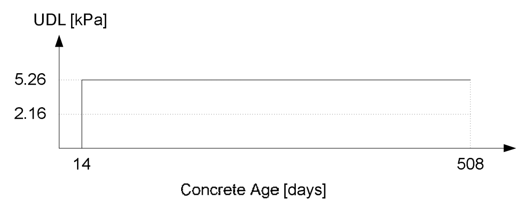	
Slab Thickness	90 mm	
Column Support Conditions	II	
Reinforcement Layout	Fixed	
Age at First Loading	14 days	
Test Period	508 days	

One of two different steel reinforcement layouts, designated in Table 5-2 as either I or II, was used in each slab. The reinforcement details are illustrated in Figure 5-2 and Figure 5-3.

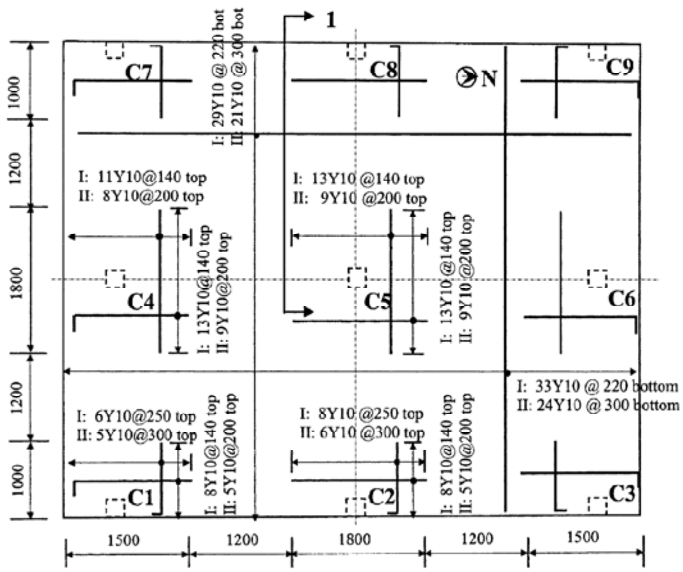

Figure 5-2: Slab reinforcement shown in plan for slab specimens (Gilbert and Guo, 2005).

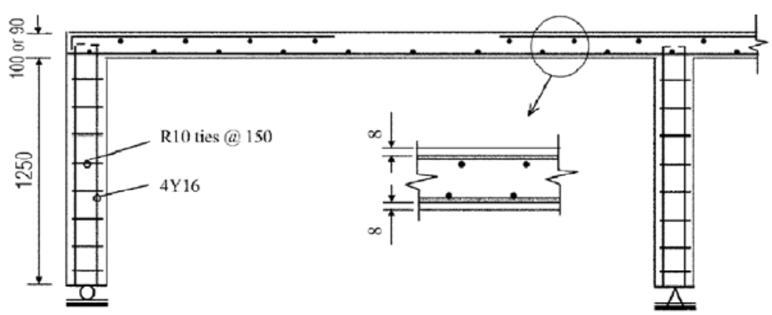

Figure 5-3: Slab and column Section 1-1 for slab specimens (Gilbert and Guo, 2005).

Each slab was reinforced with 10 mm deformed bars (Y10) in four layers (two in the bottom and two in the top slab). The bars placed in the east-west direction were located in the first and fourth layers (that is closest to the bottom and top surfaces, respectively) and the bars in the north-south direction were placed in the second and third layers.

For each slab, all supporting columns contained four 16 mm longitudinal bars (Y16) with 10 mm transverse ties at 150 mm centres and the clear concrete cover to the nearest steel bar at all concrete surfaces in the slabs and columns was 8 mm and 30 mm, respectively.

The columns for specimens S1 and S6 were pinned at their base, with all external columns mounted on rollers (to eliminate, as far as possible, in-plane restraint imposed by the columns to drying shrinkage in the slab). The central column was also pinned, but fixed in position at its base. For specimen S2, S3, S4, S5, and S7, all exterior columns were fixed at their base through 700 x 700 x 300 mm pad footings, while the central column C5 was fixed in position only at its base. The pad footings were fixed to the laboratory floor via embedded reinforcement bars. After the footings were cast, timber formwork was constructed for the slab-column system and the reinforcement placed and tied within the forms. The concrete for both the column and the slab was cast and the top surface of the slab levelled and finished with steel trowels. Each slab was covered with wet hessian and plastic sheets within 4 hours of casting and kept under moist conditions to eliminate early drying shrinkage until the formwork was removed at an age of between 10 and 14 days. The formwork props were kept in place under the slab to support its self-weight until the test loading was applied.

A number of companion cylinders and prisms were cast together with each slab specimen and were used to measure the properties of the concrete throughout the period of testing. Measured properties included the compressive strength, the elastic modulus, the flexural tensile strength, and the creep coefficient. Also measured was the time-dependent development of drying shrinkage strain. The companion specimens were standard cylinders (either 150 or 100 mm diameter) and prisms with dimensions of 100 x 100 x 150 mm. The companion specimens were kept in the laboratory and exposed to the same curing and drying conditions as the slab specimens.

The measured cylinder compressive strength f'_c, elastic modulus E_c, and the flexural tensile strength f_t for the concrete at ages 14 days and 28 days (average over four specimens for each batch) are given in Table 5-2. The average yield stress for the reinforcement is f_y = 650 MPa and its elastic modulus is E_s = 219.0 MPa. All materials properties were determined in accordance with the relevant ASTM Standard (Gilbert and Guo, 2005).

Table 5-2: Concrete properties at 14 and 28 days for experimental slabs (Gilbert and Guo, 2005).

Concrete Batch no.	Slab	E_c [GPa]		f'_c [MPa]		f_t [MPa]	
		14 days	28 days	14 days	28 days	14 days	28 days
1	S1	30.02	-	34.5	37.9	4.29	-
2	S2	29.10	29.60	28.9	33.9	2.72	4.64
3	S3	22.08	22.62	13.1	18.1	-	2.48
4	S4 and S5	22.01	23.15	18.1	23.4	2.76	-
5	S6 and S7	19.03	21.67	15.4	20.9	2.37	2.68

For each batch of concrete, creep strains were measured on two or three 150 mm diameter cylinders mounted in a standard creep rig. The cylinders in each creep rig were subjected to a constant sustained stress of 5.0 MPa first applied at the same age as the relevant slab at its time of first loading. Two other unloaded companion cylinders were used to measure the drying shrinkage strains. The creep strain was determined by subtracting the sum of the measured shrinkage strain and the instantaneous strain from the total strain measured on the creep cylinders. The creep coefficient at any time Φ is defined as the measured creep strain at that time divided by the instantaneous (or elastic) strain and this parameter can be readily used to determine the effects of creep on the total time-dependent deformation of the slab specimen. For some concrete batches, several creep rigs were set up with cylinders loaded at different ages and at different stress levels, so that the effect of aging on the creep coefficient could be measured and assessed. The variation of the creep coefficient with time for each batch of concrete loaded at age 14 days is given in Table 5-3.

To acquire a more realistic knowledge of the drying shrinkage occurring in the slabs, shrinkage was also measured on specimens with the same thickness as the slab. One or two concrete block specimens, 600 x 600 mm in plan and with the same thickness as the slab, were cast at the same time as each slab. The measured shrinkage strains, ε_{cs} (x 10^{-6}), for each batch are also given in Table 5-3 (Gilbert and Guo, 2005).

Table 5-3: Creep coefficient and shrinkage strain (x 10^{-6}) over time for experimental slab (Gilbert and Guo, 2005).

Age [days]	Batch (S1)		Batch (S2)		Batch (S3)		Batch (S4 and S5)		Batch (S6 and S7)	
	Φ	ε_{cs}	Φ	ε_{cs}	Φ	ε_{cs}	Φ	ε_{cs}	Φ	ε_{cs}
14	0.00	52	0.00	219	-	-6	0	70	0	39
20	0.73	80	0.84	296	0.00	55	0.75	123	0.80	90
28	0.88	156	1.25	416	0.58	85	1.20	208	1.06	170
40	1.26	188	1.58	462	0.81	182	1.68	301	1.27	245
80	1.64	313	2.41	581	1.30	448	2.20	450	1.77	308
120	1.84	365	2.57	640	1.55	504	2.41	540	1.99	388
200	2.06	471	2.74	744	1.89	621	2.55	670	2.25	515
250	2.22	477	2.79	751	1.95	625	2.85	722	2.43	555
300	2.29	504	2.81	779	2.05	735	3.00	765	2.48	632
400	2.32	545	2.85	823	2.18	763	3.22	831	2.59	564
450	2.34	562	2.89	842	2.34	791	3.30	859	2.73	634

Up to 21 dial gauges were used to measure the transverse deflection at different locations on the underside of each slab specimen. The locations of 16 dial gauges (no. 1 to 16) used to measure the deflections in every slab are shown in Figure 5-1. The average of the deflections measured at the four mid-panel points (no. 4, 6, 11, and 13 in Figure 5-1) are designated as Δ_1. The average deflections at the symmetric points no. 8 and 9 (Δ_2); no. 1, 2, 15, and 16 (Δ_3); no. 5 and 12 (Δ_4); and no. 3, 7, 10, and 14 (Δ_5).

5.3 Simulated Finite Element Model

The process by which to construct the finite element model was discussed in Section 4.5. An example of such a model is discussed in this section. The process was repeated for every of the seven slab specimens tested by Gilbert and Guo (2005). The finite element model example follows from Slab S3. The model is verified in Section 5.4.3 with the comparison to the experimental slab results. Section 5.3 simply discusses and example of how the cracked finite element model is compiled.

5.3.1 Finite Element Model Example: S3

Two different finite element models are evaluated within the finite element model approach for deflection prediction. The first deflection model is obtained by assuming a fully elastic model, as would be modelled in most design offices. To include the effect of creep on the model, the modulus of elasticity for both the beam elements (columns) and shell elements (slab), are reduced to an effective modulus of elasticity. The effective modulus of elasticity is calculated using Equation 2-21. Thus, the stiffness of the slab is uniformly reduced to include the effect of creep, irrespective whether certain areas on the slab have undergone cracking or not. The second deflection model approximates the occurrence of cracking by calculating a cracked modulus of elasticity (Section 4.4) and allocating this property to certain areas on the slab. The cracked modulus of elasticity is also reduced with Equation 2-21 to account for the effect of creep. However, this model neglects the effect of moment redistribution due to creep.

The first deflection result is produced from the uncracked finite element model and is designated as Δ_{P_UNCR}. The second deflection result is produced from the cracked finite element model, thus Δ_{P_CR}. The process to produce Δ_{P_UNCR} does not differ from a normal shell and beam element model analysed using a linear elastic analysis. The process to produce Δ_{P_CR} follows the process as was discussed in Section 4.5.

Finite Element Example: SLAB S3

UNCRACKED FINITE ELEMENT MODEL

The uncracked finite element model is constructed using beam (columns) and shell (slab) elements having the properties of slab S3. The properties for the slab are shown in Tables 5-1 to 5-3. The loading history for the slab is reproduced in Figure 5-4.

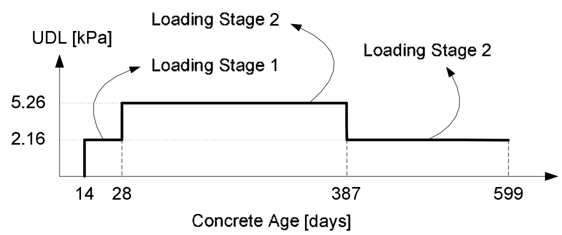

Figure 5-4: Loading History for Slab S3 (Gilbert and Guo, 2005).

The loading history may be divided into three loading stages where the second loading stage represents the period with the largest load. To obtain the largest moments, the largest load needs to be applied to the slab. It is expected that the largest moments will be obtained by applying the loads from Loading Stage 2.

By applying the loads from Loading Stage 2 and the effective modulus of elasticity, E_{eff} at 28 days to the uncracked finite element model, Δ_{P_UNCR} may be obtained.

CRACKED FINITE ELEMENT MODEL

The cracked finite element model is produced by following the process as depicted in Section 4.5.

Step 1: Calculate the Properties for the Critical Span

The first step requires the slab to be divided into column and middle strips and the calculation of the cracking moment, M_{cr}, in the critical panel for each strip. The positions at which M_{cr} needs to be calculated are determined by the position of the maximum moment, thus M_{cr} at the left and right supports of the span under consideration and at the midspan of the strip.

Slab S3 was already divided into column and middle strips by Gilbert and Gou (2005). The symmetrical quality of the experimental specimen allows that the moments from only one panel to be compared with the M_{cr}. Any cracking observed in the single panel is symmetrically duplicated in the adjacent panels.

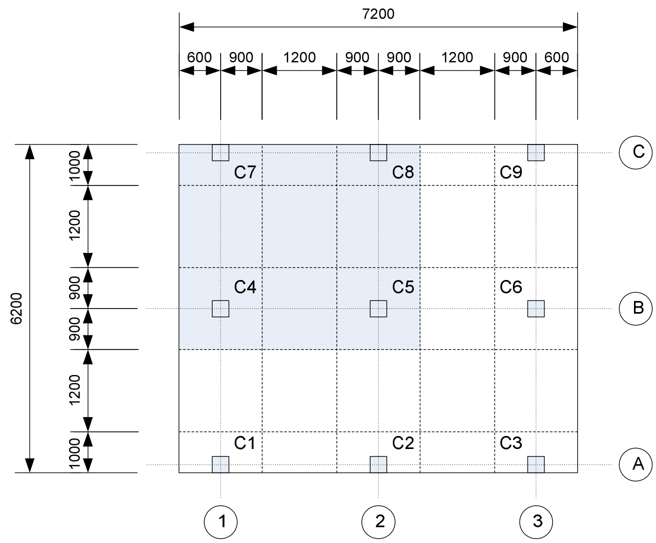

Figure 5-5: Column and Middle Strips for Slab S3 (Gilbert and Guo, 2005).

There are various equations available to calculate the cracking moment, M_{cr}, as presented in Table 2-6. The table presents two distinct equations available for cracking moment calculation. The first is suggested by the SABS 0100-1 (2000) and ACI 318 (2002) in Equation 2-71, while EC2 (2004) presents Equation 2-62.

From Section 3.3, it was concluded that EC2 (2004) presents the equations which best model the true behaviour of lightly reinforced members. Slab S3 has a percentage tension reinforcement of 0.459% (less than 1.0%), which classifies the slab as a lightly reinforced member. Considering this, the EC2 (2004) equation is used to calculate the cracking moment, M_{cr}. The M_{cr} may be calculated for the supports and midspan of each column and middle strip.

Step 2: Simplify the Loading History and identify the zones of Cracking

The M_{cr} may be compared with the moments obtained from the uncracked finite element analysis for the particular loading stage. As was discussed above, the second loading stage is the critical loading stage, having the largest load over the loading history of the slab.

The basic approach by which the M_{cr} is compared to the moments obtained from the uncracked analysis is presented in Figure 5-6. The moments for the column strip along Gridline B are presented in Figure 5-6. The distances along the moment diagram where the moments are larger than M_{cr} are allocated as areas in the two-dimensional frame of the column strip on the slab. These areas identify the location on the slab where cracking is expected.

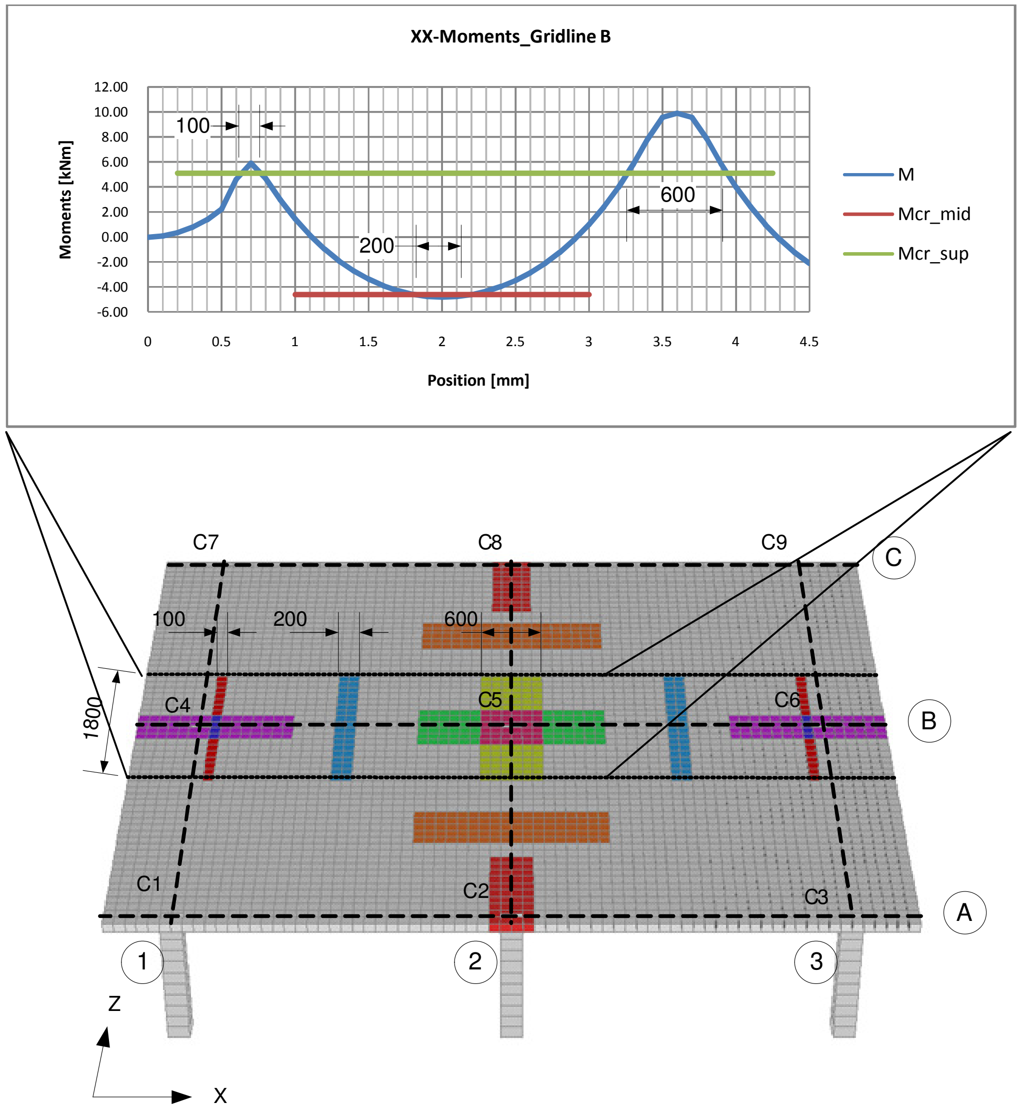

Figure 5-6: Allocating areas of cracking on the slab by comparing the cracking moment, M_{cr} to the moment along Gridline B.

This process may be repeated for all the column and middle strips. For a typical panel four column strips and two middle strips are expected (two column strips and one middle strip in each orthogonal direction). The bending moment for the other columns and middle strips are presented in Appendix F. The resulting crack pattern is presented in Figure 5-7.

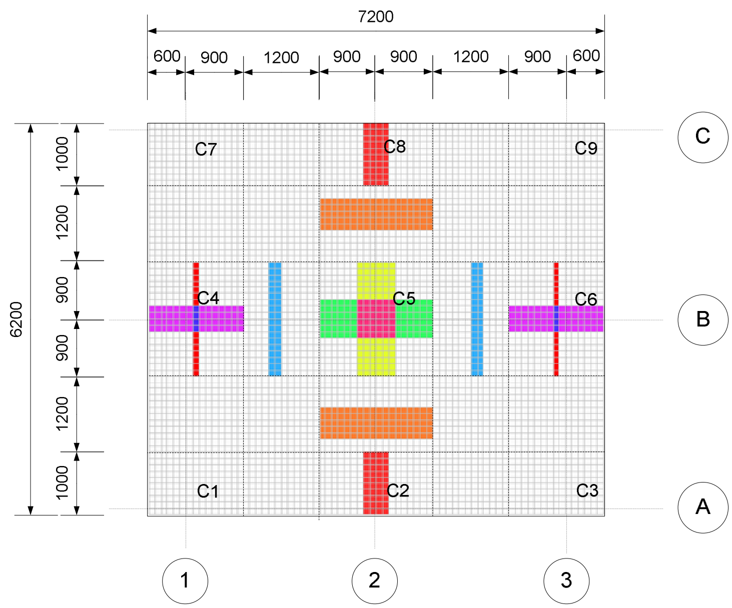

Figure 5-7: Cracked Finite Element Model for Slab S3: Predicted Crack Pattern.

The predicted crack pattern (Figure 5-7) may be compared with the observed crack pattern (Figure 5-8) as recorded by Gilbert and Guo (2005). In both the predicted and observed crack patterns, large areas of cracking are indicated above the supports. The observed pattern shows additional cracking above supports C1, C3, C7 and C9 not presented in the predicted crack pattern. Gilbert and Guo (2005) recorded no significant cracking on the bottom surface of the slab, however the predicted model shows some crack development in spans C2 – C5, C4 – C5, C8 – C5 and C6 – C5.

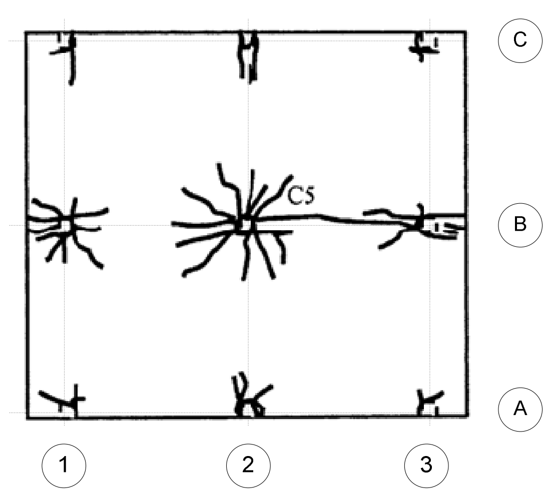

Figure 5-8: Observed Crack Pattern for top slab surface for Slab S3 (Gilbert and Guo, 2005).

Step 3: Calculate E_{cr} for the Loading Stage and Apply to Model

The value of the cracking moment, M_{cr}, was determined in Step 1. The areas which undergo cracking have been identified in Step 2. Step 3 involves the calculation of the cracked modulus of elasticity, E_{cr}, and applying the property to the identified shells from Step 2.

The cracking moment is predicted using the EC2 (2004) approach, thus the expression require that the calculate I_e should also be taken from the EC2 (2007) approach. Equation 2-61 presents expression to calculate I_e. In Equation 2-61 M_{cr} is the cracking moment as calculated from Step 1 and M_a is the maximum serviceable moment at midspan. The maximum serviceable moment is the maximum moment obtained when applying the serviceability load factors to the load combinations in order to obtain the bending moment diagram for the serviceability limit state.

The values of E_{cr} have been calculated for Slab S3 at 28 days and are presented in Table 5-4. For the areas that overlap, for example the strips of grid B and grid 2 (Figure 5-7) at column C5, an average E_{cr} value is calculated. The average E_{cr} values for areas of column and middle strips that overlap are presented in the bottom two rows of Table 5-4. From Figure 5-7 and Table 5-4 it is evident that column strips from Gridline 1 and Gridline B; and from Gridline 2 and Gridline B overlap at Supports C4 and C5, respectively.

Note that the E_{cr} values for the different column and middle strips should be allocated to the shell elements as an orthogonal property in the direction in which the strip behaves. The shell elements that fall within the overlap areas should be allocated an average E_{cr} value as an isotropic property. The overlap areas require an isotropic property to prevent singular matrices from developing during the analysis procedure in the finite element software used in this study.

Table 5-4: Calculated cracked modulus of elasticity, E_{cr} for Slab S3.

E_{cr} for Slab S3 during Loading Stage 2 at 28 days						
C8: Grid C	E_{cr} =	8.16	GPa	G =	3.40	GPa
C4: Grid B	E_{cr} =	10.07	GPa	G =	4.19	GPa
C5: Grid B	E_{cr} =	6.62	GPa	G =	2.76	GPa
mid C4 - C5: Grid B	E_{cr} =	12.03	GPa	G =	5.01	GPa
C4: Grid 1	E_{cr} =	7.83	GPa	G =	3.26	GPa
C5: Grid 2	E_{cr} =	6.59	GPa	G =	2.75	GPa
mid C8 - C5: Grid 2	E_{cr} =	10.65	GPa	G =	4.44	GPa
C4	AVG	8.95	GPa			
C5	AVG	6.61	GPa			

Step 4: Obtain Mid-Panel Deflections

The cracked finite element model was completed in Steps 1 to 3. The model may be analysed using a linear analysis to obtain the mid-panel deflections. Figure 5-9 presents the results for both the uncracked and cracked finite element model at 28 days (start of Loading Stage 2). The mid-panel deflection for the cracked model is larger than the uncracked model by approximately 17%.

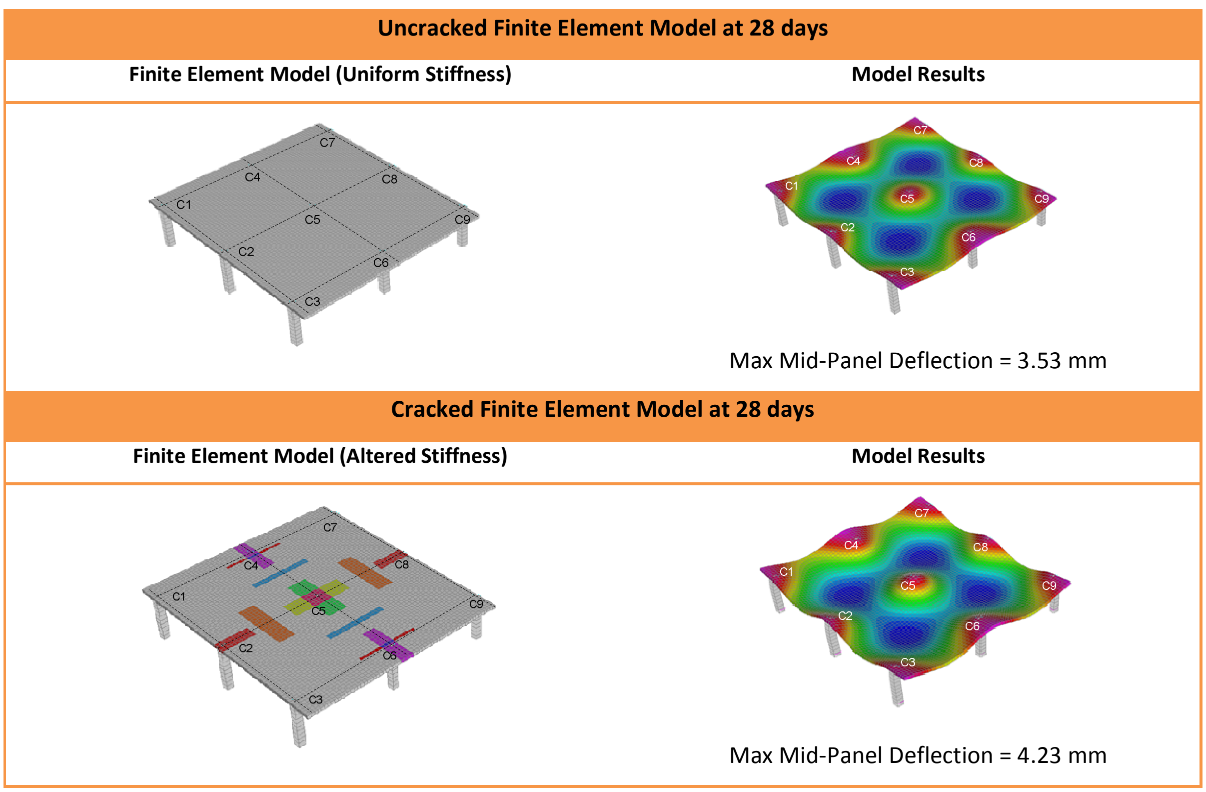

Figure 5-9: Visual Comparison for the uncracked and cracked finite element models for Slab S3.

From the experimental data it was noted that the deflection at 28 days after the load was applied, is 2.84 mm (Gilbert and Guo, 2005). This is far less than the predicted deflection from the uncracked and cracked finite element models. The predicted deflection from the uncracked finite element model is 1.24 times the recorded deflection. This ratio is increased with the less stiff cracked finite element model to a value 1.48 times the recorded deflection.

Gilbert and Guo (2005) observed that the slab remained uncracked prior to the age of 28 days. From Figure 5-4 it may be seen that the first and third loading stage are similar, showing a load of 2.16 kPa. This corresponds to the self-weight of the structure. While the slab only carries its self-weight, no cracking occurred, suggesting that the slab is able to fully carry its own weight below the point of cracking. The slab is kept at this state until an age of 28 days, thus the concrete had time to develop to its 28 days strength in an uncracked state. An increased concrete strength increased the point of first cracking.

The tensile strength of concrete, f_t used to calculate M_{cr} and in turn the value of E_{cr} is based on the 14 day properties of the concrete. The 14 day properties correspond to the day on which the slab was subjected to first loading when all formwork was removed and curing ceased. Even though the effective modulus of elasticity at 28 days (taking the effect of creep into account) was used to estimate E_{cr}, the point of first cracking is under-estimated using f_t at 14 days. Thus, the cracked finite element model is less stiff than the actual slab specimen.

On further inspection to find the reasons for the differences between the finite element model deflections and the experimental deflection result, the following was observed. The finite element models were modelled with an effective modulus of elasticity taking the effects creep into account. This produces a reduced modulus of elasticity and so a reduction in stiffness for both finite element models. It was observed that the creep factors obtained from the concrete samples part of the experimental data was exposed to different conditions relative to the experimental slab. Using these creep factors to model the finite element models produced more flexible slab models than actually occurred. It is for this reason that the uncracked finite element model and the experimental results are not similar. This error due to the creep factor was magnified in the cracked finite element model analysis, thus over-predicting the deflection for Slab S3 with an even larger difference.

5.4 Predicted Deflection from Empirical and Finite Element Models

This section explains some of the concepts of simulating cumulative crack development within the scope of both empirical and finite element models. The predicted deflection results from the empirical and the finite element models are presented for each of the seven slab specimens. A discussion on the crack development and time-dependent predicted deflections accompany the results for each experimental slab specimen. An example of the calculations done to obtain the predicted deflection from the presented empirical methods is presented in Appendix G. It should be noted that no loading factors were used to combine the dead and imposed loads. The permanent load was assumed to be the largest load constantly kept on the slab specimen throughout the test period. In some instances the permanent load included a portion of the imposed load, depending on the load history applied to the slab.

5.4.1 Empirical Model for Deflection Prediction: Cumulative Crack Development

The empirical methods introduced in Section 2.3 and discussed in Chapter 3, normally aim at predicting a short-term deflection, a long-term deflection, and a shrinkage deflection. The total deflection can be estimated from the sum of the long-term and shrinkage deflections. The set of equations used within each of the empirical models do not take the effect of the loading history in account. The loading history effects the crack development within the slab as was seen in the discussion of the cracked finite element model example from Section 5.3.1.

To approach the concept of cumulative cracking in a logical way, it is assumed that most cracking would occur during the loading stage with the largest level of load. The level of cracking is dependent on the level of loading which in turn produces the deflections. Thus, it may be assumed that at the point in time where the most cracking (or load) occurs, the largest deflection shall be obtained.

The set of equations for each empirical model from the design standards may be repeated for each loading stage until the loading stage where the maximum load occurs. In order to calculate the time-dependent deflection beyond the point of maximum load the similar effective moments of inertia, I_e from the maximum loading stage should be used. This implies that the I_e is only calculated up to the point of maximum loading and kept constant for loading stages beyond the point of maximum load. Using I_e from the maximum loading stage ensures that the slab has cracked and stays cracked beyond the point of maximum load. An example where this principle is applied to the empirical modelling for deflection prediction is presented for Slab S1 in Section 5.4.3.

The concept of where the cumulative cracking is sustained even when a model is unloaded may be presented as the non-linear unloading curve for the bilinear behaviour of a cracked flexural member. To simulate this occurrence mathematically, the approximation is made to use the calculated I_e for the maximum loading stage, as was discussed in the previous paragraph. The difference between the actual occurrence of cumulative cracking and the mathematical approximation using the I_e from the maximum loading stage is presented in Figure 5-10.

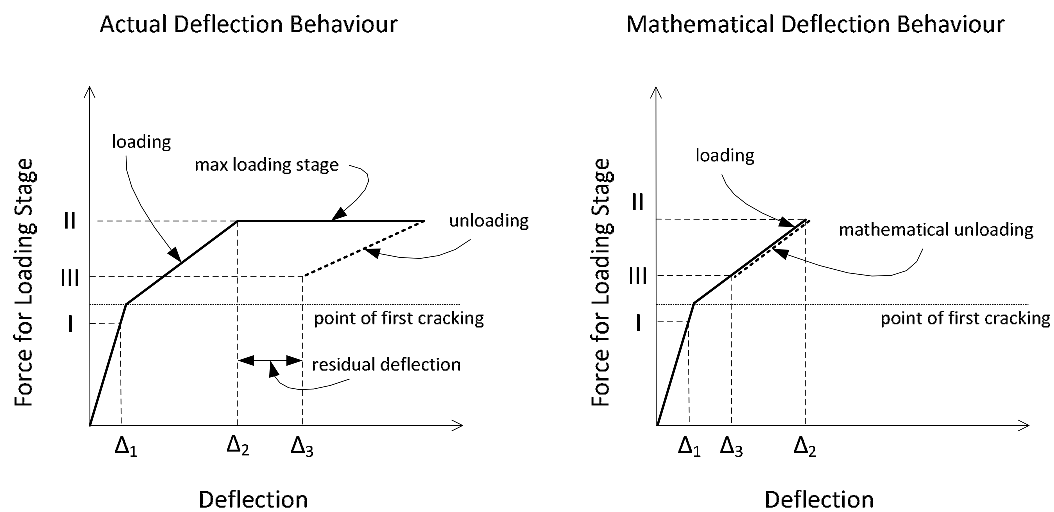

Figure 5-10: Actual and mathematical deflection behaviour.

Loading Stage I presents loading below the point of cracking, while Loading Stage II goes beyond the point of first cracking to reach the maximum loading stage. Up to this point the loss of stiffness due to cracking can be accounted for by both the actual and mathematical models.

As time continues the loading stays constant and the deflection increases due to time-dependent cracking. Loading Stage III presents a load reduction or unloading. During the unloading, according to the actual deflection behaviour, the stiffness gradient changes to show a less stiff member. The curve unloads at a new deflection position taking the residual deflection from the previous loading stage into consideration. This time-dependent cumulative loss in stiffness cannot be accounted for within the mathematical deflection behaviour. It may be observed that the unloading curve has a similar gradient as the loading curve. It is for this reason than the deflection after Loading Stage III, for the mathematical model, is under-predicted. The mathematical deflection behaviour assumes linear unloading along the same curve as produced from Loading Stage II.

Even though the cumulative cracking approximation tries to account for the cumulative reduced stiffness in the cracked slab; the mathematical model fails to account for the actual deflection behaviour during slab unloading.

It should be noted that the material properties at day 14 were used in all the deflection prediction calculations. At day 14 all curing ceased and the formwork for the slabs were removed. All slab specimens were loaded at day 14 whether this load consisted of applied uniform loading or only the self-weight of the structure. It is thus assumed that the slab was allowed to deflect from day 14 onwards. Only the value of the modulus of elasticity $E_{c,t}$, taking into account the effect of creep with time, was changed to account for the concrete stiffness at the point in time where the deflections were considered.

5.4.2 Finite Element Model for Deflection Prediction: Cumulative Crack Development

The cracked finite element model is also dependent on the crack development due to the loading history applied to the slab. As was described in Section 5.3.1., the cracked finite element model aims to represent the crack pattern by reducing the stiffness of the shell elements that have been identified to undergo cracking. The stiffness is reduced by using a cracked modulus of elasticity, E_{cr}.

As was discussed in Section 5.3.1., the level of cracking is determined by the maximum loading stage. Therefore, the crack development in the slab increases up to the point at which the maximum loading stage occurs. Thus, to find the most extreme crack pattern for the cracked section, the maximum loading stage should be considered.

It may then be assumed that the slab undergoes an increase in crack development up to the point of maximum loading. Beyond the point of maximum loading, the crack pattern is kept in the subsequent analysis, irrespective whether the load decreases in the next loading stage. An example where this principle is applied to the partially cracked finite element model for deflection prediction is presented for Slab S1 in Section 5.4.3.

5.4.3 Deflection Prediction for Experimental Slabs

The empirical models normally apply to beams elements. In this investigation the experimental slabs were divided into middle and columns strips as done by the authors. The deflections were calculated for the middle and column strips as though the strips were equivalent beam sections. The Equivalent Frame Method was then implemented to obtain the final mid-span deflection. More detail on the Equivalent Frame Method is provided in Section 2.5.

All the deflections are presented as the final deflection at mid-span. The predicted deflections from the empirical models are presented as the short-term, long-term and shrinkage deflections. The total deflection at the end of the loading stage is the sum of the shrinkage and long-term deflections. The following notation is allocated to the different deflections:

- Δ_{EXP} – the recorded experimental mid-panel deflection, assigned Δ_1 by Gilbert and Guo (2005) at specific time instances.
- Δ_{P_UNCR} – the predicted deflection from the uncracked finite element model as discussed in Section 5.3
- Δ_{P_CR} – the predicted deflection from the cracked finite element model as discussed in Section 5.3
- Δ_{SABS} – the predicted deflection from the empirical model, using the SABS 0100-1 (2000) as discussed in Section 2.3.4
- Δ_{EC2} – the predicted deflection from the empirical model, using the EC2 (2004) as discussed in Section 2.3.3
- Δ_{BS} – the predicted deflection from the empirical model, using the BS 8110 (1997) as discussed in Section 2.3.2
- Δ_{ACI} – the predicted deflection from the empirical model, using the ACI 318 (2002) as discussed in Section 2.3.1
- Δ_{ALT} – the predicted deflection from the proposed (alternative) empirical model, as discussed in Section 3.7

- Δ_{EXP} vs t – the recorded experimental mid-panel deflection presented as a function of time. The horizontal axis for the time is presented at the top of the figure.

Reference is also made to the percentage tension reinforcement for the slab mid-panel, the M_a/M_{cr} ratio (level of cracking) and the I_u/I_{cr} ratio (stiffness ratio). These parameters were used to compare the expected predicted deflection tendencies relative to the actual deflection behaviour.

SLAB: S1

Slab S1 is the slab specimen containing the most comprehensive loading history. The slab properties and loading history is presented in Section 5.2.1. The slab has a total of four loading stages and the slab was wetted over a 48 hour period during the second loading stage. Refer to Figure 5-11 for the loading history applied to Slab S1.

Figure 5-11: Loading History for Slab S1 (Gilbert and Guo, 2005).

As was discussed in Section 5.4.1, it is expected that maximum cracking would occur at loading stage 2. Some cracking did occur during Loading Stage 1 as was observed by Gilbert and Guo (2005), but most cracking occurred during Loading Stage 2. Table 5-5 illustrates the cracked finite element model for Slab S1 at day 169, which is the starting day for Loading Stage 2. The observed experimental crack patterns are the crack patterns recorded at the end of the testing period, thus 512 days.

Table 5-5: Cracked finite element model for slab S1 at day 169.

<table>
<tr><th>Cracked Finite Element Model</th><th>Experimental Crack Patterns</th></tr>
<tr><td>Predicted Crack Pattern</td><td>Observed Cack Pattern</td></tr>
<tr><td>The finite element model predicted cracking over columns C4, C6 and a relatively large area over column C5. The experimental pattern observed additional cracking above columns C2 and C8, and along the mid-panels. This is not predicted by the finite element model.</td><td>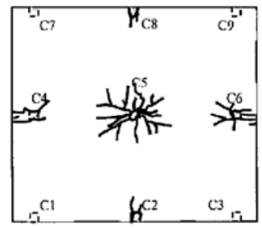
Top of S1
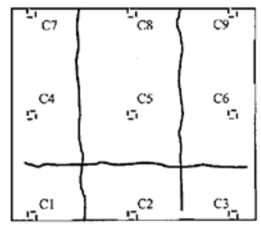
Bottom of S1</td></tr>
</table>

Some differences are observed between the crack patterns from the cracked finite element model and the observed experimental crack pattern in Table 5-5. Gilbert and Guo (2005) noted that the cracks on the bottom surface of the slab developed after the top surface was thoroughly wetted and kept wet for 48 hours. During this crack development the mid-panel deflection also suddenly increased by more than 1.0 mm. Throughout Loading Stages 3 and 4, there was no change in the crack pattern and no appreciable change in the crack widths, despite removal of the load (Gilbert and Guo, 2005).

Table 5-6 presents the results of the predicted deflections from the various models compared to the recorded experimental data.

Table 5-6: Predicted deflection comparison relative to the experimental deflections for Slab S1.

Predicted Deflection Comparison for SLAB: S1

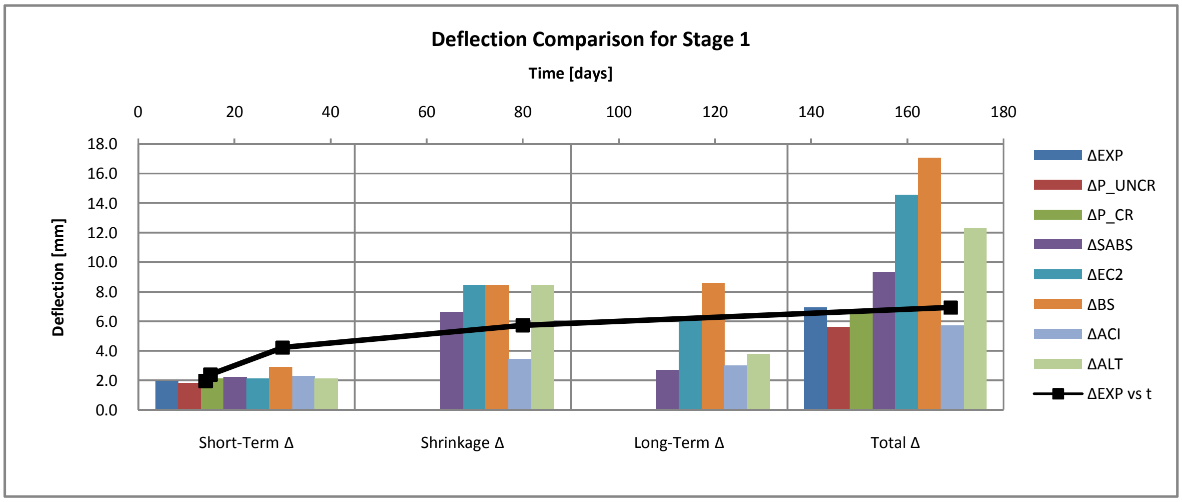

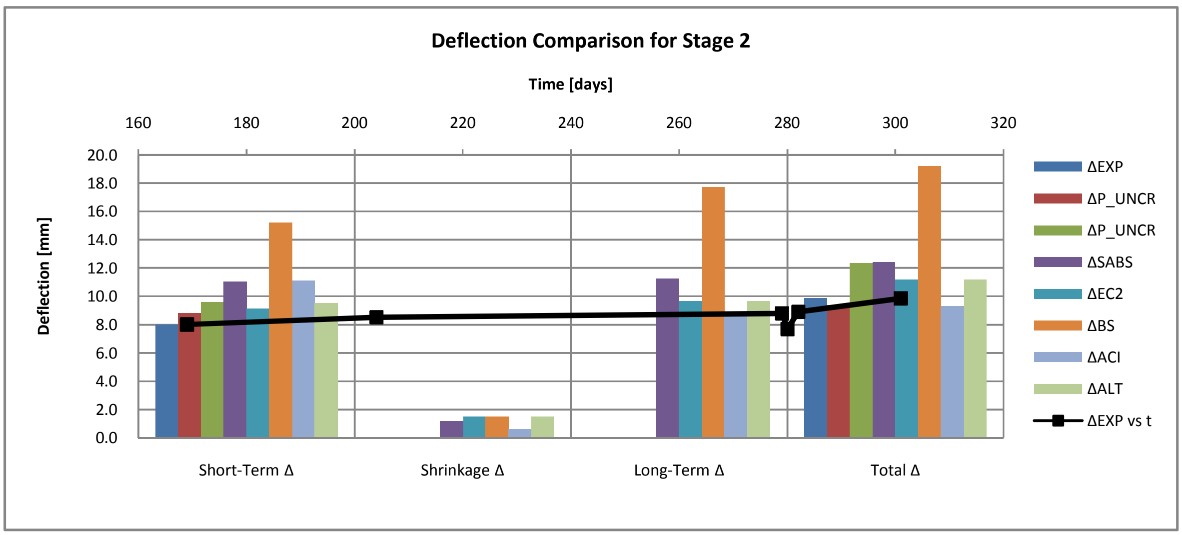

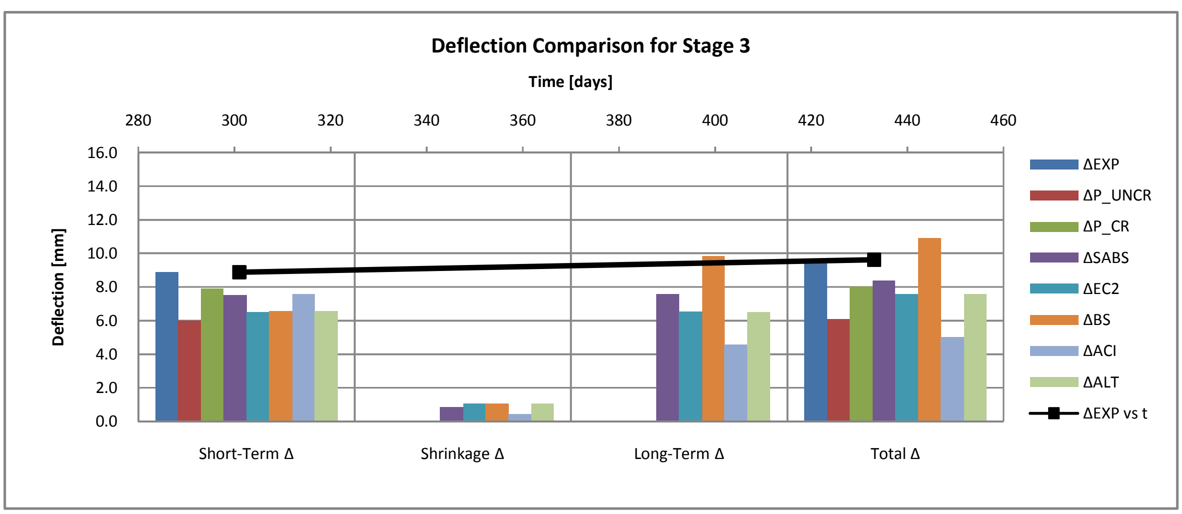

Table 5-6: (Continued).

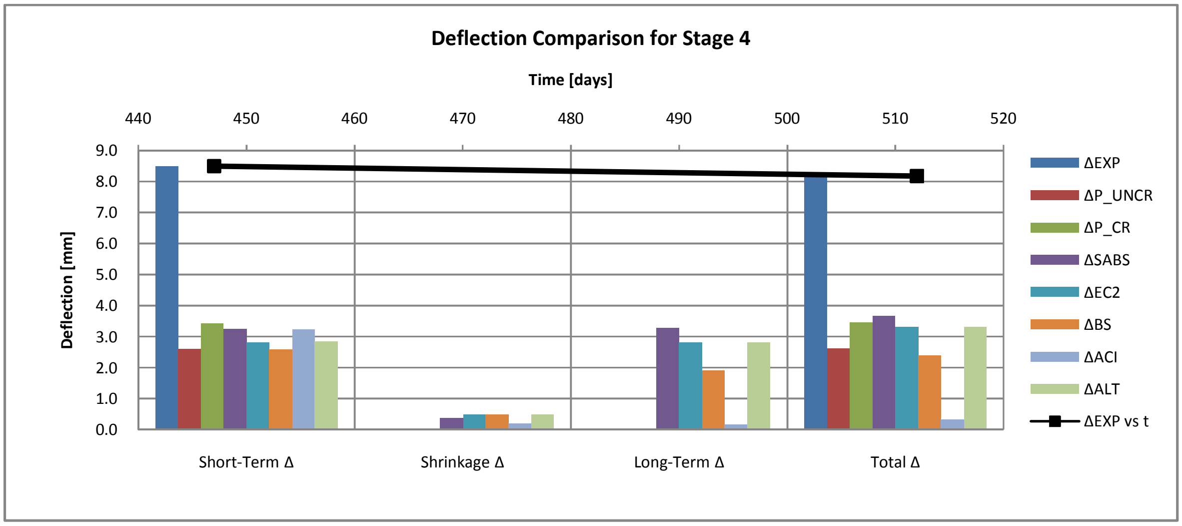

As explained in Sections 5.4.1 and 5.4.2, the amount of cumulative cracking can be accounted for until Loading Stage 2. Beyond the point of Loading Stage 2 after which unloading occurred in the test setup, the amount of cracking (value of the effective moment of inertia, I_e for the empirical models and crack pattern for the finite element models) is kept as it was calculated in Loading Stage 2. Only the time-dependent property, the modulus of elasticity, $E_{c,t}$ and the loading specific to that period is changed. The resulting predicted deflections for Loading Stages 3 and 4 in Table 5-6, are mostly underestimated. Thus, the effect of unloading beyond the point of the maximum loading stage is not effectively accounted for (Section 5.4.1).

Most designers are only interested in the maximum time-dependent deflection at the point of maximum load. Thus, it may be assumed that if the methods predict the deflections within reasonable limit up to the point of maximum load, the exercise is deemed satisfactory.

The deflection ratios of the predicted deflection relative to the experimental deflections are presented in Table 5-7.

Table 5-7: Deflection Ratios relative to the experimental deflections for Slab S1.

DEFLECTION RATIO for Slab S1								
time [days]	$\Delta_{P\_UNCR}/\Delta_{EXP}$	$\Delta_{P\_CR}/\Delta_{EXP}$	$\Delta_{SABS}/\Delta_{EXP}$	$\Delta_{EC2}/\Delta_{EXP}$	Δ_{BS}/Δ_{EXP}	$\Delta_{ACI}/\Delta_{EXP}$	$\Delta_{ALT}/\Delta_{EXP}$	Loading Stage
14	**0.93**	**1.08**	1.14	**1.09**	1.49	1.16	**1.09**	1
169	0.81	**0.94**	1.35	2.10	2.46	0.83	1.77	
169	**1.10**	1.20	1.38	1.14	1.90	1.39	1.19	2
301	**0.95**	1.25	1.26	1.13	1.95	**0.94**	1.13	

The ratio of the predicted deflection relative to the experimental deflection provides a swift indication of which method of deflection prediction provided the most accurate results. By assigning a level of good accuracy, as defined by a deflection ratio range of between 0.90 and 1.10, the best deflection method for Slab S1 may be identified.

From Table 5-7 it is seen that the uncracked finite element model presented the best fit to the experimental data. The deflections from the SABS 0100-1 (2000), the BS 8100 (1997) and the ACI 318 (2002) over-predicted the short-term deflections, while the ACI 318 (2002) is the only empirical method which presented a reasonable prediction of the total deflection. The EC2 (2004) and the Alternative Approach presented good short-term deflections, while over-predicting the total deflection. Even though the EC2 (2004) and the Alternative Approach over-predicted the total deflections, their predictions are still better than that of the SABS 0100-1 (2000) and the BS 8110 (1997). The BS 8110 (1997) presented the least accurate results.

The columns on the perimeter of Slab S1 are only pinned. This was done to eliminate the in-plane restraint imposed by the columns to drying shrinkage (Gilbert and Guo, 2005). The fact that the columns are pinned is not taken into account by either of the finite element methods. The SABS 0100-1 (2000) presents an equation for the unrestraint slab conditions. The expression presented calculates a larger modulus of rupture. The other deflection prediction methods do not account for any slab unrestraint, thus the over-prediction of the deflections for Loading Stages 1 and 2.

The cracked finite element model amplified the low level of cracking for Slab S1 and over-predicts the deflections. Therefore, due to the low level of cracking within the slab, the recorded deflections were simulated well by the uncracked finite element model.

Slab S1 has a percentage tension reinforcement of 0.421% at midspan, a M_a/M_{cr} ratio of 0.81 for Loading Stage 2 and a I_u/I_{cr} ratio of 2.50, according to the EC2 (2004) approach. The ratios as calculated from the EC2 (2004) were used, as the discussions from Chapter 3 present the EC2 (2004) approach to be the more reliable method for deflection prediction for lightly reinforced concrete flexural members. The low percentage tension reinforcement indicates that the predicted deflections from the different methods may vary, but the low level of the M_a/M_{cr} ratio indicates that the slab does not have mid-panel cracking. It has been shown (Section 3.3) that the deflection calculation methods have been calibrated to predict deflection effectively for a I_u/I_{cr} ratio at about 2.2. Slab S1 has a I_u/I_{cr} ratio of 2.50. It is for this reason that the short-term deflections for Loading Stage 1 and the total deflection for Loading Stage 2 are fairly similar for all the deflection prediction methods. Even though the total deflection for Loading Stage 2 vary more, the predicted deflections all fall within a narrow range of 5% lower or 20% higher than the experimental deflection. The total deflection from the BS 8110 (1997) is the exception.

SLAB: S2

Slab S2 is the slab specimen almost exactly similar in design and material properties than Slab S1. There is one exception concerning the column fixity. All the columns along the perimeter of the slab are fixed and it causes slab cracking due to shrinkage restraint. The slab properties are presented in Section 5.2.1. The slab has a single loading stage with cycles of drying between days 100 and 225. Refer to Figure 5-12 for the reproduced loading history applied to Slab S2.

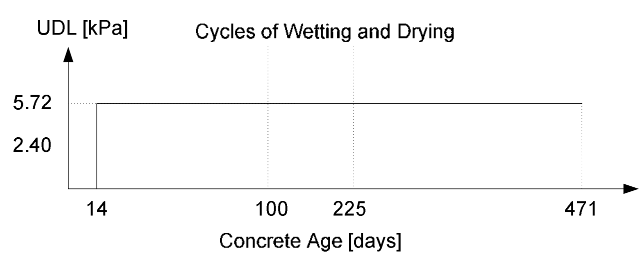

Figure 5-12: Loading History for Slab S2 (Gilbert and Guo, 2005).

Gilbert and Guo (2005) observed some fine cracks on the top slab surface due to early shrinkage. The authors also noted that most of the cracks formed within one month of loading. Table 5-8 illustrates the partially cracked finite element model for Slab S2 at day 14. The observed experimental crack patterns are the crack patterns recorded at the end of the testing period, thus 471 days.

Table 5-8: Cracked finite element model for Slab S2 at day 14.

<table>
<tr><th>Cracked Finite Element Model</th><th>Experimental Crack Patterns</th></tr>
<tr><td>Predicted Crack Pattern</td><td>Observed Cack Pattern</td></tr>
<tr><td>The finite element model predicted cracking at C5. The experimental pattern predicted large areas of cracking over column C4 and C6, crossing over to column C5. Cracks also developed at columns C7, C8, C9, C1, C2 and C3. Additional cracking along the mid-panels were also observed. This is not predicted by the finite element model. The finite element model poorly predicted the crack development of S2.</td><td>
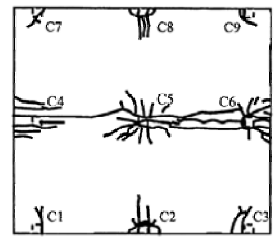

Top of S2
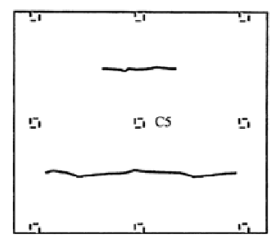

Bottom of S2
</td></tr>
</table>

Some differences are observed between the crack patterns for the cracked finite element model and the observed experimental crack pattern in Table 5-8. Gilbert and Guo (2005) noted that the cracks on the bottom surface of the slab develop after the top surface was exposed to cycles of wetting drying at 180 days. These mid-panel bottom surface cracks remained very fine for the remainder of the test and may be ignored. Thus, it is acceptable if the partially cracked finite element model did not predict any crack formation in the mid-panel of the slab model.

Table 5-9 presents the results of the predicted deflections from the various models compared to the recorded experimental data for specimen Slab S2.

Table 5-9: Predicted deflection comparison relative to the experimental deflections for Slab S2.

Predicted Deflection Comparison for SLAB: S2

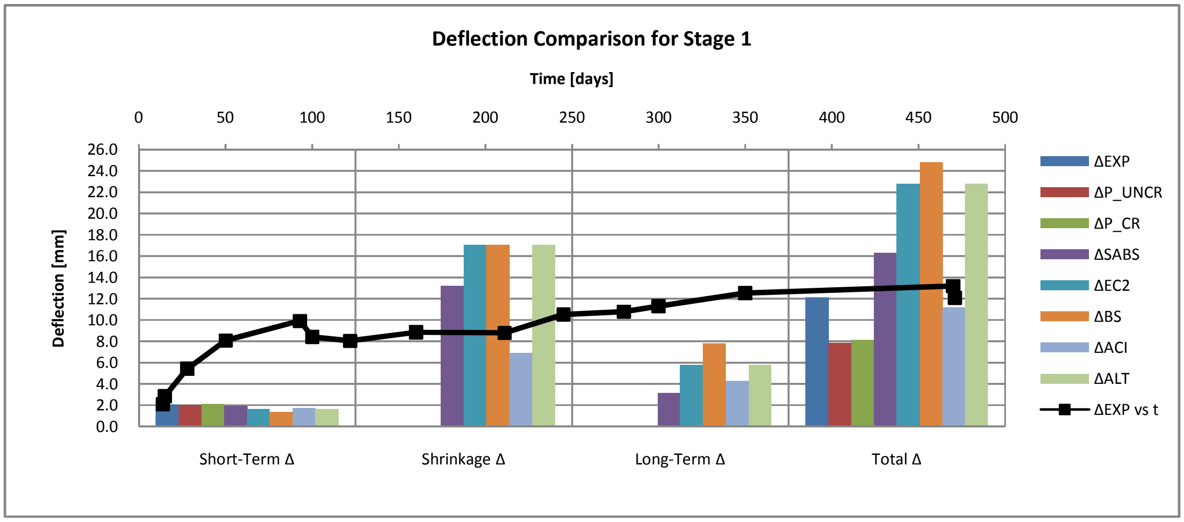

The deflection ratios of the predicted deflection relative to the experimental deflections are presented in Table 5-10.

Table 5-10: Deflection Ratios relative to the experimental deflections for Slab S2.

DEFLECTION RATIO for Slab S2								
time [days]	$\Delta_{P\_UNCR}/\Delta_{EXP}$	$\Delta_{P\_CR}/\Delta_{EXP}$	$\Delta_{SABS}/\Delta_{EXP}$	$\Delta_{EC2}/\Delta_{EXP}$	Δ_{BS}/Δ_{EXP}	$\Delta_{ACI}/\Delta_{EXP}$	$\Delta_{ALT}/\Delta_{EXP}$	Loading Stage
14	**0.96**	**1.01**	**0.90**	0.78	0.65	0.83	0.78	1
471	0.65	0.67	1.35	1.88	2.05	**0.92**	1.88	

The ratio of the predicted deflection relative to the experimental deflection provides a swift indication of which method of deflection prediction provided the most accurate results. By assigning a level of good accuracy, as defined by a deflection ratio range of between 0.90 and 1.10, the best deflection method for Slab S2 may be identified.

From Table 5-10 it is seen that the uncracked and cracked finite element models and the SABS 0100-1 (2000) presented the best fit to the short-term experimental deflection data. The rest of the empirical deflection prediction methods under-predicted the short-term deflection and over-predicted the total deflection for the slab. The one exception is the ACI 318 (2002) which presented slightly under-predicted total deflection that compared relatively well relative to the other empirical methods. The finite element methods both predicted a very accurate short-term deflection, but greatly under-predicted the long-term deflection. Due to the poor comparison between the predicted areas of cracking and the observed crack pattern the partially cracked finite element model under-predicted the total deflection. The BS 8110 (1997) model again showed the largest degree of inaccuracy of all the empirical methods of prediction.

Referring to Table 5-9, it is evident that the shrinkage deflection formed a large component of the total deflection for all the empirical methods. The ACI 318 (2002) predicted a smaller value for the shrinkage deflection, thus producing a total deflection prediction close the experimental deflection.

All the columns have fixed supports for Slab S2, since the fixity contributes to shrinkage restraint within the slab plane; the slab experienced much more cracking as shown in the experimental crack pattern in Table 5-11. The slab restraint is not accounted for by any deflection prediction method, except the SABS 0100-1 (2000). The SABS 0100-1 (2000) present different expressions for the modulus of rupture dependent on whether the slab is restrained or not.

Slab S2 has a percentage tension reinforcement of 0.421% at midspan, a M_a/M_{cr} ratio of 0.51 and a I_u/I_{cr} ratio of 5.44, according to the EC2 (2004) approach. The low percentage tension reinforcement indicates that the predicted deflections from the different methods may vary, but the low level of the M_a/M_{cr} ratio indicates that the slab does not have mid-panel cracking. Little cracking indicates the slab behaves linearly. The methods have been calibrated to predict deflections effectively for a I_u/I_{cr} ratio at about 2.2 (Section 3.3). The I_u/I_{cr} = 5.44 for Slab S2 and this indicates that the deflection predictions may vary for the different prediction methods. It is true that the predicted deflection vary greatly as is presented in Table 5-10. The predicted deflection methods over-estimate the behaviour of the slab. The slab is exposed to cycles of wetting and drying initiating some deflection recovery (Gilbert and Guo, 2005). This is not taken into account by any of the deflection prediction methods, therefore the over-predicted deflections in Table 5-10.

SLAB: S3

The specimens from Slab S3 through to Slab S7 have a smaller cross-sectional height. Slabs S1 and S2 have a depth of a 100 mm, while Slabs S3 to S7 have a depth of 90 mm. The results from Slab S3 to S7 may be compared due to similarities in the dimensions of the slab structure. The rest of the slab properties are presented in Section 5.2.1. Slab S3 has three loading stages, where the second loading stage presents the maximum applied loading. Refer to Figure 5-13 where the loading history for slab S3 is shown.

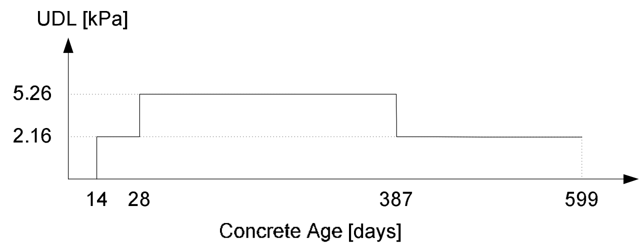

Figure 5-13: Loading History for Slab S3 (Gilbert and Guo, 2005).

Gilbert and Guo (2005) observed that the slab remained uncracked under its self-weight during the first loading stage. It was observed that most of the cracks form within 3 months after loading. Table 5-15 illustrates the cracked finite element model for slab S3 at day 28. The observed experimental crack pattern is the crack pattern recorded at 387 days within the testing period. Gilbert and Guo (2005) observed no significant cracking on the bottom of the surface of the slab throughout the test, except for a few short and very fine cracks near the mid-span of interior east-west column lines.

Table 5-11: Cracked finite element model for slab S3 at day 28.

Cracked Finite Element Model	Experimental Crack Patterns
Predicted Crack Pattern	Observed Cack Pattern
The finite element model predicted cracking above all the columns as well as cracking at the mid column strips. The experimental pattern observed large areas of cracking over all the columns as well. The finite element model suggested additional cracking in the midspan areas next to columns on the perimeter of the slab.	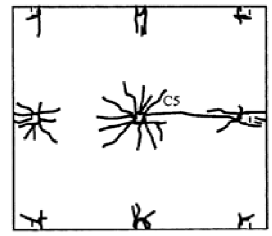 Top of S3

Some differences are observed between the crack patterns for the partially cracked finite element model and the observed experimental crack pattern in Table 5-11. The cracked finite element model predicts additional cracking not observed in the experimental crack pattern.

Table 5-12 presents the results of the predicted deflections from the various models compared to the recorded experimental data.

Table 5-12: Predicted deflection comparison relative to the experimental deflection for Slab S3.

Predicted Deflection Comparison for SLAB: S3

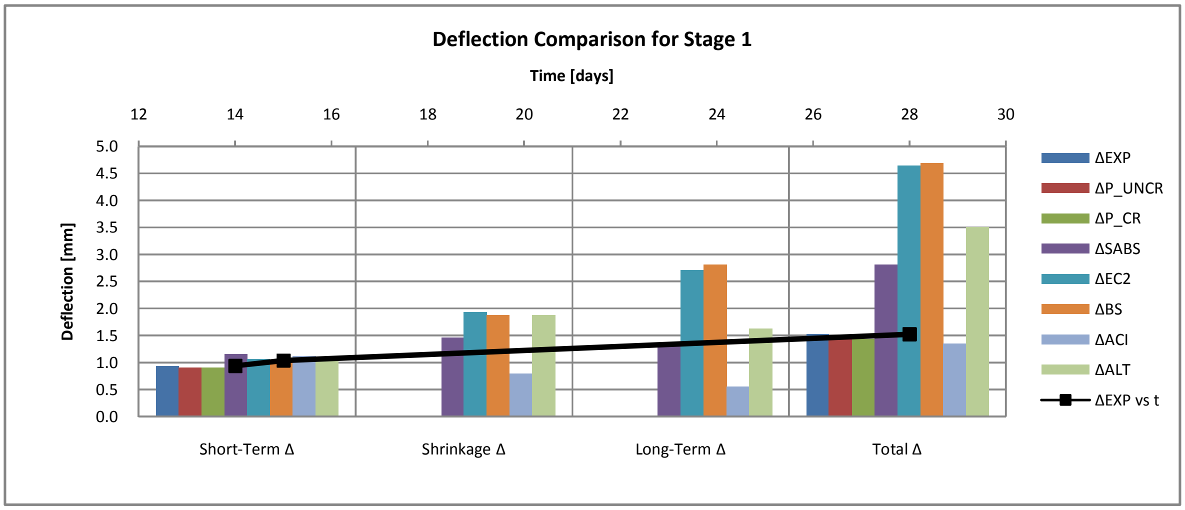

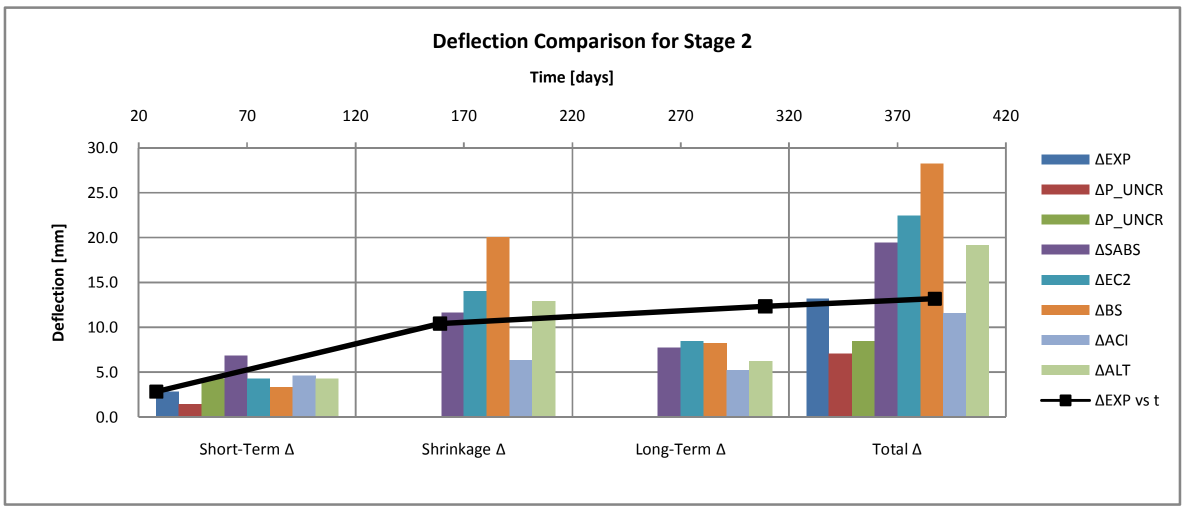

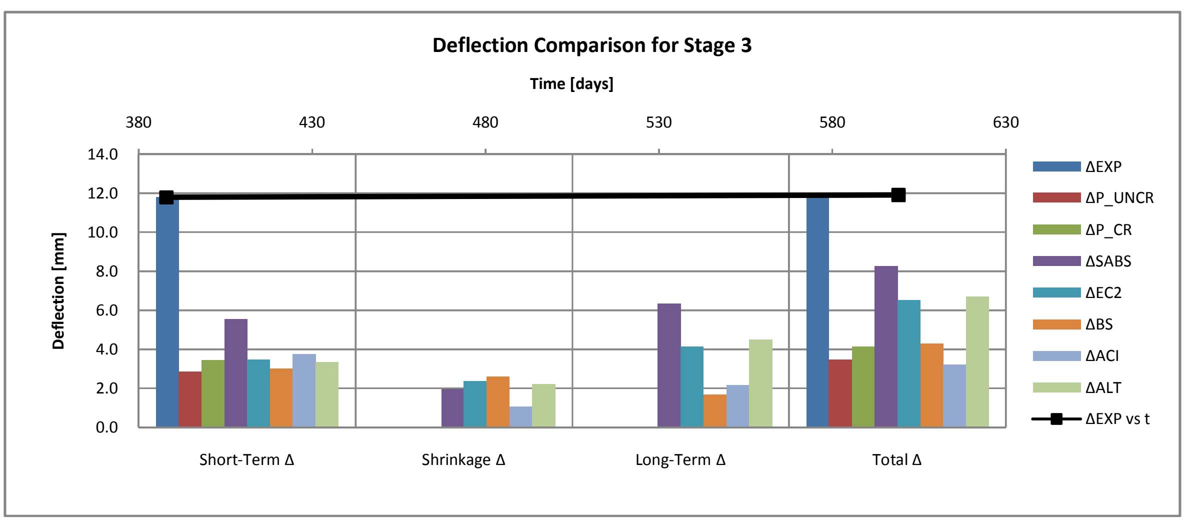

The deflection ratios of the predicted deflections relative to the experimental deflections are presented in Table 5-13.

Table 5-13: Deflection Ratios relative to the experimental deflections for Slab S3.

DEFLECTION RATIO for Slab S3								
time [days]	$\Delta_{P\_UNCR}/\Delta_{EXP}$	$\Delta_{P\_CR}/\Delta_{EXP}$	$\Delta_{SABS}/\Delta_{EXP}$	$\Delta_{EC2}/\Delta_{EXP}$	Δ_{BS}/Δ_{EXP}	$\Delta_{ACI}/\Delta_{EXP}$	$\Delta_{ALT}/\Delta_{EXP}$	Loading Stage
14	**0.96**	**0.96**	1.23	1.13	1.12	1.19	1.13	1
28	**0.94**	**0.94**	1.85	3.05	1.27	0.89	2.30	
28	0.50	1.49	2.40	1.49	1.17	1.62	1.49	2
387	0.54	0.64	1.47	1.70	2.14	0.87	1.45	

From Table 5-13 it is seen that the uncracked and the cracked finite element models presented the best fit to the short-term experimental data. All the empirical deflection prediction methods over-predicted the short-term deflections at day 14. At this point the slab only had to carry its own weight in an uncracked state. Loading applied during Loading Stage 2 at 28 days, produced moments beyond the point of first cracking.

Both the finite element models under-predict the total deflection at day 387, as was discussed in Section 5.3.1. The empirical models all over-predicted the total-deflection except the prediction from the ACI 318 (2002) which under-predicted the total deflection. The BS 8110 (1997) model showed the largest degree of inaccuracy for the time-dependent deflection prediction for Slab S3.

Slab S3 has a percentage tension reinforcement of 0.476% at midspan, a M_a/M_{cr} ratio of 0.89 for Loading Stage 2 and a I_u/I_{cr} ratio of 3.03, according to the EC2 (2004) approach. The low percentage tension reinforcement indicates that the predicted deflections from the different methods may vary, but the low level of the M_a/M_{cr} ratio indicates that the slab does not have mid-panel cracking. Little cracking indicates the slab behaves linearly. The methods have been calibrated to predict deflections effectively for a I_u/I_{cr} ratio at about 2.2 (Section 3.3). The I_u/I_{cr} = 3.03 for Slab S3 does not vary much from 2.2, thus it is expected that the results from the different prediction methods do not vary so much. This is true for the short-term deflections predicted for Loading Stage 1, but not for the total deflections predicted for Loading Stage 2 as presented in Table 5-13. The predicted deflection methods over-estimate the total deflection for Loading Stage 2.

The large shrinkage deflection contributes to the over-estimation of the total deflection. It is suspected that the shrinkage deflection is over-estimated by the empirical methods. In the second loading cases, the ACI 318 (2002) presented a good estimate of the total deflection. The long-term deflections are similar for all the empirical prediction methods, while the shrinkage deflection from the ACI 318 (2002) presented the smallest value. The result is a good total deflection approximation from the ACI 318 (2002) approach and an over-estimation from the rest of the empirical methods.

SLAB: S4

The specimen Slab S4 has a single loading stage. Refer to Figure 5-14 for the loading history for Slab S4. The test period is 776 days.

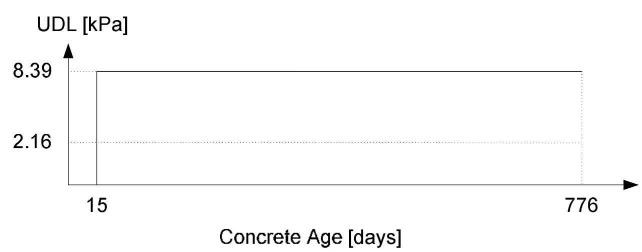

Figure 5-14: Loading History for Slab S4 (Gilbert and Guo, 2005).

Gilbert and Guo (2005) observed that the slab cracked the instance the load was applied at day 15. These cracks continued to develop as time increased. Most cracks formed within four weeks of loading. Table 5-14 illustrates the cracked finite element model for Slab S3 at day 15. The observed experimental crack pattern for the top of the slab is the crack pattern recorded at 776 days. Gilbert and Guo (2005) observed that the bottom surface cracks did not develop with the top surface cracks but a few days after the load was applied. Unlike the top cracks, bottom cracks continued to develop throughout the test and by the end of the test the bottom surface was extensively cracked, with cracks forming a roughly circular pattern around the column supports in each span. The experimental crack pattern presented for the bottom surface of the experimental slab in Table 5-20 is the recorded crack pattern at 776 days.

Table 5-14: Cracked finite element model for Slab S4 at day 15.

Cracked Finite Element Model	**Experimental Crack Patterns**
Predicted Crack Pattern	Observed Cack Pattern
The finite element model and the experimental crack pattern are very similar. Large areas of top surface cracking above all columns and bottom surface cracking at mid-panel were observed for both the predicted and observed crack patterns.	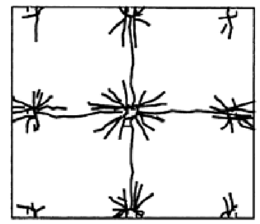 Top of S4 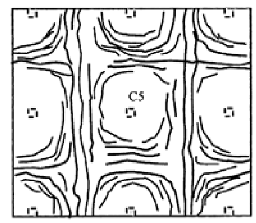 Bottom of S4

Little differences are observed between the crack pattern from the cracked finite element model and the observed experimental crack pattern in Table 5-14. Table 5-15 presents the results from the predicted deflections from the various models and compared to the recorded experimental data.

Table 5-15: Predicted deflection comparison relative to the experimental deflections for Slab S4.

Predicted Deflection Comparison for SLAB: S4
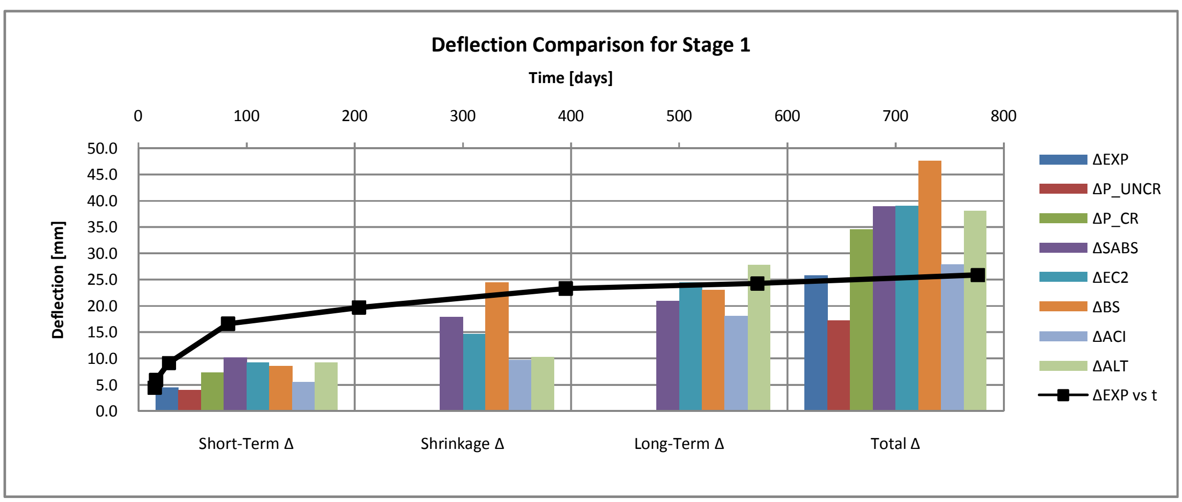

The deflection ratios of the predicted deflection relative to the experimental deflections are presented in Table 5-16.

Table 5-16: Deflection Ratios relative to the experimental deflections for Slab S4.

DEFLECTION RATIO for Slab S4								
time [days]	$\Delta_{P\_UNCR}/\Delta_{EXP}$	$\Delta_{P\_CR}/\Delta_{EXP}$	$\Delta_{SABS}/\Delta_{EXP}$	$\Delta_{EC2}/\Delta_{EXP}$	Δ_{BS}/Δ_{EXP}	$\Delta_{ACI}/\Delta_{EXP}$	$\Delta_{ALT}/\Delta_{EXP}$	Loading Stage
15	0.89	1.63	2.26	2.06	1.92	1.24	2.06	1
776	0.67	1.33	1.50	1.51	1.84	**1.08**	1.47	

From Table 5-16 it is seen that the uncracked finite element model under-predicts both the short-term and total deflection, while the cracked finite element model over-predict both the short-term and total deflection. This indicates that the applied loading forces the slab beyond the point of cracking, thus to a cracked state, hence the under-prediction by the uncracked finite element model. The fact that the partially cracked finite element model over-predicts the deflection indicates that the model over-predicted the amount of cracking to produce a far more flexible slab than what is observed in reality. All the empirical deflection prediction methods over-predicted the short-term deflections at day 15. One out of the five empirical models predicted the total deflection within the desired accuracy limit. This empirical method includes the ACI 318 (2002). The SABS 0100-1 (2000), EC2 (2004), the BS 8110 (1997) and the Alternative Approach model showed very large inaccuracies for the deflection prediction of Slab S4.

Slab S4 has a percentage tension reinforcement of 0.476% at midspan, a M_a/M_{cr} ratio of 1.21 and a I_u/I_{cr} ratio of 4.19, according to the EC2 (2004) approach. The low percentage tension reinforcement indicates that the predicted deflections from the different methods may vary, but the critical level of the M_a/M_{cr} ratio indicates that the slab does have mid-panel cracking. The applied moment is just above the cracking moment, indicating that there are large variations between the different deflection prediction methods (Section 3.5). The methods have been calibrated to predict deflections effectively for a I_u/I_{cr} ratio at about 2.2. The I_u/I_{cr} = 4.71 for Slab S4 and this indicates that the deflection predictions may vary for the different prediction methods. The short-term deflections vary greatly. The predicted total deflections do vary, but not excessively so, as would be expected (Table 5-15). The results from the SABS 0100-1 (2000), the EC2 (2004), the BS 8110 (1997) and the Alternative Approach over-estimate the behaviour of the slab. The ACI 318 (2002) presents good deflection approximations.

Similar to what was explained in for Slab S3, concerning the prediction of shrinkage deflections, a similar tendency is observed in Table 5-15. The shrinkage deflection for the methods over-predicting the total deflections have a high predicted shrinkage deflection.

SLAB: S5

The specimen Slab S5 has two loading stages. Refer to Figure 5-15 for the loading history for Slab S5. The test period for the slab is 747 days.

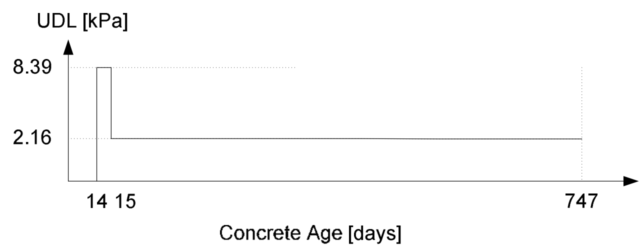

Figure 5-15: Loading History for Slab S5 (Gilbert and Guo, 2005).

The loading for Slab S5 is similar to the early age loading for a flat slab structure during slab construction. Flat slab systems within buildings designed with several storeys of flat slabs, experience this type of loading during the hastily construction of the next storey above. Large construction loading is applied to the slab below, which usually has just completed its curing process. These loads can be close to the design loads and initiate immediate crack development within the slab.

Gilbert and Guo (2005) observed that the slab cracked immediately after first loading at 14 days. Cracks occurred on the top surface of the slab over most columns. The load was kept on the slab for one day. Even though the load was only applied for one day, more cracks still develop on the top surface of the slab with time. Most cracks formed within 3 weeks of first loading, thereafter, no significant change in the crack pattern was observed. The final observed crack pattern is presented in Table 5-17. Gilbert and Guo (2005) observed that no cracks formed on the bottom surface of Slab S5 immediately after first loading. However, when the slab's self-weight of 2.16 kPa was applied; bottom cracks gradually appeared in the first 4 weeks after unloading, most probably due to shrinkage causing the opening of load-induced cracks that were initially too fine to be noticed.

Table 5-17: Cracked finite element model for slab S5 at day 15.

Cracked Finite Element Model	Experimental Crack Patterns
Predicted Crack Pattern	Observed Cack Pattern
The finite element model predicted cracking on the top surface of the slab above all the columns. The predicted crack pattern also showed mid-panel cracking and cracking around all edge and corner columns. The observed crack pattern for the top surface cracks is shown. Only the cracking above the columns are presented by both models.	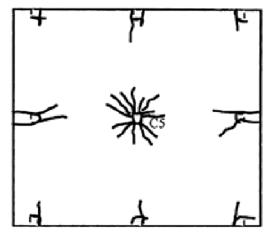 Top of S5

Some mid-panel cracking differences are observed between the crack patterns for the cracked finite element model and the observed experimental crack patterns in Table 5-17. Table 5-18 presents the results from the predicted deflections from the various models compared to the recorded experimental data.

The test period for Loading Stage 1 is only one day. The deflections recorded at different instances during that day was denote as follows:

- $\Delta_{14.1}$ denotes the deflection recorded at day 14 after the first layer of loading blocks were applied
- $\Delta_{14.2}$ denotes the deflection recorded at day 14 after the second layer of loading blocks were applied

Table 5-18: Predicted deflection comparison relative to the experimental deflections for Slab S5.

Predicted Deflection Comparison for SLAB: S5

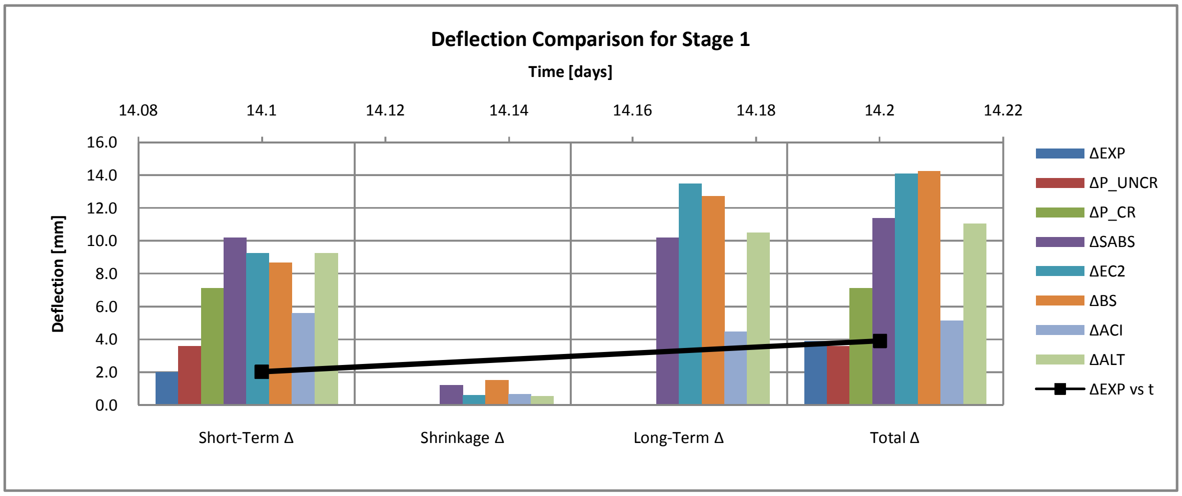

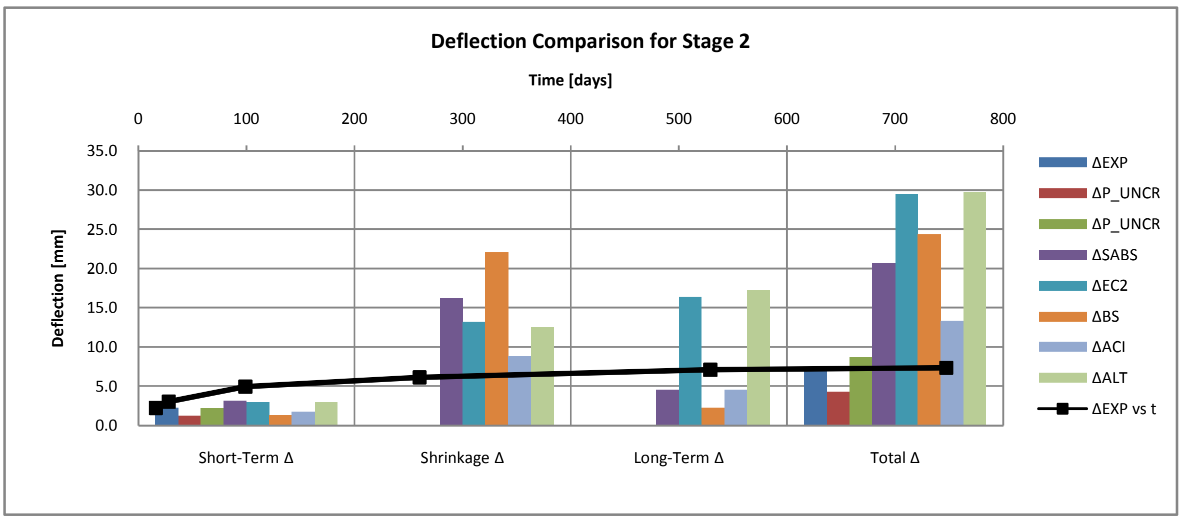

The deflection ratios of the predicted deflection relative to the experimental deflections are presented in Table 5-19.

Table 5-19: Deflection Ratios relative to the experimental deflections for Slab S5.

DEFLECTION RATIO for Slab S5								
time [days]	$\Delta_{P\_UNCR}/\Delta_{EXP}$	$\Delta_{P\_CR}/\Delta_{EXP}$	$\Delta_{SABS}/\Delta_{EXP}$	$\Delta_{EC2}/\Delta_{EXP}$	Δ_{BS}/Δ_{EXP}	$\Delta_{ACI}/\Delta_{EXP}$	$\Delta_{ALT}/\Delta_{EXP}$	Loading Stage
14.1	1.77	3.53	5.05	4.59	4.29	2.77	4.59	1
14.2	**0.92**	1.82	2.91	3.60	3.64	1.31	2.83	
16	0.55	**0.98**	1.44	1.31	0.58	0.79	1.31	2
747	0.59	1.17	2.81	4.01	3.30	1.81	4.03	

The deflection ratios in Table 5-19 all greatly under-predict or over-predict the slab deflections. Both the finite element models and the empirical models over-estimate the amount of cracking (decrease in slab stiffness) at day 14 and predict deflections up to 2.37 times the recorded experimental deflection. The error of over-estimating the amount of cracking is carried forward in the deflection prediction for the second loading stage. The total deflections at day 747 are predicted up to 4.03 times the recorded experimental deflection. As in all the other slabs the uncracked finite element model under-predicts the total deflection at the end of the test period. Even though no model presented a relatively accurate predicted deflection result, the best result was obtained with the ACI 318 (2002) approach.

The poor predicted results for Slab S5 indicates that the prediction methods struggle to accurate account for early age loading of flat slabs. The prediction models over-estimate the effect of early construction loading on the flat slab structure, thus the results are unreliable.

Slab S5 has a percentage tension reinforcement of 0.476% at midspan, a M_a/M_{cr} ratio of 1.21 for loading stage 2 and a I_u/I_{cr} ratio of 4.19, according to the EC2 (2004) approach. The low percentage tension reinforcement indicates that the predicted deflections from the different methods may vary, but the critical level of the M_a/M_{cr} ratio indicates that the slab does have mid-panel cracking. The applied moment is just above the cracking moment, indicating that there are large variations between the different deflection prediction methods (Section 3.5). The methods have been calibrated to predict deflections effectively for a I_u/I_{cr} ratio at about 2.2 (Section 3.3). The I_u/I_{cr} = 4.19 for Slab S4 and this indicates that the deflection predictions may vary for the different prediction methods. These results are similar to those obtained for Slab S5. Slabs S4 and S5 have a similar maximum load applied to the similar slab layout and characteristics. The only difference is the test period over which this maximum load was applied to the slab. Even though there are some similarities between the slab setup, the resulting observations are not similar. It is observed that the loading history greatly influences slab behaviour. None of the results from the deflection prediction methods show any tendency to predict the actual deflection behaviour.

SLAB: S6

The specimens Slab S6 and Slab S7 both have a single loading stage. Refer to Figure 5-19 for the loading history for slab S6. The test period for the slab is 508 days.

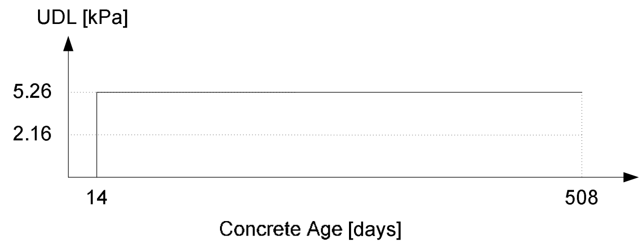

Figure 5-16: Loading History for Slab S6 (Gilbert and Guo, 2005).

The difference between Slabs S6 and S7 is their column fixity for the columns along the perimeter of the slab. The columns along the perimeter for Slab S6 are pinned, thus reducing the amount of in-plane restraint due to shrinkage. The columns along the perimeter for Slab S7 are fixed, thus allowing restraint against shrinkage. It is expected that the crack pattern for Slab S7 would be more than the pattern for Slab S6, due to the fixed columns. The difference in applied loading is relatively small (0.29 kPa) between Slabs S6 and S7, thus the specimens are a good choice to observe the effect of restrained shrinkage.

Gilbert and Guo (2005) observed that cracking appeared on the top surface of the slab over each column, except the corner columns C1, C3, C7 and C9 after first loading at 14 days. These cracks continued to develop with time. Cracks over the corner columns were first observed at 63 days. The final observed crack pattern is presented in Table 5-20. No cracks were observed on the bottom surface immediately after first loading. Bottom cracks, however, gradually developed with time.

Table 5-20: racked finite element model for Slab S6 at day 14.

Cracked Finite Element Model	**Experimental Crack Patterns**
Predicted Crack Pattern	Observed Cack Pattern
In both the predicted and observed crack patterns much cracking is observed above columns C2, C6, C8, C4 and C5. Both patterns also observed cracking in the mid-panels circulating around the columns.	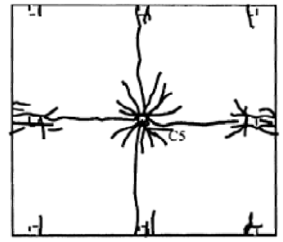 Top of S6 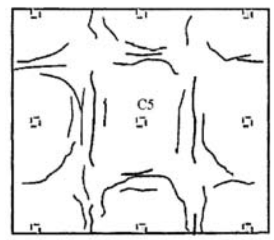 Bottom of S6

Little differences are observed between the crack patterns from the cracked finite element model and the observed experimental crack patterns in Table 5-20. Table 5-21 presents the results from the predicted deflections from the various models compared to the recorded experimental data.

Table 5-21: Predicted deflection comparison relative to the experimental deflections for Slab S6.

Predicted Deflection Comparison for SLAB: S6
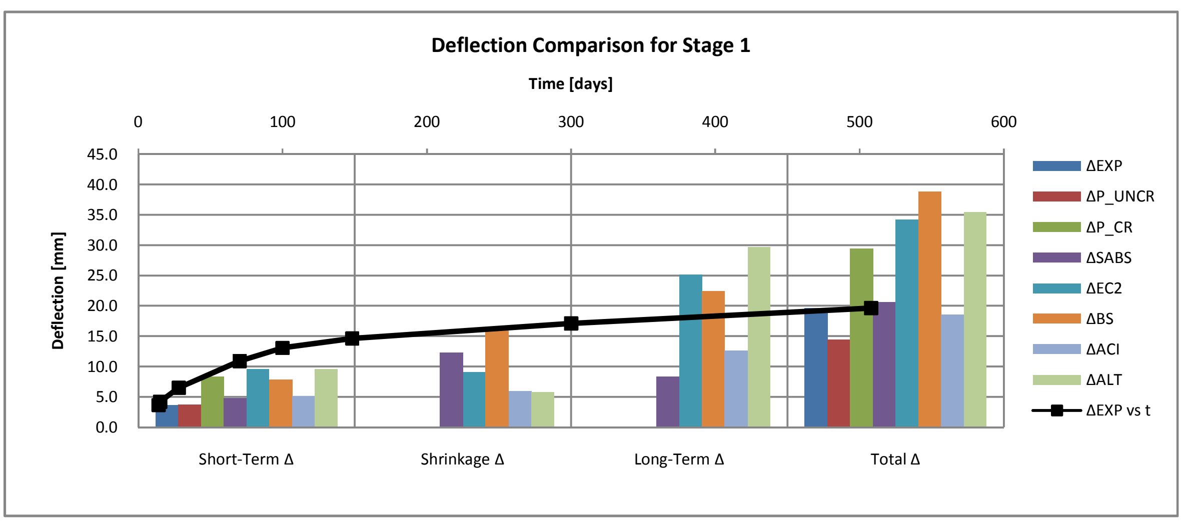

The deflection ratios of the predicted deflection relative to the experimental deflections are presented in Table 5-22.

Table 5-22: Deflection Ratios relative to the experimental deflections for Slab S6.

DEFLECTION RATIO for Slab S6							
time [days]	$\Delta_{P\_UNCR}/\Delta_{EXP}$	$\Delta_{P\_CR}/\Delta_{EXP}$	$\Delta_{SABS}/\Delta_{EXP}$	$\Delta_{EC2}/\Delta_{EXP}$	Δ_{BS}/Δ_{EXP}	$\Delta_{ACI}/\Delta_{EXP}$	$\Delta_{ALT}/\Delta_{EXP}$
14	**1.01**	2.27	1.31	2.60	2.13	1.39	2.60
508	0.74	1.50	**1.05**	1.75	1.98	**0.95**	1.81

The deflection ratios indicate that the all the prediction method over-predicted the short-term deflections at day 14. The uncracked finite element model shows the best results almost predicting a short-term deflection identical to the recorded deflection. The empirical models over-predicted the short-term deflections up to 2.6 times the recorded deflection. Both the SABS 0100-1 (2000) model and the ACI 318 (2002) model presented the best prediction for the total deflection.

Slab S6 has a percentage tension reinforcement of 0.340% at midspan, a M_a/M_{cr} ratio of 1.16 and a I_u/I_{cr} ratio of 5.11, according to the EC2 (2004) approach. The low percentage tension reinforcement indicates that the predicted deflections from the different methods may vary, but the critical level of the M_a/M_{cr} ratio indicates that the slab does have mid-panel cracking. The applied moment is just above the cracking moment, indicating that there are large variations between the different deflection prediction methods (Section 3.5). The methods have been calibrated to predict deflections effectively for a I_u/I_{cr} ratio at about 2.2 (Section 3.3). The I_u/I_{cr} = 5.11 for Slab S6 and this indicates that the deflection predictions may vary for the different prediction methods.

The short-term and total deflections vary greatly as presented in Table 5-22. The results from the EC2 (2004), the BS 8110 (1997) and the Alternative Approach over-estimate the behaviour of the slab. The ACI 318 (2002) and the SABS 0100-1 (20002) present good deflection approximations.

SLAB: S7

The specimen Slab S7 has a single loading stage. Refer to Figure 5-17 for the loading history for slab S7. The test period for the slab is 508 days.

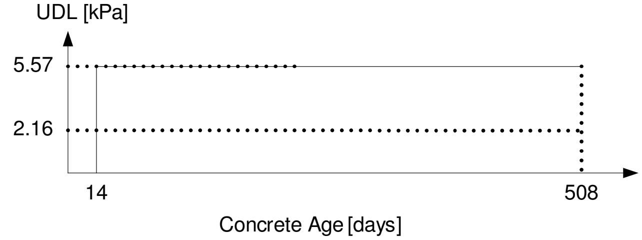

Figure 5-17: Loading History for Slab S7 (Gilbert and Guo, 2005).

Gilbert and Guo (2005) observed that cracks appeared on the top surface of the slab over each column immediately after first loading. Cracks continued to develop with time, with most cracks forming within one month of loading. The crack pattern on the top surface at the end of the test is presented in Table 5-23. There were some differences between Slab S7 (Table 5-23) and Slab S6 (Table 5-20) in the top crack pattern, particularly over the edge columns C1, C2, C3, C7, C8, and C9, due to the different fixity conditions for the columns. Similar to Slab S6, no cracks were observed on the bottom surface immediately after first loading, but bottom cracks gradually developed with time.

Table 5-23: Cracked finite element model for slab S7 at day 14.

Cracked Finite Element Model	**Experimental Crack Patterns**
Predicted Crack Pattern	Observed Cack Pattern
The predicted crack pattern shows cracking above all columns, similar to the observed crack pattern. Some cracking is predicted adjacent to the centre edge columns by the finite element model. The observed crack pattern shows extensive mid-panel cracking not predicted by the finite element crack pattern.	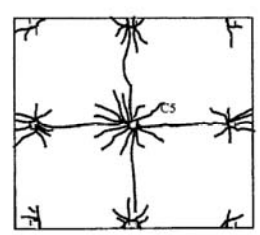 Top of S7 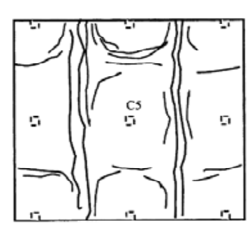 Bottom of S7

There are many differences between the crack patterns at the mid-panel points for the cracked finite element model and the observed experimental crack patterns in Table 5-23.

The predicted crack pattern for Slab S7 is far more excessive, than the crack pattern observed for Slab S6. This is due to the restrained drying shrinkage induced by the fixed supports of Slab S7. Unfortunately, this trend is not observed for the predicted crack patterns from the cracked finite element model. More cracking is predicted for Slab S6 than for Slab S7 according to the observed crack patterns from Tables 5-20 and 5-23. The bending action from the pinned columns in finite element model for Slab S6 allows the mid-panel sections to carry larger moments, thus suggesting larger mid-panel areas to crack. The stiffer supports in the finite element model for Slab S7 reduce the amount of moments redistributed to the mid-panel areas, suggesting that less cracking occurs at these sections. This occurrence within the finite element model results, allow a larger prediction of cracking for Slab S6 than Slab S7.

Table 5-24 presents the results from the predicted deflections from the various models compared to the recorded experimental data.

Table 5-24: Partially cracked finite element model for Slab S7 at day 14.

Predicted Deflection Comparison for SLAB: S7

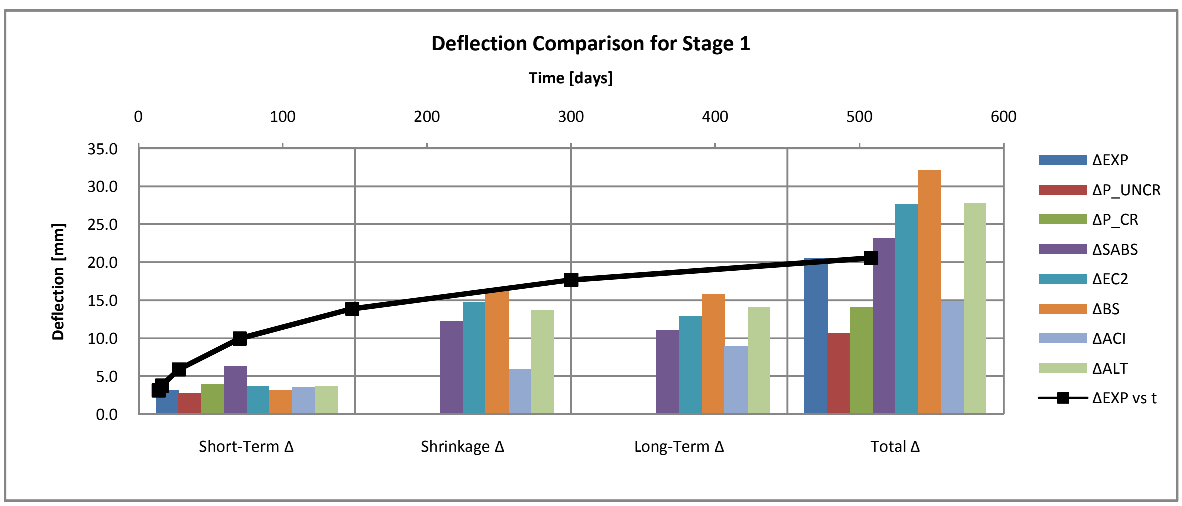

The deflection ratios of the predicted deflection relative to the experimental deflections are presented in Table 5-25.

Table 5-25: Deflection Ratios relative to the experimental deflections for Slab S7.

DEFLECTION RATIO for Slab S7							
time [days]	$\Delta_{P\_UNCR}/\Delta_{EXP}$	$\Delta_{P\_CR}/\Delta_{EXP}$	$\Delta_{SABS}/\Delta_{EXP}$	$\Delta_{EC2}/\Delta_{EXP}$	Δ_{BS}/Δ_{EXP}	$\Delta_{ACI}/\Delta_{EXP}$	$\Delta_{ALT}/\Delta_{EXP}$
14	0.87	1.24	2.01	1.18	**0.99**	1.16	1.18
508	0.52	0.68	1.13	1.34	1.56	0.72	1.34

The uncracked finite element model under-predict both the short and total deflections by not taking any cracking into account. The cracked finite element model over-predicts the short-term deflection and under-predicts the total deflection. The model over-estimates the short-term cracking and under-estimates the long-term cracking. The empirical methods predict fairly similar short-term deflections, up to roughly 1.18 times the experimental deflection. The EC2 (2004), the BS 8110 (1997) and the Alternative Approach presented the largest over-prediction for the total deflection.

Slab S7 has a percentage tension reinforcement of 0.340% at midspan, a M_a/M_{cr} ratio of 0.91 and a I_u/I_{cr} ratio of 5.11, according to the EC2 (2004) approach. The low percentage tension reinforcement indicates that the predicted deflections from the different methods may vary, but the low level of the M_a/M_{cr} ratio indicates that the slab does not have mid-panel cracking. The applied moment is just below the cracking moment, indicating that the slab behaves linearly at mid-panel. The methods have been calibrated to predict deflections effectively for a I_u/I_{cr} ratio at about 2.2 (Section 3.3). The I_u/I_{cr} = 5.11 for Slab S7 and this indicates that the deflection predictions may vary for the different prediction methods. The short-term and total deflections vary greatly as presented in Table 5-25.

5.4.4 Concluding Summary

The results for Slabs S1 to S7 confirmed that the time-dependent cracking greatly affects the serviceability of flat slab. In all specimens, new cracking occurred with time and existing cracks extended (usually on the top surface). The predicted total deflection was generally higher than the measured experimental deflection, primarily due to the loss of stiffness associated with time-dependent cracking under the combined influences of restraint shrinkage. The extent of time-dependent shrinkage induced cracking and its effect on the behaviour of concrete slabs was significant and tended to be the most important and dominant factor influencing long-term behaviour (Gilbert and Guo, 2005).

As expected, the uncracked finite element models always under-predicted the midspan deflection, except in the case of Slabs S1 and S6. The cracked finite element model produced no consistent results. Even though the predicted deflections were far better than those predicted by the cracked finite element model, the model was dependent on simulating the amount of cracking in the slab. In some cases many similarities in the crack patterns between the predicted and observed crack patterns were observed (Slab S4) but other times, many differences occurred (Slab S2).

All the empirical and finite element models predicted the short-term deflections very well in cases where the slabs were exposed to a single loading stage with a constant load applied over the entire test period. The models struggled to predict accurate deflection in cases where the loading histories changed such as the results for Slabs S1, S3 and S5. The predicted results for the slabs exposed to cycles of drying and wetting (Slabs S1 and S2) were also poor.

The empirical methods presenting the best overall accuracy level are the SABS 0100-1 (2000), the ACI 318 (2002) and for cases with a varying loading history, the Alternative Approach. The SABS 0100-1 always over-predicts deflections (both short-term and total), together with the Alternative Approach. The ACI 318 (2002) always under-predicts deflections. It may be observed that the SABS 0100-1 provided an upper limit to the predicted deflections, while the ACI 318 provided a lower limit. The Alternative Approach predict deflections either larger than the SABS 0100-1 or in between the upper and lower limit.

Both the EC2 (2004) and the BS 8110 (1997) greatly over-predicted most of the deflections. These methods also presented the largest degree of inaccuracy compared with all the other methods of deflection prediction. The EC2 (2004) and the BS 8110 (1997) consider only the section stiffness at the point of maximum deflection for a member. The ACI 318 (2002) and the SABS 0100-1 (2000) incorporate the additional stiffness at the sections above the columns for continuous members, such as flat slabs. Including these stiffness allow the ACI 318 (2002) and the SABS 0100-1 (2002) to predict more accurate deflection. Refer to Section 2.5 for the discussion on member continuity. By not including the effect of the stiffness of the sections above the column the member stiffness is over-predicted and larger deflections results as in the case for the EC2 (2004) and the BS 8110 (1997).

It was also observed that the column fixity, responsible for the slab shrinkage restraint and thus the slab crack development is not accounted for by any of the deflection prediction methods with the exception of the SABS 0100-1 (2000). The SABS 0100-1 (2000) presents separate expressions to calculate the modulus of rupture for deflection prediction, depending on whether the slab is restrained or not. The column fixity is not related to the shrinkage deflection predictions. It is however, observed that the over-estimated shrinkage deflection is not predicted effectively and is usually the reason why most of the total deflections for the empirical methods, are over-predicted.

The percentage tension reinforcement, the M_a/M_{cr} ratio and the I_u/I_g ratio provided a good indication on what to expect concerning the degree of variation for the predicted deflections from the various methods. Table 5-26 present a summary of the effectiveness of the deflection prediction methods to predict actual deflections. The most accurate of the finite element models and empirical models for each case considered, are presented in Table 5-26. The accuracy of the models is evaluated on the basis of the deflection ratios nearest to 1.0, irrespective if this ratio slightly under-predicts or over-predicts the deflection.

Table 5-26: Summary of the accuracy of the results for the deflection prediction methods.

Slab	Restraint	Deflection	Finite Element Model		Empirical Models					Indicators		
			Uncracked	Cracked	SABS 0100-1 (2000)	EC2 (2004)	BS 8110 (1997)	ACI 318 (2002)	ALT	M_a/M_{cr} [-]	I_u/I_{cr} [-]	ρ [%]
S1	no	Short-term	√	√		√			√	0.81	2.50	0.421
		Total				√		√				
S2	yes	Short-term	√	√	√			√		0.51	5.44	0.421
		Total			√			√				
S3	yes	Short-term	√	√		√			√	0.89	3.03	0.476
		Total			√			√	√			
S4	yes	Short-term						√		1.21	4.19	0.476
		Total						√	√			
S5	yes	Short-term	√					√		1.21	4.19	0.476
		Total		√				√				
S6	no	Short-term	√		√			√		1.16	5.11	0.476
		Total			√			√				
S7	yes	Short-term	√				√	√		0.91	5.11	0.476
		Total			√							

The slab specimens all have a percentage tension reinforcement less than 0.8%. It is therefore critical to note that these conclusions only apply to flat slab structure with percentage tension reinforcement contents within this range.

From Table 5-26 it is evident that a slab with little or no mid-panel cracking ($M_a/M_{cr} \leq 1.0$) and a $I_u/I_{cr} \leq 5.5$, the uncracked finite element model predict short-term deflection effectively. Within this range, the SABS 0100-1 (2000) and the ACI 318 (2002) provide the most effective empirical methods to calculate predicted the short-term and total deflections. For a slab with much mid-panel cracking ($M_a/M_{cr} > 1.0$) and a $I_u/I_{cr} \leq 5.5$, the uncracked finite element model does not predict short-term deflections well. The ACI 318 (2002) and the SABS 0100-1 (2000) is recommended for deflection prediction using a empirical approach. The ACI (2002) presented the most effective method to predict flat slab deflection empirically even though the results are slightly under-predicted (±10%). The SABS 0100-1 (2000) presented the second most effective method with a slightly larger range error.

5.5 Allowable Span/Depth Ratios for Experimental Slabs

Most of the design standards recommend that the span/depth ratio be calculated prior to the calculation of the predicted total deflection. It is recommended that if the slab fails the span/depth ratio test, the more rigorous approach is to calculate the predicted deflection.

The span/depth ratios for the seven experimental slabs by Gilbert and Guo (2005) are calculated and presented in this section.

5.5.1 Calculated Span/Depth Ratios

The equations used to calculate the span/depth ratios for the seven experimental slabs from Gilbert and Guo (2005) are presented in Section 2.4. All seven experimental slabs are classified as flat slabs and thus the span/depth equations should be applied to the longer of the spans. The spans for the experimental specimens are equal (Figure 5-1), therefore either of the spans may be used to calculate the allowable span/depth ratio. The middle strip C7,C8 – C4,C5 was used to calculate the allowable span/ratio for the experimental slabs as is shown in Figure 5-18. The dimensions of the middle strip are also presented in Figure 5-18.

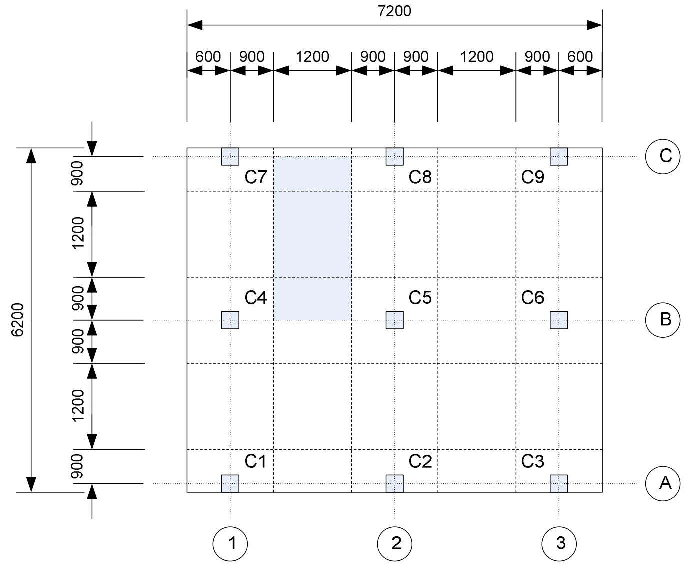

Figure 5-18: Position of the Middle Strip C7,C8 – C4,C5.

The properties of each experimental slab specimen are presented in Table 5-1. The allowable and actual span/depth ratios for each slab specimen are presented in Table 5-27. When the actual span/depth ratio is less than the allowable span/depth ratio, the slab meets the serviceability criteria. Equation 5-1 presents this inequality.

$$\left({}^{L}/_{d}\right)_{ACTUAL} \leq \left({}^{L}/_{d}\right)_{ALLOWABLE} \tag{5-1}$$

Figure 5-19 graphically represents the allowable span/depth (L/d) ratio for the seven slab specimens. The calculations for the span/depth ratios are presented in Appendix G.

Table 5-27: The Actual and Allowable span/depth ratios for the seven experimental slabs.

Slab	SABS 0100-1 (L/d Ratio)			EC2 (L/d Ratio)			BS 8110 (L/d Ratio)			ACI 318 (L/h Ratio)		
	Actual	Allowable	Serviceable	Actual	Allowable	Serviceable	Actual	Allowable	Serviceable	Actual	Allowable	Serviceable
S1	34.48	40.36	OK	34.48	58.63	OK	34.48	52.00	OK	28.00	25.40	NO
S2	34.48	43.20	OK	34.48	101.5	OK	34.48	52.00	OK	28.00	25.40	NO
S3	38.96	43.20	OK	38.96	68.40	OK	38.96	52.00	OK	31.11	25.40	NO
S4	38.96	43.20	OK	38.96	46.23	OK	38.96	52.00	OK	31.11	25.40	NO
S5	38.96	43.20	OK	38.96	46.23	OK	38.96	52.00	OK	31.11	25.40	NO
S6	38.96	42.69	OK	38.96	41.47	OK	38.96	52.00	OK	31.11	25.40	NO
S7	38.96	43.20	OK	38.96	52.91	OK	38.96	52.00	OK	31.11	25.40	NO

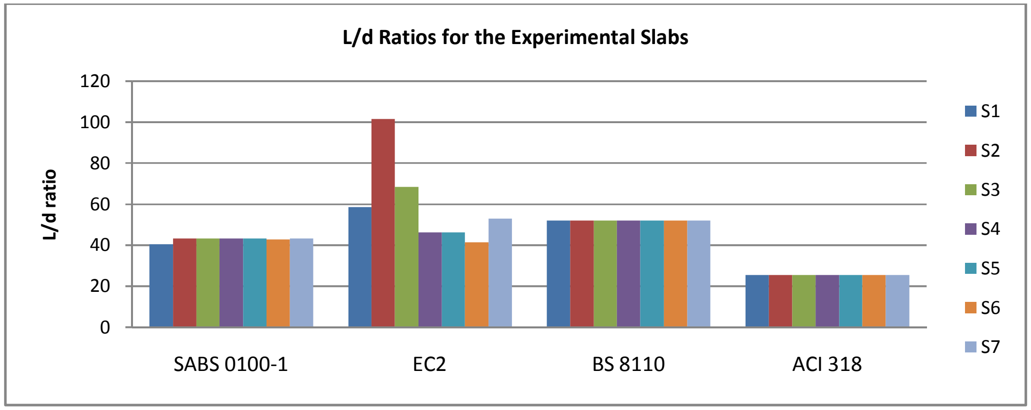

Figure 5-19: Graphical representation of the allowable span/depth ratios for the seven experimental slabs.

From Figure 5-19, the SABS 0100-1 (2000) shows the most conservative span/depth ratios for the specimens, having the lesser allowable span/depth ratios of the first three design standard approaches. The BS 8110 (1997) and the EC2 (2004) show a less conservative span/depth ratio. The EC2 (2004) shows the greatest variation for the allowable span/depth ratios. Slab S1 and Slab S2 have a smaller ratio of percentage tension reinforcement relative to the other slab specimens. Using EC2 (2004) the allowable span/depth ratio for Slab S1 and S2 are noticeably larger than the ratios calculated for the other slabs. This suggests that the span/depth ratio method of calculation presented for the EC2 (2004) approach is far more sensitive to the percentage tension reinforcement of a slab than the other design standards. The ACI 318 (2002) shows the least ratios. It must be remembered that the ACI 318 (2002) uses the span/height ratios and not the span/depth ratios (Section 2.4.4).

According to the SABS 0100-1 (2000), the EC2 (2004) and the BS 8110 (1997), all the slab specimens are serviceable. This is indicated in Table 5-27 where the span/depth ratios are larger than the actual span/depth ratios, which is 34.84 (Slabs S1 and S2) and 38.96 (rest of slab specimens). The ACI 318 (2002) approach presented results indicating that the slab specimens are not serviceable and are expected to undergo excessive deflections.

5.6 CONCLUDING SUMMARY

The experimental study conducted by Gilbert and Guo (2005) presented seven large-scale slab specimens tested under sustained load for test periods up 750 days. The data recorded from the experimental study was used to predict the time-dependent deflection for all seven specimens. The span/depth ratios for the specimens were also calculated to investigate the variability between the different design standards.

The predicted deflections were obtained from a finite element models and empirical hand-calculations. Two different finite element models were considered. The first was an uncracked finite element model (conventional stiffness) and the second was a cracked finite element model (altered stiffness). The uncracked finite element model mostly under-predict slab deflections as expected, since the model only accounts for linear slab behaviour. The cracked finite element model presented no real deflection prediction trend for the seven slab specimens, thus the use of the model is unreliable. The unreliable results prove that the cracked finite element model is not suitable for application in a finite element environment and should not be used to predict deflection for slender lightly reinforced members.

The empirical deflection prediction methods included the methods presented by the SABS 0100-1 (2000), the EC2 (2004), the BS 8110 (1997), the ACI 318 (2002) and Alternative Approach (Section 3.8). It was observed that an upper deflection limit is presented by the SABS 0100-1 (2000) method, while the ACI 318 (20002) present a lower deflection limit. The recorded deflection usually occurred between these limit. The results for the Alternative Approach presented results also within these limits, but not coinciding to the experimental results in a significant way. The results for the EC2 (2004) and the BS 8100 (1997) methods mostly over-predicted the deflections of the slab specimens.

It is suspected that the over-prediction of the shrinkage deflection causes the over-prediction of the total deflection in most slab specimens. The deflection predictions are also highly dependent on the loading history and the environmental exposure of the slab to different conditions of wetting and drying. The more constant the loading and the more controlled the environmental exposure, the higher the probability that the predicted deflections will be similar to the actual deflections. The motive for deflection prediction is to allow the designer to determine the maximum deflection, irrespective of the loading history, and make the necessary provisions to keep the structure within the serviceability criteria. It may be stated that if the loading occurs in a gradual increase or decrease, the effect of the loading history is not as extensive as sudden peak changes, as was observed for Slab S5. For deflection prediction at a specific point in time, an accurate assessment of the loading history is however required.

The reduction in cracking due to no shrinkage restraint is not accounted for by any of the deflection prediction methods, except for the SABS 0100-1 (2000). The SABS 0100-1 (2000) presents separate expressions for the modulus of rupture, f_r, for restrained and unrestrained members. The modulus of rupture determines the point of first cracking of the slab section. It is important to account for the influence of restraint for a slender member, since this determines the amount of cracking resulting predicted at mid-span. The deflection prediction expression is dependent on the amount of cracking accounted for at mid-span of a flexural member. For no restraint, more cracking is observed at mid-span and the exact opposite is observed during much restraint. For much restraint, the majority of the crack development is observed over the supports. Only the SABS 0100-1 (2002) provide expression to account for this effect. The other deflection prediction methods assume that the structure has a certain amount of restraint. To observe the effect of the expression for the unrestrained effect as presented by the SABS 0100-1 (2000), the comparative results for Slab S6 (unrestraint slab) in Table 5-26 should be observed. The SABS 0100-1 (2000) presented the more accurate results, while the results from the other design standards over-predicted the deflections. This implies that the amount of loss in stiffness (crack development) was over-predicted by assuming more slab restraint.

The percentage tension reinforcement, the M_a/M_{cr} ratio and the I_u/I_g ratio provided a good indication on what to expect concerning the degree of variation for the predicted deflections from the various methods. Table 5-27 presented a summary of the results discussed in Section 5.4.3. It is observed that for a flat slab structure with a percentage tension reinforcement less than 0.8% and $I_u/I_{cr} \leq 5.5$, the following methods present the best approximation for the short-term and total deflections. When $M_a/M_{cr} \leq 1.0$, the uncracked finite element model presents an accurate prediction of the short-term deflection, while the SABS 0100-1 (2000) and the ACI 318 (2002) effectively predicts both short-term and total deflections. When $M_a/M_{cr} > 1.0$, the ACI 318 (2002) and the SABS 0100-1 (2000) is recommended for both short-term and total deflection prediction. The ACI 318 (2002) provides a lower deflection limit, while the SABS 0100-1 (2000) provides a upper deflection limit. The Alternative Approach produced relatively good results, but requires more comparison for different flat slab loading and support conditions. The ACI 318 (2002) is the most accurate for deflection prediction of the experimental slab specimens even though most of the deflections are slightly under-predicted.

The EC2 (2004) presents the least conservative and variable span/depth ratios. The span/depth ratios of the EC2 (2004) approach is very sensitive to the amount of tension reinforcement present in the section. The ACI 318 (2002) presented the least span/height (L/h) ratios. Only the ACI 318 (2002) ratios indicated that the experimental slabs do not meet the serviceability criteria.

6 SERVICEABILITY OF SOUTH AFRICAN FLAT SLAB DESIGN

6.1 INTRODUCTION

The South African designers apply the specifications as stipulated in the SABS 0100-1 (2000) to evaluate the serviceability of a structure. The comparisons of the two serviceability methods presented in the SABS 0100-1 (2000) with other design standards, such as the EC2 (2004), the BS 8110 (1997) and the ACI 318 (2002), provide insight to whether the South African designers apply the most appropriate methods to estimate the serviceability of a structure. The following section presents three slab examples from the South African design offices. The first two examples present actual flat slabs built in Southern Africa and the third example consists of tests on one-way spanning lightly reinforced slabs that were used in a study to investigate short-term deflections.

The examples presented in this chapter have different reinforcement layouts and unsymmetrical spans in each orthogonal direction, thus only the empirical methods were used to predict mid-panel deflections. The uncertainty of the finite element models' results when applied to irregular slab layouts has not been investigated in the previous chapter, thus the finite element modelling method was not applied in this chapter.

6.2 CURRENT SOUTH AFRICAN FLAT SLAB SERVICEABILITY METHODS

The South African designers often use the span/depth ratio verification as presented by SABS 0100-1, Clause 4.3.6.2 (2000), to evaluate whether a slab is serviceable or not. From Section 3.3.2 it is evident that the span/depth ratio for the SABS 0100-1 (2000) approach presents the most conservative results for flat slab serviceability design. Thus, it may be assumed that many flat slab designs in South Africa are mostly conservatively designed and present little serviceability problems.

The problem occurs when a flat slab design narrowly passes the span/depth test. If this occurs, it is uncertain what the serviceability implications for the design may be. The examples that follow in this chapter either narrowly fail or pass the span/depth ratio test. The allowable span/depth ratios and the predicted mid-panel deflections are calculated for each example.

6.3 Flat Slab Case Studies from Practice

The three slab examples, presented in this chapter, include two two-way spanning slabs with column drops (slab thickening) around the columns and an experimental study of lightly reinforced one-way spanning slabs.

The first two-way spanning slab is a section as part of a slab for a multi-level parking area. Some excessive cracking and deflections were reported in certain areas. The predicted deflection for a specific slab panel is calculated.

The second two-way spanning slab is a section is part of an office building. The edge panels were reported to have presented excessive deflections. The predicted deflections for the specific slab panels are calculated.

The last example, an experimental study by Maritz (2009), presents recorded short-term deflections for one-way spanning slabs with two spans. The predicted deflections are presented relative to the M_a/M_{cr} ratio (level of cracking).

6.3.1 Example 1: Parking Deck Two-Way Spanning Slab

The slab section modelled for the parking deck is presented in Figure 6-1. The slab section is bordered by Gridlines D to G and 8 to 11. The slab was modelled by the finite element software program, PROKON (2008) to obtain the serviceable moments for the slab. The slab within Gridlines D to G and 8 to 9 has a slab thickness of 250 mm, with drop panels at columns locations (1800 x 1800 x 400 mm). At the drop panels the total depths of the column drops include the slab depth. The remainder of the slab has a thickness of 200 mm. The concrete cover is 20 mm plus 5 mm to the centre of the reinforcement.

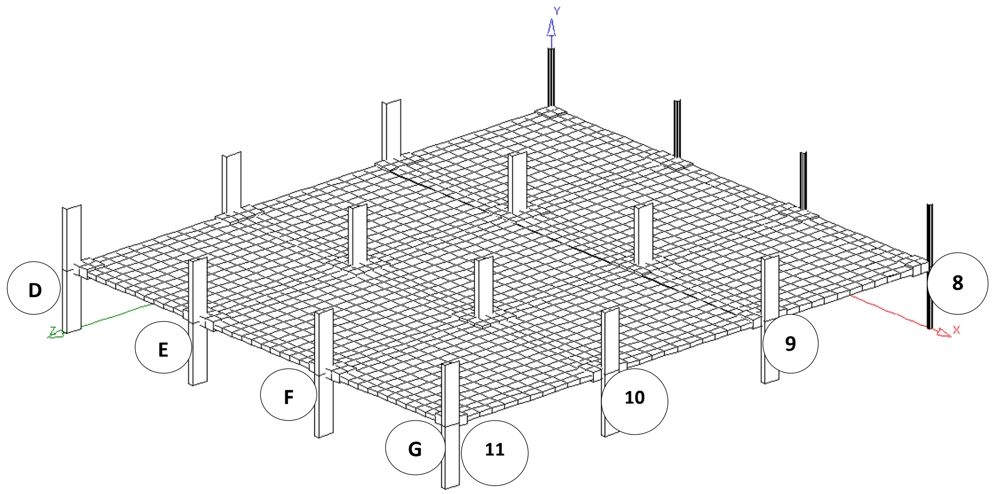

Figure 6-1: Parking deck slab gridline layout.

Table 6-1 presents the slab characteristics for the parking deck. It is assumed that 60% of the applied imposed load contributes to the permanent loading applied to the slab (SABS 0160, 1989).

Table 6-1: Slab Characteristics for the parking deck.

Slab Characteristics		Reference
f_c [MPa]	30.0	Table 1, SABS 0100-1 (2000)
f'_c [MPa]	24.0	Robberts and Marshall, 2008
E_c [GPa]	28.0	Table 1, SABS 0100-1 (2000)
Imposed Load	2.0 kPa	Table 4, SABS 1060 (1989)
Creep	2.75	Fig C.1, SABS 0100-1 (2000)
Shrinkage	4.20×10^{-4}	Fig C.2, SABS 0100-1 (2000)

The panel layout for the parking deck is presented in Figure 6-2. Serviceability problems were observed in Panel 3.

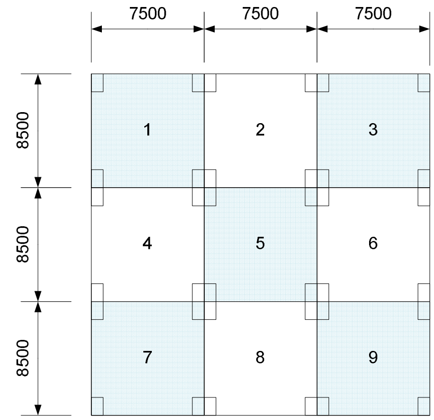

Figure 6-2: Panel layout for the parking deck.

The details for Panel 3 are shown in Figure 6-3. The slab is divided into column and middle strips according to SABS 0100-1 (2000). The dimensions for the column and middle strips are also presented in Figure 6-3.

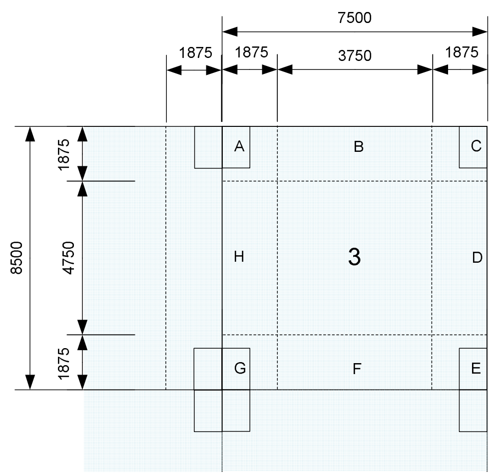

Figure 6-3: Dimensioning details for Panel 3 for the parking deck.

Before the predicted deflections were calculated, the span/depth ratios from the various design standards were calculated. The values in Table 6-2 present the allowable and actual span/depth ratios (L/d) calculated for Middle Strip B – F. For two-way spanning slabs, the span/depth expressions should be applied to the longer of the spans (SABS 0100-1, 2000). The expressions for the span/depth ratios are presented in Section 2.4. The slab is serviceable when the allowable span/depth ratio is larger than the actual span/depth ratio. From Table 6-2 it can be seen that the slab is serviceable according to the span/depth tests from the SABS 0100-1 (2000), the BS 8110

(1997) and the EC2 (2004). The allowable span/depth ratios present a similar trend as was observed for the allowable span/depth ratios for the seven experimental slab specimens as presented in Section 5.5.

The percentage tension reinforcement for the middle strip is 0.295%. This small percentage justifies the large allowable span/depth ratio for the EC2 (2004), being the method greatly affected by the percentage of tension reinforcement. The allowable span/depth ratios for the SABS 0100-1 (2000) and the BS 8110 (1997) are not drastically effected by low level of tension reinforcement; therefore the span/depth ratios produced from these methods are in close range of each other. The span/height ratio produced from the ACI 318 (2002) approach presented the most conservative result and indicates that the slab is not serviceable. The calculations for the span/depth ratios are presented in Appendix H.

Table 6-2: Span/depth ratios from the various design standards as calculated for the parking deck.

L/d Ratios for Middle Strip B - F				
	SABS 0100-1 (2000)	ACI 318 (2002)	BS 8110 (1997)	EC2 (2004)
Allowable	41.15	32.50	45.59	60.21
Actual	37.78	33.20	37.78	37.78
Serviceable	OK	NO	OK	OK

After an evaluation of the span/depth ratios, the mid-panel deflections were obtained by calculating the average deflection for two column strips at the edges of the panel and then adding the deflection from the orthogonal middle strip. Figure 6-4 illustrates this process. The average deflection from Column Strips A – G and C – E is calculated and the deflection of Middle Strips H – D is added to obtain a mid-panel deflection. It is assumed, for the purpose of this study, that the mid-panel deflection calculated from the column and middle strips in the orthogonal direction will produce a relatively similar deflection. The process is similar to the Equivalent Frame Method as was discussed in Section 2.5.

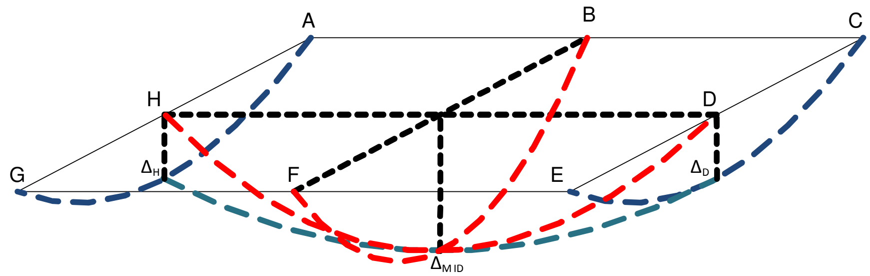

Figure 6-4: Process to obtain mid-panel deflection: Δ_{MID}.

The predicted deflections were calculated for the SABS 0100-1 (2000), the EC2 (2004), the BS 8110 (1997), the ACI 318 (2002) and the Alternative Approach (Section 3.8). The EC2 (2004) requires the use of the quasi-permanent moments to calculate the deflections and not the serviceability moments due to the total load (Webster and Brooker, 2006). The similar moments were used for the Alternative Approach. The deflection methods for the rest of the design standards require that the full serviceability moment be used to calculate the deflections. The predicted deflections are presented in Figure 6-5. The calculations of the deflections are presented in Appendix H.

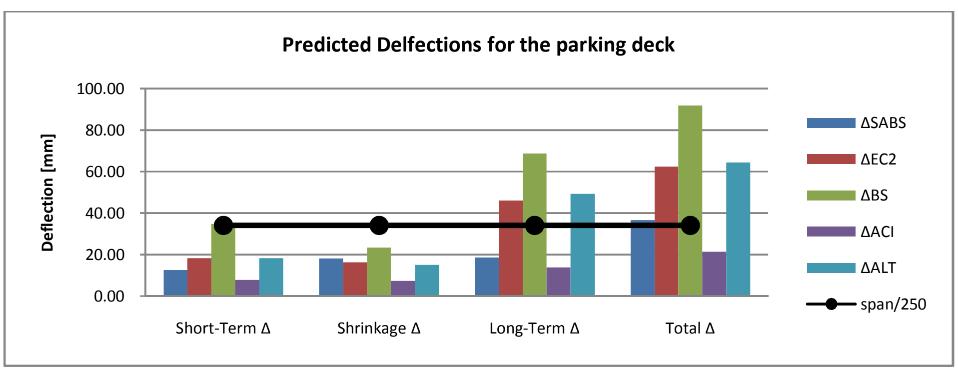

Figure 6-5: Graphical representation of the predicted deflection for the parking deck for the various design standards.

From Figure 6-5 it is evident that the ACI 318 (2002) predicts the smallest deflection prediction while the BS 8110 (1997) predicts the largest deflection prediction. The SABS 0100-1 (2002), the EC2 (2004) and the BS 8110 (1997) limit the final allowable deflection to span/250, while the ACI 318 (2002) presents a span/240 limit. These limits produce similar values, thus only the span/250 limit is presented in Figure 6-5. If this limit is assumed to govern the serviceability evaluation of the parking deck example, it is observed that all the deflection calculation methods predict total deflections larger than the allowable limit with the exception of the ACI 318 (2002) approach. The SABS 0100-1

(2000) deflection result also borders on this limit. The slab was designed according to the SABS 0100-1 (2000), therefore the slab does complies with the serviceability limits as stipulated by the design standards.

In a report by L&S Consulting (Pty) Ltd (2008) on the structural assessment of the parking deck, it was observed that the actual measured deflection as noted by the contractor, was approximately two to three times the allowable long-term deflection as stipulated in the SABS 0160 (1989). The SABS 0160 (1989) presents an allowable long-term deflection for the parking area of span/300 (28.3 mm for the 8500.0 mm span). This suggests that the maximum measured deflection was about 85.0 mm. This is not consistent with the results of the predicted deflections from the SABS 0100-1 (2000) and the ACI 318 (2002) as presented in Figure 6-5. According to L&S Consulting (Pty) Ltd (2008), the reasons for these excessive deflections include:

- Early de-propping of slabs in the affected area, which could have caused cracking of Sections and an additional loss in stiffness.
- Strength of the concrete mix was below the specified strength.
- The slab could have been overloaded during the first two years of the structure life, causing cracking and irreversible loss in stiffness.
- During construction an initial curvature may have resulted due to slab decking out and the measured deflection may be a combination of the actual deflection and the initial deflection.
- The actual built dimensions of the slab could be less than what was specified from the design plans.
- The actual bottom reinforcement in the slab may be less than what was detailed in the design plans.

6.3.2 Example 2: Office Block Two-Way Spanning Slabs

The slab section modelled for office block is presented in Figure 6-6. The slab section is bordered by Gridlines F to H and 3 to 11. The slab was modelled by the finite element software program, PROKON (2008) to obtain the serviceability moments of the slab. The slab panels within Gridlines F to H and 4 to 11 have a slab thickness of 230 mm, with drop panels at the interior columns located along Gridline G (2400 x 2400 x 400 mm). At the drop panels the total depths of the column drops include the slab depth. The slab within Gridlines F to H and 3 to 4 has a thickness of 180 mm. The concrete cover is 15 mm plus 8 mm to the centre of the reinforcement. The slab perimeter is supported by either a 190 x 900 mm or 230 x 900 mm beam. This supporting beam is located along Gridline F up to the intersection with Gridline 5, Gridlines 4, H and 11.

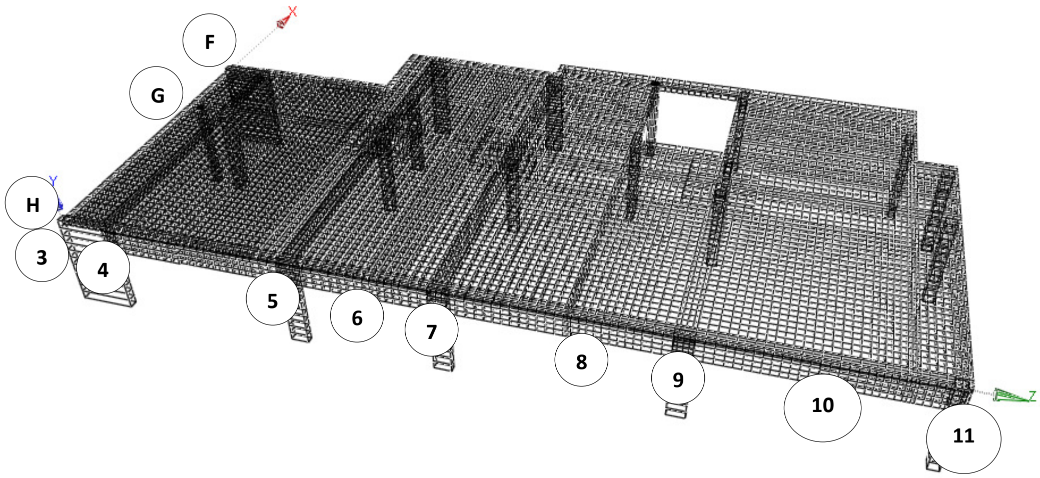

Figure 6-6: Office block slab gridline layout.

Excessive deflections occurred in the two panels located in between Gridlines G to H and 7 to 11. Figure 6-7 shows the deflections calculated to obtain the mid-panel deflection for the first and second panel.

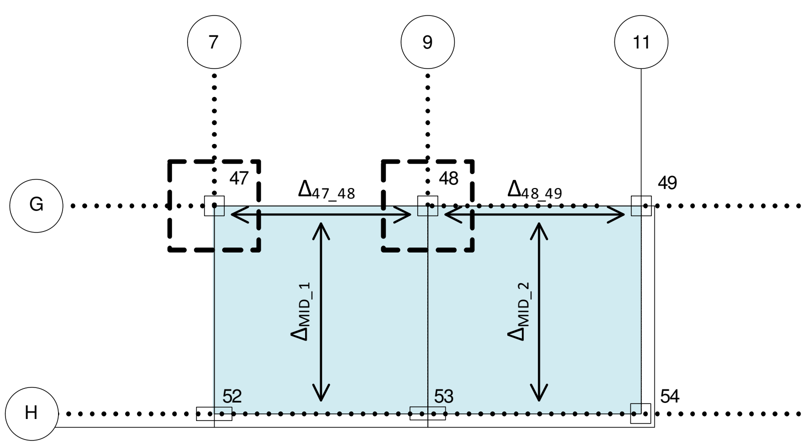

Figure 6-7: The two slab panels, part of the office block slab, which have experienced excessive deflections.

The mid-panel deflection of each panel was calculated by taking the average column strip deflections and adding the orthogonal middle strip deflection. The presence of the supporting beam along Gridlines H and G (Figure 6-7), provide significant stiffness for the column strip deflections between Columns 52 and 53 and Columns 53 and 54. The deflections at these points are assumed to be zero. Thus, only the deflection in the column strip along Gridline B and the deflection for the orthogonal middle strip were calculated.

Table 6-3 presents the slab characteristics for the office block slab. It is assumed that 30% of the applied imposed load contributes to the permanent loading applied to the slab (SABS 0160, 1989).

Table 6-3: Slab Characteristics for Office block Slab.

Slab Characteristics		Reference
f_c [MPa]	25.0	Table 1, SABS 0100-1 (2000)
f'_c [MPa]	20.0	Robberts and Marshall, 2008
E_c [GPa]	26.0	Table 1, SABS 0100-1 (2000)
Creep	2.50	Fig C.1, SABS 0100-1 (2000)
Shrinkage	3.50×10^{-4}	Fig C.2, SABS 0100-1 (2000)

The design loads comply with the SABS 0160 (1989) and include the following:

- Concrete: 24.0 kN/m^3
- Imposed Load (office areas): 2.5 kN/m^2
- Imposed Load (toilet areas): 3.0 kN/m^2
- Light weight partioning: 1.0 kN/m^2
- Suspended ceilings, light fittings, ect: 0.25 kN/m^2
- Line Load on Building Perimeter: 5.5 kN/m

More detail on the loads applied to the slab structure is presented in Appendix I.

The panel layouts for the office block slab are presented in Figure 6-8 where the details for the two panels under consideration, are shown. The slab is divided into column and middle strips according to SABS 0100-1 (2000). The dimensions for the column and middle strips are also presented in Figure 6-8.

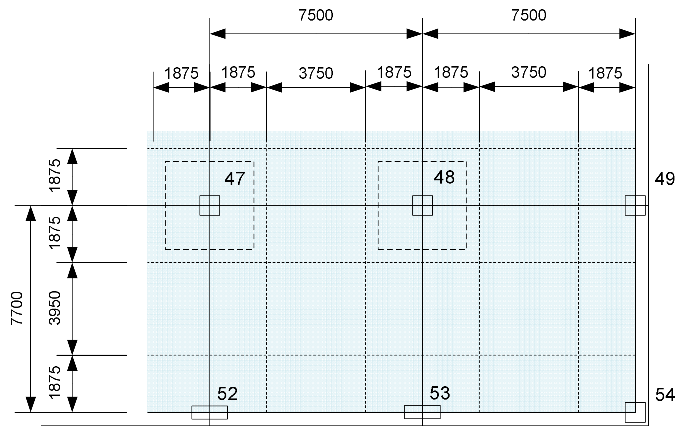

Figure 6-8: Column and Middle Strip dimensions for the two panels part of the office block slab.

Before the predicted deflections were calculated, the span/depth ratios from the various design standards were calculated. The values in Table 6-4 present the allowable and actual span/depth ratios (L/d) calculated for Middle Strip 52,53 – 47,48. The mid-span reinforcement and dimensions for both panels are similar, thus the span/depth ratio test for only the first panel was calculated. For the two-way spanning slabs, the span/depth ratio expressions should be applied to the longer of the spans (SABS 0100-1, 2000). The expressions for the span/depth ratio are presented in Section 2.4. The slab is serviceable when the allowable span/depth ratio is larger than the actual span/depth ratio.

Table 6-4: Span/depth ratios from the various design standards as calculated for the office block slab.

L/d Ratios for Middle Strip 52,53 – 47,48				
	SABS 0100-1 (2000)	ACI 318 (2002)	BS 8110 (1997)	EC2 (2004)
Allowable	39.98	32.50	44.03	39.25
Actual	37.20	31.96	37.20	37.20
Serviceable	OK	OK	OK	OK

The slab is serviceable according to the span/depth ratio tests from the SABS 0100-1 (2000), the BS 8110 (1997) and the EC2 (2004). In this case, the result from the BS 8110 (1997) presented the largest allowable span/depth ratio, while the EC2 (2004) presented the least allowable span/depth ratio. This example slab has a relatively low concrete compressive strength relative to the other slabs discussed in this investigation. The EC2 (2004) approach is dependent on the value of the concrete compressive strength, which is significantly low in this case. This is the reason for the sudden change in the trend for the span/depth ratios relative to the results obtained from the other slabs. The expressions for the span/depth ratio evaluation of the other design standards do not directly take the concrete compressive strength into account, thus showing no real change in their results due to a smaller value of the concrete compressive strength. The low concrete compressive strength allows the span/depth ratio result for the EC2 (2004) to be more conservative than both the SABS 0100-1 (2000) and the BS 8110 (1997). The span/height ratio produced from the ACI 318 (2002) approach presented the most conservative result and indicates that the slab is serviceable. The calculations for the span/depth ratio are presented in Appendix I.

The mid-panel deflections were obtained by calculating the average deflection for two column strips at the edges of the panel and then adding the deflection from orthogonal middle strip. The finite element results for the slab example showed predominantly one way slab behaviour; therefore the calculation of the slab deflections in the direction as presented in Figure 6-7 was more appropriate. The process is similar to the Equivalent Frame Method as was discussed in Section 2.5. The predicted deflections were calculated for the SABS 0100-1 (2000), the EC2 (2004), the BS 8110 (1997), the ACI 318 (2002) and the Alternative Approach (Section 3.8). The EC2 (2004) require the use of the quasi-permanent moments to calculate the deflections and not the serviceability moments due to the total load (Webster and Brooker, 2006). The similar moments were used for the Alternative Approach. The deflection methods for the rest of the design standards require that the full serviceability moment be used to calculate the deflections. The predicted deflections for the first and second panels are presented in Figures 6-9 and 6-10. The calculations of the deflections are presented in Appendix I.

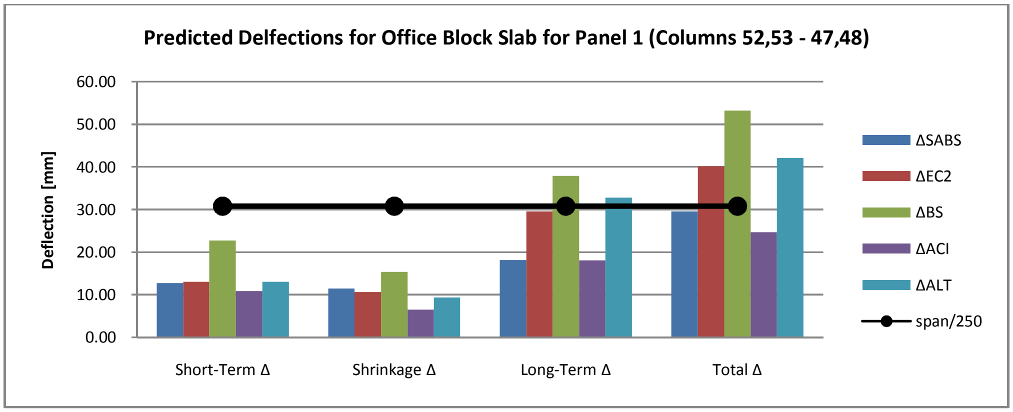

Figure 6-9: Graphical representation of the predicted deflections for the first office block panel for the various design standards.

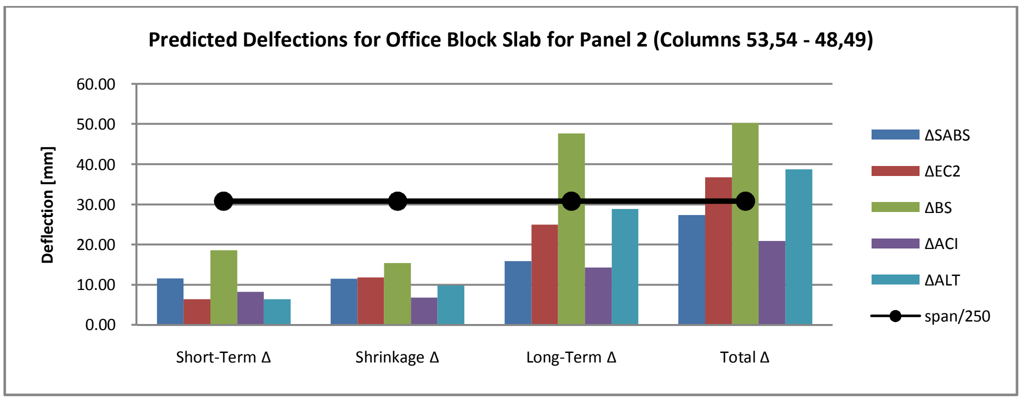

Figure 6-10: Graphical representation of the predicted deflection for the second office block panel for the various design standards.

Similar deflections tendencies are presented for both panels from Figures 6-9 and 6-10. In both cases the ACI 318 (2002) presents the smallest deflection prediction while the BS 8110 (1997) presented the largest deflection prediction.

It was recorded that the actual mid-panel deflection reached 70.0 mm. This value is far larger than what is predicted in Figures 6-9 and 6-10. The SABS 0100-1 (2002), the EC2 (2004) and the BS 8110 (1997) limit the final allowable deflection to span/250, while the ACI 318 (2002) presents a span/240 limit. These limits produce similar values, thus only the span/250 limit is presented in Figures 6-9 and 6-10. If this limit is assumed to govern the serviceability evaluation of the office block slab example, it is observed that the EC2 (2004), the BS 8110 (1997) and the Alternative Approach methods predict the total deflections larger than the allowable. The ACI 318 (2002) and the SABS 0100-1 (2000) predict the total deflections below the span/250 limit. The actual deflection of 70.0 mm is larger than the 30.8 mm limit, thus the slab does not comply with the serviceability limits as stipulated by the design standards. This may potentially be due to the following reasons:

- The early removal of propping and incorrect curing of the slab result in early cracking, causing in early irreversible reduction in slab stiffness that is not accounted for by the deflection prediction methods.
- If the slab is overloaded for short periods during the structure life, the additional cracks also reduce the slab stiffness not accounted for by the deflection prediction methods.
- Actual reinforcement in the built structure may not be what is detailed in the design plans.
- A faulty concrete mix may change the expected slab behaviour and may be the cause of excessive slab deflections.
- Possible changes to actual slab dimensions as to what is indicated in the may contribute to excessive slab deflections.

According to the span/250 limit the slab does comply with the deflection serviceability requirements, since being designed according to the SABS 0100-1 (2000). In Table 6-4, the SABS 0100-1 (2000), the ACI 318 (2002) and the EC2 (2004) produce a span/depth ratio evaluations where the slab narrowly complies with the required span/depth ratio limit. This suggests that it is required to calculate the predicted deflection for slab structure.

The first panel (Figure 6-9) of the office block slabs shows the larger deflections for the two panels under consideration. Seeing that the first panel governs the serviceability behaviour of the office block slab, thus only the behaviour of the first panel is discussed.

The first office block slab panel has a percentage tension reinforcement content of 0.492%. Using the M_{cr} as calculated for the EC2 (2004), the M_a/M_{cr} ratio is 1.25 and the I_u/I_{cr} ratio is 4.56. These values indicate that the slab is lightly reinforced with the applied moment slightly above the cracking moment of the slab. It has been seen in Chapter 3 that for such ratios it is expected that the BS 8110 (1997) will produce the largest deflections, the SABS 0100-1 (2000) and the ACI 318 (2002) the least deflections. The EC2 (2004) and Alternative Approach produced deflections within the limits provided by the other calculation methods. The short-term deflections produced from the different design standards are very similar with the exception of the excessive deflection from BS 8110 (1997). The deflection variability increases for the total deflections. From the discussions in Chapter 3, concerning the effectiveness of the different deflection prediction methods, it may be observed that BS 8110 (1997) greatly over-estimated the slab deflections. The EC2 (2004) results provide an upper limit for the predicted deflections and the SABS 0100-1 (2000) provides a lower limit. The results from the Alternative Approach are similar to the EC2 (2004) results, thus it may be assumed that the either the EC2 (2004) or the Alternative Approach results may be used as the upper limit.

6.3.3 Example 3: Maritz One-Way Spanning Slabs

The experimental study by Maritz (2009) involved the testing of nine one-way spanning slabs with varying percentages of tension reinforcement. The slabs were tested in a controlled environment in a laboratory. Each set of three slab specimens respectively contained 0.4%, 0.8% or 1.1% tension reinforcement. The study focused on obtaining short-term deflections from experimental slab specimens and comparing the recorded data to calculated deflections from the design standards. The dimension of the slab specimens are presented in Table 6-5.

Table 6-5: Dimensions and properties of the nine slab specimens from Maritz (2009).

Slab Set	ρ [%]	h [mm]	b [mm]	d [mm]	Span [mm]	E_c [GPa]	f_c [MPa]	$A_{s,prov}$ [mm^2]	$\rho = A_{s,prov}/bh$ [%]
Slab 1a	0.40	100	600	75	2400	27.76	41.4	236	0.39
Slab 1b	0.40	100	600	75	2400	26.08	40.1	236	0.39
Slab 1c	0.40	100	600	75	2400	26.08	40.1	236	0.39
Slab 2a	0.80	100	600	75	2400	31.37	45.2	471	0.79
Slab 2b	0.80	100	600	75	2400	31.37	45.2	471	0.79
Slab 2c	0.80	100	600	75	2400	31.37	45.2	471	0.79
Slab 3a	1.10	100	400	75	2400	33.11	51.1	452	1.13
Slab 3b	1.10	100	400	75	2400	33.11	51.1	452	1.13
Slab 3c	1.10	100	400	75	2400	33.11	51.1	452	1.13

The study by Maritz (2009) presented recorded short-term deflections for nine one-way slab specimens. The empirical methods from the design standards were used to calculate the predicted short-term deflections to present a comparison between the recorded and predicted results.

The experimental setup used by Maritz (2009) to obtain the experimental slab deflections, is presented in Figure 6-11. Two point loads were applied 1.2 m from the interior support to obtain the mid-span deflections for both Spans 1 and 2.

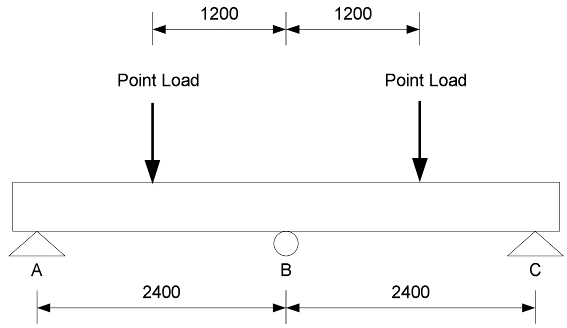

Figure 6-11: Experimental setup and load application (Maritz, 2009).

The short-term deflections from the experimental slabs are presented in Table 6-6. Each specimen set contained deflections from three specimens, such as Slabs 1a, 1b and 1c, as well as deflections from both spans in for each specimen. The average deflection for all 6 spans, for each specimen set, was calculated. The results for each span did not provide much variance and produced approximately similar results.

Table 6-6: Recorded short-term deflection results from the experimental slab specimens (Maritz, 2009).

Slab Specimens	ρ [%]	Δ_{EXP} [mm]	Applied Moment, M_a [kNm]
Slab 1a – 1c	0.39	4.62	4.62
Slab 2a – 2c	0.79	6.30	8.81
Slab 3a – 3c	1.13	7.68	8.02

The recorded deflections and the predicted deflections from the empirical methods were compared using a M_a/M_{cr} ratio versus deflection curve and are presented in Tables 6-7 to 6-9. The M_a/M_{cr} (applied moment over cracking moment) ratio depicts the level of cracking within a member. A M_a/M_{cr} ratio of less than one, represents an uncracked member, while a M_a/M_{cr} larger than one, represents a member undergoing cracking. The predicted deflection behaviour is shown for the methods from the various design standards as the M_a/M_{cr} increases from zero. The experimental behaviour is plotted on the predicted deflection behaviour curves in order to observe which curve follows the experimental behaviour.

Different methods are available to obtain a value for M_{cr}. There are no real distinctions which of these methods are the most effective. For this reason, the M_a/M_{cr} ratio for each M_{cr} is presented in the comparisons. The M_{cr} for the EC2 (2004), the SABS 0100-1 (2000) and the ACI 318 (2002) are presented. As a result from the discussion in Section 3.2, where the EC2 (2004) was identified to predict short-term deflections most effectively, the M_{cr} from the EC2 (2004) was used to predict the M_a/M_{cr} ratio for the BS 8110 (1997). Table 6-7 presents the comparisons for the slab specimens with 0.39% tension reinforcement content. Using the correct M_a/M_{cr} ratio relative for the deflection prediction method, the appropriate point of first cracking is included in the comparison with the experimental data. The calculations to produce the graph presented in Table 6-7 are presented in Appendix J.

Table 6-7: Short-term deflection comparison for slab specimens at 0.39 % tension reinforcement.

Deflection versus M_a/M_{cr} Ratio curves for the Different design standards

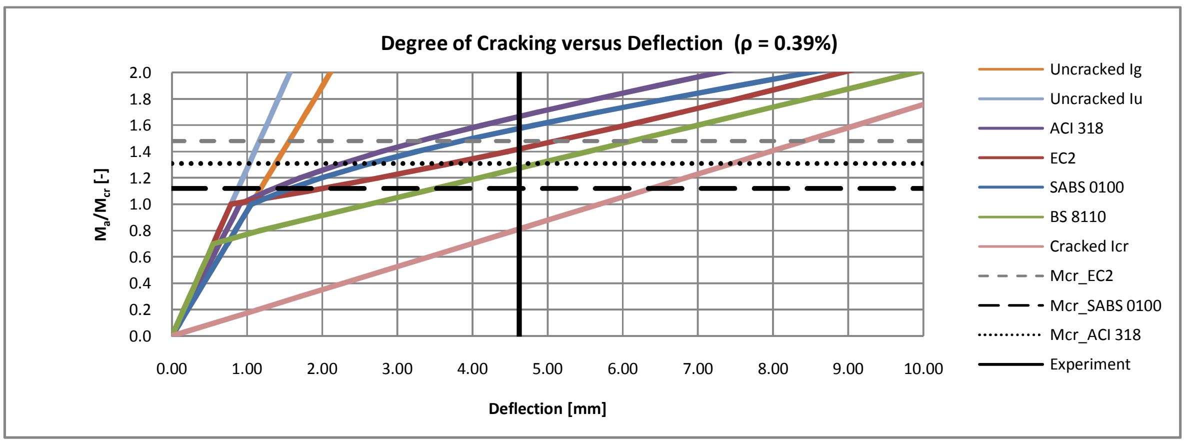

Maritz (2009) **Δ_{EXP} = 4.62 mm** **M_a = 4.62 kNm**

design standards				
	ACI 318 (2002)	EC 2 (2004)	SABS 0100-1 (2000)	BS 8110 (1997)
M_{cr} [kNm]	3.53	3.13	4.12	3.13
M_a/M_{cr}	1.31	1.48	1.12	1.48
Δ_i [mm]	2.25	5.10	1.58	6.12
Δ_i/Δ_{EXP}	0.49	1.10	0.34	1.32

The predicted deflection at the M_a/M_{cr} for the specific method may be obtained from the graph in Table 6-9. For example, according the EC2 (2004) approach the M_{cr} = 3.13 kNm and produces a M_a/M_{cr} ratio of 1.48. Following the M_a/M_{cr} ratio curve to the point of interSection with the predicted deflection curve from the EC2, a deflection of 5.10 mm is obtained. In comparison to the experimental deflection, the Δ_i/Δ_{EXP} is calculated to be 1.10. This ratio indicates that the EC2 (2004) approach slightly over-predicts the point of first cracking and in response over-predicts the short-term deflection at an applied moment of 4.62 kNm. However, the EC2 (2004) still presented the more accurate results in comparison with the deflection ratios of the other approaches.

It may be interpreted that the M_{cr} as calculated by the EC2 (2004), present the point of cracking acceptably in order to predict slab behaviour that follows the experimental behaviour. This is only appliable to slab specimens with a percentage tension reinforcement of 0.39%. The stiffening ratio, I_g/I_{cr} = 7.1 for the slab specimen. The high stiffening ratio indicates that the EC2 (2004) will most likely predict the defleciton behaviour of the slab more effectively.

The next set of slab specimens are those for with a percentage tension reinforcement of 0.79%. Table 6-8 presents the comparisons for the slab specimens.

Table 6-8: Short-term deflection comparison for slab specimens at 0.79 % tension reinforcement.

Deflection versus M_a/M_{cr} Ratio curves for the different design standards

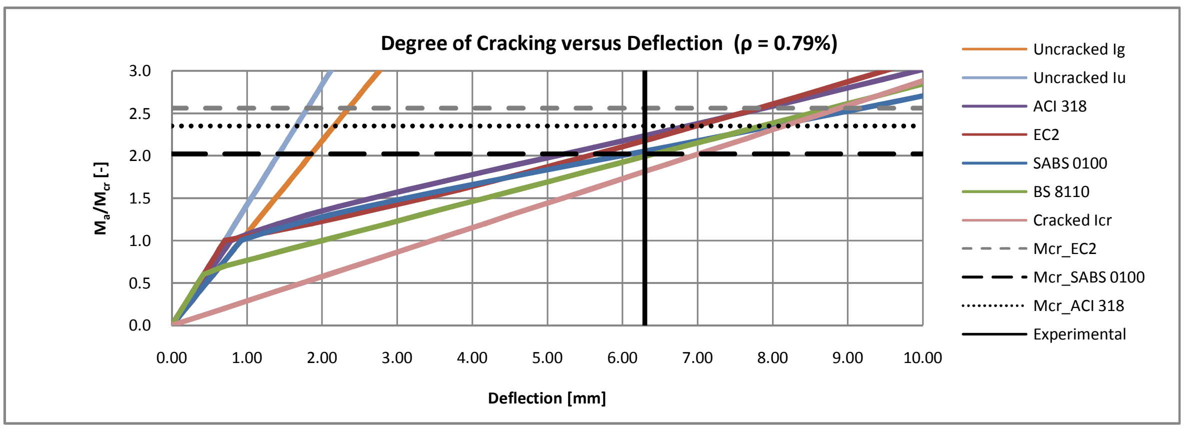

Maritz (2009)	Δ_{EXP} **= 6.30 mm**		M_a **= 8.81 kNm**	
	design standards			
	ACI 318 (2002)	EC 2 (2004)	SABS 0100-1 (2000)	BS 8110 (1997)
M_{cr} [kNm]	3.75	3.45	4.37	3.45
M_a/M_{cr}	2.35	2.56	2.02	2.56
Δ_i [mm]	7.80	2.09	3.86	8.76
Δ_i/Δ_{EXP}	1.09	1.24	0.97	1.39

As explained for the results in Table 6-7, the same procedure is applied to obtain the results as presented below the graph in Table 6-8.

From the deflection ratios it is evident that the ACI 318 (2002) and the SABS 0100-1 (2000) present the most accurate deflection predictions to produce a deflection similar to the experimental deflection. It is therefore also assumed that the ACI 318 (2002) and the SABS 0100 (2000) accurately account for the point of first cracking affectively to follow the experimental behaviour.The EC2 (2004) and the BS 8110 (1997) over-predict the deflections. This is only applicable to slab specimens with a percentage tension reinforcement of 0.79% and a stiffening ratio of I_g/I_{cr} = 4.8. The low stiffness ratio indicates that the SABS 0100-1 (2000) and the ACI 318 (2002) are suitable to predict the defleciton behaviour of the slab more effectively.

The next set of slab specimens are those with a percentage tension reinforcement of 1.13%. Table 6-9 presents the comparisons for the slab.

Table 6-9: Short-term deflection comparison for slab specimens at 1.13 % tension reinforcement.

Deflection versus M_a/M_{cr} Ratio curves for the Different design standards

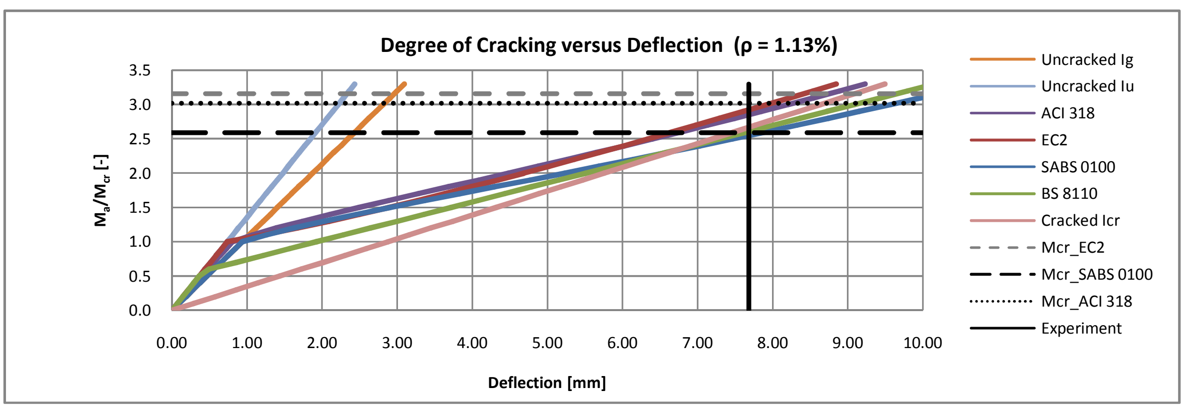

Maritz (2009)	Δ_{EXP} = 7.68 mm		M_a = 8.02 kNm	
design standards				
	ACI 318 (2002)	EC 2 (2004)	SABS 0100-1 (2000)	BS 8110 (1997)
M_{cr} [kNm]	2.66	2.54	3.10	2.54
M_a/M_{cr}	3.02	3.16	2.59	3.16
Δ_i [mm]	8.27	8.42	7.85	9.65
Δ_i/Δ_{EXP}	1.08	1.10	1.02	1.26

As explained for the results in Table 6-7, the same procedure is applied to obtain the results as presented below the graph in Table 6-9.

From the deflection ratios it is evident that the SABS 0100-1 (2000) presents the most accurate deflection prediction to produce a deflection similar to the experimental deflection. It is therefore also assumed that the SABS 0100 (2000) accurately accounts for the point of first cracking effectively to follow the experimental behaviour.The EC2 (2004) and the ACI 318 (2002) also predict the deflections with only a slight over-prediction. The BS 8110 (1997) greatly over-predicts the deflections. This conclusion is only applicable to slab specimens with a percentage tension reinforcement of 1.13%. The stiffening ratio, I_g/I_{cr} = 4.7 for the slab specimens. The low stiffness ratio indicates that the SABS 0100-1 (2000), the ACI 318 (2002) and the EC2 (2004) approaches are suiTable to predict the defleciton behaviour of the slab effectively.

The BS 8110 (1997) method of deflection prediction over-predicts the deflection behaviour for the all slab specimens, as presented in Tables 6-9 to 6-11. This justifies the observation that the BS 8110 (1997) is not suitable to predict deflections for lightly reinforced concrete members. For low reinforcement content the EC2 (2004) presents the more effective deflection prediction method. At higher reinforcement contents, also producing section with a lower stiffening ratio, the ACI 318 (2002) and the SABS 0100-1 (2000) prove to be more effective. For slabs with a percentage reinforcement content larger than 1.13%, any of the presented deflection prediction may be applied, with the exception of the BS 8110 (1997) approach.

6.4 IMPLICATIONS OF THE PREDICTION OF FLAT SLAB DEFLECTIONS ON SOUTH AFRICAN DESIGN

The use of better quality construction materials and more effective construction methods allow flat slab designs to stretch over longer spans with thinner sections. The calculation of the predicted time-dependent deflection is important in order to produce flat slab designs that meet both the ultimate limit state and serviceability limit state requirements. While a flat slab may comply with the ultimate limit state requirements, the governing design requirement may be the serviceability limit state. If the serviceability deflection requirements are over-predicted, indicating the need for thicker slabs than what are actually required, the structures become too expensive. By presenting a more effective method of deflection prediction, flat slab designs can be cost effective, but with adequate assurance that no serviceability problems will occur, such as the examples presented in Section 6.3.

Another advantage of presenting more effective flat slab deflection predictions is that existing flat slab structures that have deflection problems, may be re-evaluated to observe whether the excessive deflections is a product of poor construction or of engineering design error.

6.5 CONCLUDING SUMMARY

It is important to evaluate flat slab structures for the serviceability limit state. There is a need for South African designers to have effective deflection prediction methods available to predict the time-dependent deflection for slender structures. The deflection methods need to be able to predict deflections specifically for lightly reinforced concrete members, such as flat slab structures.

Three slab examples are presented in this chapter. The deflections are predict using the empirical deflection prediction methods including the SABS 0100-1 (2000), the EC2 (2004), the BS 8110 (1997), the ACI 318 (2002) and the Alternative Approach (Section 3.8). The first two examples are flat slab examples with columns drops, which have undergone excessive deflections over time. The predicted deflections are calculated and the results presented. It was observed that the SABS 0100-1 (2000) and the ACI 318 (2002) predicted a total deflection below the allowable span/250 limit as presented by the design standards. The results from the other deflection methods presented results above this limit. Even though the span/depth ratio evaluation suggested that the slabs narrowly conform to the serviceability requirements, the calculated deflections suggest that the slab borders on producing unacceptable deflections.

It was observed that the actual measured deflections exceed the calculated deflections from the deflection prediction methods for both the parking deck and the office block. It was postulated that the possible reasons for this may include:

- The early removal of propping and incorrect curing of the slab result in early cracking. Such cracking irreversibly reduces the slab stiffness.
- Spontaneous slab overloading for short periods during the structure life causes additional cracking and thus a loss of slab stiffness.
- Actual reinforcement in the built structure may be different from the designed reinforcement layout, thus changing the slab behaviour
- A faulty concrete mix with concrete of a decreased concrete strength may cause excessive deflections.
- Possible changes to actual slab dimensions during construction alter slab behaviour and may cause excessive deflections.

Such occurrences during or immediately after slab construction, is not accounted for by the deflection prediction methods. In cases where the slab suffers these influences the calculated deflection is far less than the actual measured deflection. It may therefore be recommended that there is a need to incorporate the effects of construction methods into deflection prediction methods. By incorporating those effects, the deflection prediction methods may predict actual deflection taking actual conditions into consideration.

The third example presents deflection of one-way slab specimens which is part of a study to investigate short-term deflections by Maritz (2009). The deflection behaviour is evaluated and it is demonstrated that the expressions used to evaluate the point of first cracking is also of importance to predict deflections effectively. It is observed that the EC2 (2004) approach predict deflections effectively for one-way slabs with a percentage tension reinforcement of 0.39%, while the ACI 318 (2002) and the SABS 0100-1 (2000) present the more effective results for the 0.79% tension reinforcement slabs. Above and at the percentage tension reinforcement of 1.13% the ACI 318 (2002), the SABS 0100-1 (2000) and the EC2 (2004) predict acceptable deflections for one-way slabs. The BS 8110 (1997) approach over-predicts deflections for all the slab specimens.

In this chapter it has been proven that the flat slab case studies are serviceable as were designed according to the SABS 0100-1 (2000). Therefore, South African designers produce designs that fall within the required serviceability of other design standards as well and the serviceability requirements as presented in the SABS 0100-1 (2000) are effective.

The implications of being capable of predicting relatively accurate deflections include the advantage of less over-design and thus more inexpensive flat slab designs.

7 SUMMARY, CONCLUSIONS AND RECOMMENDATIONS

The summary, conclusions and recommendations for this study are based on the findings as stipulated in Chapters 3, 4, 5 and 6.

7.1 SUMMARY

7.1.1 Modelling Approach for Predicting Deflections

The aim of this study was to identify a deflection prediction method that effectively predicts mid-panel deflections for a flat slab structure. The deflection prediction method should take the necessary factors into account which influence the two-dimensional behaviour of a flat slab structure. The deflection prediction methods considered in this study include finite element models solved within a commercial finite element software package and empirical hand-calculations from various design standards.

To acquire such a solution the problem was first simplified to a two-dimensional problem. The deflection solution for a one-way spanning slab was investigated and was presented in Chapter 3. The limitations of the deflection methods to predict one-way spanning slab deflections were identified. Knowing the limitations of the methods, it is possible to know what to expect from the results of the deflection prediction methods. The parameters that play a role are identified as the percentage tension reinforcement content, the level of cracking (M_a/M_{cr} ratio) and the stiffness ratio (I_u/I_{cr}).

The next step was to evaluate these parameters together with the deflection prediction methods and to apply the procedures to a three-dimensional flat slab example. Gilbert and Guo (2005) conducted an experimental study with seven large-scale flat slab specimens under a sustained distributed load, for a test period of up to 750 days. The recorded data from the test specimens are compared with the predicted deflection methods to evaluate the competency of the deflection methods. This evaluation was done in Chapter 5.

The comparisons in Chapter 5 identified some tendencies for the various deflection prediction methods. A further comparison was conducted for three case studies of real slab designed and built using the South African standards. These comparisons are presented in Chapter 6. This comparison was done to evaluate the serviceability requirements for South African slab designs.

The evaluations with the test results (Chapter 5) and the case studies (Chapter 6) assisted to draw conclusions for a suitable approach to determine deflections of slender reinforced concrete elements.

7.1.2 Linear Finite Element Model for Flat Slab Serviceability Design

The finite element deflection prediction methods considered in this study include the analyses of a finite element model within a commercial software packages. Chapter 4 discussed how the nonlinear behaviour of a composite concrete – steel reinforcement element is required to account for the elasto-plastic behaviour of reinforced concrete. The limitations of the commercial finite element software required an approximation of the localised behaviour of crack development and tension stiffening within the slab structure. The global flexural behaviour of the slab structure was obtained using a slab model composed of eight-node quadrilateral shell elements for the slab, and beam elements for the columns. The stiffness of the shell elements was reduced to incorporate the effect of cracking within certain slab locations. The model is analysed with a linear analysis, because the effect of concrete cracking is taken into account using a reduced stiffness of identified shell elements.

Two finite element models are presented for the finite element deflection prediction methods. The first was an uncracked finite element model consisting of a flat slab model with shell (slab) and beam elements (columns). The uncracked finite element model represented the conventional method for flat slab modelling. The second model was a cracked finite element model with a similar element composition as the uncracked finite element model, but with certain shells allocated a reduced stiffness to simulate cracked stiffness (cracked modulus of elasticity). These shells were located at areas in the slab where the bending moment is larger than the cracking moment.

The deflections obtained from the two finite element models therefore included the deflections using the uncracked finite element model and the deflection using the cracked finite element model.

7.1.3 Methods Available for Predicting Deflections

Methods to predict deflection include either finite element software or applying a set of expressions to empirically calculate the deflections by hand. It was decided to investigate the empirical methods available from four different design standards. These design standards are:

- The American Concrete Institute 318-02 (ACI 318, 2002)
- The British Standards 8110: Part 2: 1997 (BS 8110, 1997)
- EN 1992 -1-1 Eurocode 2: Part 1-1 (EC2, 2004)
- South African Bureau of Standards 0100-1 (SABS 0100-1, 2000)

Each empirical method allows the calculation of the short-term, the long-term and shrinkage deflections. The maximum total deflection of a slender member is the sum of the long-term and shrinkage deflections.

The BS 8110 (1997) approach assumes that a section is either uncracked or cracked under loading. The method provides no means of estimating the gradual change of the increasing loss in stiffness for a section during loading. The SABS 0100-1 (2000) and the ACI 318 (2002) have accepted Branson's (1977) approach to model the gradual development of a section from an uncracked to cracked state, while the EC2 (2004) follows similar to Bischoff's (2005) approach.

Chapter 3 discussed the differences between the empirical deflection prediction methods. These differences have been quantified using identified parameters. The parameters are the percentage tension reinforcement, the level of cracking (M_a/M_{cr} ratio) and the stiffening ratio (I_u/I_{cr} or I_g/I_{cr}). Branson's (1977) approach, adopted by the ACI 318 (2001) and the SABS 0100-1 (2000), have been calibrated to predict the deflection for beams with a percentage tension reinforcement content of equal to or large than 1.0%, a M_a/M_{cr} ratio of between 2.0 and 3.0 and a I_u/I_{cr} ratio of between 2.5 and 4.0. The EC2 (2004) approach is capable of effectively predicting deflections for beam with a percentage tension reinforcement of less than 1.0%, a M_a/M_{cr} ratio of just above 1.0 and a I_u/I_{cr} ratio of larger than 4.0.

The discussions from the literature study in Chapter 2 initiated the development of a proposed Alternative Approach. This approach is also used and evaluated as a deflection prediction method. The approach is described in Chapter 3. The results using this method are summarized below.

7.1.4 Methods Available for Calculating Span/Depth Ratios

The span/depth test is the first approach used by a designer to evaluate the serviceability of a slender member. The deflection prediction methods are usually only employed if a specific deflection is required. Therefore, this study also included a comparison of the span/depth methods as found in the different design standards.

Chapter 2 described the set of expressions required for each of the span/depth methods, while Chapter 3 presented a comparison between the different methods. The comparison aimed to investigating the influence of low percentages of tension reinforcement on the variability of the span/depth ratios for the various design standards. The effect of compression reinforcement was not taken into account, since compression reinforcement is usually not provided at midspan for flat slab structures.

It was found that the calculated allowable span/depth (L/d) ratios show a particular trend for reinforced concrete sections with less than or up to 1.0% tension reinforcement and with normal concrete strength (approximately 30 MPa concrete characteristic cube strength). The SABS 0100-1 (2000) presented the most conservative span/depth ratios, while BS 8110 (1997) presented less conservative span/depth ratios. The span/depth ratios for the EC2 (2004) presented the largest variability as the percentage tension reinforcement decreases, producing very high span/depth ratios at very low reinforcement percentages. For a percentage tension reinforcement of larger than 1.0%, the span/depth ratio for the EC2 (2004) approach stabilises to a value slightly less than the value from the BS 8110 (1997).

The EC2 (2004) approach is also influenced by the concrete compressive strength as discussed in Chapter 6. Decreasing the concrete compressive strength, decreases the span/depth ratio for the EC2 (2004) approach to span/depth ratios less than both the SABS 0100-1 (2000) and BS 8110 (1997) results.

The ACI 318 (2002) presents approximations for the span/height ratios of a slender member, rather than the usual span/depth ratios. These ratios stay constant for a particular slab, irrespective if the percentage tension reinforcement or the concrete compressive strength is varied. The span/height ratio is a function of the reinforcement yield strength, the type of slab and the slab span length. The results from the ACI 318 (2002) approach present no real trend relative to the span/depth ratio results from the other design standards.

7.2 CONCLUSIONS

7.2.1 Different Deflection Prediction Methods Available

The deflection prediction limits discussed in Chapter 3 and Section 7.3, are reliable indicators on what tendencies to expect if the deflection is calculated from the various deflection prediction methods. The deflections limits do not take irregular loading stages or extreme environmental exposure into consideration. If such effects are present, then the deflection prediction limits are not reliable as seen from the discussion from Slab S2 and Slab S5 in Chapter 5.

The predicted deflections for the experimental flat slab specimens in Chapter 5 show a particular trend. The deflections obtained from the SABS 0100-1 (2000) provide an upper deflection limit; while the deflections obtained from the ACI 318 (2002) provide a lower deflection limit. The SABS 0100-1 (2000) and the ACI 318 (2002) approach require an estimate of the average stiffness of the sections above the supports and the mid-panel section, while the other deflection prediction methods only account for crack development at mid-span. It is for this reason that these two prediction methods provided a more acceptable deflection prediction for the experimental slabs. The different approximations of the long-term and shrinkage deflections from the ACI 318 (2002) and the SABS 0100-1 (2000), result in the upper and lower deflection limits from these methods. The inclusion of the section stiffness above the column during the deflection calculation presented improves estimations of the member stiffness and similarly the deflections. This is not included by the EC2 (2004) and BS 8110 (1997) models. The EC2 (2004) and the BS 8110 (1997) usually over-predicted the predicted deflection by only accounting for over-predicted mid-panel crack development.

The Alternative Approach predicted the experimental deflection far better than the EC2 (2004) approach, even though the two methods are almost similar. The Alternative Approach presents a different approach to compute the long-term deflections and the results proved that this approximation is far more effective for cases where the loading history changes. The Alternative Approach results usually provided results within the upper and lower limits provided by the methods of SABS 0100-1 (2000) and the ACI 318 (2002).

The uncracked finite element models usually under-predicted the deflections (as expected), while the cracked finite element model presented no real tendency throughout the comparison. The finite element models, using the approach investigated in this study, are therefore not recommended for deflection prediction and should not be used in the design office.

7.2.2 Adequacy of the Deflection Prediction Methods for a South African design office

The empirical methods were used to predict the deflection for the three South African case studies. As stated in Section 7.2.1, the results from the finite element models have proved to be inconsistent and thus were not included in this comparison. Chapter 6 discussed the deflection predictions as applied to South African case studies.

The first two examples predicted similar deflection tendencies for both slabs. The design standards present an allowable final deflection limit of span/250. Taking this into account, it was observed from the deflection results in Chapter 6 that BS 8110 (1997), EC2 (2004) and the Alternative Approach greatly over-estimated the maximum total slab deflections. The SABS 0100-1 (2000) and the ACI 318 (2002) presents deflection results close to and below the span/250 limit. These conclusions are similar to what is observed from the discussion is Chapter 5. The SABS 0100-1 (2000) and the ACI 318 (2002) present the most effective method to predict deflection for flat slab structures. In both case studies it was observed that the actual measured deflection exceed the calculated deflections from the deflection prediction methods. Reasons for these differences potentially include:

- Slab overloading for short periods during the structure life causes additional cracking and thus a loss of slab stiffness.

- The incorrect curing and early removal of propping for the slab result in early cracking. Such cracking also irreversibly reduces the slab stiffness.
- Actual reinforcement in the built slab possibly different from the designed reinforcement layout, thus changing the slab behaviour
- An incorrect concrete mix with concrete of a reduced concrete strength may cause excessive deflections.
- Possible changes to actual slab dimensions during construction alter slab behaviour and may cause excessive deflections.

The third case study consists of an experimental investigation conducted by Maritz (2009). The investigation aimed at measuring the short-term deflection for one-way spanning slab with low percentages of tension reinforcement. Three sets of slab specimens were tested with percentages tension reinforcement of 0.39%, 0.79% and 1.13%. From these results, it was observed that the cracking moment (estimated point of first cracking) is of importance to predict deflections effectively. The results show the EC2 (2004) approach is the most effective method for deflection prediction for a slab with 0.39% tension reinforcement, while the SABS 0100-1 (2000) and the ACI 318 (2002) are the best approaches for the slab specimens with 0.79% and 1.13% tension reinforcement. The EC2 (2004) also presented good results for the slab specimens with a percentage tension reinforcement of 1.13%. The discussions in Chapter 3 support these observations.

7.3 Recommendations

From the different discussions presented in the study, the following recommendations are presented:

- Three parameters were identified as guidance tools to determine which deflection method will predict a more accurate deflection. The parameters include the M_a/M_{cr} ratio, the stiffening ratio I_g/I_{cr} and the percentage tension reinforcement (ρ). Several parameter conditions are presented to suggest appropriate deflection prediction methods when the slab under investigation falls within these ranges.

PARAMETER CONDITION 1: $M_a/M_{cr} \leq 1.0$

The slender member behaves linearly thus any of the methods may be used to predict the deflections, with the exception of the BS 8110 (1997) method.

PARAMETER CONDITION 2: $1.0 < M_a/M_{cr} \leq 2.0$, $\rho \leq 1.0$ %, $I_g/I_{cr} > 3$

For a flat slab that falls within this category, the ACI 318 (2002) and the SABS 0100-1 (2000) present the most effective methods of deflection prediction. This also applies to one-way spanning slabs. When the percentage tension falls below 0.4%, then the EC2 (2004) is the more effective method of deflection prediction for one-way spanning slabs.

PARAMETER CONDITION 3: $M_a/M_{cr} > 2.0$, $\rho > 1.0$%, $I_g/I_{cr} < 3$

For these conditions the ACI 318 (2002), the SABS 0100-1 (2000) and the EC2 (2004) provide good deflection predictions.

It should be noted that in all cases the BS 8110 (1997) is not recommended and always over-predict deflection results.

- It is recommended that the method of the SAB S0100-1 (2000) be considered as the most conservative approach. The EC2 (2004) span/depth ratio is not to be used for a span/depth ratio evaluation for flat slabs with $\rho \leq 1.0$%.

  It should however be noted that if the slab narrowly passes the span/depth ratio evaluation, it is necessary to calculate the deflection with the preferred method and compare it to the allowable deflection limit from the design standard, such as the span/250 limit.

- There is also no real indication from the experimental data which part of the total deflection occurred due to long-term shrinkage effects. It is therefore not clear which part of the deflection prediction methods does not predict the actual deflection effectively. It is suggested that more effective means of time-dependent deflection recording be developed to evaluate which part of the total deflection (long-term and shrinkage deflection) is not effectively accounted for using empirical expressions.

- The residual deflection after unloading is not accounted for by the deflection prediction methods and the deflection beyond the point of maximum loading cannot effectively be predicted. Therefore, the deflection prediction methods are not effective in accounting for the deflection behaviour of flat slab structures with many excessive variations within the loading history.

- The excessive loading variations are, however, of importance if the slab was exposed to accidental overloading for short periods of time during the structure life. The additional loss of stiffness due to the peak loads, are not accounted for by the deflection prediction methods presented in this study. More research is required on how to account for such slab overloading.

- It is also observed that the predicted point of first cracking varies between the different empirical deflection methods. Further investigation on the topic is required.

- It is evident from this study that an adequate finite element approach is required to accurately account for the elasto-plastic behaviour of a flat slab structure. Both the localised phenomena, such as tension stiffening and shrinkage restraint should be accounted for.

- There is a need to study the effects of construction procedures, such as curing and de-propping, on the serviceability of flat slab structures. If it is observed that the construction methods are a prominent influence of the slab serviceability, specific construction regulations need to be employed to reduce these effects. Alternatively, a more rigorous deflection prediction method should be suggested that incorporates the effects of the construction procedure into the deflection prediction methods.

8 REFERENCES

1. Ahmed, M., Dad Khan, M.K. & Warniq, M. 2008. Effect of Concrete Cracking on the Lateral Response of RCC Buildings. *Asian Journal of Civil Engineering (Building and Housing),* 9(1): 25 – 34.
2. *American Concrete Institute (ACI) 318-02*. 2002. Building Code Requirements for Structural Concrete, American Concrete Institute, United States.
3. Bailey, C.G. 2001. Membrane Action of Unrestrained Lightly Reinforced Concrete Slabs at Large Displacements. *Engineering Structures 23*: 470 – 483.
4. Bailey, C.G., Toh, W.S. & Chan, B.M. 2008. Simplified and Advanced Analysis of Membrane Action of Concrete Slabs. *ACI Structural Journal*: 30 – 40.
5. Bangash, M.Y.H. 1989. *Concrete and Concrete Structures: Numerical Modelling and Applications*. London: Elsevier Science Publishers Ltd.
6. Barr, B.I.G., Howells, R.W. & Lark R.J. 2004. A Sensitivity Study of Parameters Used in Shrinkage and Creep Prediction Models. *Magazine of Concrete Research* 57(10): 589 – 602.
7. Beeby, A.W. & Scott, R.H. 2006. Mechanisms of Long-Term Decay of Tension Stiffening. *Magazine of Concrete Research,* 58(5): 255 – 266.
8. Beeby, A.W., Scott, R.H. & Jones A.E.K. 2005. Revised Code Provisions for Long-Term Deflection Calculations. *Proceedings of the Institution of Civil Engineers, Structures & Buildings 158*, SBI: 71 – 75.
9. Bischoff, P.H. 2005. Re-evaluation of Deflection Prediction for Concrete Beams Reinforced with Steel and Fiber Reinforced Polymer Bars. *ASCE Journal of Structural Engineering,* 131(5): 752 – 767.
10. Bischoff, P.H. 2007. Rational Model for Calculating Deflection of Reinforced Concrete Beams and Slabs. *Canadian Journal of Civil Engineering*, 34: 992 – 1002.
11. Bischoff, P.H. 2008. Discussion of "Tension Stiffening in Lightly Reinforced Concrete Slabs" by R.I. Gilbert. *ASCE Journal of Structural Engineering,* 134(7): 1259 – 1260.
12. Branson, D.E. 1977. *Deformation of Concrete Structures. United States of America*. McGraw-Hill International Book Company.
13. *British Standards 8110: Structural Use of Concrete: Part 1: 1997*. Code of Practice for Design and Construction, British Standards Institute, London.
14. Burns, C., Seelhofer, H. & Marti, P.M. 2008. Discussion if "Tension Stiffening in Lightly Reinforced Concrete Slabs" by R.I Gilbert. *ASCE Journal of Structural Engineering*: 1262 – 1264.

15. Divakar, M.P. & Dilger, W.H. 1988. Analysis of Shrinkage Deformation in Concrete Structures. *Sädhanä*, 12(4): 307 – 320.
16. *EN 1992-1-1 European Standards, Eurocode 2*. 2004. Design of Concrete Structures, Part 1-1: General Rules and Rules for Buildings, British Standards Institute, London.
17. Fanourakis, G.C. & Ballim, Y. 2003. Predicting Creep Deformation of Concrete: A Comparison of Results from Different Investigations. *Proceedings, 11th FIG Symposium of Deformation Measurement*. Greece: Santorini
18. Fanourakis, G.C. & Ballim, Y. 2006. An Assessment of the Accuracy of Nine Design Models for Predicting Creep in Concrete. *Journal of the South African Institution of Civil Engineering*, 48(5): 2 – 8.
19. Gilbert, R.I. & Guo, X.H. 2005. Time-Dependent Deflection and Deformation of Reinforced Concrete Flat Slabs – An Experimental Study. *ACI Structural Journal*, 102(3): 363 – 373.
20. Gilbert, R.I. 1999. Deflection Calculation for Reinforced Concrete Structures – Why We Sometimes Get It Wrong. *ACI Structural Journal*, 96(6): 1027 – 1032.
21. Gilbert, R.I. 2001. Shrinkage, Cracking and Deflection - The Serviceability of Concrete Structures. *Electronic Journal of Structural Engineering*, 1(1).
22. Gilbert, R.I. 2007. Tension Stiffening in Lightly Reinforced Concrete Slabs. *ASCE Journal of Structural Engineering*, 113(6): 899 – 903.
23. Gilbert, R.I. 2008. Closure to “Tension Stiffening in Lightly Reinforced Concrete Slabs” by R.I. Gilbert. *ASCE Journal of Structural Engineering*: 1264 – 1265.
24. Goto, Y. 1971. Cracks formed in Concrete around Deformed Tension Bars. *Journal of the American Concrete Institute*, 68(4): 244 – 251.
25. Hill, G. 2009. E-mail Communication with Strand7 Support, e-mail to Strand7 Support [Online]. 26 March. Available e-mail: supports@strand7.com.
26. Illston, J.M. & Domone, P.L.J. 2001. *Construction Materials: their Nature and Behaviour – 3rd Edition*. Great Britain: Spon Press – Taylor & Francis Group
27. Jones, A.E.K. & Morrison, J. 2005. Flat Slab Design: Past, Present and Future. *Proceedings of the Institution of Civil Engineers, Structures & Buildings*, 158(SB2): 133 – 140.
28. Kaklauskas, G., Gribniak, V. & Bacinskas, D. 2007. Discussion of “Tension Stiffening in Lightly Reinforced Concrete Slabs” by R.I. Gilbert. *ASCE Journal of Structural Engineering*: 1261 – 1262.
29. Kara, I.F. & Dundar, C. 2009. Effect of Loading Types and Reinforcement Ratio on an Effective Moment of inertia and Deflection of a Reinforced Concrete Beam. *Advances in Engineering Software 40*: 836 – 846.

30. Kong, F.K. & Evans, R.H. 1987. *Reinforced and Prestressed Concrete – Third Edition*. United Kingdom: Spon Press of the Taylor and Francis Group.
31. L&s Consulting (Pty.) Ltd. Structural & Civil Engineers. 2008. Maerua Mall: Windhoek, Structural Assessment of Basement Parking Slab. 5 September. Bryanstan, South Africa.
32. Maaddawy, T.E., Soudki, K. & Topper, T. 2005. Analytical Model to Predict Nonlinear Flexural Behaviour of Corroded Reinforced Concrete Beams. *American Concrete Institute, Structural Journal*, 102(4): 550 – 559.
33. Maritz, J. 2009. Deflections of Reinforced Concrete Elements. Thesis Nr. S34-2009. Unpublished dissertation. Stellenbosch: University of Stellenbosch, Structural Engineering Department.
34. Mazloom, M. 2008. Estimating Long-Term Creep and Shrinkage of High-Strength Concrete. *Cement and Concrete Composites 30*: 316 – 326.
35. Montgomery, D.C. & Runger, G.C. 2003. Applied Statistics and Probability for Engineers – 3rd Edition. United States of America: John Wiley & Sons, Inc.
36. Pillai, S.U. & Menon, D. 2003. *Reinforced Concrete Design – 2nd Edition*. New Delhi: Tata McGraw Hill.
37. PROKON. 2008. Edition W2.4.12 – 27 November 2008, South Africa, PROKON Software Consultants Ltd.
38. Raz, S.A. 2001. *Analytical Methods in Structural Engineering - 2nd Edition*. New Age International
39. Robberts, J.M. & Marshall, V. 2008. *Analysis and Design of Concrete Structures*. South Africa: School of Concrete Technology, Cement & Concrete Institute.
40. Scanlon, A. & Bischoff, P.H. 2008. Shrinkage Restraint and Loading History Effects on Deflections of Flexural Members, *ACI Structural Journal*: 498 – 506.
41. Scott, R.H. & Beeby, A.W. 2005. Long-Term Tension-Stiffening Effects in Concrete. *ACI Structural Journal*: 31 – 39.
42. *South African Bureau of Standards (SABS) 0100-1. 1992*. The Structural Use of Concrete – Part 1: Design, South African Bureau of Standards, Pretoria.
43. *Strand 7 Application Programming Interface Manual – Edition 6a* [Online]. Available: http://www.strand7.com [2005, January]
44. Strand 7. 2005. Edition 69. Release 2.3. Sydney, Australia, Strand7 Pty. Ltd.
45. Taylor, J.P. 2009. *The Deflection of Reinforced Concrete* [Online]. Available: http://www.tlbengineers.com [2009, April].

46. Taylor, P.J. & Heiman, J.L. 1977. Long-Term Deflection of Reinforced Concrete Flat Slabs and Plates. *ACI Journal*: 556 – 561.
47. Update to specifiers regarding BS 8110, Eurocode 2 and Building Regulations. [Online]. Available: http://www.eurocode2.info [2009, August 17].
48. Varghese, P.C. 2005. Advanced Reinforced Concrete Design – 2nd Edition. India: Prentice-Hall of India.
49. Vollum, R.L. & Hossain, T.R. 2002. Are Existing Span-to-Depth Rules Conservative for Flat Slabs?. *Magazine of Concrete Research*, 54(6): 411 – 421.
50. Vollum, R.L. 2002. Influences of Shrinkage and Construction Loading on Loss of Tension Stiffening in Slabs. *Magazine of Concrete Research,* 54(4): 273 – 282.
51. Vollum, R.L. 2003. Multipliers for Deflections in Reinforced Concrete Flat Slabs. *Magazine of Concrete Research*, 55(2): 95 – 104.
52. Vollum, R.L. 2009. Comparison of deflection calculations and span-to-depth ratios in BS 8110 and Eurocode 2. *Magazine of Concrete Research*, 61(6): 465 – 476.

Webster, R. & Brooker, O. 2006. *How to Design Concrete Structures using Eurocode 2*. United Kingdom: The Concrete Centre and British Cement Association.

APPENICES

Estée M. Eigelaar

Appendices part of the thesis “Deflections of Reinforced Concrete Flat Slabs”

Supervisor: Professor J.A. Wium

Date of Award: March 2010

TABLE OF CONTENTS

APPENDIX A

In this appendix the derivation of the deflection calculation equation using the two moment curvature theorems are presented and discussed.

As apparent from the discussions in Chapter 2, the difficulties concerning the calculation of deflections of concrete beams arise from the uncertainties regarding the flexural stiffness EI and the effects of creep and shrinkage. The Moment-Area Theorem expresses the slopes and deflections of a bending member in term of the properties of the M/EI diagram. For flexural elastic members, the quantity M/EI is equal to the curvature 1/r for each of application. The Moment-Area Theorem is rephrased as the Curvature-Area Theorem (Kong & Evans, 1987). The two Moment-Area Theorems (Curvature-Area Theorems) may often be used in easily evaluating structural deformation. These are formulated as follows:

Moment-Area Theorem I: *The change of slope between any two points on a deflected beam is given by the area of the M/EI-diagram between them* (Raz, 2001).

Here M denotes the bending moment, E the modulus of elasticity and I the moment of inertia of the beam cross section. In an elastic element, E and I are constant over the beam length so that the M/EI-diagram is obtained by dividing the moment by EI. If the moment of inertia varies along the length, the moments are divided by EI-values corresponding to their respective positions on the beam.

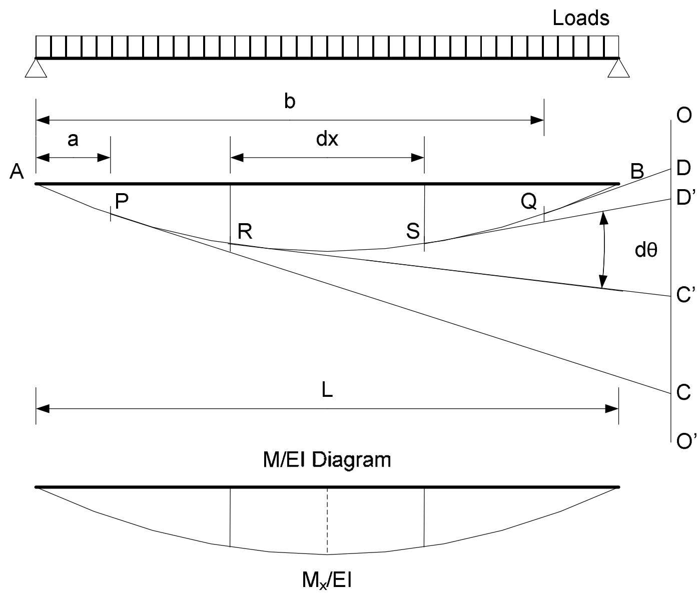

Figure A-1: Moment-Area Theorem based on a simply-supported, uniformly loaded beam (Raz, 2001).

Figure A-1 shows a beam AB subjects to a system of loads. The corresponding M/EI-diagram is indicated below. Let the tangents at the points P and Q on the deflected beam be inclined at θ_p and θ_q respectively to the horizontal so that $\theta = (\theta_p - \theta_q)$ is the change in slope between P and Q. Let $d\theta$ be the angle between the tangents at the two points R and S as shown in the figure.

If I_x and M_x denote the sectional moment of inertia and the bending moment respectively at R then:

$$d\theta = \frac{M_x}{EI_x} dx \tag{A-1}$$

Integrating the above expression between P and Q:

$$\int_P^Q d\theta = \int_a^b \frac{M_x}{EI_x} dx \tag{A-2}$$

therefore $(\theta_P - \theta_Q) = \theta$ = Area of the M/EI-diagram between P and Q.

Moment Area Theorem II: *The vertical intercept by tangents at any two points of a deflected beam on a vertical line through a point O in its plane is given by the moment of the area of the M/EI-diagram between those points about O* (Raz, 2001).

Consider the beam in Figure A-1. Let OO' be a vertical line through an arbitrary point O in the plane of the beam and let CD be the intercept on OO' by the tangents at R and S, i.e. C'D' is given by the following expression:

$$C'D' = xd\theta = x\frac{M_x}{EI_x}dx \quad \text{(A-3)}$$

Integrating the above expression between P and Q:

$$\int_P^Q xd\theta = \int_a^b \frac{xM_x}{EI_x}dx \quad \text{(A-4)}$$

therefore CD = Moment of the area of the M/EI-diagram between P and Q about O.

For estimating the deflections of concrete structures, the Curvature-Area Theorems have distinct advantages over the conventional Moment-Area Theorems (Kong & Evans, 1987)(Varghese, 2005):

- Unlike the Moment-Area Theorems, the Curvature-Area Theorems express the purely geometrical relations between the slopes, θ, the deflections Δ and the curvature 1/r. Since the relations are purely geometrical, their validity is independent of the mechanical properties of the materials. That is, the Curvature-Area Theorems are equally applicable irrespective of whether the structure is elastic, plastic or elasto-plastic.

- Unlike the Moment-Area Theorems, the Curvature-Area theorems can be used even where the deformations are caused by other effects than bending moments, for example shrinkage and creep. Once the curvatures are known, the slopes and deflections are completely defined by the Curvature-Area Theorems. Whether the curvatures have been caused by bending moment or by shrinkage and creep does not affect the results.

Applying the Moment-Area Theorems the following equation for deflection may be obtained (Kong & Evans, 1987):

Refer to Figure 2-4, Chapter 2 for the equivalent section from a cracked concrete section where the bending formula is applicable:

$$f_c = \frac{M}{I_x} x \qquad \text{(A-5)}$$

Where f_c is the concrete stress at a distance x from the neutral axis, M is the bending moment acting on the section and I_x is the moment of inertia of the (equivalent) section. If r is the radius of curvature of the beam at the section under consideration, then the curvature 1/r is immediately obtained from the strain diagram as shown in Figure 2-4, Chapter 2.

$$\frac{1}{r} = \frac{\varepsilon_c}{x} \qquad \text{(A-6)}$$

Substituting Equation A-5 into Equation A-6, and noting that $\varepsilon_c = f_c / E_c$, we have

$$\frac{1}{r} = \frac{M}{E_c I_x} \qquad \text{(A-7)}$$

Deflections may be calculated directly from Equation A-7 by calculations of the curvatures at successive sections along the element and the use of a numerical integration technique such as that proposed by Newmark. Alternatively, it is shown that a simplified approach may be used. The deflection is calculated using Equation A-8.

$$\Delta = KL^2 \frac{M}{E_c I_e} = KL^2 \frac{1}{r} \qquad \text{(A-8)}$$

where K is the deflection coefficient dependent on the bending moment diagram, L is the effective span of the member, M the applied moment, E_c is the modulus of elasticity of the member, I_e is the effective moment of inertia, and 1/r refers to the curvature.

APPENDIX B

Calculations for the short-term moment-deflection response for a section with a percentage tension reinforcement of 0.84% for the various design standard methods are presented in this appendix. Similar equations were used for section with different dimensions and percentage tension reinforcements.

Also, the calculations to obtain the values for the allowable and actual span/effective depth ratios are presented for the various design standard approaches.

Data obtianed from Article: "Tension Stiffening in Lightly Reinforced Concrete Slabs" by R.I. Gilbert
Journal of Structural Engineering (ASCE) June 2007

SLAB: Z4

Calculation of the Immediate Deflection according to SABS 0100-1, clause A.2.4

Slab Panel Parameters:

Material Properties:

f'_c = 48.4 MPa
f_c = 60.50 MPa
f_t = 4.04 MPa
E_c = 30.5 GPa

Wide Beam:

b = 850.0 mm
L = 2000.0 mm
d = 79.0 mm
d' = 21.0 mm
h = 100.0 mm

Modulus of Rupture: (for unrestrained slabs)

$$f_r = 0.65\sqrt{f_c}$$

f_r = 5.06 MPa

Cracking Moment:

$$M_{cr} = \frac{f_r I_g}{y_t}$$

I_g = 7.1E+07 mm^4
y_t = 50.0 mm
M_{cr} = 7.16 kNm

Momenf of Inertia of Cracked Section: Equations used

x_{cr} for the Cracked Condition	I_{cr} for the Cracked Condition	Modular Ratio
$x_{cr\_1} = \dfrac{\frac{1}{2}x_{cr\_2}^{2}b + A_s d\alpha_e}{x_{cr\_2}b + A_s\alpha_e}$ where $x_{cr\_1} = x_{cr\_2}$	$I_{cr} = \frac{1}{3}bx_{cr}^{3} + A_s(d - x_{cr})^2\alpha_e$	$\alpha_e = \dfrac{E_s}{E_c}$

ρ	[%]	0.18	0.29	0.52	0.84	0.90	1.10	1.30	1.50	1.70	1.90	2.10	2.30	2.50	2.70	2.90	3.10
x_{cr_1}	[mm]	11.2	14.0	18.1	22.3	22.9	24.9	26.6	28.1	29.5	30.8	32.0	33.1	34.1	35.1	36.0	36.8
b	[mm]	850.0	850.0	850.0	850.0	850.0	850.0	850.0	850.0	850.0	850.0	850.0	850.0	850.0	850.0	850.0	850.0
A_s	[mm^2]	120.9	196.7	349.9	565.4	604.4	738.7	873.0	1007.3	1141.6	1275.9	1410.2	1544.5	1678.8	1813.1	1947.4	2081.7
d	[mm]	79.0	79.0	79.0	79.0	79.0	79.0	79.0	79.0	79.0	79.0	79.0	79.0	79.0	79.0	79.0	79.0
E_s	[GPa]	200.0	200.0	200.0	200.0	200.0	200.0	200.0	200.0	200.0	200.0	200.0	200.0	200.0	200.0	200.0	200.0
E_c	[GPa]	30.5	30.5	30.5	30.5	30.5	30.5	30.5	30.5	30.5	30.5	30.5	30.5	30.5	30.5	30.5	30.5
α_e	[-]	6.6	6.6	6.6	6.6	6.6	6.6	6.6	6.6	6.6	6.5	6.6	6.6	6.6	6.6	6.6	6.6
x_{cr_2}	[mm]	11.2	14.0	18.1	22.3	22.9	24.8	26.6	28.1	29.5	30.8	32.0	33.1	34.1	35.1	36.0	36.8
I_{cr}	[mm^4]	4.0E+06	6.2E+06	1.0E+07	1.5E+07	1.6E+07	1.9E+07	2.1E+07	2.3E+07	2.6E+07	2.8E+07	3.0E+07	3.2E+07	3.3E+07	3.5E+07	3.7E+07	3.8E+07

I_e for Partially Cracked Condition	Immediate Curvature $1/r_i$
$I_e = \left(\dfrac{M_{cr}}{M_a}\right)^3 I_g + \left[1 - \left(\dfrac{M_{cr}}{M_a}\right)^3\right] I_{cr} \leq I_g$	$\dfrac{1}{r_i} = \dfrac{M_a}{E_c I_e}$

ρ [%]		0.18		0.293		0.521		0.84		0.9		1.1		1.3		1.5	
M_{cr}/M_a	M_a/M_{cr}	I_e	$1/r_i$	I_e	$1/r_i$	I_e	$1/r_i$	I_e	$1/r_i$	I_e	$1/r_i$	I_e	$1/r_i$	I_e	$1/r_i$	I_e	$1/r_i$
[-]	[-]	[mm^4]	[10^6 mm^{-1}]	[mm^4]	[10^6 mm^{-1}]	[mm^4]	[10^6 mm^{-1}]	[mm^4]	[10^6 mm^{-1}]	[mm^4]	[10^6 mm^{-1}]	[mm^4]	[10^6 mm^{-1}]	[mm^4]	[10^6 mm^{-1}]	[mm^4]	[10^6 mm^{-1}]
5.00	0.20	7.1E+07	0.7	7.1E+07	0.7	7.1E+07	0.7	7.1E+07	0.7	7.1E+07	0.7	7.1E+07	0.7	7.1E+07	0.7	7.1E+07	0.7
2.50	0.40	7.1E+07	1.3	7.1E+07	1.3	7.1E+07	1.3	7.1E+07	1.3	7.1E+07	1.3	7.1E+07	1.3	7.1E+07	1.3	7.1E+07	1.3
1.67	0.60	7.1E+07	2.0	7.1E+07	2.0	7.1E+07	2.0	7.1E+07	2.0	7.1E+07	2.0	7.1E+07	2.0	7.1E+07	2.0	7.1E+07	2.0
1.25	0.80	7.1E+07	2.7	7.1E+07	2.7	7.1E+07	2.7	7.1E+07	2.7	7.1E+07	2.7	7.1E+07	2.7	7.1E+07	2.7	7.1E+07	2.7
1.00	1.00	7.1E+07	3.3	7.1E+07	3.3	7.1E+07	3.3	7.1E+07	3.3	7.1E+07	3.3	7.1E+07	3.3	7.1E+07	3.3	7.1E+07	3.3

0.83	1.20	4.3E+07	6.6	4.4E+07	6.5	4.5E+07	6.2	4.7E+07	6.0	4.8E+07	5.9	4.9E+07	5.8	5.0E+07	5.7	5.1E+07	5.5
0.71	1.40	2.8E+07	11.6	3.0E+07	11.0	3.2E+07	10.2	3.5E+07	9.3	3.6E+07	9.2	3.8E+07	8.7	3.9E+07	8.4	4.1E+07	8.1
0.63	1.60	2.0E+07	18.5	2.2E+07	17.1	2.5E+07	15.0	2.9E+07	13.1	2.9E+07	12.8	3.1E+07	12.0	3.3E+07	11.3	3.5E+07	10.7
0.56	1.80	1.5E+07	27.3	1.7E+07	24.4	2.1E+07	20.5	2.5E+07	17.2	2.5E+07	16.7	2.8E+07	15.4	3.0E+07	14.3	3.2E+07	13.4
0.50	2.00	1.2E+07	37.9	1.4E+07	32.8	1.8E+07	26.4	2.2E+07	21.3	2.3E+07	20.6	2.5E+07	18.7	2.7E+07	17.2	2.9E+07	16.0
0.45	2.20	1.0E+07	50.1	1.2E+07	42.0	1.6E+07	32.5	2.0E+07	25.5	2.1E+07	24.6	2.3E+07	22.0	2.6E+07	20.1	2.8E+07	18.5
0.42	2.40	8.9E+06	63.5	1.1E+07	51.7	1.5E+07	38.7	1.9E+07	29.5	2.0E+07	28.4	2.2E+07	25.2	2.5E+07	22.9	2.7E+07	21.0
0.38	2.60	7.8E+06	77.9	9.9E+06	61.6	1.4E+07	44.8	1.8E+07	33.5	1.9E+07	32.1	2.2E+07	28.4	2.4E+07	25.6	2.6E+07	23.4
0.36	2.80	7.1E+06	92.8	9.2E+06	71.7	1.3E+07	50.8	1.8E+07	37.4	1.8E+07	35.8	2.1E+07	31.4	2.3E+07	28.2	2.6E+07	25.7
0.33	3.00	6.5E+06	108.1	8.6E+06	81.7	1.2E+07	56.7	1.7E+07	41.1	1.8E+07	39.3	2.0E+07	34.4	2.3E+07	30.8	2.5E+07	28.0
0.31	3.20	6.1E+06	123.6	8.2E+06	91.6	1.2E+07	62.4	1.7E+07	44.8	1.8E+07	42.8	2.0E+07	37.3	2.3E+07	33.3	2.5E+07	30.2
0.29	3.40	5.7E+06	139.1	7.9E+06	101.4	1.2E+07	68.1	1.6E+07	48.4	1.7E+07	46.2	2.0E+07	40.2	2.2E+07	35.8	2.5E+07	32.4
0.28	3.60	5.5E+06	154.5	7.6E+06	111.0	1.1E+07	73.6	1.6E+07	52.0	1.7E+07	49.6	2.0E+07	43.0	2.2E+07	38.2	2.4E+07	34.6

ρ [%]		1.7		1.9		2.1		2.3		2.5		2.7		2.9		3.1	
M_{cr}/M_a [-]	M_a/M_{cr} [-]	I_e [mm^4]	$1/r_i$ [10^6 mm^{-1}]	I_e [mm^4]	$1/r_i$ [10^6 mm^{-1}]	I_e [mm^4]	$1/r_i$ [10^6 mm^{-1}]	I_e [mm^4]	$1/r_i$ [10^6 mm^{-1}]	I_e [mm^4]	$1/r_i$ [10^6 mm^{-1}]	I_e [mm^4]	$1/r_i$ [10^6 mm^{-1}]	I_e [mm^4]	$1/r_i$ [10^6 mm^{-1}]	I_e [mm^4]	$1/r_i$ [10^6 mm^{-1}]
5.00	0.20	7.1E+07	0.7	7.1E+07	0.7	7.1E+07	0.7	7.1E+07	0.7	7.1E+07	0.7	7.1E+07	0.7	7.1E+07	0.7	7.1E+07	0.7
2.50	0.40	7.1E+07	1.3	7.1E+07	1.3	7.1E+07	1.3	7.1E+07	1.3	7.1E+07	1.3	7.1E+07	1.3	7.1E+07	1.3	7.1E+07	1.3
1.67	0.60	7.1E+07	2.0	7.1E+07	2.0	7.1E+07	2.0	7.1E+07	2.0	7.1E+07	2.0	7.1E+07	2.0	7.1E+07	2.0	7.1E+07	2.0
1.25	0.80	7.1E+07	2.7	7.1E+07	2.7	7.1E+07	2.7	7.1E+07	2.7	7.1E+07	2.7	7.1E+07	2.7	7.1E+07	2.7	7.1E+07	2.7
1.00	1.00	7.1E+07	3.3	7.1E+07	3.3	7.1E+07	3.3	7.1E+07	3.3	7.1E+07	3.3	7.1E+07	3.3	7.1E+07	3.3	7.1E+07	3.3
0.83	1.20	5.2E+07	5.4	5.3E+07	5.4	5.4E+07	5.3	5.4E+07	5.2	5.5E+07	5.1	5.6E+07	5.0	5.7E+07	5.0	5.7E+07	4.9
0.71	1.40	4.2E+07	7.8	4.3E+07	7.6	4.5E+07	7.4	4.6E+07	7.2	4.7E+07	7.0	4.8E+07	6.8	4.9E+07	6.7	5.0E+07	6.5
0.63	1.60	3.7E+07	10.3	3.8E+07	9.8	4.0E+07	9.5	4.1E+07	9.1	4.3E+07	8.8	4.4E+07	8.6	4.5E+07	8.3	4.6E+07	8.1
0.56	1.80	3.3E+07	12.7	3.5E+07	12.0	3.7E+07	11.5	3.8E+07	11.0	4.0E+07	10.6	4.1E+07	10.2	4.3E+07	9.9	4.4E+07	9.6
0.50	2.00	3.1E+07	15.0	3.3E+07	14.2	3.5E+07	13.5	3.7E+07	12.9	3.8E+07	12.3	4.0E+07	11.9	4.1E+07	11.4	4.2E+07	11.1
0.45	2.20	3.0E+07	17.3	3.2E+07	16.3	3.4E+07	15.4	3.5E+07	14.6	3.7E+07	14.0	3.9E+07	13.4	4.0E+07	12.9	4.1E+07	12.5
0.42	2.40	2.9E+07	19.5	3.1E+07	18.3	3.3E+07	17.2	3.4E+07	16.4	3.6E+07	15.6	3.8E+07	14.9	3.9E+07	14.3	4.1E+07	13.8
0.38	2.60	2.8E+07	21.7	3.0E+07	20.2	3.2E+07	19.1	3.4E+07	18.0	3.6E+07	17.2	3.7E+07	16.4	3.9E+07	15.8	4.0E+07	15.2
0.36	2.80	2.8E+07	23.8	3.0E+07	22.2	3.2E+07	20.8	3.3E+07	19.7	3.5E+07	18.7	3.7E+07	17.9	3.8E+07	17.1	4.0E+07	16.5
0.33	3.00	2.7E+07	25.8	2.9E+07	24.0	3.1E+07	22.6	3.3E+07	21.3	3.5E+07	20.2	3.6E+07	19.3	3.8E+07	18.5	4.0E+07	17.8
0.31	3.20	2.7E+07	27.8	2.9E+07	25.9	3.1E+07	24.3	3.3E+07	22.9	3.5E+07	21.7	3.6E+07	20.7	3.8E+07	19.8	3.9E+07	19.1
0.29	3.40	2.7E+07	29.8	2.9E+07	27.7	3.1E+07	26.0	3.3E+07	24.5	3.4E+07	23.2	3.6E+07	22.1	3.8E+07	21.2	3.9E+07	20.3
0.28	3.60	2.7E+07	31.8	2.9E+07	29.5	3.1E+07	27.6	3.2E+07	26.1	3.4E+07	24.7	3.6E+07	23.5	3.8E+07	22.5	3.9E+07	21.6

Uncracked Condition			
M_{cr}/M_a [-]	M_a/M_{cr} [-]	I_g [mm^4]	$1/r_i$ [10^6 mm^{-1}]
5.00	0.20	7.1E+07	0.7
2.50	0.40	7.1E+07	1.3
1.67	0.60	7.1E+07	2.0
1.25	0.80	7.1E+07	2.7
1.00	1.00	7.1E+07	3.3
0.83	1.20	7.1E+07	4.0
0.71	1.40	7.1E+07	4.6
0.63	1.60	7.1E+07	5.3
0.56	1.80	7.1E+07	6.0
0.50	2.00	7.1E+07	6.6
0.45	2.20	7.1E+07	7.3
0.42	2.40	7.1E+07	8.0
0.38	2.60	7.1E+07	8.6
0.36	2.80	7.1E+07	9.3
0.33	3.00	7.1E+07	9.9
0.31	3.20	7.1E+07	10.6
0.29	3.40	7.1E+07	11.3
0.28	3.60	7.1E+07	11.9

Experimental Behaviour: Gilbert 2007 (Tension Stiffening in Lightly Reinforced Concrete Slabs)

ρ = 0.842 %

M_{cr} = 6.05 kNm

For simpel supported one-way slab

K = 0.104

M_{cr}/M_a [-]	M_a/M_{cr} [-]	Δ [mm]	I_e [mm^4]	$1/r_i$ [10^6 mm^{-1}]
0.91	1.1	2.38	3.8E+07	5.7
0.83	1.2	3.45	2.9E+07	8.3
0.77	1.3	4.15	2.6E+07	10.0

Immediate Curvature $1/r_i$	I_e for Partially Cracked Condition
$\frac{1}{r_i} = \frac{\Delta}{KL^2}$	$I_e = \frac{M_a}{E_c \frac{1}{r_i}}$

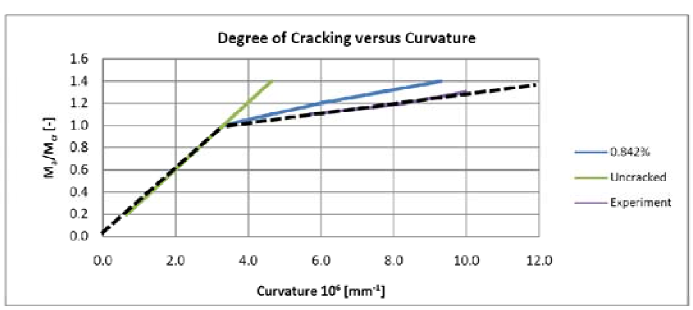

Data obtianed from Article: "Tension Stiffening in Lightly Reinforced Concrete Slabs" by R.I. Gilbert
Journal of Structural Engineering (ASCE) June 2007

SLAB: Z4

Calculation of the Immediate Deflection according to Eurocode 2, Section 7.4

Slab Panel Parameters:

Material Properties:	f'_c =	48.4 MPa
	f_c =	60.50 MPa
	f_t =	4.04 MPa
	E_c =	30.5 GPa
Wide Beam:	b =	850.0 mm
	L =	2000.0 mm
	d =	79.0 mm
	d' =	21.0 mm
	h =	100.0 mm

Momenf of Inertia for a Partailly Cracked Section: Equation used

x_u for the Uncracked Condition	I_u for the Uncracked Condition	Modular Ratio
$x_u = \dfrac{\frac{bh^2}{2} + (\alpha_e - 1)(A_s d + A'_s d')}{bh + (\alpha_e - 1)(A_s + A'_s)}$	$I_u = \dfrac{bh^3}{12} + bh\left(\dfrac{h}{2} - x_u\right)^2 + (\alpha_e - 1)\left[A_s(d - x_u)^2 + A'_s(x_u - d')^2\right]$	$\alpha_e = \dfrac{E_s}{E_c}$

x_{cr} for the Cracked Condition	I_{cr} for the Cracked Condition	Cracking Moment
$\omega = A_s\alpha_e + A'_s(\alpha_e - 1)$ $x_{cr} = \left\{\left[\omega^2 + 2b(A_s d\alpha_e + A'_s d'(\alpha_e - 1))\right]^{0.5} - \omega\right\}/b$	$I_{cr} = \dfrac{bx_{cr}^3}{3} + \alpha_e A_s (d - x_{cr})^2 + (\alpha_e - 1)A'_s(d' - x_{cr})^2$	$M_{cr} = \dfrac{f_t I_u}{h - x_u}$

ρ	[%]	0.18	0.29	0.52	0.84	0.90	1.10	1.30	1.50	1.70	1.90	2.10	2.30	2.50	2.70	2.90	3.10
b	[mm]	850.0	850.0	850.0	850.0	850.0	850.0	850.0	850.0	850.0	850.0	850.0	850.0	850.0	850.0	850.0	850.0
h	[mm]	100.0	100.0	100.0	100.0	100.0	100.0	100.0	100.0	100.0	100.0	100.0	100.0	100.0	100.0	100.0	100.0
A_s	[mm^2]	120.9	196.7	349.9	565.4	604.4	738.7	873.0	1007.3	1141.6	1275.9	1410.2	1544.5	1678.8	1813.1	1947.4	2081.7
d	[mm]	79.0	79.0	79.0	79.0	79.0	79.0	79.0	79.0	79.0	79.0	79.0	79.0	79.0	79.0	79.0	79.0
E_s	[GPa]	200.0	200.0	200.0	200.0	200.0	200.0	200.0	200.0	200.0	200.0	200.0	200.0	200.0	200.0	200.0	200.0
E_c	[GPa]	30.5	30.5	30.5	30.5	30.5	30.5	30.5	30.5	30.5	30.5	30.5	30.5	30.5	30.5	30.5	30.5
α_e	[-]	6.6	6.6	6.6	6.6	6.6	6.6	6.6	6.6	6.6	6.6	6.6	6.6	6.6	6.6	6.6	6.6
x_u	[mm]	50.2	50.4	50.6	51.0	51.1	51.3	51.6	51.8	52.0	52.2	52.4	52.7	52.9	53.1	53.3	53.5
I_u	[mm^4]	7.1E+07	7.2E+07	7.2E+07	7.3E+07	7.4E+07	7.4E+07	7.5E+07	7.5E+07	7.6E+07	7.6E+07	7.7E+07	7.7E+07	7.8E+07	7.8E+07	7.9E+07	7.9E+07
ω	[mm^2]	792.6	1290.2	2294.1	3707.6	3963.0	4843.6	5724.3	6604.9	7485.6	8366.2	9246.9	10127.5	11008.2	11888.9	12769.5	13650.2
x_{cr}	[mm]	11.2	14.0	18.1	22.3	22.9	24.8	26.6	28.1	29.5	30.8	32.0	33.1	34.1	35.1	36.0	36.8
I_{cr}	[mm^4]	4.0E+06	6.2E+06	1.0E+07	1.5E+07	1.6E+07	1.9E+07	2.1E+07	2.3E+07	2.6E+07	2.8E+07	3.0E+07	3.2E+07	3.3E+07	3.5E+07	3.7E+07	3.8E+07
M_{cr}	[kNm]	5.8	5.8	5.9	6.1	6.1	6.2	6.2	6.3	6.4	6.5	6.5	6.6	6.7	6.8	6.8	6.9

I_e for Partially Cracked Condition	Immediate Curvature $1/r_i$
$I_e = \dfrac{I_{cr}}{1 - \left(1 - \dfrac{I_{cr}}{I_u}\right)\left(\dfrac{M_{cr}}{M_a}\right)^2}$	$\dfrac{1}{r_i} = \dfrac{M_a}{E_c I_e}$

ρ [%]		0.18		0.293		0.521		0.842		0.9		1.1		1.3		1.5	
M_{cr}/M_a	M_a/M_{cr}	I_e	$1/r_i$	I_e	$1/r_i$	I_e	$1/r_i$	I_e	$1/r_i$	I_e	$1/r_i$	I_e	$1/r_i$	I_e	$1/r_i$	I_e	$1/r_i$
[-]	[-]	[mm^4]	[$10^6\ mm^{-1}$]	[mm^4]	[$10^6\ mm^{-1}$]	[mm^4]	[$10^6\ mm^{-1}$]	[mm^4]	[$10^6\ mm^{-1}$]	[mm^4]	[$10^6\ mm^{-1}$]	[mm^4]	[$10^6\ mm^{-1}$]	[mm^4]	[$10^6\ mm^{-1}$]	[mm^4]	[$10^6\ mm^{-1}$]
5.00	0.20	7.1E+07	0.5	7.2E+07	0.5	7.2E+07	0.5	7.3E+07	0.5	7.4E+07	0.5	7.4E+07	0.5	7.5E+07	0.5	7.5E+07	0.5
2.50	0.40	7.1E+07	1.1	7.2E+07	1.1	7.2E+07	1.1	7.3E+07	1.1	7.4E+07	1.1	7.4E+07	1.1	7.5E+07	1.1	7.5E+07	1.1
1.67	0.60	7.1E+07	1.6	7.2E+07	1.6	7.2E+07	1.6	7.3E+07	1.6	7.4E+07	1.6	7.4E+07	1.6	7.5E+07	1.6	7.5E+07	1.6
1.25	0.80	7.1E+07	2.1	7.2E+07	2.1	7.2E+07	2.1	7.3E+07	2.2	7.4E+07	2.2	7.4E+07	2.2	7.5E+07	2.2	7.5E+07	2.2
1.00	1.00	7.1E+07	2.7	7.2E+07	2.7	7.2E+07	2.7	7.3E+07	2.7	7.4E+07	2.7	7.4E+07	2.7	7.5E+07	2.7	7.5E+07	2.7
0.83	1.20	1.2E+07	19.5	1.7E+07	13.5	2.5E+07	9.2	3.4E+07	7.1	3.5E+07	6.9	3.9E+07	6.3	4.2E+07	5.8	4.5E+07	5.5
0.71	1.40	7.8E+06	34.1	1.2E+07	23.0	1.8E+07	15.0	2.5E+07	11.0	2.6E+07	10.5	3.0E+07	9.4	3.3E+07	8.6	3.6E+07	8.0
0.63	1.60	6.4E+06	47.5	9.7E+06	31.6	1.5E+07	20.3	2.2E+07	14.5	2.3E+07	13.9	2.6E+07	12.3	2.9E+07	11.2	3.2E+07	10.3

0.56	1.80	5.7E+06	60.0	8.7E+06	39.7	1.4E+07	25.2	2.0E+07	17.9	2.1E+07	17.1	2.4E+07	15.0	2.7E+07	13.6	3.0E+07	12.5
0.50	2.00	5.3E+06	71.8	8.1E+06	47.4	1.3E+07	30.0	1.9E+07	21.1	2.0E+07	20.2	2.3E+07	17.7	2.6E+07	15.9	2.8E+07	14.6
0.45	2.20	5.0E+06	83.3	7.7E+06	54.9	1.2E+07	34.5	1.8E+07	24.2	1.9E+07	23.1	2.2E+07	20.2	2.5E+07	18.2	2.7E+07	16.7
0.42	2.40	4.8E+06	94.4	7.4E+06	62.1	1.2E+07	39.0	1.7E+07	27.3	1.8E+07	26.0	2.1E+07	22.7	2.4E+07	20.4	2.7E+07	18.7
0.38	2.60	4.7E+06	105.2	7.2E+06	69.1	1.2E+07	43.3	1.7E+07	30.2	1.8E+07	28.8	2.1E+07	25.1	2.4E+07	22.6	2.6E+07	20.6
0.36	2.80	4.6E+06	115.8	7.0E+06	76.0	1.1E+07	47.6	1.7E+07	33.2	1.8E+07	31.6	2.1E+07	27.5	2.3E+07	24.7	2.6E+07	22.6
0.33	3.00	4.5E+06	126.3	6.9E+06	82.9	1.1E+07	51.8	1.7E+07	36.0	1.7E+07	34.4	2.0E+07	29.9	2.3E+07	26.8	2.5E+07	24.5
0.31	3.20	4.5E+06	136.6	6.8E+06	89.6	1.1E+07	55.9	1.6E+07	38.9	1.7E+07	37.1	2.0E+07	32.3	2.3E+07	28.9	2.5E+07	26.4
0.29	3.40	4.4E+06	146.8	6.8E+06	96.3	1.1E+07	60.1	1.6E+07	41.7	1.7E+07	39.8	2.0E+07	34.6	2.2E+07	30.9	2.5E+07	28.3
0.28	3.60	4.4E+06	156.9	6.7E+06	102.9	1.1E+07	64.1	1.6E+07	44.5	1.7E+07	42.4	2.0E+07	36.9	2.2E+07	33.0	2.5E+07	30.1

ρ [%]		1.7		1.9		2.1		2.3		2.5		2.7		2.9		3.1	
M_{cr}/M_a [-]	M_a/M_{cr} [-]	I_e [mm⁴]	$1/r_i$ [10^6 mm⁻¹]	I_e [mm⁴]	$1/r_i$ [10^6 mm⁻¹]	I_e [mm⁴]	$1/r_i$ [10^6 mm⁻¹]	I_e [mm⁴]	$1/r_i$ [10^6 mm⁻¹]	I_e [mm⁴]	$1/r_i$ [10^6 mm⁻¹]	I_e [mm⁴]	$1/r_i$ [10^6 mm⁻¹]	I_e [mm⁴]	$1/r_i$ [10^6 mm⁻¹]	I_e [mm⁴]	$1/r_i$ [10^6 mm⁻¹]
5.00	0.20	7.6E+07	0.6	7.6E+07	0.6	7.7E+07	0.6	7.7E+07	0.6	7.8E+07	0.6	7.8E+07	0.6	7.9E+07	0.6	7.9E+07	0.6
2.50	0.40	7.6E+07	1.1	7.6E+07	1.1	7.7E+07	1.1	7.7E+07	1.1	7.8E+07	1.1	7.8E+07	1.1	7.9E+07	1.1	7.9E+07	1.1
1.67	0.60	7.6E+07	1.7	7.6E+07	1.7	7.7E+07	1.7	7.7E+07	1.7	7.8E+07	1.7	7.8E+07	1.7	7.9E+07	1.7	7.9E+07	1.7
1.25	0.80	7.6E+07	2.2	7.6E+07	2.2	7.7E+07	2.2	7.7E+07	2.2	7.8E+07	2.2	7.8E+07	2.3	7.9E+07	2.3	7.9E+07	2.3
1.00	1.00	7.6E+07	2.8	7.6E+07	2.8	7.7E+07	2.8	7.7E+07	2.8	7.8E+07	2.8	7.8E+07	2.8	7.9E+07	2.8	7.9E+07	2.8
0.83	1.20	4.7E+07	5.3	5.0E+07	5.1	5.2E+07	5.0	5.4E+07	4.8	5.5E+07	4.7	5.7E+07	4.7	5.8E+07	4.6	6.0E+07	4.5
0.71	1.40	3.9E+07	7.6	4.1E+07	7.2	4.3E+07	6.9	4.5E+07	6.7	4.7E+07	6.5	4.9E+07	6.3	5.1E+07	6.2	5.2E+07	6.1
0.63	1.60	3.5E+07	9.7	3.7E+07	9.2	3.9E+07	8.8	4.1E+07	8.4	4.3E+07	8.1	4.5E+07	7.9	4.7E+07	7.7	4.8E+07	7.5
0.56	1.80	3.2E+07	11.7	3.4E+07	11.0	3.7E+07	10.5	3.9E+07	10.1	4.1E+07	9.7	4.2E+07	9.4	4.4E+07	9.1	4.6E+07	8.9
0.50	2.00	3.1E+07	13.6	3.3E+07	12.8	3.5E+07	12.2	3.7E+07	11.7	3.9E+07	11.2	4.1E+07	10.9	4.2E+07	10.5	4.4E+07	10.2
0.45	2.20	3.0E+07	15.5	3.2E+07	14.6	3.4E+07	13.8	3.6E+07	13.2	3.8E+07	12.7	4.0E+07	12.3	4.1E+07	11.9	4.3E+07	11.6
0.42	2.40	2.9E+07	17.4	3.1E+07	16.3	3.3E+07	15.5	3.5E+07	14.8	3.7E+07	14.2	3.9E+07	13.7	4.1E+07	13.2	4.2E+07	12.9
0.38	2.60	2.8E+07	19.2	3.1E+07	18.0	3.3E+07	17.0	3.5E+07	16.3	3.7E+07	15.6	3.8E+07	15.0	4.0E+07	14.5	4.2E+07	14.1
0.36	2.80	2.8E+07	20.9	3.0E+07	19.6	3.2E+07	18.6	3.4E+07	17.7	3.6E+07	17.0	3.8E+07	16.4	4.0E+07	15.8	4.1E+07	15.4
0.33	3.00	2.8E+07	22.7	3.0E+07	21.3	3.2E+07	20.1	3.4E+07	19.2	3.6E+07	18.4	3.7E+07	17.7	3.9E+07	17.1	4.1E+07	16.6
0.31	3.20	2.7E+07	24.4	3.0E+07	22.9	3.2E+07	21.7	3.4E+07	20.7	3.5E+07	19.8	3.7E+07	19.1	3.9E+07	18.4	4.0E+07	17.9
0.29	3.40	2.7E+07	26.2	2.9E+07	24.5	3.1E+07	23.2	3.3E+07	22.1	3.5E+07	21.2	3.7E+07	20.4	3.9E+07	19.7	4.0E+07	19.1
0.28	3.60	2.7E+07	27.9	2.9E+07	26.1	3.1E+07	24.7	3.3E+07	23.5	3.5E+07	22.5	3.7E+07	21.7	3.8E+07	21.0	4.0E+07	20.3

Uncracked Condition			Cracked Condition	
M_a/M_{cr} [-]	I_u [mm⁴]	$1/r_i$ [10^6 mm⁻¹]	I_{cr} [mm⁴]	$1/r_i$ [10^6 mm⁻¹]
0.00	7.3E+07	0.0	1.5E+07	0
0.20	7.3E+07	0.5	1.5E+07	2.6
0.40	7.3E+07	1.1	1.5E+07	5.3
0.60	7.3E+07	1.6	1.5E+07	7.9
0.80	7.3E+07	2.2	1.5E+07	10.5
1.00	7.3E+07	2.7	1.5E+07	13.2
1.20	7.3E+07	3.2	1.5E+07	15.8
1.40	7.3E+07	3.8	1.5E+07	18.5
1.60	7.3E+07	4.3	1.5E+07	21.1
1.80	7.3E+07	4.9	1.5E+07	23.7
2.00	7.3E+07	5.4	1.5E+07	26.4
2.20	7.3E+07	6.0	1.5E+07	29.0
2.40	7.3E+07	6.5	1.5E+07	31.6
2.60	7.3E+07	7.0	1.5E+07	34.3
2.80	7.3E+07	7.6	1.5E+07	36.9
3.00	7.3E+07	8.1	1.5E+07	39.5
3.20	7.3E+07	8.7	1.5E+07	42.2
3.40	7.3E+07	9.2	1.5E+07	44.8
3.60	7.3E+07	9.7	1.5E+07	47.4

Experimental Behaviour: Gilbert 2007 (Tension Stiffening in Lightly Reinforced Concrete Slabs)

ρ = 0.842 %

M_{cr} = 6.05 kNm

For simpel supported one-way slab

K = 0.104

M_{cr}/M_a [-]	M_a/M_{cr} [-]	Δ [mm]	I_e [mm⁴]	$1/r_i$ [10^6 mm⁻¹]
0.91	1.1	2.38	3.8E+07	5.7
0.83	1.2	3.45	2.9E+07	8.3
0.77	1.3	4.15	2.6E+07	10.0

Immediate Curvature $1/r_i$	I_e for Partially Cracked Condition
$\frac{1}{r_i} = \frac{\Delta}{KL^2}$	$I_e = \frac{M_a}{E_c \frac{1}{r_i}}$

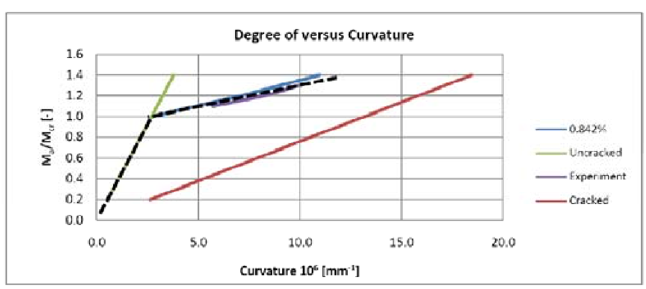

Data obtianed from Article: "Tension Stiffening in Lightly Reinforced Concrete Slabs" by R.I. Gilbert
Journal of Structural Engineering (ASCE) June 2007

SLAB: Z4

Calculation of the Immediate Deflection according to BS 8110, 3.6

Slab Panel Parameters:

Material Properties:

f'_c = 48.4 MPa
f_c = 60.50 MPa
f_t = 4.04 MPa
E_c = 30.5 GPa

Wide Beam:

b = 850.0 mm
L = 2000.0 mm
d = 79.0 mm
d' = 21.0 mm
h = 100.0 mm

Cracking Moment: M_{cr} = 6.05 kNm (from data)

Momenf of Inertia of Cracked Section: Equations used

x_u for the Uncracked Condition	I_u for the Uncracked Condition	Modular Ratio
$x_u = \dfrac{\frac{bh^2}{2} + (\alpha_e)(A_s d + A'_s d')}{bh + (\alpha_e)(A_s + A'_s)}$	$I_u = \dfrac{bh^3}{12} + bh\left(\dfrac{h}{2} - x_u\right)^2 + (\alpha_e)\left[A_s(d - x_u)^2 + A'_s(x_u - d')^2\right]$	$\alpha_e = \dfrac{E_s}{E_c}$

x_{cr} for the Cracked Condition	I_{cr} for the Cracked Condition
$\dfrac{x_{cr}}{d} = -\alpha_e(\rho + \rho') + \sqrt{\left\{\alpha_e^2(\rho + \rho')^2 + 2\alpha_e\left(\rho + \dfrac{d'}{d}\rho'\right)\right\}}$	$\dfrac{I_{cr}}{bd^3} = \dfrac{1}{3}\left(\dfrac{x_{cr}}{d}\right)^3 + \alpha_e\rho\left(1 - \dfrac{x_{cr}}{d}\right)^2 + \alpha_e\rho'\left(\dfrac{x_{cr}}{d} - \dfrac{d'}{d}\right)^2$

ρ	[%]	0.18	0.29	0.52	0.84	0.90	1.10	1.30	1.50	1.70	1.90	2.10	2.30	2.50	2.70	2.90	3.10
b	[mm]	850.0	850.0	850.0	850.0	850.0	850.0	850.0	850.0	850.0	850.0	850.0	850.0	850.0	850.0	850.0	850.0
d	[mm]	79.0	79.0	79.0	79.0	79.0	79.0	79.0	79.0	79.0	79.0	79.0	79.0	79.0	79.0	79.0	79.0
A_s	[mm^2]	120.9	196.7	349.9	565.4	604.4	738.7	873.0	1007.3	1141.6	1275.9	1410.2	1544.5	1678.8	1813.1	1947.4	2081.7
ρ	[-]	0.0018	0.0029	0.0052	0.0084	0.0090	0.0110	0.0130	0.0150	0.0170	0.0190	0.0210	0.0230	0.0250	0.0270	0.0290	0.0310
E_s	[GPa]	200.0	200.0	200.0	200.0	200.0	200.0	200.0	200.0	200.0	200.0	200.0	200.0	200.0	200.0	200.0	200.0
E_c	[GPa]	30.5	30.5	30.5	30.5	30.5	30.5	30.5	30.5	30.5	30.5	30.5	30.5	30.5	30.5	30.5	30.5
α_e	[-]	6.6	6.6	6.6	6.6	6.6	6.6	6.6	6.6	6.6	6.6	6.6	6.6	6.6	6.6	6.6	6.6
x_u	[mm]	50.3	50.4	50.8	51.2	51.3	51.6	51.8	52.1	52.3	52.6	52.8	53.1	53.3	53.6	53.8	54.0
I_u	[mm^4]	7.1E+07	7.2E+07	7.3E+07	7.4E+07	7.4E+07	7.5E+07	7.5E+07	7.6E+07	7.7E+07	7.7E+07	7.8E+07	7.8E+07	7.9E+07	8.0E+07	8.0E+07	8.1E+07
x_{cr}/d	[-]	0.142	0.178	0.229	0.282	0.290	0.314	0.336	0.356	0.374	0.390	0.405	0.419	0.432	0.444	0.455	0.466
X_{cr}	[mm]	11.2	14.0	18.1	22.3	22.9	24.8	26.6	28.1	29.5	30.8	32.0	33.1	34.1	35.1	36.0	36.8
I_{cr}/bd^3	[-]	0.0096	0.0149	0.0243	0.0359	0.0379	0.0443	0.0502	0.0558	0.0611	0.0661	0.0709	0.0754	0.0798	0.0839	0.0879	0.0917
I_{cr}	[mm^4]	4.0E+06	6.2E+06	1.0E+07	1.5E+07	1.6E+07	1.9E+07	2.1E+07	2.3E+07	2.6E+07	2.8E+07	3.0E+07	3.2E+07	3.3E+07	3.5E+07	3.7E+07	3.8E+07
ΔM	[kNm]	2.92	2.77	2.55	2.35	2.32	2.22	2.14	2.07	2.00	1.95	1.90	1.85	1.81	1.77	1.73	1.69

Immediate Curvature $1/r_i$ for Uncracked Section	Net Applied Moment for Partially Cracked Section	Immediate Curvature $1/r_i$ for Partially Cracked Section
$\dfrac{1}{r_i} = \dfrac{M_a}{E_c I_u}$	$M_{net} = M_a - \Delta M = M_a - \frac{1}{3}\dfrac{b(h - x_{cr})^3}{d - x_{cr}} f_t$	$\dfrac{1}{r_i} = \dfrac{M_{net}}{E_c I_{cr}}$

ρ [%]		0.18		0.29		0.521		0.84		0.9		1.1		1.3		1.5	
M_{cr}/M_a	M_a/M_{cr}	I_u	$1/r_i$	I_u	$1/r_i$	I_u	$1/r_i$	I_u	$1/r_i$	I_u	$1/r_i$	I_u	$1/r_i$	I_u	$1/r_i$	I_u	$1/r_i$
[-]	[-]	[mm^4]	[10^6 mm^{-1}]	[mm^4]	[10^6 mm^{-1}]	[mm^4]	[10^6 mm^{-1}]	[mm^4]	[10^6 mm^{-1}]	[mm^4]	[10^6 mm^{-1}]	[mm^4]	[10^6 mm^{-1}]	[mm^4]	[10^6 mm^{-1}]	[mm^4]	[10^6 mm^{-1}]
5.00	0.20	7.1E+07	0.6	7.2E+07	0.6	7.3E+07	0.5	7.4E+07	0.5	7.4E+07	0.5	7.5E+07	0.5	7.5E+07	0.5	7.6E+07	0.5
2.50	0.40	7.1E+07	1.1	7.2E+07	1.1	7.3E+07	1.1	7.4E+07	1.1	7.4E+07	1.1	7.5E+07	1.1	7.5E+07	1.1	7.6E+07	1.0
1.67	0.60	4.0E+06	5.7	6.2E+06	4.5	1.0E+07	3.5	1.5E+07	2.8	1.6E+07	2.7	1.9E+07	2.5	2.1E+07	2.3	2.3E+07	2.2

1.25	0.80	4.0E+06	15.5	6.2E+06	10.9	1.0E+07	7.4	1.5E+07	5.4	1.6E+07	5.2	1.9E+07	4.6	2.1E+07	4.2	2.3E+07	3.9
1.00	1.00	4.0E+06	25.4	6.2E+06	17.3	1.0E+07	11.2	1.5E+07	8.1	1.6E+07	7.7	1.9E+07	6.8	2.1E+07	6.1	2.3E+07	5.6
0.83	1.20	4.0E+06	35.2	6.2E+06	23.6	1.0E+07	15.1	1.5E+07	10.7	1.6E+07	10.2	1.9E+07	8.9	2.1E+07	8.0	2.3E+07	7.3
0.71	1.40	4.0E+06	45.0	6.2E+06	30.0	1.0E+07	19.0	1.5E+07	13.3	1.6E+07	12.7	1.9E+07	11.0	2.1E+07	9.9	2.3E+07	9.0
0.63	1.60	4.0E+06	54.8	6.2E+06	36.4	1.0E+07	22.9	1.5E+07	16.0	1.6E+07	15.2	1.9E+07	13.2	2.1E+07	11.7	2.3E+07	10.7
0.56	1.80	4.0E+06	64.6	6.2E+06	42.7	1.0E+07	26.8	1.5E+07	18.6	1.6E+07	17.7	1.9E+07	15.3	2.1E+07	13.6	2.3E+07	12.4
0.50	2.00	4.0E+06	74.4	6.2E+06	49.1	1.0E+07	30.7	1.5E+07	21.2	1.6E+07	20.2	1.9E+07	17.5	2.1E+07	15.5	2.3E+07	14.1
0.45	2.20	4.0E+06	84.3	6.2E+06	55.5	1.0E+07	34.6	1.5E+07	23.9	1.6E+07	22.7	1.9E+07	19.6	2.1E+07	17.4	2.3E+07	15.8
0.42	2.40	4.0E+06	94.1	6.2E+06	61.9	1.0E+07	38.5	1.5E+07	26.5	1.6E+07	25.2	1.9E+07	21.7	2.1E+07	19.3	2.3E+07	17.4
0.38	2.60	4.0E+06	103.9	6.2E+06	68.2	1.0E+07	42.4	1.5E+07	29.1	1.6E+07	27.7	1.9E+07	23.9	2.1E+07	21.2	2.3E+07	19.1
0.36	2.80	4.0E+06	113.7	6.2E+06	74.6	1.0E+07	46.3	1.5E+07	31.8	1.6E+07	30.2	1.9E+07	26.0	2.1E+07	23.1	2.3E+07	20.8
0.33	3.00	4.0E+06	123.5	6.2E+06	81.0	1.0E+07	50.2	1.5E+07	34.4	1.6E+07	32.7	1.9E+07	28.2	2.1E+07	24.9	2.3E+07	22.5
0.31	3.20	4.0E+06	133.3	6.2E+06	87.3	1.0E+07	54.1	1.5E+07	37.0	1.6E+07	35.2	1.9E+07	30.3	2.1E+07	26.8	2.3E+07	24.2
0.29	3.40	4.0E+06	143.2	6.2E+06	93.7	1.0E+07	58.0	1.5E+07	39.7	1.6E+07	37.7	1.9E+07	32.4	2.1E+07	28.7	2.3E+07	25.9
0.28	3.60	4.0E+06	153.0	6.2E+06	100.1	1.0E+07	61.9	1.5E+07	42.3	1.6E+07	40.2	1.9E+07	34.6	2.1E+07	30.6	2.3E+07	27.6

ρ [%]		1.7		1.9		2.1		2.3		2.5		2.7		2.9		3.1	
M_{cr}/M_a [-]	M_a/M_{cr} [-]	I_e [mm⁴]	$1/r_i$ [10^6 mm^{-1}]	I_e [mm⁴]	$1/r_i$ [10^6 mm^{-1}]	I_e [mm⁴]	$1/r_i$ [10^6 mm^{-1}]	I_e [mm⁴]	$1/r_i$ [10^6 mm^{-1}]	I_e [mm⁴]	$1/r_i$ [10^6 mm^{-1}]	I_e [mm⁴]	$1/r_i$ [10^6 mm^{-1}]	I_e [mm⁴]	$1/r_i$ [10^6 mm^{-1}]	I_e [mm⁴]	$1/r_i$ [10^6 mm^{-1}]
5.00	0.20	7.7E+07	0.5	7.7E+07	0.5	7.8E+07	0.5	7.8E+07	0.5	7.9E+07	0.5	8.0E+07	0.5	8.0E+07	0.5	8.1E+07	0.5
2.50	0.40	7.7E+07	1.0	7.7E+07	1.0	7.8E+07	1.0	7.8E+07	1.0	7.9E+07	1.0	8.0E+07	1.0	8.0E+07	1.0	8.1E+07	1.0
1.67	0.60	2.6E+07	2.1	2.8E+07	2.0	3.0E+07	1.9	3.2E+07	1.8	3.3E+07	1.8	3.5E+07	1.7	3.7E+07	1.7	3.8E+07	1.7
1.25	0.80	2.6E+07	3.6	2.8E+07	3.4	3.0E+07	3.2	3.2E+07	3.1	3.3E+07	3.0	3.5E+07	2.9	3.7E+07	2.8	3.8E+07	2.7
1.00	1.00	2.6E+07	5.2	2.8E+07	4.9	3.0E+07	4.6	3.2E+07	4.4	3.3E+07	4.2	3.5E+07	4.0	3.7E+07	3.8	3.8E+07	3.7
0.83	1.20	2.6E+07	6.7	2.8E+07	6.3	3.0E+07	5.9	3.2E+07	5.6	3.3E+07	5.3	3.5E+07	5.1	3.7E+07	4.9	3.8E+07	4.7
0.71	1.40	2.6E+07	8.3	2.8E+07	7.7	3.0E+07	7.3	3.2E+07	6.9	3.3E+07	6.5	3.5E+07	6.3	3.7E+07	6.0	3.8E+07	5.8
0.63	1.60	2.6E+07	9.8	2.8E+07	9.1	3.0E+07	8.6	3.2E+07	8.1	3.3E+07	7.7	3.5E+07	7.4	3.7E+07	7.1	3.8E+07	6.8
0.56	1.80	2.6E+07	11.4	2.8E+07	10.6	3.0E+07	9.9	3.2E+07	9.4	3.3E+07	8.9	3.5E+07	8.5	3.7E+07	8.2	3.8E+07	7.8
0.50	2.00	2.6E+07	12.9	2.8E+07	12.0	3.0E+07	11.3	3.2E+07	10.6	3.3E+07	10.1	3.5E+07	9.6	3.7E+07	9.2	3.8E+07	8.9
0.45	2.20	2.6E+07	14.5	2.8E+07	13.4	3.0E+07	12.6	3.2E+07	11.9	3.3E+07	11.3	3.5E+07	10.8	3.7E+07	10.3	3.8E+07	9.9
0.42	2.40	2.6E+07	16.0	2.8E+07	14.9	3.0E+07	13.9	3.2E+07	13.1	3.3E+07	12.5	3.5E+07	11.9	3.7E+07	11.4	3.8E+07	10.9
0.38	2.60	2.6E+07	17.6	2.8E+07	16.3	3.0E+07	15.3	3.2E+07	14.4	3.3E+07	13.7	3.5E+07	13.0	3.7E+07	12.5	3.8E+07	12.0
0.36	2.80	2.6E+07	19.1	2.8E+07	17.7	3.0E+07	16.6	3.2E+07	15.7	3.3E+07	14.8	3.5E+07	14.1	3.7E+07	13.5	3.8E+07	13.0
0.33	3.00	2.6E+07	20.7	2.8E+07	19.2	3.0E+07	17.9	3.2E+07	16.9	3.3E+07	16.0	3.5E+07	15.3	3.7E+07	14.6	3.8E+07	14.0
0.31	3.20	2.6E+07	22.2	2.8E+07	20.6	3.0E+07	19.3	3.2E+07	18.2	3.3E+07	17.2	3.5E+07	16.4	3.7E+07	15.7	3.8E+07	15.1
0.29	3.40	2.6E+07	23.8	2.8E+07	22.0	3.0E+07	20.6	3.2E+07	19.4	3.3E+07	18.4	3.5E+07	17.5	3.7E+07	16.8	3.8E+07	16.1
0.28	3.60	2.6E+07	25.3	2.8E+07	23.5	3.0E+07	21.9	3.2E+07	20.7	3.3E+07	19.6	3.5E+07	18.7	3.7E+07	17.8	3.8E+07	17.1

Uncracked Condition			
M_{cr}/M_a [-]	M_a/M_{cr} [-]	I_u [mm⁴]	$1/r_i$ [10^6 mm^{-1}]
5.00	0.20	7.4E+07	0.5
2.50	0.40	7.4E+07	1.1
1.67	0.60	7.4E+07	1.6
1.25	0.80	7.4E+07	2.1
1.00	1.00	7.4E+07	2.7
0.83	1.20	7.4E+07	3.2
0.71	1.40	7.4E+07	3.8
0.63	1.60	7.4E+07	4.3
0.56	1.80	7.4E+07	4.8
0.50	2.00	7.4E+07	5.4
0.45	2.20	7.4E+07	5.9
0.42	2.40	7.4E+07	6.4
0.38	2.60	7.4E+07	7.0
0.36	2.80	7.4E+07	7.5
0.33	3.00	7.4E+07	8.1
0.31	3.20	7.4E+07	8.6
0.29	3.40	7.4E+07	9.1
0.28	3.60	7.4E+07	9.7

Experimental Behaviour: Gilbert 2007 (Tension Stiffening in Lightly Reinforced Concrete Slabs)

ρ = 0.842 %

M_{cr} = 6.05 kNm

For simpel supported one-way slab

K = 0.104

M_{cr}/M_a [-]	M_a/M_{cr} [-]	Δ [mm]	I_e [mm⁴]	$1/r_i$ [10^6 mm^{-1}]
0.91	1.1	2.38	3.8E+07	5.7
0.83	1.2	3.45	2.9E+07	8.3
0.77	1.3	4.15	2.6E+07	10.0

Immediate Curvature $1/r_i$	I_e for Partially Cracked Condition
$\frac{1}{r_i} = \frac{\Delta}{KL^2}$	$I_e = \frac{M_a}{E_c \frac{1}{r_i}}$

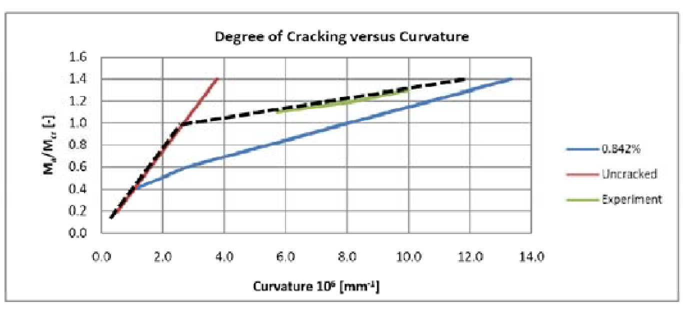

Data obtianed from Article: "Tension Stiffening in Lightly Reinforced Concrete Slabs" by R.I. Gilbert
Journal of Structural Engineering (ASCE) June 2007

SLAB: Z4

Calculation of the Immediate Deflection according to ACI 318, Chapter 9.

Slab Panel Parameters:

Material Properties:

f'_c = 48.4 MPa
f_c = 60.50 MPa
f_r = 4.04 MPa
E_c = 30.5 GPa

Wide Beam:

b = 850.0 mm
L = 2000.0 mm
d = 79.0 mm
d' = 21.0 mm
h = 100.0 mm

Modulus of Rupture: (for unrestrained slabs)

$$f_r = 0.623\sqrt{f'_c}$$

f'_c = 48.4 MPa
f_r = 4.33 MPa

Cracking Moment:

$$M_{cr} = \frac{f_r I_g}{y_t}$$

I_g = 7.1E+07 mm^4
y_t = 50.0 mm
M_{cr} = 6.14 kNm

Momenf of Inertia of Cracked Section: Equations used

x_{cr} for the Cracked Condition	I_{cr} for the Cracked Condition	Modular Ratio
$\omega = A_s\alpha_e + A'_s(\alpha_e - 1)$ $x_{cr} = \left\{[\omega^2 + 2b(A_s d\alpha_e + A'_s d'(\alpha_e - 1))]^{0.5} - \omega\right\}/b$	$I_{cr} = \frac{bx_{cr}^3}{3} + \alpha_e A_s(d - x_{cr})^2 + (\alpha_e - 1)A'_s(d' - x_{cr})^2$	$\alpha_e = \frac{E_s}{E_c}$

ρ	[%]	0.18	0.29	0.52	0.84	0.90	1.10	1.30	1.50	1.70	1.90	2.10	2.30	2.50	2.70	2.90	3.10
b	[mm]	850.0	850.0	850.0	850.0	850.0	850.0	850.0	850.0	850.0	850.0	850.0	850.0	850.0	850.0	850.0	850.0
A_s	[mm^2]	120.9	196.7	349.9	565.4	604.4	738.7	873.0	1007.3	1141.6	1275.9	1410.2	1544.5	1678.8	1813.1	1947.4	2081.7
d	[mm]	79.0	79.0	79.0	79.0	79.0	79.0	79.0	79.0	79.0	79.0	79.0	79.0	79.0	79.0	79.0	79.0
E_s	[GPa]	200.0	200.0	200.0	200.0	200.0	200.0	200.0	200.0	200.0	200.0	200.0	200.0	200.0	200.0	200.0	200.0
E_c	[GPa]	30.5	30.5	30.5	30.5	30.5	30.5	30.5	30.5	30.5	30.5	30.5	30.5	30.5	30.5	30.5	30.5
α_e	[-]	6.6	6.6	6.6	6.6	6.6	6.6	6.6	6.6	6.6	6.6	6.6	6.6	6.6	6.6	6.6	6.6
ω	[mm^2]	792.6	1290.2	2294.1	3707.6	3963.0	4843.6	5724.3	6604.9	7485.6	8366.2	9246.9	10127.5	11008.2	11888.9	12769.5	13650.2
x_{cr}	[mm]	11.2	14.0	18.1	22.3	22.9	24.8	26.6	28.1	29.5	30.8	32.0	33.1	34.1	35.1	36.0	36.8
I_{cr}	[mm^4]	4.0E+06	6.2E+06	1.0E+07	1.5E+07	1.6E+07	1.9E+07	2.1E+07	2.3E+07	2.6E+07	2.8E+07	3.0E+07	3.2E+07	3.3E+07	3.5E+07	3.7E+07	3.8E+07

I_e for Partially Cracked Condition	Immediate Curvature $1/r_i$
$I_e = \left(\frac{M_{cr}}{M_a}\right)^3 I_g + \left[1 - \left(\frac{M_{cr}}{M_a}\right)^3\right] I_{cr} \le I_g$	$\frac{1}{r_i} = \frac{M_a}{E_c I_e}$

ρ [%]		0.18		0.293		0.521		0.842		0.9		1.1		1.3		1.5	
M_{cr}/M_a	M_a/M_{cr}	I_e	$1/r_i$	I_e	$1/r_i$	I_e	$1/r_i$	I_e	$1/r_i$	I_e	$1/r_i$	I_e	$1/r_i$	I_e	$1/r_i$	I_e	$1/r_i$
[-]	[-]	[mm^4]	[10^6 mm^{-1}]	[mm^4]	[10^6 mm^{-1}]	[mm^4]	[10^6 mm^{-1}]	[mm^4]	[10^6 mm^{-1}]	[mm^4]	[10^6 mm^{-1}]	[mm^4]	[10^6 mm^{-1}]	[mm^4]	[10^6 mm^{-1}]	[mm^4]	[10^6 mm^{-1}]
5.00	0.20	7.1E+07	0.6	7.1E+07	0.6	7.1E+07	0.6	7.1E+07	0.6	7.1E+07	0.6	7.1E+07	0.6	7.1E+07	0.6	7.1E+07	0.6
2.50	0.40	7.1E+07	1.1	7.1E+07	1.1	7.1E+07	1.1	7.1E+07	1.1	7.1E+07	1.1	7.1E+07	1.1	7.1E+07	1.1	7.1E+07	1.1
1.67	0.60	7.1E+07	1.7	7.1E+07	1.7	7.1E+07	1.7	7.1E+07	1.7	7.1E+07	1.7	7.1E+07	1.7	7.1E+07	1.7	7.1E+07	1.7
1.25	0.80	7.1E+07	2.3	7.1E+07	2.3	7.1E+07	2.3	7.1E+07	2.3	7.1E+07	2.3	7.1E+07	2.3	7.1E+07	2.3	7.1E+07	2.3
1.00	1.00	7.1E+07	2.8	7.1E+07	2.8	7.1E+07	2.8	7.1E+07	2.8	7.1E+07	2.8	7.1E+07	2.8	7.1E+07	2.8	7.1E+07	2.8
0.83	1.20	4.3E+07	5.7	4.4E+07	5.5	4.5E+07	5.3	4.7E+07	5.1	4.8E+07	5.1	4.9E+07	4.9	5.0E+07	4.8	5.1E+07	4.8
0.71	1.40	2.8E+07	9.9	3.0E+07	9.5	3.2E+07	8.7	3.5E+07	8.0	3.6E+07	7.9	3.8E+07	7.5	3.9E+07	7.2	4.1E+07	6.9

0.63	1.60	2.0E+07	15.8	2.2E+07	14.6	2.5E+07	12.9	2.9E+07	11.2	2.9E+07	11.0	3.1E+07	10.3	3.3E+07	9.7	3.5E+07	9.2
0.56	1.80	1.5E+07	23.4	1.7E+07	20.9	2.1E+07	17.6	2.5E+07	14.7	2.5E+07	14.3	2.8E+07	13.2	3.0E+07	12.2	3.2E+07	11.5
0.50	2.00	1.2E+07	32.5	1.4E+07	28.1	1.8E+07	22.7	2.2E+07	18.3	2.3E+07	17.7	2.5E+07	16.1	2.7E+07	14.8	2.9E+07	13.7
0.45	2.20	1.0E+07	42.9	1.2E+07	36.0	1.6E+07	27.9	2.0E+07	21.8	2.1E+07	21.1	2.3E+07	18.9	2.6E+07	17.2	2.8E+07	15.9
0.42	2.40	8.9E+06	54.5	1.1E+07	44.3	1.5E+07	33.1	1.9E+07	25.3	2.0E+07	24.3	2.2E+07	21.6	2.5E+07	19.6	2.7E+07	18.0
0.38	2.60	7.8E+06	66.7	9.9E+06	52.8	1.4E+07	38.4	1.8E+07	28.7	1.9E+07	27.5	2.2E+07	24.3	2.4E+07	21.9	2.6E+07	20.1
0.36	2.80	7.1E+06	79.6	9.2E+06	61.5	1.3E+07	43.5	1.8E+07	32.0	1.8E+07	30.7	2.1E+07	26.9	2.3E+07	24.2	2.6E+07	22.1
0.33	3.00	6.5E+06	92.7	8.6E+06	70.1	1.2E+07	48.6	1.7E+07	35.3	1.8E+07	33.7	2.0E+07	29.5	2.3E+07	26.4	2.5E+07	24.0
0.31	3.20	6.1E+06	106.0	8.2E+06	78.6	1.2E+07	53.5	1.7E+07	38.4	1.8E+07	36.7	2.0E+07	32.0	2.3E+07	28.5	2.5E+07	25.9
0.29	3.40	5.7E+06	119.2	7.9E+06	86.9	1.2E+07	58.3	1.6E+07	41.5	1.7E+07	39.6	2.0E+07	34.4	2.2E+07	30.7	2.5E+07	27.8
0.28	3.60	5.5E+06	132.4	7.6E+06	95.2	1.1E+07	63.1	1.6E+07	44.6	1.7E+07	42.5	2.0E+07	36.8	2.2E+07	32.8	2.4E+07	29.7

ρ [%]		1.7		1.9		2.1		2.3		2.5		2.7		2.9		3.1	
M_{cr}/M_a [-]	M_a/M_{cr} [-]	I_c [mm^4]	$1/r_i$ [10^6 mm^{-1}]	I_c [mm^4]	$1/r_i$ [10^6 mm^{-1}]	I_c [mm^4]	$1/r_i$ [10^6 mm^{-1}]	I_c [mm^4]	$1/r_i$ [10^6 mm^{-1}]	I_c [mm^4]	$1/r_i$ [10^6 mm^{-1}]	I_c [mm^4]	$1/r_i$ [10^6 mm^{-1}]	I_c [mm^4]	$1/r_i$ [10^6 mm^{-1}]	I_c [mm^4]	$1/r_i$ [10^6 mm^{-1}]
5.00	0.20	7.1E+07	0.6	7.1E+07	0.6	7.1E+07	0.6	7.1E+07	0.6	7.1E+07	0.6	7.1E+07	0.6	7.1E+07	0.6	7.1E+07	0.6
2.50	0.40	7.1E+07	1.1	7.1E+07	1.1	7.1E+07	1.1	7.1E+07	1.1	7.1E+07	1.1	7.1E+07	1.1	7.1E+07	1.1	7.1E+07	1.1
1.67	0.60	7.1E+07	1.7	7.1E+07	1.7	7.1E+07	1.7	7.1E+07	1.7	7.1E+07	1.7	7.1E+07	1.7	7.1E+07	1.7	7.1E+07	1.7
1.25	0.80	7.1E+07	2.3	7.1E+07	2.3	7.1E+07	2.3	7.1E+07	2.3	7.1E+07	2.3	7.1E+07	2.3	7.1E+07	2.3	7.1E+07	2.3
1.00	1.00	7.1E+07	2.8	7.1E+07	2.8	7.1E+07	2.8	7.1E+07	2.8	7.1E+07	2.8	7.1E+07	2.8	7.1E+07	2.8	7.1E+07	2.8
0.83	1.20	5.2E+07	4.7	5.3E+07	4.6	5.4E+07	4.5	5.4E+07	4.4	5.5E+07	4.4	5.6E+07	4.3	5.7E+07	4.3	5.7E+07	4.2
0.71	1.40	4.2E+07	6.7	4.3E+07	6.5	4.5E+07	6.3	4.6E+07	6.1	4.7E+07	6.0	4.8E+07	5.9	4.9E+07	5.7	5.0E+07	5.6
0.63	1.60	3.7E+07	8.8	3.8E+07	8.4	4.0E+07	8.1	4.1E+07	7.8	4.3E+07	7.6	4.4E+07	7.3	4.5E+07	7.1	4.6E+07	7.0
0.56	1.80	3.3E+07	10.9	3.5E+07	10.3	3.7E+07	9.9	3.8E+07	9.5	4.0E+07	9.1	4.1E+07	8.8	4.3E+07	8.5	4.4E+07	8.2
0.50	2.00	3.1E+07	12.9	3.3E+07	12.2	3.5E+07	11.6	3.7E+07	11.0	3.8E+07	10.6	4.0E+07	10.2	4.1E+07	9.8	4.2E+07	9.5
0.45	2.20	3.0E+07	14.8	3.2E+07	13.9	3.4E+07	13.2	3.5E+07	12.5	3.7E+07	12.0	3.9E+07	11.5	4.0E+07	11.1	4.1E+07	10.7
0.42	2.40	2.9E+07	16.7	3.1E+07	15.7	3.3E+07	14.8	3.4E+07	14.0	3.6E+07	13.4	3.8E+07	12.8	3.9E+07	12.3	4.1E+07	11.8
0.38	2.60	2.8E+07	18.6	3.0E+07	17.3	3.2E+07	16.3	3.4E+07	15.5	3.6E+07	14.7	3.7E+07	14.1	3.9E+07	13.5	4.0E+07	13.0
0.36	2.80	2.8E+07	20.4	3.0E+07	19.0	3.2E+07	17.8	3.3E+07	16.9	3.5E+07	16.0	3.7E+07	15.3	3.8E+07	14.7	4.0E+07	14.1
0.33	3.00	2.7E+07	22.1	2.9E+07	20.6	3.1E+07	19.3	3.3E+07	18.3	3.5E+07	17.3	3.6E+07	16.6	3.8E+07	15.9	4.0E+07	15.2
0.31	3.20	2.7E+07	23.9	2.9E+07	22.2	3.1E+07	20.8	3.3E+07	19.6	3.5E+07	18.6	3.6E+07	17.8	3.8E+07	17.0	3.9E+07	16.3
0.29	3.40	2.7E+07	25.6	2.9E+07	23.8	3.1E+07	22.3	3.3E+07	21.0	3.4E+07	19.9	3.6E+07	19.0	3.8E+07	18.2	3.9E+07	17.4
0.28	3.60	2.7E+07	27.3	2.9E+07	25.3	3.1E+07	23.7	3.2E+07	22.3	3.4E+07	21.2	3.6E+07	20.2	3.8E+07	19.3	3.9E+07	18.5

Uncracked Condition			
M_{cr}/M_a [-]	M_a/M_{cr} [-]	I_g [mm^4]	$1/r_i$ [10^6 mm^{-1}]
5.00	0.20	7.1E+07	0.6
2.50	0.40	7.1E+07	1.1
1.67	0.60	7.1E+07	1.7
1.25	0.80	7.1E+07	2.3
1.00	1.00	7.1E+07	2.8
0.83	1.20	7.1E+07	3.4
0.71	1.40	7.1E+07	4.0
0.63	1.60	7.1E+07	4.5
0.56	1.80	7.1E+07	5.1
0.50	2.00	7.1E+07	5.7
0.45	2.20	7.1E+07	6.3
0.42	2.40	7.1E+07	6.8
0.38	2.60	7.1E+07	7.4
0.36	2.80	7.1E+07	8.0
0.33	3.00	7.1E+07	8.5
0.31	3.20	7.1E+07	9.1
0.29	3.40	7.1E+07	9.7
0.28	3.60	7.1E+07	10.2

Experimental Behaviour: Gilbert 2007 (Tension Stiffening in Lightly Reinforced Concrete Slabs)

ρ = 0.842 %

M_{cr} = 6.05 kNm

For simpel supported one-way slab

K = 0.104

M_{cr}/M_a [-]	M_a/M_{cr} [-]	Δ [mm]	I_e [mm^4]	$1/r_i$ [10^6 mm^{-1}]
0.91	1.1	2.38	3.8E+07	5.7
0.83	1.2	3.45	2.9E+07	8.3
0.77	1.3	4.15	2.6E+07	10.0

Immediate Curvature $1/r_i$	I_c for Partially Cracked Condition
$\frac{1}{r_i} = \frac{\Delta}{KL^2}$	$I_e = \frac{M_a}{E_c \frac{1}{r_i}}$

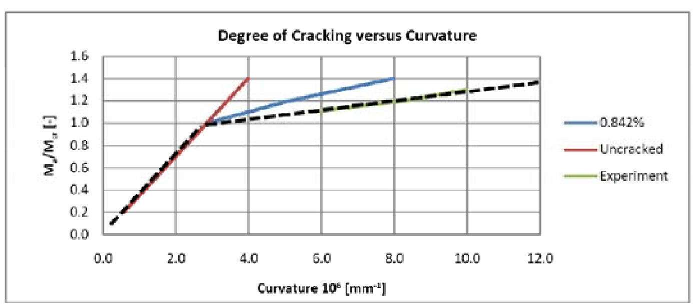

Predicted Results from Design Codes

		SABS 0100		EC2		BS 8110		ACI 318		Uncracked Section		Uncracked Section	
ρ [%]		0.842		0.842		0.842		0.842		I_g (SABS)		I_u (EC2)	
M_{cr}/M_a [-]	M_a/M_{cr} [-]	I_e [mm^4]	$1/r_i$ [$10^6\ mm^{-1}$]	I_e [mm^4]	$1/r_i$ [$10^6\ mm^{-1}$]	I_e [mm^4]	$1/r_i$ [$10^6\ mm^{-1}$]	I_e [mm^4]	$1/r_i$ [$10^6\ mm^{-1}$]	I_e [mm^4]	$1/r_i$ [$10^6\ mm^{-1}$]	I_e [mm^4]	$1/r_i$ [$10^6\ mm^{-1}$]
0.00	0.00	7.1E+07	0.0	7.3E+07	0.0	7.4E+07	0.0	7.1E+07	0.0	7.1E+07	0.0	7.3E+07	0.0
5.00	0.20	7.1E+07	0.7	7.3E+07	0.5	7.4E+07	0.5	7.1E+07	0.6	7.1E+07	0.7	7.3E+07	0.5
2.50	0.40	7.1E+07	1.3	7.3E+07	1.1	7.4E+07	1.1	7.1E+07	1.1	7.1E+07	1.3	7.3E+07	1.1
1.67	0.60	7.1E+07	2.0	7.3E+07	1.6	1.5E+07	2.8	7.1E+07	1.7	7.1E+07	2.0	7.3E+07	1.6
1.25	0.80	7.1E+07	2.7	7.3E+07	2.2	1.5E+07	5.4	7.1E+07	2.3	7.1E+07	2.7	7.3E+07	2.2
1.00	1.00	7.1E+07	3.3	7.3E+07	2.7	1.5E+07	8.1	7.1E+07	2.8	7.1E+07	3.3	7.3E+07	2.7
0.83	1.20	4.7E+07	6.0	3.4E+07	7.1	1.5E+07	10.7	4.7E+07	5.1	7.1E+07	4.0	7.3E+07	3.2
0.71	1.40	3.5E+07	9.3	2.5E+07	11.0	1.5E+07	13.3	3.5E+07	8.0	7.1E+07	4.6	7.3E+07	3.8
0.63	1.60	2.9E+07	13.1	2.2E+07	14.5	1.5E+07	16.0	2.9E+07	11.2	7.1E+07	5.3	7.3E+07	4.3
0.56	1.80	2.5E+07	17.2	2.0E+07	17.9	1.5E+07	18.6	2.5E+07	14.7	7.1E+07	6.0	7.3E+07	4.9
0.50	2.00	2.2E+07	21.3	1.9E+07	21.1	1.5E+07	21.2	2.2E+07	18.3	7.1E+07	6.6	7.3E+07	5.4
0.45	2.20	2.0E+07	25.5	1.8E+07	24.2	1.5E+07	23.9	2.0E+07	21.8	7.1E+07	7.3	7.3E+07	6.0
0.42	2.40	1.9E+07	29.5	1.7E+07	27.3	1.5E+07	26.5	1.9E+07	25.3	7.1E+07	8.0	7.3E+07	6.5
0.38	2.60	1.8E+07	33.5	1.7E+07	30.2	1.5E+07	29.1	1.8E+07	28.7	7.1E+07	8.6	7.3E+07	7.0
0.36	2.80	1.8E+07	37.4	1.7E+07	33.2	1.5E+07	31.8	1.8E+07	32.0	7.1E+07	9.3	7.3E+07	7.6
0.33	3.00	1.7E+07	41.1	1.7E+07	36.0	1.5E+07	34.4	1.7E+07	35.3	7.1E+07	9.9	7.3E+07	8.1
0.31	3.20	1.7E+07	44.8	1.6E+07	38.9	1.5E+07	37.0	1.7E+07	38.4	7.1E+07	10.6	7.3E+07	8.7
0.29	3.40	1.6E+07	48.4	1.6E+07	41.7	1.5E+07	39.7	1.6E+07	41.5	7.1E+07	11.3	7.3E+07	9.2
0.28	3.60	1.6E+07	52.0	1.6E+07	44.5	1.5E+07	42.3	1.6E+07	44.6	7.1E+07	11.9	7.3E+07	9.7

Experimental Behaviour: Gilbert 2007 (Tension Stiffening in Lightly Reinforced Concrete Slabs)

ρ = 0.842 %

M_{cr} = 6.05 kNm

M_{cr}/M_a [-]	M_a/M_{cr} [-]	Δ [mm]	I_e [mm^4]	$1/r_i$ [$10^6\ mm^{-1}$]
0.91	1.1	2.38	3.8E+07	5.7
0.83	1.2	3.45	2.9E+07	8.3
0.77	1.3	4.15	2.6E+07	10.0

For simpel supported one-way slab

K = 0.104

Immediate Curvature $1/r_i$	I_e for Partially Cracked Condition
$\frac{1}{r_i} = \frac{\Delta}{KL^2}$	$I_e = \frac{M_a}{E_c \frac{1}{r_i}}$

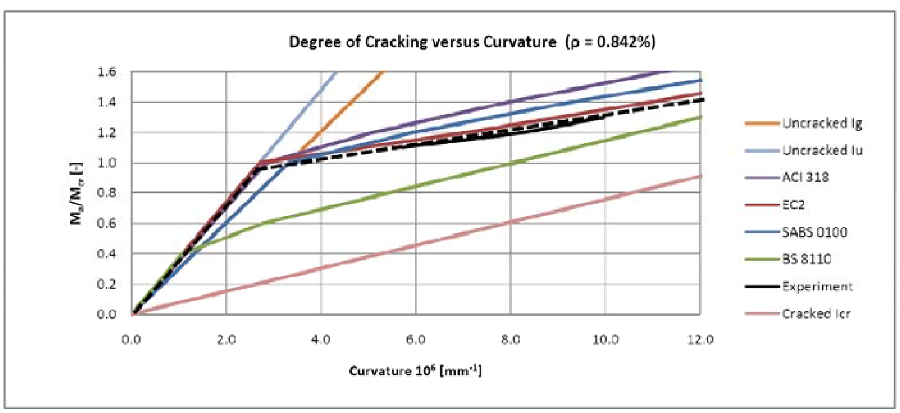

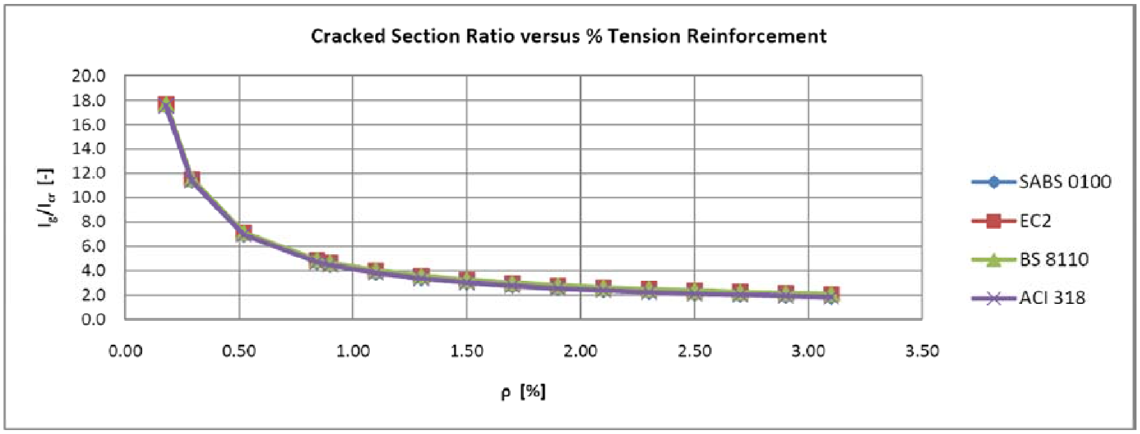

Cracked Section Ratio versus % Tension Reinforcement
20.0
18.0
16.0
14.0
12.0
10.0
8.0
6.0
4.0
2.0
0.0
I_g/I_{cr} [-]
0.00
0.50
1.00
1.50
2.00
2.50
3.00
3.50
ρ [%]
SABS 0100
EC2
BS 8110
ACI 318

Data obtianed from Article: "Tension Stiffening in Lightly Reinforced Concrete Slabs" by R.I. Gilbert
Journal of Structural Engineering (ASCE) June 2007

SLAB: SS2

Obtain the Allowable L/d ratio according to SABS 0100-1, clause 4.3.6

Slab Panel Parameters:

Material Properties:

f'_c = 38.0 MPa
f_c = 47.50 MPa
f_t = 4.42 MPa
E_c = 27.47 GPa
f_y = 500.0 MPa

Wide Beam:

b = 850.0 mm
L = 2000.0 mm
d = 81.7 mm
d' = 20.3 mm
h = 102.0 mm

Provided Reinforcement:

ρ [%]	0.2	0.3	0.6	0.8	1.0	1.2	1.4	1.6	1.8	2.0	2.2	2.4
A_s [mm^2]	138.9	227.1	416.7	555.6	694.5	833.3	972.2	1111.1	1250.0	1388.9	1527.8	1666.7

A'_s [mm^2]	0.0

Allowable Span/Depth Ratio compared to the Actual Span/Depth Ratio:

Step 1: Basic span/depth ratio for rectangular beams

Support Condition	Rectangular Section
Simply supported beam	16

L > 10.0 m ? FALSE

Condition		
TRUE	k_1 =	10/L
FALSE	k_1 =	1.0

k_1 = 1.0

Step 2: Modification of span/depth ratio due to tension reinforcement

Design Service Stress:

assume that the ratio required tension reinforcement and provided tension reinforcement is 1.0

$A_{s,req}$ = $A_{s,prov}$ = 1.0

assume the normal partial load combination factors apply

γ_1 = 1.1
γ_2 = 1.0
γ_3 = 1.2
γ_4 = 1.6

assume no moment redistribution occurs

β_b = 1.0

$$f_s = 0.87 f_y \cdot \frac{\gamma_1 + \gamma_2}{\gamma_3 + \gamma_4} \cdot \frac{A_{s,req}}{A_{s,prov}} \cdot \frac{1}{\beta_b}$$

f_y = 500.0 MPa

f_s = 326.25 MPa

Calculate the Design Ultimate Bending Moment (clause 4.3.3.4):

assume only tension reinforcement is required, therefore $K \leq K'$

assume $z = 0.95d$

therefore $$M = A_s(0.87 f_y \cdot 0.95d)$$

f_y = 500.0 MPa
d = 81.7 mm

ρ [%]	0.2	0.4	0.6	0.8	1.0	1.2	1.4	1.6	1.8	2.0	2.2	2.4
A_s [mm^2]	138.9	227.1	416.7	555.6	694.5	833.3	972.2	1111.1	1250.0	1388.9	1527.8	1666.7
M [kNm]	4.69	7.67	14.07	18.76	23.45	28.14	32.82	37.51	42.20	46.89	51.58	56.27

1st Iteration:

check assumption $$K = \frac{M}{bd^2 f_c}$$

b = 850.0 mm
f_c = 47.50 MPa
d = 81.70 mm

ρ [%]	0.2	0.4	0.6	0.8	1.0	1.2	1.4	1.6	1.8	2.0	2.2	2.4
A_s [mm^2]	138.89	227.09	416.67	555.56	694.45	833.34	972.23	1111.12	1250.01	1388.90	1527.79	1666.68
K [-]	0.0174	0.0284	0.0522	0.0696	0.0870	0.1044	0.1218	0.1392	0.1566	0.1740	0.1914	0.2088

$$z = d\left\{0.5 + \sqrt{0.25 - \frac{K}{0.9}}\right\} \leq 0.95d \qquad M = A_s(0.87 f_y \cdot 0.95d)$$

ρ [%]	0.2	0.4	0.6	0.8	1.0	1.2	1.4	1.6	1.8	2.0	2.2	2.4
A_s [mm^2]	138.9	227.1	416.7	555.6	694.5	833.3	972.2	1111.1	1250.0	1388.9	1527.8	1666.7
z [mm]	0.980	0.967	0.938	0.916	0.892	0.866	0.839	0.809	0.776	0.738	0.693	0.634
> 0.95d	0.95	0.95	0.94	0.92	0.89	0.87	0.84	0.81	0.78	0.74	0.69	0.63
M [kNm]	4.69	7.67	13.89	18.08	22.00	25.65	28.98	31.94	34.46	36.43	37.64	37.56

2nd Iteration:

check assumption $$K = \frac{M}{bd^2 f_c}$$

b = 850.0 mm
f_c = 47.50 MPa
d = 81.70 mm

ρ [%]	0.2	0.4	0.6	0.8	1.0	1.2	1.4	1.6	1.8	2.0	2.2	2.4
A_s [mm^2]	138.89	227.09	416.67	555.56	694.45	833.34	972.23	1111.12	1250.01	1388.90	1527.79	1666.68
K [-]	0.0174	0.0284	0.0516	0.0671	0.0816	0.0952	0.1075	0.1185	0.1279	0.1352	0.1397	0.1394

$$z = d\left\{0.5 + \sqrt{0.25 - \frac{K}{0.9}}\right\} \leq 0.95d \qquad M = A_s(0.87 f_y \cdot 0.95d)$$

ρ [%]	0.2	0.4	0.6	0.8	1.0	1.2	1.4	1.6	1.8	2.0	2.2	2.4
A_s [mm^2]	138.9	227.1	416.7	555.6	694.5	833.3	972.2	1111.1	1250.0	1388.9	1527.8	1666.7
z [mm]	0.980	0.967	0.939	0.919	0.899	0.880	0.861	0.844	0.829	0.816	0.808	0.808
> 0.95d	0.95	0.95	0.94	0.92	0.90	0.88	0.86	0.84	0.83	0.82	0.81	0.81
M [kNm]	4.69	7.67	13.90	18.14	22.19	26.06	29.76	33.33	36.81	40.27	43.87	47.89

3rd Iteration:

check assumption $$K = \frac{M}{bd^2 f_c}$$

b = 850.0 mm
f_c = 47.50 MPa
d = 81.70 mm

ρ [%]	0.2	0.4	0.6	0.8	1.0	1.2	1.4	1.6	1.8	2.0	2.2	2.4
A_s [mm^2]	138.89	227.09	416.67	555.56	694.45	833.34	972.23	1111.12	1250.01	1388.90	1527.79	1666.68
K [-]	0.0174	0.0284	0.0516	0.0673	0.0823	0.0967	0.1104	0.1237	0.1366	0.1494	0.1628	0.1777

$$z = d\left\{0.5 + \sqrt{0.25 - \frac{K}{0.9}}\right\} \leq 0.95d \qquad M = A_s(0.87 f_y \cdot 0.95d)$$

ρ [%]	0.2	0.4	0.6	0.8	1.0	1.2	1.4	1.6	1.8	2.0	2.2	2.4
A_s [mm^2]	138.9	227.1	416.7	555.6	694.5	833.3	972.2	1111.1	1250.0	1388.9	1527.8	1666.7
z [mm]	0.980	0.967	0.939	0.919	0.898	0.878	0.857	0.836	0.813	0.790	0.763	0.729
> 0.95d	0.95	0.95	0.94	0.92	0.90	0.88	0.86	0.84	0.81	0.79	0.76	0.73
M [kNm]	4.69	7.67	13.90	18.14	22.17	25.99	29.60	32.99	36.14	38.98	41.43	43.20

4th Iteration:

check assumption

$$K = \frac{M}{bd^2 f_c}$$

b = 850.0 mm

f_c = 47.50 MPa

d = 81.70 mm

ρ [%]	0.2	0.4	0.6	0.8	1.0	1.2	1.4	1.6	1.8	2.0	2.2	2.4
A_s [mm^2]	138.89	227.09	416.67	555.56	694.45	833.34	972.23	1111.12	1250.01	1388.90	1527.79	1666.68
K [-]	0.0174	0.0284	0.0516	0.0673	0.0823	0.0964	0.1099	0.1224	0.1341	0.1446	0.1537	0.1603

$$z = d\left\{0.5 + \sqrt{0.25 - \frac{K}{0.9}}\right\} \le 0.95d \qquad M = A_s\left(0.87 f_y \cdot 0.95d\right)$$

ρ [%]	0.2	0.4	0.6	0.8	1.0	1.2	1.4	1.6	1.8	2.0	2.2	2.4
A_s [mm^2]	138.9	227.1	416.7	555.6	694.5	833.3	972.2	1111.1	1250.0	1388.9	1527.8	1666.7
z [mm]	0.980	0.967	0.939	0.919	0.898	0.878	0.858	0.838	0.818	0.799	0.781	0.768
> 0.95d	0.95	0.95	0.94	0.92	0.90	0.88	0.86	0.84	0.82	0.80	0.78	0.77
M [kNm]	4.69	7.67	13.90	18.14	22.17	26.00	29.64	33.08	36.33	39.43	42.43	45.50

5th Iteration:

check assumption

$$K = \frac{M}{bd^2 f_c}$$

b = 850.0 mm

f_c = 47.50 MPa

d = 81.70 mm

ρ [%]	0.2	0.4	0.6	0.8	1.0	1.2	1.4	1.6	1.8	2.0	2.2	2.4
A_s [mm^2]	138.89	227.09	416.67	555.56	694.45	833.34	972.23	1111.12	1250.01	1388.90	1527.79	1666.68
K [-]	0.0174	0.0284	0.0516	0.0673	0.0823	0.0965	0.1100	0.1227	0.1348	0.1463	0.1574	0.1688

$$z = d\left\{0.5 + \sqrt{0.25 - \frac{K}{0.9}}\right\} \le 0.95d \qquad M = A_s\left(0.87 f_y \cdot 0.95d\right)$$

ρ [%]	0.2	0.4	0.6	0.8	1.0	1.2	1.4	1.6	1.8	2.0	2.2	2.4
A_s [mm^2]	138.9	227.1	416.7	555.6	694.5	833.3	972.2	1111.1	1250.0	1388.9	1527.8	1666.7
z [mm]	0.980	0.967	0.939	0.919	0.898	0.878	0.858	0.837	0.817	0.796	0.774	0.750
> 0.95d	0.95	0.95	0.94	0.92	0.90	0.88	0.86	0.84	0.82	0.80	0.77	0.75
M [kNm]	4.69	7.67	13.90	18.14	22.17	26.00	29.63	33.06	36.28	39.28	42.02	44.41

5th Iteration:

check assumption

$$K = \frac{M}{bd^2 f_c}$$

b = 850.0 mm

f_c = 47.50 MPa

d = 81.70 mm

ρ [%]	0.2	0.4	0.6	0.8	1.0	1.2	1.4	1.6	1.8	2.0	2.2	2.4
A_s [mm^2]	138.89	227.09	416.67	555.56	694.45	833.34	972.23	1111.12	1250.01	1388.90	1527.79	1666.68
K [-]	0.0174	0.0284	0.0516	0.0673	0.0823	0.0965	0.1099	0.1227	0.1346	0.1457	0.1559	0.1648

$$z = d\left\{0.5 + \sqrt{0.25 - \frac{K}{0.9}}\right\} \le 0.95d \qquad M = A_s\left(0.87 f_y \cdot 0.95d\right)$$

ρ [%]	0.2	0.4	0.6	0.8	1.0	1.2	1.4	1.6	1.8	2.0	2.2	2.4
A_s [mm^2]	138.9	227.1	416.7	555.6	694.5	833.3	972.2	1111.1	1250.0	1388.9	1527.8	1666.7
z [mm]	0.980	0.967	0.939	0.919	0.898	0.878	0.858	0.837	0.817	0.797	0.777	0.759
> 0.95d	0.95	0.95	0.94	0.92	0.90	0.88	0.86	0.84	0.82	0.80	0.78	0.76
M [kNm]	4.69	7.67	13.90	18.14	22.17	26.00	29.63	33.06	36.29	39.33	42.19	44.94

Modification Factor k_2:

$$k_2 = 0.55 + \frac{(477 - f_s)}{120\left(0.9 + \frac{M}{bd^2}\right)} \leq 2.0$$

b = 850.0 mm
d = 81.7 mm
f_s = 326.25 MPa

ρ [%]	0.2	0.4	0.6	0.8	1.0	1.2	1.4	1.6	1.8	2.0	2.2	2.4
A_s [mm^2]	138.9	227.1	416.7	555.6	694.5	833.3	972.2	1111.1	1250.0	1388.9	1527.8	1666.7
M [kNm]	4.69	7.67	13.90	18.14	22.17	26.00	29.63	33.06	36.29	39.33	42.19	44.94
k_2	1.28	1.11	0.92	0.86	0.81	0.78	0.76	0.74	0.72	0.71	0.70	0.69
> 2.0	1.28	1.11	0.92	0.86	0.81	0.78	0.76	0.74	0.72	0.71	0.70	0.69

Step 3: Modification of span/depth ratio due to compression reinforcement

no compression reinforcement provided
therefore k_3 = 1.00

Step 4: Deflection due to creep and shrinkage

assume normal creep and shrinkage occurs and is accounted for from step 1 to 3
therefore k_4 = 1.00

Step 5: Span/depth ratio for flanged beams

beam is rectangular and not flanged, step 5 is not applicable
therefore k_5 = 1.00

Compare Actual and Allowable L/d Ratios

$$\left(\frac{L}{d}\right)_{ACTUAL} \leq \left(\frac{L}{d}\right)_{ALLOWABLE} \cdot k_1 \cdot k_2 \cdot k_3 \cdot k_4 \cdot k_5$$

L = 2000.0 mm
d = 81.7 mm

$(L/d)_{ACTUAL}$ = 24.48

$(L/d)_{BASIS}$ = 16

ρ [%]	0.2	0.4	0.6	0.8	1.0	1.2	1.4	1.6	1.8	2.0	2.2	2.4
A_s [mm^2]	138.9	227.1	416.7	555.6	694.5	833.3	972.2	1111.1	1250.0	1388.9	1527.8	1666.7
k_1	1.0	1.0	1.0	1.0	1.0	1.0	1.0	1.0	1.0	1.0	1.0	1.0
k_2	1.3	1.1	0.9	0.9	0.8	0.8	0.8	0.7	0.7	0.7	0.7	0.7
k_3	1.0	1.0	1.0	1.0	1.0	1.0	1.0	1.0	1.0	1.0	1.0	1.0
k_4	1.0	1.0	1.0	1.0	1.0	1.0	1.0	1.0	1.0	1.0	1.0	1.0
k_5	1.0	1.0	1.0	1.0	1.0	1.0	1.0	1.0	1.0	1.0	1.0	1.0
$(L/d)_{ALLOWABLE}$	20.44	17.73	14.80	13.71	12.98	12.47	12.08	11.79	11.55	11.37	11.21	11.08
Serviceable ?	NO	NO	NO	NO	NO	NO	NO	NO	NO	NO	NO	NO

Data obtianed from Article: "Tension Stiffening in Lightly Reinforced Concrete Slabs" by R.I. Gilbert
Journal of Structural Engineering (ASCE) June 2007

SLAB: SS2

Obtain the Allowable L/d ratio according to EC2, clause 7.4.2

Slab Panel Parameters:

Material Properties:
f'_c = 38.0 MPa
f_c = 47.50 MPa
f_t = 4.42 MPa
E_c = 27.47 GPa
f_y = 500.0 MPa

Wide Beam:
b = 850.0 mm
L = 2000.0 mm
d = 81.7 mm
d' = 20.3 mm
h = 102.0 mm

Provided Reinforcement:

ρ [%]	0.2	0.3	0.6	0.8	1.0	1.2	1.4	1.6	1.8	2.0	2.2	2.4
A_s [mm^2]	138.9	227.1	416.7	555.6	694.5	833.3	972.2	1111.1	1250.0	1388.9	1527.8	1666.7

A'_s [mm^2]	0.0

Allowable Span/Depth Ratio compared to the Actual Span/Depth Ratio:

Determine which L/d Equation is applicable:

$\boxed{1}$ $$\frac{L}{d} = K\left[11 + 1.5\sqrt{f_c^{'}}\cdot\frac{\rho_o}{\rho} + 3.2\sqrt{f_c^{'}}\cdot\left(\frac{\rho_o}{\rho} - 1\right)^{3/2}\right]$$ if $\rho \le \rho_o$

$\boxed{2}$ $$\frac{L}{d} = K\left[11 + 1.5\sqrt{f_c^{'}}\cdot\frac{\rho_o}{\rho - \rho'} + \frac{1}{12}\sqrt{f_c^{'}}\cdot\sqrt{\frac{\rho'}{\rho_o}}\right]$$ if $\rho > \rho_o$

where $\rho_o = 10^{-3}\sqrt{f_c^{'}}$

ρ_o = 0.006

f'_c = 38.0 MPa

b = 850.0 mm
d = 81.7 mm

ρ [%]	0.2	0.3	0.6	0.8	1.0	1.2	1.4	1.6	1.8	2.0	2.2	2.4
A_s [mm^2]	138.9	227.1	416.7	555.6	694.5	833.3	972.2	1111.1	1250.0	1388.9	1527.8	1666.7
A'_s [mm^2]	0.0	0.0	0.0	0.0	0.0	0.0	0.0	0.0	0.0	0.0	0.0	0.0
$\rho = A_s/bd$ [-]	0.002	0.0033	0.006	0.008	0.01	0.012	0.014	0.016	0.018	0.02	0.022	0.024
$\rho' = A'_s/bd$ [-]	0	0	0	0	0	0	0	0	0	0	0	0
eq. ?	1	1	1	2	2	2	2	2	2	2	2	2

Flanged Sections:

if b_f/b_w > 3.0 then k_1 = 0.8

b_f/b_w = 0.00 therefore k_1 = 1.00

Beam and Slab Elements:

if $L >$ 7.0 which support partitions liable to be damaged by excessive deflection then $k_2 = 7 / L_{eff}$

$L <$ 7.00 therefore $k_2 =$ 1.00

Flat Slabs:

if greater span $>$ 8.5 which support partitions liable to be damaged by excessive deflections then $k_3 = 8.5 / L_{eff}$

greater span $<$ 8.50 therefore $k_3 =$ 1.00

Basic Span/Depth Ratio:

Structural System	K	Concrete Highly Stressed $\rho = 1.5\%$	Concrete Lightly Stressed $\rho = 0.5\%$
Simply supported beam, one- or two-way spanning simply supported slab	1.0	14	20
End span of continuouse beam or one-way continuous slab or two-way spanning slab continuous over one long side	1.3	18	26
Interior span of beam or one-way or two-way spanning slab	1.5	20	30
Slab supported on columns without beams (flat slab)(based on longer span)	1.2	17	24
Cantilever	0.4	6	8

Compare Actual and Allowable L/d Ratios

$$\left(L/d\right)_{ACTUAL} \le \left(L/d\right)_{ALLOWABLE}$$

$L =$ 2000.0 mm $(L/d)_{ACTUAL} =$ 24.48

$d =$ 81.7 mm

eq. 1

$$\left(L/d\right)_{ALLOWABLE} = K\left[11 + 1.5\sqrt{f_c'} \cdot \frac{\rho_o}{\rho} + 3.2\sqrt{f_c'} \cdot \left(\frac{\rho_o}{\rho} - 1\right)^{3/2}\right] \cdot k_1 \cdot k_2 \cdot k_3$$

eq. 2

$$\left(L/d\right)_{ALLOWABLE} = K\left[11 + 1.5\sqrt{f_c'} \cdot \frac{\rho_o}{\rho - \rho'} + \frac{1}{12}\sqrt{f_c'} \cdot \sqrt{\frac{\rho'}{\rho_o}}\right] \cdot k_1 \cdot k_2 \cdot k_3$$

$f'_c =$ 38.0 MPa

$\rho_o =$ 0.006

ρ [%]	0.2	0.4	0.6	0.8	1.0	1.2	1.4	1.6	1.8	2.0	2.2	2.4
A_s [mm^2]	138.9	227.1	416.7	555.6	694.5	833.3	972.2	1111.1	1250.0	1388.9	1527.8	1666.7
A'_s [mm^2]	0.0	0.0	0.0	0.0	0.0	0.0	0.0	0.0	0.0	0.0	0.0	0.0
$\rho = A_s/bd$ [-]	0.002	0.003	0.006	0.008	0.010	0.012	0.014	0.016	0.018	0.020	0.022	0.024
$\rho' = A'_s/bd$ [-]	0.00	0.00	0.00	0.00	0.00	0.00	0.00	0.00	0.00	0.00	0.00	0.00
eq. ?	1	1	1	2	2	2	2	2	2	2	2	2
k_1	1.0	1.0	1.0	1.0	1.0	1.0	1.0	1.0	1.0	1.0	1.0	1.0
k_2	1.0	1.0	1.0	1.0	1.0	1.0	1.0	1.0	1.0	1.0	1.0	1.0
k_3	1.0	1.0	1.0	1.0	1.0	1.0	1.0	1.0	1.0	1.0	1.0	1.0
K	1.0	1.0	1.0	1.0	1.0	1.0	1.0	1.0	1.0	1.0	1.0	1.0
$(L/d)_{ALLOWABLE}$	39.50	28.43	20.50	18.13	16.70	15.75	15.07	14.56	14.17	13.85	13.59	13.38
Serviceable ?	OK	OK	NO	NO	NO	NO	NO	NO	NO	NO	NO	NO

Data obtianed from Article: "Tension Stiffening in Lightly Reinforced Concrete Slabs" by R.I. Gilbert
Journal of Structural Engineering (ASCE) June 2007

SLAB: SS2

Obtain the Allowable L/d ratio according to BS 8110, clause 3.4.6

Slab Panel Parameters:

Material Properties:

f'_c = 38.0 MPa
f_c = 47.50 MPa
f_t = 4.42 MPa
E_c = 27.47 GPa
f_y = 500.0 MPa

Wide Beam:

b = 850.0 mm
L = 2000.0 mm
d = 81.7 mm
d' = 20.3 mm
h = 102.0 mm

Provided Reinforcement:

ρ [%]	0.2	0.3	0.6	0.8	1.0	1.2	1.4	1.6	1.8	2.0	2.2	2.4
A_s [mm^2]	138.9	227.1	416.7	555.6	694.5	833.3	972.2	1111.1	1250.0	1388.9	1527.8	1666.7

A'_s [mm^2]	0.0

Allowable Span/Depth Ratio compared to the Actual Span/Depth Ratio:

Step 1: Basic span/depth ratio for rectangular beams

Support Condition	Rectangular Section	Flanged Section $b_w/b \leq 0.3$
Simply Supported	20	16

L > 10.0 m ? FALSE

Condition	
TRUE	k_1 = 10/L
FALSE	k_1 = 1.0

k_1 = 1.0

Step 2: Modification of span/depth ratio due to tension reinforcement

Design Service Stress:

assume that the ratio required tension reinforcement and provided tension reinforcement is 1.0

$A_{s,req}$ = $A_{s,prov}$ = 1.0

assume the normal partial load combination factors apply

γ_1 = 1.1
γ_2 = 1.0
γ_3 = 1.2
γ_4 = 1.6

assume no moment redistribution occurs

β_b = 1.0

$$f_s = \frac{5f_y}{8} \cdot \frac{A_{s,req}}{A_{s,prov}} \cdot \frac{1}{\beta_b}$$

f_y = 500.0 MPa

f_s = 312.5 MPa

Calculate the Design Ultimate Bending Moment (SABS 0100-1, clause 4.3.3.4):

assume only tension reinforcement is required, therefore $K \leq K'$

assume z = 0.95d

therefore $$M = A_s\left(0.87 f_y \cdot 0.95 d\right)$$

f_y = 500.0 MPa
d = 81.7 mm

ρ [%]	0.2	0.4	0.6	0.8	1.0	1.2	1.4	1.6	1.8	2.0	2.2	2.4
A_s [mm^2]	138.9	227.1	416.7	555.6	694.5	833.3	972.2	1111.1	1250.0	1388.9	1527.8	1666.7
M [kNm]	4.69	7.67	14.07	18.76	23.45	28.14	32.82	37.51	42.20	46.89	51.58	56.27

<u>1st Iteration:</u>

check assumption $$K = \frac{M}{bd^2 f_c}$$

b = 850.0 mm
f_c = 47.50 MPa
d = 81.70 mm

ρ [%]	0.2	0.4	0.6	0.8	1.0	1.2	1.4	1.6	1.8	2.0	2.2	2.4
A_s [mm^2]	138.89	227.09	416.67	555.56	694.45	833.34	972.23	1111.12	1250.01	1388.90	1527.79	1666.68
K [-]	0.0174	0.0284	0.0522	0.0696	0.0870	0.1044	0.1218	0.1392	0.1566	0.1740	0.1914	0.2088

$$z = d\left\{0.5 + \sqrt{0.25 - \frac{K}{0.9}}\right\} \leq 0.95d \qquad M = A_s\left(0.87 f_y \cdot 0.95 d\right)$$

ρ [%]	0.2	0.4	0.6	0.8	1.0	1.2	1.4	1.6	1.8	2.0	2.2	2.4
A_s [mm^2]	138.9	227.1	416.7	555.6	694.5	833.3	972.2	1111.1	1250.0	1388.9	1527.8	1666.7
z [mm]	0.980	0.967	0.938	0.916	0.892	0.866	0.839	0.809	0.776	0.738	0.693	0.634
> 0.95d	0.95	0.95	0.94	0.92	0.89	0.87	0.84	0.81	0.78	0.74	0.69	0.63
M [kNm]	4.69	7.67	13.89	18.08	22.00	25.65	28.98	31.94	34.46	36.43	37.64	37.56

<u>2nd Iteration:</u>

check assumption $$K = \frac{M}{bd^2 f_c}$$

b = 850.0 mm
f_c = 47.50 MPa
d = 81.70 mm

ρ [%]	0.2	0.4	0.6	0.8	1.0	1.2	1.4	1.6	1.8	2.0	2.2	2.4
A_s [mm^2]	138.89	227.09	416.67	555.56	694.45	833.34	972.23	1111.12	1250.01	1388.90	1527.79	1666.68
K [-]	0.0174	0.0284	0.0516	0.0671	0.0816	0.0952	0.1075	0.1185	0.1279	0.1352	0.1397	0.1394

$$z = d\left\{0.5 + \sqrt{0.25 - \frac{K}{0.9}}\right\} \leq 0.95d \qquad M = A_s\left(0.87 f_y \cdot 0.95 d\right)$$

ρ [%]	0.2	0.4	0.6	0.8	1.0	1.2	1.4	1.6	1.8	2.0	2.2	2.4
A_s [mm^2]	138.9	227.1	416.7	555.6	694.5	833.3	972.2	1111.1	1250.0	1388.9	1527.8	1666.7
z [mm]	0.980	0.967	0.939	0.919	0.899	0.880	0.861	0.844	0.829	0.816	0.808	0.808
> 0.95d	0.95	0.95	0.94	0.92	0.90	0.88	0.86	0.84	0.83	0.82	0.81	0.81
M [kNm]	4.69	7.67	13.90	18.14	22.19	26.06	29.76	33.33	36.81	40.27	43.87	47.89

<u>3rd Iteration:</u>

check assumption $$K = \frac{M}{bd^2 f_c}$$

b = 850.0 mm
f_c = 47.50 MPa
d = 81.70 mm

ρ [%]	0.2	0.4	0.6	0.8	1.0	1.2	1.4	1.6	1.8	2.0	2.2	2.4
A_s [mm^2]	138.89	227.09	416.67	555.56	694.45	833.34	972.23	1111.12	1250.01	1388.90	1527.79	1666.68
K [-]	0.0174	0.0284	0.0516	0.0673	0.0823	0.0967	0.1104	0.1237	0.1366	0.1494	0.1628	0.1777

$$z = d\left\{0.5 + \sqrt{0.25 - \frac{K}{0.9}}\right\} \leq 0.95d \qquad M = A_s\left(0.87 f_y \cdot 0.95 d\right)$$

ρ [%]	0.2	0.4	0.6	0.8	1.0	1.2	1.4	1.6	1.8	2.0	2.2	2.4
A_s [mm^2]	138.9	227.1	416.7	555.6	694.5	833.3	972.2	1111.1	1250.0	1388.9	1527.8	1666.7
z [mm]	0.980	0.967	0.939	0.919	0.898	0.878	0.857	0.836	0.813	0.790	0.763	0.729
> 0.95d	0.95	0.95	0.94	0.92	0.90	0.88	0.86	0.84	0.81	0.79	0.76	0.73
M [kNm]	4.69	7.67	13.90	18.14	22.17	25.99	29.60	32.99	36.14	38.98	41.43	43.20

<u>4th Iteration:</u>

check assumption $$K = \frac{M}{bd^2 f_c}$$

b = 850.0 mm
f_c = 47.50 MPa
d = 81.70 mm

ρ [%]	0.2	0.4	0.6	0.8	1.0	1.2	1.4	1.6	1.8	2.0	2.2	2.4
A_s [mm^2]	138.89	227.09	416.67	555.56	694.45	833.34	972.23	1111.12	1250.01	1388.90	1527.79	1666.68
K [-]	0.0174	0.0284	0.0516	0.0673	0.0823	0.0964	0.1099	0.1224	0.1341	0.1446	0.1537	0.1603

$$z = d\left\{0.5 + \sqrt{0.25 - \frac{K}{0.9}}\right\} \leq 0.95d \qquad M = A_s\left(0.87 f_y \cdot 0.95d\right)$$

ρ [%]	0.2	0.4	0.6	0.8	1.0	1.2	1.4	1.6	1.8	2.0	2.2	2.4
A_s [mm^2]	138.9	227.1	416.7	555.6	694.5	833.3	972.2	1111.1	1250.0	1388.9	1527.8	1666.7
z [mm]	0.980	0.967	0.939	0.919	0.898	0.878	0.858	0.838	0.818	0.799	0.781	0.768
> 0.95d	0.95	0.95	0.94	0.92	0.90	0.88	0.86	0.84	0.82	0.80	0.78	0.77
M [kNm]	4.69	7.67	13.90	18.14	22.17	26.00	29.64	33.08	36.33	39.43	42.43	45.50

5th Iteration:

check assumption

$$K = \frac{M}{bd^2 f_c}$$

b = 850.0 mm
f_c = 47.50 MPa
d = 81.70 mm

ρ [%]	0.2	0.4	0.6	0.8	1.0	1.2	1.4	1.6	1.8	2.0	2.2	2.4
A_s [mm^2]	138.89	227.09	416.67	555.56	694.45	833.34	972.23	1111.12	1250.01	1388.90	1527.79	1666.68
K [-]	0.0174	0.0284	0.0516	0.0673	0.0823	0.0965	0.1100	0.1227	0.1348	0.1463	0.1574	0.1688

$$z = d\left\{0.5 + \sqrt{0.25 - \frac{K}{0.9}}\right\} \leq 0.95d \qquad M = A_s\left(0.87 f_y \cdot 0.95d\right)$$

ρ [%]	0.2	0.4	0.6	0.8	1.0	1.2	1.4	1.6	1.8	2.0	2.2	2.4
A_s [mm^2]	138.9	227.1	416.7	555.6	694.5	833.3	972.2	1111.1	1250.0	1388.9	1527.8	1666.7
z [mm]	0.980	0.967	0.939	0.919	0.898	0.878	0.858	0.837	0.817	0.796	0.774	0.750
> 0.95d	0.95	0.95	0.94	0.92	0.90	0.88	0.86	0.84	0.82	0.80	0.77	0.75
M [kNm]	4.69	7.67	13.90	18.14	22.17	26.00	29.63	33.06	36.28	39.28	42.02	44.41

5th Iteration:

check assumption

$$K = \frac{M}{bd^2 f_c}$$

b = 850.0 mm
f_c = 47.50 MPa
d = 81.70 mm

ρ [%]	0.2	0.4	0.6	0.8	1.0	1.2	1.4	1.6	1.8	2.0	2.2	2.4
A_s [mm^2]	138.89	227.09	416.67	555.56	694.45	833.34	972.23	1111.12	1250.01	1388.90	1527.79	1666.68
K [-]	0.0174	0.0284	0.0516	0.0673	0.0823	0.0965	0.1099	0.1227	0.1346	0.1457	0.1559	0.1648

$$z = d\left\{0.5 + \sqrt{0.25 - \frac{K}{0.9}}\right\} \leq 0.95d \qquad M = A_s\left(0.87 f_y \cdot 0.95d\right)$$

ρ [%]	0.2	0.4	0.6	0.8	1.0	1.2	1.4	1.6	1.8	2.0	2.2	2.4
A_s [mm^2]	138.9	227.1	416.7	555.6	694.5	833.3	972.2	1111.1	1250.0	1388.9	1527.8	1666.7
z [mm]	0.980	0.967	0.939	0.919	0.898	0.878	0.858	0.837	0.817	0.797	0.777	0.759
> 0.95d	0.95	0.95	0.94	0.92	0.90	0.88	0.86	0.84	0.82	0.80	0.78	0.76
M [kNm]	4.69	7.67	13.90	18.14	22.17	26.00	29.63	33.06	36.29	39.33	42.19	44.94

Modification Factor k_2:

$$k_2 = 0.55 + \frac{(477 - f_s)}{120\left(0.9 + \frac{M}{bd^2}\right)} \leq 2.0$$

b = 850.0 mm
d = 81.7 mm
f_s = 312.5 MPa

ρ [%]	0.2	0.4	0.6	0.8	1.0	1.2	1.4	1.6	1.8	2.0	2.2	2.4
A_s [mm^2]	138.9	227.1	416.7	555.6	694.5	833.3	972.2	1111.1	1250.0	1388.9	1527.8	1666.7
M [kNm]	4.69	7.67	13.90	18.14	22.17	26.00	29.63	33.06	36.29	39.33	42.19	44.94
k_2	1.34	1.16	0.96	0.88	0.84	0.80	0.77	0.75	0.74	0.73	0.71	0.71
> 2.0	1.34	1.16	0.96	0.88	0.84	0.80	0.77	0.75	0.74	0.73	0.71	0.71

Step 4: Deflection due to creep and shrinkage

assume normal creep and shrinkage occurs and is accounted for from step 1 to 3

therefore k_4 = 1.00

Step 5: Span/depth ratio for flanged beams

beam is rectangular and not flanged, step 5 is not applicable

therefore k_5 = 1.00

Compare Actual and Allowable L/d Ratios

$$\left(L/d\right)_{ACTUAL} \leq \left(L/d\right)_{ALLOWABLE} \cdot k_1 \cdot k_2 \cdot k_3 \cdot k_4 \cdot k_5$$

L = 2000.0 mm $\quad$ $(L/d)_{ACTUAL}$ = 24.48

d = 81.7 mm

$(L/d)_{BASIS}$ = 20

ρ [%]	0.2	0.4	0.6	0.8	1.0	1.2	1.4	1.6	1.8	2.0	2.2	2.4
A_s [mm^2]	138.9	227.1	416.7	555.6	694.5	833.3	972.2	1111.1	1250.0	1388.9	1527.8	1666.7
k_1	1.0	1.0	1.0	1.0	1.0	1.0	1.0	1.0	1.0	1.0	1.0	1.0
k_2	1.3	1.2	1.0	0.9	0.8	0.8	0.8	0.8	0.7	0.7	0.7	0.7
k_3	1.0	1.0	1.0	1.0	1.0	1.0	1.0	1.0	1.0	1.0	1.0	1.0
k_4	1.0	1.0	1.0	1.0	1.0	1.0	1.0	1.0	1.0	1.0	1.0	1.0
k_5	1.0	1.0	1.0	1.0	1.0	1.0	1.0	1.0	1.0	1.0	1.0	1.0
$(L/d)_{ALLOWABLE}$	26.88	23.18	19.18	17.69	16.70	16.00	15.48	15.08	14.76	14.50	14.29	14.11
Serviceable ?	OK	NO	NO	NO	NO	NO	NO	NO	NO	NO	NO	NO

Data obtianed from Article: "Tension Stiffening in Lightly Reinforced Concrete Slabs" by R.I. Gilbert
Journal of Structural Engineering (ASCE) June 2007

SLAB: SS2

Obtain the Allowable L/d ratio according to ACI 318, Chapter 9, Clause 9.5

Slab Panel Parameters:

Material Properties:

f'_c = 38.0 MPa
f_c = 47.50 MPa
f_t = 4.42 MPa
E_c = 27.47 GPa
f_y = 500.0 MPa

Wide Beam:

b = 850.0 mm
L = 2000.0 mm
d = 81.7 mm
d' = 20.3 mm
h = 102.0 mm

Provided Reinforcement:

ρ [%]	0.2	0.3	0.6	0.8	1.0	1.2	1.4	1.6	1.8	2.0	2.2	2.4
A_s [mm^2]	138.9	227.1	416.7	555.6	694.5	833.3	972.2	1111.1	1250.0	1388.9	1527.8	1666.7

A'_s [mm^2]	0.0

Allowable Span/Depth Ratio compared to the Actual Span/Depth Ratio:

One-way Construction (Nonprestressed): (clause 9.5.2)

L/h Ratios for Nonprestresses Beams or One-way Slabs				
	Simply-Supported	One End Continuous	Both Ends Continuous	Cantilever
Member	Members not supporting or attached to partitions or other construction likely to be damaged by large deflections.			
Solid one-way slabs	20	24	28	10
Beams or ribbed one-way slabs	16	18.5	21	8

Two-way Construction (Nonprestressed): (clause 9.5.3)

L_n/h Ratios for Nonprestressed Slabs without Interior Beam						
Yield Stength	Without Drop Panels			With Drop Panels		
	Exterior Panels		Interior Panels	Exterior Panels		Interior Panels
f_y [MPa]	Without Edge Beams	With Edge Beams		Without Edge Beams	With Edge Beams	
300.0	33	36	36	36	40	40
420.0	30	33	33	33	36	36
520.0	28	31	31	31	34	34

For slabs without interior beams spanning between the supports and having ratio of long to short span not greater than 2, the minimum thickness shall be in accordance with the provision as stated above for two-way construction.

Consider the L/h ratio for One-way Construction

Compare Actual and Allowable L/d Ratios

$$\left(\frac{L}{h}\right)_{ACTUAL} \leq \left(\frac{L}{h}\right)_{ALLOWABLE}$$

L = 2000.0 mm (L/h)$_{ACTUAL}$ = 19.61
h = 102.0 mm

(L/h)$_{BASIS}$ = 20

ρ [%]	0.2	0.4	0.6	0.8	1.0	1.2	1.4	1.6	1.8	2.0	2.2	2.4
A_s [mm^2]	138.9	227.1	416.7	555.6	694.5	833.3	972.2	1111.1	1250.0	1388.9	1527.8	1666.7
(L/h)$_{ALLOWABLE}$	20.00	20.00	20.00	20.00	20.00	20.00	20.00	20.00	20.00	20.00	20.00	20.00
Serviceable ?	OK	OK	OK	OK	OK	OK	OK	OK	OK	OK	OK	OK

Predicted Results from Design Codes

ρ [%]	SABS 0100		EC2		BS 8110		ACI 318		Allowable	Allowable	% diff
	Actual	Allowable	Actual	Allowable	Actual	Allowable	Actual	Allowable	MAX	MIN	
0.20	24.48	20.44	24.48	39.50	24.48	26.88	19.61	20.00	39.50	20.44	48.25%
0.40	24.48	17.73	24.48	28.43	24.48	23.18	19.61	20.00	28.43	17.73	37.65%
0.60	24.48	14.80	24.48	20.50	24.48	19.18	19.61	20.00	20.50	14.80	27.81%
0.80	24.48	13.71	24.48	18.13	24.48	17.69	19.61	20.00	18.13	13.71	24.38%
1.00	24.48	12.98	24.48	16.70	24.48	16.70	19.61	20.00	16.70	12.98	22.28%
1.20	24.48	12.47	24.48	15.75	24.48	16.00	19.61	20.00	16.00	12.47	22.09%
1.40	24.48	12.08	24.48	15.07	24.48	15.48	19.61	20.00	15.48	12.08	21.93%
1.60	24.48	11.79	24.48	14.56	24.48	15.08	19.61	20.00	15.08	11.79	21.81%
1.80	24.48	11.55	24.48	14.17	24.48	14.76	19.61	20.00	14.76	11.55	21.70%
2.00	24.48	11.37	24.48	13.85	24.48	14.50	19.61	20.00	14.50	11.37	21.61%
2.20	24.48	11.21	24.48	13.59	24.48	14.29	19.61	20.00	14.29	11.21	21.54%
2.40	24.48	11.08	24.48	13.38	24.48	14.11	19.61	20.00	14.11	11.08	21.47%

Allowable Maximum: Maximum value taken from SABS 0100, EC2 and BS 8110. The values of the ACI 318 not included because the ACI 318 considered a L/h ratio and not a L/d ratio.

Allowable Maximum: Minimum value taken from SABS 0100, EC2 and BS 8110. The values of the ACI 318 not included because the ACI 318 considered a L/h ratio and not a L/d ratio.

% diff: $\%diff = (AllowableMAX - AllowableMIN) / AllowableMAX$

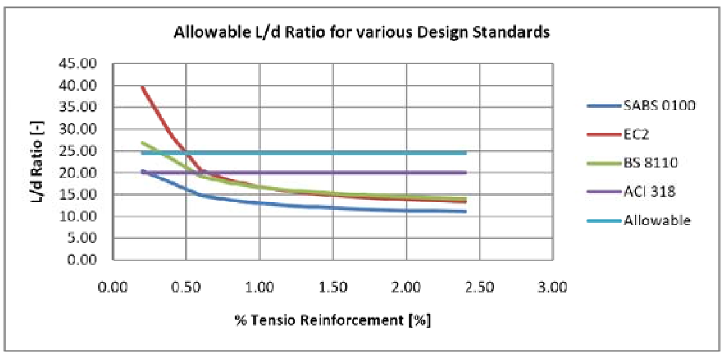

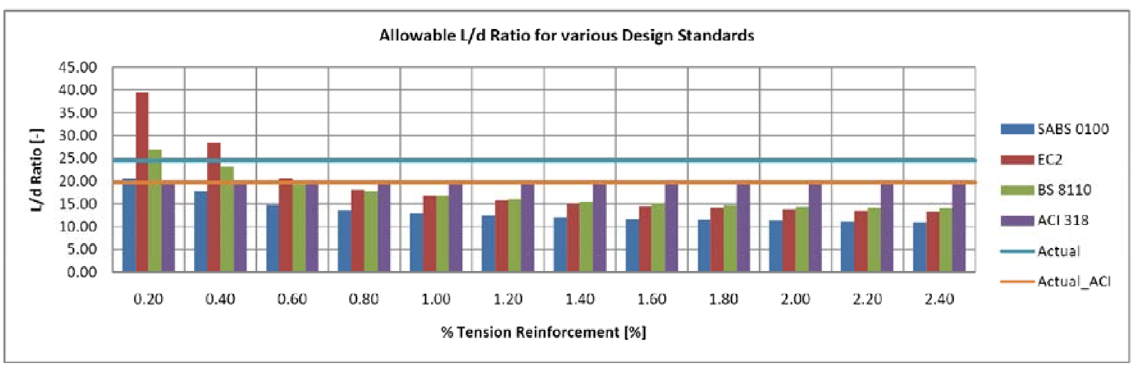

APPENDIX C

Calculations to obtain short-term deflection using the SABS 0100-1 (2000) for the one-way slab specimens as presented by Gilbert (2007) are presented in this appendix.

Initial Defleciton according to SABS 0100-1, Annexure A, Clause A.2.4

Slab Number = S1 (select slab number from drop-down menue)

h =	110.0	mm
L =	3500.0	mm
d =	92.0	mm
d' =	18.0	mm
b =	850.0	mm
A_s =	141.0	mm^2
f_c =	46.6	MPa
E_c =	26.8	GPa
E_s =	200.0	GPa

M_{cr} = 5.93 kNm

Applied Moment

M_a = 1.10 M_{cr}

= 6.52 kNm

(select M_a using drop-down menue)

* Determine K for Bending Moment Diagram

K = 0.1040

* Modulus of Rupture: (for unrestrained slabs)

$$f_r = 0.65\sqrt{f_c}$$

f_r = 4.44 MPa

Critical Positive Moment Section:

Cracking Moment:

$$M_{cr} = \frac{f_r I_g}{y_t}$$

I_g = 9.43E+07 mm^4

y_t = 55.0 mm

M_{cr} = 7.6 kNm

Momenf of Inertia of Cracked Section:

(change x_{cr_1} until $x_{cr\_1} = x_{cr\_2}$)

$$x_{cr\_1} = \frac{\frac{1}{2} x_{cr\_2}{}^2 b + A_s d \alpha_e}{x_{cr\_2} b + A_s \alpha_e}$$

where $\alpha_e = \frac{E_s}{E_c}$

x_{cr_1} =	13.9	mm
b =	850.0	mm
A_s =	141.0	mm^2
d =	92.0	mm
E_s =	200.0	GPa
E_c =	26.8	GPa
α_e =	7.5	
x_{cr_2} =	13.9	mm

$$I_{cr} = \tfrac{1}{3} b x_{cr}{}^3 + A_s (d - x_{cr})^2 \alpha_e$$

I_{cr} = 7.2E+06 mm^4

$$I_e = \left(\frac{M_{cr}}{M_a}\right)^3 I_g + \left[1 - \left(\frac{M_{cr}}{M_a}\right)^3\right] I_{cr}$$

M_a = 6.52 kNm

I_e = 1.5E+08 mm^4

I_e > I_g Section is Uncracked

then I_e = 1.5E+08 mm^4

* Initial Deflection: Δ_i

$$\Delta_i = KM_a \frac{L^2}{E_c I_e}$$

K = 0.104

M_a = 6.52 kNm

L = 3500.0 mm

E_c = 26.8 GPa

I_e = 9.4E+07 mm^4

Δ_i = 3.29 mm

Results for all 9 Slabs

SLAB	M_a	Δ_{exp}	Δ_{SABS}	$\Delta_{SABS}/\Delta_{exp}$
S1	$1.1M_{cr}$	8.31	3.29	0.40
	$1.2M_{cr}$	13.2	3.59	0.27
	$1.3M_{cr}$	17.5	4.03	0.23
S2	$1.1M_{cr}$	6.37	3.32	0.52
	$1.2M_{cr}$	8.23	3.62	0.44
	$1.3M_{cr}$	10.8	4.18	0.39
S3	$1.1M_{cr}$	4.78	3.37	0.71
	$1.2M_{cr}$	6.09	3.67	0.60
	$1.3M_{cr}$	9.03	4.36	0.48
S8	$1.1M_{cr}$	6.45	3.57	0.55
	$1.2M_{cr}$	8.48	3.90	0.46
	$1.3M_{cr}$	11.04	4.97	0.45
SS2	$1.1M_{cr}$	3.45	1.98	0.57
	$1.2M_{cr}$	5.13	2.69	0.52
	$1.3M_{cr}$	6.71	3.52	0.52
SS3	$1.1M_{cr}$	2.16	1.93	0.89
	$1.2M_{cr}$	3.49	2.58	0.74
	$1.3M_{cr}$	4.5	3.32	0.74
SS4	$1.1M_{cr}$	2.9	1.91	0.66
	$1.2M_{cr}$	3.83	2.56	0.67
	$1.3M_{cr}$	4.78	3.32	0.69
Z1	$1.1M_{cr}$	3.86	1.23	0.32
	$1.2M_{cr}$	6.18	1.34	0.22
	$1.3M_{cr}$	9.49	1.70	0.18
Z2	$1.1M_{cr}$	2.2	1.24	0.56
	$1.2M_{cr}$	3.21	1.35	0.42
	$1.3M_{cr}$	4.55	1.75	0.38
Z3	$1.1M_{cr}$	3.04	1.25	0.41
	$1.2M_{cr}$	4.03	1.37	0.34
	$1.3M_{cr}$	5.09	1.81	0.36
Z4	$1.1M_{cr}$	2.38	1.28	0.54
	$1.2M_{cr}$	3.45	1.44	0.42
	$1.3M_{cr}$	4.15	1.88	0.45

Data reproduced form article:

Tension Stiffening in Lightly Reinforced Concrete Slabs by RI Gilbert
Journal of Strucutral Engineering (ASCE), June 2007

Data presented as shown in the article

ACI 318			$1.1M_{cr}$			$1.2M_{cr}$			$1.3M_{cr}$		
Slab	M_{cr}	ρ	Δ_{exp}	Δ_{ACI}	$\Delta_{ACI}/\Delta_{exp}$	Δ_{exp}	Δ_{ACI}	$\Delta_{ACI}/\Delta_{exp}$	Δ_{exp}	Δ_{ACI}	$\Delta_{ACI}/\Delta_{exp}$
s1	5.93	0.18%	8.31	3.82	0.46	13.2	5.22	0.40	17.5	6.89	0.39
z1	5.2	0.20%	3.86	1.61	0.42	6.18	2.18	0.35	9.49	2.94	0.31
s2	5.99	0.29%	6.37	3.79	0.59	8.23	5.11	0.62	10.8	6.66	0.62
ss2	6.7	0.33%	3.45	1.59	0.46	5.13	2.15	0.42	6.71	2.82	0.42
z2	5.25	0.33%	2.20	1.59	0.72	3.21	2.05	0.64	4.55	2.84	0.62
s8	7.38	0.45%	6.45	4.00	0.62	8.48	5.28	0.62	11.04	6.84	0.62
s3	6.07	0.46%	4.78	3.74	0.78	6.09	4.94	0.81	9.03	6.34	0.70
ss4	7.3	0.48%	2.90	1.50	0.52	3.83	2.01	0.52	4.78	2.61	0.55
ss3	7.4	0.49%	2.16	1.49	0.69	3.49	1.98	0.57	4.5	2.65	0.59
z3	5.32	0.52%	3.04	1.59	0.52	4.03	2.1	0.52	5.09	2.72	0.53
z4	6.05	0.84%	2.38	1.59	0.67	3.45	2.07	0.60	4.15	2.63	0.63
MEAN					0.59			0.55			0.54

Data presented as shown in the article

Eurocode 2			$1.1M_{cr}$			$1.2M_{cr}$			$1.3M_{cr}$		
Slab	M_{cr}	ρ	Δ_{exp}	Δ_{EC2}	$\Delta_{EC2}/\Delta_{exp}$	Δ_{exp}	Δ_{EC2}	$\Delta_{EC2}/\Delta_{exp}$	Δ_{exp}	Δ_{EC2}	$\Delta_{EC2}/\Delta_{exp}$
s1	5.93	0.18%	8.31	9.21	1.11	13.2	15.1	1.14	17.5	20.5	1.17
z1	5.2	0.20%	3.86	3.70	0.96	6.18	6.21	1.00	9.49	8.66	0.91
s2	5.99	0.29%	6.37	7.08	1.11	8.23	11	1.34	10.8	14.70	1.36
ss2	6.7	0.33%	3.45	3.00	0.87	5.13	4.71	0.92	6.71	6.31	0.94
z2	5.25	0.33%	2.20	2.98	1.35	3.21	4.47	1.39	4.55	6.16	1.35
s8	7.38	0.45%	6.45	6.30	0.98	8.48	10.1	1.19	11.04	13.20	1.20
s3	6.07	0.46%	4.78	5.72	1.20	6.09	8.42	1.38	9.03	11.00	1.22
ss4	7.3	0.48%	2.90	2.44	0.84	3.83	3.7	0.97	4.78	4.87	1.02
ss3	7.4	0.49%	2.16	2.30	1.06	3.49	3.43	0.98	4.5	4.49	1.00
z3	5.32	0.52%	3.04	2.43	0.80	4.03	3.55	0.88	5.09	4.65	0.91
z4	6.05	0.84%	2.38	2.15	0.90	3.45	3.13	0.91	4.15	3.85	0.93
MEAN					1.02			1.10			1.09

Data presented as shown in the article

BS 8110			$1.1M_{cr}$			$1.2M_{cr}$			$1.3M_{cr}$		
Slab	M_{cr}	ρ	Δ_{exp}	Δ_{BS}	Δ_{BS}/Δ_{exp}	Δ_{exp}	Δ_{BS}	Δ_{BS}/Δ_{exp}	Δ_{exp}	Δ_{BS}	Δ_{BS}/Δ_{exp}
s1	5.93	0.18%	8.31	20.30	2.44	13.2	23.7	1.80	17.5	26.9	0.54
z1	5.2	0.20%	3.86	7.08	1.83	6.18	8.21	1.33	9.49	9.35	0.01
s2	5.99	0.29%	6.37	14.50	2.28	8.23	16.7	2.03	10.8	19.00	0.76
ss2	6.7	0.33%	3.45	7.21	2.09	5.13	8.72	1.70	6.71	9.16	0.37
z2	5.25	0.33%	2.20	5.04	2.29	3.21	5.82	1.81	4.55	6.62	0.45
s8	7.38	0.45%	6.45	14.10	2.19	8.48	16	1.89	11.04	17.90	0.62
s3	6.07	0.46%	4.78	10.90	2.28	6.09	12.4	2.04	9.03	14.00	0.55
ss4	7.3	0.48%	2.90	5.42	1.87	3.83	6.16	1.61	4.78	6.89	0.44
ss3	7.4	0.49%	2.16	5.09	2.36	3.49	5.76	1.65	4.5	6.44	0.43
z3	5.32	0.52%	3.04	3.78	1.24	4.03	4.34	1.08	5.09	4.91	0.04
z4	6.05	0.84%	2.38	3.39	1.42	3.45	3.84	1.11	4.15	4.29	0.03
MEAN					2.03			1.64			0.39

APPENDIX D

The calculations are similar to the calculations of Appendix A, to obtain the values as shown in this appendix. The reinforced concrete beam dimensions are kept constant while the percentage tension reinforcement is varied. Refer to the data disks for more calculation detail.

Predicted Results from Design Codes

		SABS 0100-1		EC2		BS 8110		ACI 318		Uncracked Section		Uncracked Section		Cracked Section	
p [%]		0.18		0.18		0.18		0.18		I_g (SABS)		I_u (EC2)		I_{cr} (EC2)	
M_{cr}/M_s [-]	M_s/M_{cr} [-]	I_e [mm^4]	$1/r_i$ [10^6 mm^{-1}]	I_e [mm^4]	$1/r_i$ [10^6 mm^{-1}]	I_e [mm^4]	$1/r_i$ [10^6 mm^{-1}]	I_e [mm^4]	$1/r_i$ [10^6 mm^{-1}]	I_e [mm^4]	$1/r_i$ [10^6 mm^{-1}]	I_e [mm^4]	$1/r_i$ [10^6 mm^{-1}]	I_e [mm^4]	$1/r_i$ [10^6 mm^{-1}]
0.00	0.00	7.1E+07	0.00	7.1E+07	0.00	7.1E+07	0.00	7.1E+07	0.00	7.1E+07	0.00	7.1E+07	0.00	4.0E+06	0.00
5.00	0.20	7.1E+07	0.66	7.1E+07	0.53	7.1E+07	0.56	7.1E+07	0.57	7.1E+07	0.66	7.1E+07	0.51	4.0E+06	9.40
2.50	0.40	7.1E+07	1.33	7.1E+07	1.06	7.1E+07	1.11	7.1E+07	1.14	7.1E+07	1.33	7.1E+07	1.03	4.0E+06	18.81
1.67	0.60	7.1E+07	1.99	7.1E+07	1.60	4.0E+06	5.73	7.1E+07	1.70	7.1E+07	1.99	7.1E+07	1.54	4.0E+06	28.21
1.25	0.80	7.1E+07	2.65	7.1E+07	2.13	4.0E+06	15.54	7.1E+07	2.27	7.1E+07	2.65	7.1E+07	2.05	4.0E+06	37.61
1.00	1.00	7.1E+07	3.32	7.1E+07	2.66	4.0E+06	25.36	7.1E+07	2.84	7.1E+07	3.32	7.1E+07	2.56	4.0E+06	47.01
0.83	1.20	4.3E+07	6.60	1.2E+07	19.46	4.0E+06	35.18	4.3E+07	5.66	7.1E+07	3.98	7.1E+07	3.08	4.0E+06	56.42
0.71	1.40	2.8E+07	11.58	7.8E+06	34.14	4.0E+06	44.99	2.8E+07	9.93	7.1E+07	4.64	7.1E+07	3.59	4.0E+06	65.82
0.63	1.60	2.0E+07	18.47	6.4E+06	47.50	4.0E+06	54.81	2.0E+07	15.82	7.1E+07	5.30	7.1E+07	4.10	4.0E+06	75.22
0.56	1.80	1.5E+07	27.28	5.7E+06	59.98	4.0E+06	64.63	1.5E+07	23.38	7.1E+07	5.97	7.1E+07	4.61	4.0E+06	84.62
0.50	2.00	1.2E+07	37.91	5.3E+06	71.85	4.0E+06	74.44	1.2E+07	32.48	7.1E+07	6.63	7.1E+07	5.13	4.0E+06	94.03
0.45	2.20	1.0E+07	50.09	5.0E+06	83.27	4.0E+06	84.26	1.0E+07	42.92	7.1E+07	7.29	7.1E+07	5.64	4.0E+06	103.43
0.42	2.40	8.9E+06	63.52	4.8E+06	94.35	4.0E+06	94.07	8.9E+06	54.43	7.1E+07	7.96	7.1E+07	6.15	4.0E+06	112.83
0.38	2.60	7.8E+06	77.86	4.7E+06	105.17	4.0E+06	103.89	7.8E+06	66.72	7.1E+07	8.62	7.1E+07	6.66	4.0E+06	122.23
0.36	2.80	7.1E+06	92.82	4.6E+06	115.80	4.0E+06	113.71	7.1E+06	79.54	7.1E+07	9.28	7.1E+07	7.18	4.0E+06	131.64
0.33	3.00	6.5E+06	108.13	4.5E+06	126.25	4.0E+06	123.52	6.5E+06	92.66	7.1E+07	9.95	7.1E+07	7.69	4.0E+06	141.04
0.31	3.20	6.1E+06	123.60	4.5E+06	136.58	4.0E+06	133.34	6.1E+06	105.92	7.1E+07	10.61	7.1E+07	8.20	4.0E+06	150.44
0.29	3.40	5.7E+06	139.08	4.4E+06	146.80	4.0E+06	143.16	5.7E+06	119.19	7.1E+07	11.27	7.1E+07	8.71	4.0E+06	159.84
0.28	3.60	5.5E+06	154.47	4.4E+06	156.93	4.0E+06	152.97	5.5E+06	132.37	7.1E+07	11.94	7.1E+07	9.23	4.0E+06	169.25

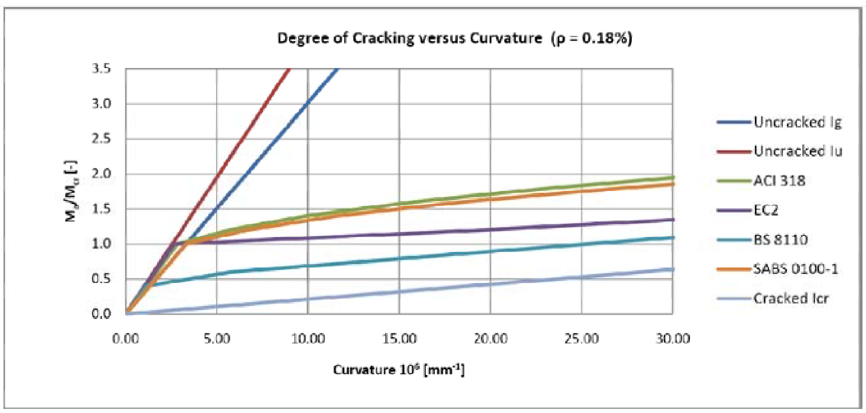

Predicted Results from Design Codes

		SABS 0100-1		EC2		BS 8110		ACI 318		Uncracked Section		Uncracked Section		Cracked Section	
p [%]		0.49		0.49		0.49		0.49		I_g (SABS)		I_u (EC2)		I_{cr} (EC2)	
M_{cr}/M_s [-]	M_s/M_{cr} [-]	I_e [mm^4]	$1/r_i$ [10^6 mm^{-1}]	I_e [mm^4]	$1/r_i$ [10^6 mm^{-1}]	I_e [mm^4]	$1/r_i$ [10^6 mm^{-1}]	I_e [mm^4]	$1/r_i$ [10^6 mm^{-1}]	I_e [mm^4]	$1/r_i$ [10^6 mm^{-1}]	I_e [mm^4]	$1/r_i$ [10^6 mm^{-1}]	I_e [mm^4]	$1/r_i$ [10^6 mm^{-1}]
0.00	0.00	7.1E+07	0.00	7.2E+07	0.00	7.2E+07	0.00	7.1E+07	0.00	7.1E+07	0.00	7.2E+07	0.00	9.6E+06	0.00
5.00	0.20	7.1E+07	0.66	7.2E+07	0.54	7.2E+07	0.55	7.1E+07	0.57	7.1E+07	0.66	7.2E+07	0.50	9.6E+06	4.04
2.50	0.40	7.1E+07	1.33	7.2E+07	1.07	7.2E+07	1.10	7.1E+07	1.14	7.1E+07	1.33	7.2E+07	1.01	9.6E+06	8.08
1.67	0.60	7.1E+07	1.99	7.2E+07	1.61	9.6E+06	3.58	7.1E+07	1.70	7.1E+07	1.99	7.2E+07	1.51	9.6E+06	12.13
1.25	0.80	7.1E+07	2.65	7.2E+07	2.15	9.6E+06	7.71	7.1E+07	2.27	7.1E+07	2.65	7.2E+07	2.02	9.6E+06	16.17
1.00	1.00	7.1E+07	3.32	7.2E+07	2.68	9.6E+06	11.85	7.1E+07	2.84	7.1E+07	3.32	7.2E+07	2.52	9.6E+06	20.21
0.83	1.20	4.5E+07	6.26	2.4E+07	9.65	9.6E+06	15.98	4.5E+07	5.36	7.1E+07	3.98	7.2E+07	3.03	9.6E+06	24.25
0.71	1.40	3.2E+07	10.30	1.7E+07	15.77	9.6E+06	20.11	3.2E+07	8.83	7.1E+07	4.64	7.2E+07	3.53	9.6E+06	28.30
0.63	1.60	2.5E+07	15.31	1.5E+07	21.38	9.6E+06	24.25	2.5E+07	13.12	7.1E+07	5.30	7.2E+07	4.04	9.6E+06	32.34
0.56	1.80	2.0E+07	21.03	1.3E+07	26.64	9.6E+06	28.38	2.0E+07	18.03	7.1E+07	5.97	7.2E+07	4.54	9.6E+06	36.38
0.50	2.00	1.7E+07	27.23	1.2E+07	31.66	9.6E+06	32.52	1.7E+07	23.33	7.1E+07	6.63	7.2E+07	5.05	9.6E+06	40.42
0.45	2.20	1.5E+07	33.66	1.2E+07	36.50	9.6E+06	36.65	1.5E+07	28.85	7.1E+07	7.29	7.2E+07	5.55	9.6E+06	44.47
0.42	2.40	1.4E+07	40.18	1.1E+07	41.20	9.6E+06	40.79	1.4E+07	34.44	7.1E+07	7.96	7.2E+07	6.06	9.6E+06	48.51
0.38	2.60	1.3E+07	46.68	1.1E+07	45.81	9.6E+06	44.92	1.3E+07	40.00	7.1E+07	8.62	7.2E+07	6.56	9.6E+06	52.55
0.36	2.80	1.2E+07	53.09	1.1E+07	50.33	9.6E+06	49.05	1.2E+07	45.50	7.1E+07	9.28	7.2E+07	7.06	9.6E+06	56.59
0.33	3.00	1.2E+07	59.38	1.1E+07	54.79	9.6E+06	53.19	1.2E+07	50.89	7.1E+07	9.95	7.2E+07	7.57	9.6E+06	60.63
0.31	3.20	1.1E+07	65.55	1.0E+07	59.20	9.6E+06	57.32	1.1E+07	56.17	7.1E+07	10.61	7.2E+07	8.07	9.6E+06	64.68
0.29	3.40	1.1E+07	71.58	1.0E+07	63.56	9.6E+06	61.46	1.1E+07	61.34	7.1E+07	11.27	7.2E+07	8.58	9.6E+06	68.72
0.28	3.60	1.1E+07	77.50	1.0E+07	67.89	9.6E+06	65.59	1.1E+07	66.41	7.1E+07	11.94	7.2E+07	9.08	9.6E+06	72.76

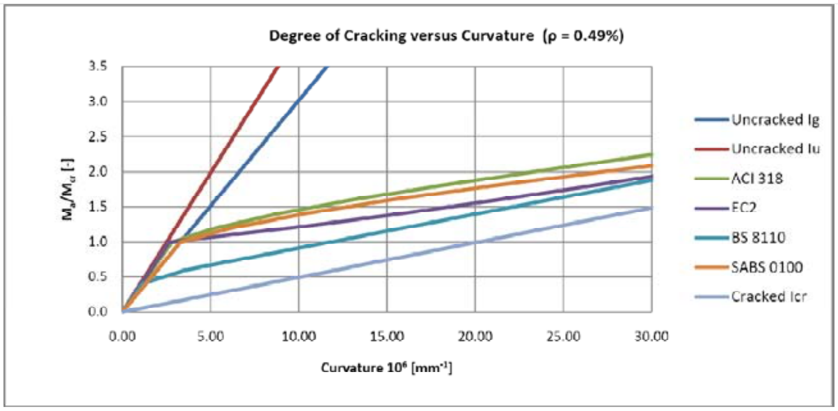

Predicted Results from Design Codes

		SABS 0100-1		EC2		BS 8110		ACI 318		Uncracked Section		Uncracked Section		Cracked Section	
ρ [%]		0.84		0.84		0.84		0.84		I_g (SABS)		I_u (EC2)		I_{cr} (EC2)	
M_{cr}/M_a	M_a/M_{cr}	I_e	$1/r_i$	I_e	$1/r_i$	I_e	$1/r_i$	I_e	$1/r_i$	I_e	$1/r_i$	I_e	$1/r_i$	I_e	$1/r_i$
[-]	[-]	[mm^4]	[10^6 mm^{-1}]	[mm^4]	[10^6 mm^{-1}]	[mm^4]	[10^6 mm^{-1}]	[mm^4]	[10^6 mm^{-1}]	[mm^4]	[10^6 mm^{-1}]	[mm^4]	[10^6 mm^{-1}]	[mm^4]	[10^6 mm^{-1}]
0.00	0.00	7.1E+07	0.00	7.3E+07	0.00	7.3E+07	0.00	7.1E+07	0.00	7.1E+07	0.00	7.3E+07	0.00	1.5E+07	0.00
5.00	0.20	7.1E+07	0.7	7.3E+07	0.5	7.3E+07	0.5	7.1E+07	0.6	7.1E+07	0.66	7.3E+07	0.50	1.5E+07	2.64
2.50	0.40	7.1E+07	1.3	7.3E+07	1.1	7.3E+07	1.1	7.1E+07	1.1	7.1E+07	1.33	7.3E+07	1.00	1.5E+07	5.27
1.67	0.60	7.1E+07	2.0	7.3E+07	1.6	1.5E+07	2.8	7.1E+07	1.7	7.1E+07	1.99	7.3E+07	1.50	1.5E+07	7.91
1.25	0.80	7.1E+07	2.7	7.3E+07	2.2	1.5E+07	5.4	7.1E+07	2.3	7.1E+07	2.65	7.3E+07	2.00	1.5E+07	10.54
1.00	1.00	7.1E+07	3.3	7.3E+07	2.7	1.5E+07	8.1	7.1E+07	2.8	7.1E+07	3.32	7.3E+07	2.50	1.5E+07	13.18
0.83	1.20	4.7E+07	6.0	3.4E+07	7.1	1.5E+07	10.7	4.7E+07	5.1	7.1E+07	3.98	7.3E+07	3.00	1.5E+07	15.82
0.71	1.40	3.5E+07	9.3	2.5E+07	11.0	1.5E+07	13.3	3.5E+07	8.0	7.1E+07	4.64	7.3E+07	3.50	1.5E+07	18.45
0.63	1.60	2.9E+07	13.1	2.2E+07	14.5	1.5E+07	16.0	2.9E+07	11.2	7.1E+07	5.30	7.3E+07	4.00	1.5E+07	21.09
0.56	1.80	2.5E+07	17.2	2.0E+07	17.9	1.5E+07	18.6	2.5E+07	14.7	7.1E+07	5.97	7.3E+07	4.50	1.5E+07	23.72
0.50	2.00	2.2E+07	21.3	1.9E+07	21.1	1.5E+07	21.2	2.2E+07	18.3	7.1E+07	6.63	7.3E+07	5.00	1.5E+07	26.36
0.45	2.20	2.0E+07	25.5	1.8E+07	24.2	1.5E+07	23.9	2.0E+07	21.8	7.1E+07	7.29	7.3E+07	5.50	1.5E+07	29.00
0.42	2.40	1.9E+07	29.5	1.7E+07	27.3	1.5E+07	26.5	1.9E+07	25.3	7.1E+07	7.96	7.3E+07	6.00	1.5E+07	31.63
0.38	2.60	1.8E+07	33.5	1.7E+07	30.2	1.5E+07	29.1	1.8E+07	28.7	7.1E+07	8.62	7.3E+07	6.50	1.5E+07	34.27
0.36	2.80	1.8E+07	37.4	1.7E+07	33.2	1.5E+07	31.8	1.8E+07	32.0	7.1E+07	9.28	7.3E+07	7.00	1.5E+07	36.90
0.33	3.00	1.7E+07	41.1	1.7E+07	36.0	1.5E+07	34.4	1.7E+07	35.2	7.1E+07	9.95	7.3E+07	7.50	1.5E+07	39.54
0.31	3.20	1.7E+07	44.8	1.6E+07	38.9	1.5E+07	37.0	1.7E+07	38.4	7.1E+07	10.61	7.3E+07	8.00	1.5E+07	42.18
0.29	3.40	1.6E+07	48.4	1.6E+07	41.7	1.5E+07	39.7	1.6E+07	41.5	7.1E+07	11.27	7.3E+07	8.50	1.5E+07	44.81
0.28	3.60	1.6E+07	52.0	1.6E+07	44.5	1.5E+07	42.3	1.6E+07	44.6	7.1E+07	11.94	7.3E+07	9.00	1.5E+07	47.45

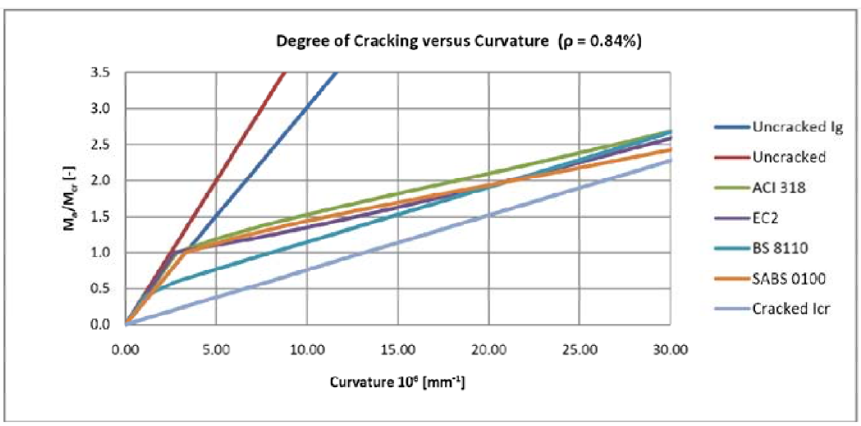

APPENDIX E

The calculations to obtain the values of the moment of inertia are similar to those of Appendix A. The calculations done to identify the Critical M_a/M_{cr} Range, for beam with a percentage tension reinforcement of 0.18%, is presented in this appendix. The calculations for different sections are presented on the data disks.

Predicted Results from Design Codes

		SABS 0100	EC2	BS 8110	ACI 318	I_g (SABS)	I_u (EC2)
ρ [%]		0.18	0.18	0.18	0.18		
M_{cr}/M_a	M_a/M_{cr}	I_e	I_e	I_e	I_e	I_e	I_e
[-]	[-]	[mm^4]	[mm^4]	[mm^4]	[mm^4]	[mm^4]	[mm^4]
10.00	0.10	7.1E+07	7.1E+07	7.1E+07	7.1E+07	7.1E+07	7.1E+07
5.00	0.20	7.1E+07	7.1E+07	7.1E+07	7.1E+07	7.1E+07	7.1E+07
3.33	0.30	7.1E+07	7.1E+07	7.1E+07	7.1E+07	7.1E+07	7.1E+07
2.50	0.40	7.1E+07	7.1E+07	7.1E+07	7.1E+07	7.1E+07	7.1E+07
2.00	0.50	7.1E+07	7.1E+07	4.0E+06	7.1E+07	7.1E+07	7.1E+07
1.67	0.60	7.1E+07	7.1E+07	4.0E+06	7.1E+07	7.1E+07	7.1E+07
1.43	0.70	7.1E+07	7.1E+07	4.0E+06	7.1E+07	7.1E+07	7.1E+07
1.25	0.80	7.1E+07	7.1E+07	4.0E+06	7.1E+07	7.1E+07	7.1E+07
1.11	0.90	7.1E+07	7.1E+07	4.0E+06	7.1E+07	7.1E+07	7.1E+07
1.00	1.00	7.1E+07	7.1E+07	4.0E+06	7.1E+07	7.1E+07	7.1E+07
0.91	1.10	5.4E+07	1.8E+07	4.0E+06	5.4E+07	7.1E+07	7.1E+07
0.83	1.20	4.3E+07	1.2E+07	4.0E+06	4.3E+07	7.1E+07	7.1E+07
0.77	1.30	3.4E+07	9.1E+06	4.0E+06	3.4E+07	7.1E+07	7.1E+07
0.71	1.40	2.8E+07	7.8E+06	4.0E+06	2.8E+07	7.1E+07	7.1E+07
0.67	1.50	2.4E+07	7.0E+06	4.0E+06	2.4E+07	7.1E+07	7.1E+07
0.63	1.60	2.0E+07	6.4E+06	4.0E+06	2.0E+07	7.1E+07	7.1E+07
0.59	1.70	1.8E+07	6.0E+06	4.0E+06	1.8E+07	7.1E+07	7.1E+07
0.56	1.80	1.5E+07	5.7E+06	4.0E+06	1.5E+07	7.1E+07	7.1E+07
0.53	1.90	1.4E+07	5.5E+06	4.0E+06	1.4E+07	7.1E+07	7.1E+07
0.50	2.00	1.2E+07	5.3E+06	4.0E+06	1.2E+07	7.1E+07	7.1E+07
0.48	2.10	1.1E+07	5.1E+06	4.0E+06	1.1E+07	7.1E+07	7.1E+07
0.45	2.20	1.0E+07	5.0E+06	4.0E+06	1.0E+07	7.1E+07	7.1E+07
0.43	2.30	9.5E+06	4.9E+06	4.0E+06	9.5E+06	7.1E+07	7.1E+07
0.42	2.40	8.9E+06	4.8E+06	4.0E+06	8.9E+06	7.1E+07	7.1E+07
0.40	2.50	8.3E+06	4.8E+06	4.0E+06	8.3E+06	7.1E+07	7.1E+07
0.38	2.60	7.8E+06	4.7E+06	4.0E+06	7.8E+06	7.1E+07	7.1E+07
0.37	2.70	7.4E+06	4.6E+06	4.0E+06	7.4E+06	7.1E+07	7.1E+07
0.36	2.80	7.1E+06	4.6E+06	4.0E+06	7.1E+06	7.1E+07	7.1E+07
0.34	2.90	6.8E+06	4.6E+06	4.0E+06	6.8E+06	7.1E+07	7.1E+07
0.33	3.00	6.5E+06	4.5E+06	4.0E+06	6.5E+06	7.1E+07	7.1E+07
0.32	3.10	6.3E+06	4.5E+06	4.0E+06	6.3E+06	7.1E+07	7.1E+07
0.31	3.20	6.1E+06	4.5E+06	4.0E+06	6.1E+06	7.1E+07	7.1E+07
0.30	3.30	5.9E+06	4.4E+06	4.0E+06	5.9E+06	7.1E+07	7.1E+07
0.29	3.40	5.7E+06	4.4E+06	4.0E+06	5.7E+06	7.1E+07	7.1E+07
0.29	3.50	5.6E+06	4.4E+06	4.0E+06	5.6E+06	7.1E+07	7.1E+07
0.28	3.60	5.5E+06	4.4E+06	4.0E+06	5.5E+06	7.1E+07	7.1E+07
0.27	3.70	5.4E+06	4.3E+06	4.0E+06	5.4E+06	7.1E+07	7.1E+07
0.26	3.80	5.3E+06	4.3E+06	4.0E+06	5.3E+06	7.1E+07	7.1E+07
0.26	3.90	5.2E+06	4.3E+06	4.0E+06	5.2E+06	7.1E+07	7.1E+07
0.25	4.00	5.1E+06	4.3E+06	4.0E+06	5.1E+06	7.1E+07	7.1E+07
0.24	4.10	5.0E+06	4.3E+06	4.0E+06	5.0E+06	7.1E+07	7.1E+07

% Difference with reference to the Gross Moment of Inertia of the Beam Section

$$\%diff = \left(I_g - I_e\right)/I_g$$

The %diff of every effective moment of inertia respective to the gross moment of inertia of the section under inspection. % diff is expressed in a percentage form.

The covariance is calculated in columns cov_A and cov_S.
The covariance returns the average of the products of the deviations for each data point pair. This is done to determine the relationship between the two data sets.

The first data set consists of the %diff percentages relative to the Gross Moment of Inertia. The second data set consists of the %diff percentages relative to the Uncracked Moment of Inertia.

cov_A: refers to the covariance where the %diff percentages from all the Design Standards are considered.
cov_S: refers to the covariance where the %diff percentages from only the SABS0100 and EC2 are considered.

It was chosen to include cov_S, because the equations from BS 8110 overestimates the effect of cracking and produces unclear results.

M_a/M_{cr} [-]	SABS 0100 I_e [mm^4]	EC2 I_e [mm^4]	BS 8110 I_e [mm^4]	ACI 318 I_e [mm^4]	I_g [mm^4]	SABS 0100 %diff [%]	EC2 %diff [%]	BS 8110 %diff [%]	ACI 318 %diff [%]	COV_A	COV_S
0.10	7.08E+07	7.14E+07	7.15E+07	7.08E+07	7.08E+07	0.00%	-0.79%	-0.93%	0.00%	0.00%	0.00%
0.20	7.08E+07	7.14E+07	7.15E+07	7.08E+07	7.08E+07	0.00%	-0.79%	-0.93%	0.00%	0.00%	0.00%
0.30	7.08E+07	7.14E+07	7.15E+07	7.08E+07	7.08E+07	0.00%	-0.79%	-0.93%	0.00%	0.00%	0.00%
0.40	7.08E+07	7.14E+07	7.15E+07	7.08E+07	7.08E+07	0.00%	-0.79%	-0.93%	0.00%	0.00%	0.00%
0.50	7.08E+07	7.14E+07	4.04E+06	7.08E+07	7.08E+07	0.00%	-0.79%	94.29%	0.00%	16.63%	0.00%
0.60	7.08E+07	7.14E+07	4.04E+06	7.08E+07	7.08E+07	0.00%	-0.79%	94.29%	0.00%	16.63%	0.00%
0.70	7.08E+07	7.14E+07	4.04E+06	7.08E+07	7.08E+07	0.00%	-0.79%	94.29%	0.00%	16.63%	0.00%
0.80	7.08E+07	7.14E+07	4.04E+06	7.08E+07	7.08E+07	0.00%	-0.79%	94.29%	0.00%	16.63%	0.00%
0.90	7.08E+07	7.14E+07	4.04E+06	7.08E+07	7.08E+07	0.00%	-0.79%	94.29%	0.00%	16.63%	0.00%
1.00	7.08E+07	7.14E+07	4.04E+06	7.08E+07	7.08E+07	0.00%	-0.79%	94.29%	0.00%	16.63%	0.00%
1.10	5.42E+07	1.83E+07	4.04E+06	5.42E+07	7.08E+07	23.45%	74.11%	94.29%	23.45%	9.66%	6.36%
1.20	4.27E+07	1.17E+07	4.04E+06	4.27E+07	7.08E+07	39.73%	83.46%	94.29%	39.73%	6.14%	4.74%
1.30	3.44E+07	9.15E+06	4.04E+06	3.44E+07	7.08E+07	51.37%	87.09%	94.29%	51.37%	3.90%	3.16%
1.40	2.84E+07	7.79E+06	4.04E+06	2.84E+07	7.08E+07	59.93%	89.00%	94.29%	59.93%	2.53%	2.10%
1.50	2.38E+07	6.96E+06	4.04E+06	2.38E+07	7.08E+07	66.36%	90.17%	94.29%	66.36%	1.68%	1.41%
1.60	2.03E+07	6.40E+06	4.04E+06	2.03E+07	7.08E+07	71.27%	90.96%	94.29%	71.27%	1.15%	0.96%
1.70	1.76E+07	6.00E+06	4.04E+06	1.76E+07	7.08E+07	75.10%	91.53%	94.29%	75.10%	0.80%	0.67%
1.80	1.55E+07	5.70E+06	4.04E+06	1.55E+07	7.08E+07	78.13%	91.95%	94.29%	78.13%	0.56%	0.47%
1.90	1.38E+07	5.47E+06	4.04E+06	1.38E+07	7.08E+07	80.55%	92.28%	94.29%	80.55%	0.41%	0.34%
2.00	1.24E+07	5.29E+06	4.04E+06	1.24E+07	7.08E+07	82.51%	92.53%	94.29%	82.51%	0.30%	0.25%
2.10	1.13E+07	5.14E+06	4.04E+06	1.13E+07	7.08E+07	84.11%	92.74%	94.29%	84.11%	0.22%	0.18%
2.20	1.03E+07	5.02E+06	4.04E+06	1.03E+07	7.08E+07	85.44%	92.91%	94.29%	85.44%	0.17%	0.14%
2.30	9.53E+06	4.92E+06	4.04E+06	9.53E+06	7.08E+07	86.54%	93.06%	94.29%	86.54%	0.13%	0.11%
2.40	8.87E+06	4.83E+06	4.04E+06	8.87E+06	7.08E+07	87.47%	93.18%	94.29%	87.47%	0.10%	0.08%
2.50	8.32E+06	4.76E+06	4.04E+06	8.32E+06	7.08E+07	88.26%	93.28%	94.29%	88.26%	0.08%	0.06%
2.60	7.84E+06	4.70E+06	4.04E+06	7.84E+06	7.08E+07	88.93%	93.37%	94.29%	88.93%	0.06%	0.05%
2.70	7.43E+06	4.64E+06	4.04E+06	7.43E+06	7.08E+07	89.50%	93.45%	94.29%	89.50%	0.05%	0.04%
2.80	7.08E+06	4.59E+06	4.04E+06	7.08E+06	7.08E+07	90.00%	93.51%	94.29%	90.00%	0.04%	0.03%
2.90	6.78E+06	4.55E+06	4.04E+06	6.78E+06	7.08E+07	90.43%	93.57%	94.29%	90.43%	0.03%	0.02%
3.00	6.52E+06	4.51E+06	4.04E+06	6.52E+06	7.08E+07	90.80%	93.63%	94.29%	90.80%	0.03%	0.02%
3.10	6.28E+06	4.48E+06	4.04E+06	6.28E+06	7.08E+07	91.13%	93.67%	94.29%	91.13%	0.02%	0.02%
3.20	6.08E+06	4.45E+06	4.04E+06	6.08E+06	7.08E+07	91.42%	93.72%	94.29%	91.42%	0.02%	0.01%
3.30	5.90E+06	4.42E+06	4.04E+06	5.90E+06	7.08E+07	91.67%	93.75%	94.29%	91.67%	0.01%	0.01%
3.40	5.74E+06	4.40E+06	4.04E+06	5.74E+06	7.08E+07	91.90%	93.79%	94.29%	91.90%	0.01%	0.01%
3.50	5.60E+06	4.38E+06	4.04E+06	5.60E+06	7.08E+07	92.10%	93.82%	94.29%	92.10%	0.01%	0.01%
3.60	5.47E+06	4.36E+06	4.04E+06	5.47E+06	7.08E+07	92.27%	93.85%	94.29%	92.27%	0.01%	0.01%
3.70	5.36E+06	4.34E+06	4.04E+06	5.36E+06	7.08E+07	92.43%	93.87%	94.29%	92.43%	0.01%	0.01%
3.80	5.26E+06	4.32E+06	4.04E+06	5.26E+06	7.08E+07	92.58%	93.90%	94.29%	92.58%	0.01%	0.00%
3.90	5.17E+06	4.31E+06	4.04E+06	5.17E+06	7.08E+07	92.70%	93.92%	94.29%	92.70%	0.01%	0.00%
4.00	5.09E+06	4.29E+06	4.04E+06	5.09E+06	7.08E+07	92.82%	93.94%	94.29%	92.82%	0.00%	0.00%
4.10	5.01E+06	4.28E+06	4.04E+06	5.01E+06	7.08E+07	92.93%	93.96%	94.29%	92.93%	0.00%	0.00%
									max	16.63%	6.36%

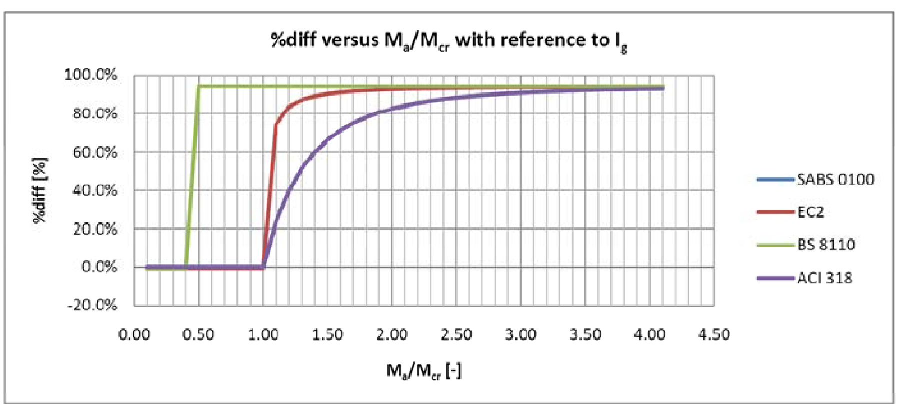

% Difference with reference to the Uncracked Moment of Inertia of the Beam Section

	SABS 0100	EC2	BS 8110	ACI 318		SABS 0100	EC2	BS 8110	ACI 318		
M_a/M_{cr}	I_e	I_e	I_e	I_e	I_u	%diff	%diff	%diff	%diff	COV_A	COV_S
[-]	[mm^4]	[mm^4]	[mm^4]	[mm^4]	[mm^4]	[%]	[%]	[%]	[%]		
0.10	7.08E+07	7.14E+07	7.15E+07	7.08E+07	7.14E+07	0.79%	0.00%	-0.14%	0.79%	0.00%	0.00%
0.20	7.08E+07	7.14E+07	7.15E+07	7.08E+07	7.14E+07	0.79%	0.00%	-0.14%	0.79%	0.00%	0.00%
0.30	7.08E+07	7.14E+07	7.15E+07	7.08E+07	7.14E+07	0.79%	0.00%	-0.14%	0.79%	0.00%	0.00%
0.40	7.08E+07	7.14E+07	7.15E+07	7.08E+07	7.14E+07	0.79%	0.00%	-0.14%	0.79%	0.00%	0.00%
0.50	7.08E+07	7.14E+07	4.04E+06	7.08E+07	7.14E+07	0.79%	0.00%	94.34%	0.79%	16.63%	0.00%
0.60	7.08E+07	7.14E+07	4.04E+06	7.08E+07	7.14E+07	0.79%	0.00%	94.34%	0.79%	16.63%	0.00%
0.70	7.08E+07	7.14E+07	4.04E+06	7.08E+07	7.14E+07	0.79%	0.00%	94.34%	0.79%	16.63%	0.00%
0.80	7.08E+07	7.14E+07	4.04E+06	7.08E+07	7.14E+07	0.79%	0.00%	94.34%	0.79%	16.63%	0.00%
0.90	7.08E+07	7.14E+07	4.04E+06	7.08E+07	7.14E+07	0.79%	0.00%	94.34%	0.79%	16.63%	0.00%
1.00	7.08E+07	7.14E+07	4.04E+06	7.08E+07	7.14E+07	0.79%	0.00%	94.34%	0.79%	16.63%	0.00%
1.10	5.42E+07	1.83E+07	4.04E+06	5.42E+07	7.14E+07	24.05%	74.31%	94.34%	24.05%	9.66%	6.36%
1.20	4.27E+07	1.17E+07	4.04E+06	4.27E+07	7.14E+07	40.20%	83.59%	94.34%	40.20%	6.14%	4.74%
1.30	3.44E+07	9.15E+06	4.04E+06	3.44E+07	7.14E+07	51.76%	87.19%	94.34%	51.76%	3.90%	3.16%
1.40	2.84E+07	7.79E+06	4.04E+06	2.84E+07	7.14E+07	60.25%	89.09%	94.34%	60.25%	2.53%	2.10%
1.50	2.38E+07	6.96E+06	4.04E+06	2.38E+07	7.14E+07	66.62%	90.25%	94.34%	66.62%	1.68%	1.41%
1.60	2.03E+07	6.40E+06	4.04E+06	2.03E+07	7.14E+07	71.50%	91.04%	94.34%	71.50%	1.15%	0.96%
1.70	1.76E+07	6.00E+06	4.04E+06	1.76E+07	7.14E+07	75.30%	91.60%	94.34%	75.30%	0.80%	0.67%
1.80	1.55E+07	5.70E+06	4.04E+06	1.55E+07	7.14E+07	78.30%	92.01%	94.34%	78.30%	0.56%	0.47%
1.90	1.38E+07	5.47E+06	4.04E+06	1.38E+07	7.14E+07	80.70%	92.34%	94.34%	80.70%	0.41%	0.34%
2.00	1.24E+07	5.29E+06	4.04E+06	1.24E+07	7.14E+07	82.64%	92.59%	94.34%	82.64%	0.30%	0.25%
2.10	1.13E+07	5.14E+06	4.04E+06	1.13E+07	7.14E+07	84.24%	92.80%	94.34%	84.24%	0.22%	0.18%
2.20	1.03E+07	5.02E+06	4.04E+06	1.03E+07	7.14E+07	85.55%	92.97%	94.34%	85.55%	0.17%	0.14%
2.30	9.53E+06	4.92E+06	4.04E+06	9.53E+06	7.14E+07	86.65%	93.11%	94.34%	86.65%	0.13%	0.11%
2.40	8.87E+06	4.83E+06	4.04E+06	8.87E+06	7.14E+07	87.57%	93.23%	94.34%	87.57%	0.10%	0.08%
2.50	8.32E+06	4.76E+06	4.04E+06	8.32E+06	7.14E+07	88.35%	93.33%	94.34%	88.35%	0.08%	0.06%
2.60	7.84E+06	4.70E+06	4.04E+06	7.84E+06	7.14E+07	89.02%	93.42%	94.34%	89.02%	0.06%	0.05%
2.70	7.43E+06	4.64E+06	4.04E+06	7.43E+06	7.14E+07	89.59%	93.50%	94.34%	89.59%	0.05%	0.04%
2.80	7.08E+06	4.59E+06	4.04E+06	7.08E+06	7.14E+07	90.08%	93.56%	94.34%	90.08%	0.04%	0.03%
2.90	6.78E+06	4.55E+06	4.04E+06	6.78E+06	7.14E+07	90.50%	93.62%	94.34%	90.50%	0.03%	0.02%
3.00	6.52E+06	4.51E+06	4.04E+06	6.52E+06	7.14E+07	90.87%	93.68%	94.34%	90.87%	0.03%	0.02%
3.10	6.28E+06	4.48E+06	4.04E+06	6.28E+06	7.14E+07	91.20%	93.72%	94.34%	91.20%	0.02%	0.02%
3.20	6.08E+06	4.45E+06	4.04E+06	6.08E+06	7.14E+07	91.48%	93.76%	94.34%	91.48%	0.02%	0.01%
3.30	5.90E+06	4.42E+06	4.04E+06	5.90E+06	7.14E+07	91.74%	93.80%	94.34%	91.74%	0.01%	0.01%
3.40	5.74E+06	4.40E+06	4.04E+06	5.74E+06	7.14E+07	91.96%	93.84%	94.34%	91.96%	0.01%	0.01%
3.50	5.60E+06	4.38E+06	4.04E+06	5.60E+06	7.14E+07	92.16%	93.87%	94.34%	92.16%	0.01%	0.01%
3.60	5.47E+06	4.36E+06	4.04E+06	5.47E+06	7.14E+07	92.33%	93.89%	94.34%	92.33%	0.01%	0.01%
3.70	5.36E+06	4.34E+06	4.04E+06	5.36E+06	7.14E+07	92.49%	93.92%	94.34%	92.49%	0.01%	0.01%
3.80	5.26E+06	4.32E+06	4.04E+06	5.26E+06	7.14E+07	92.63%	93.94%	94.34%	92.63%	0.01%	0.00%
3.90	5.17E+06	4.31E+06	4.04E+06	5.17E+06	7.14E+07	92.76%	93.96%	94.34%	92.76%	0.01%	0.00%
4.00	5.09E+06	4.29E+06	4.04E+06	5.09E+06	7.14E+07	92.88%	93.98%	94.34%	92.88%	0.00%	0.00%
4.10	5.01E+06	4.28E+06	4.04E+06	5.01E+06	7.14E+07	92.98%	94.00%	94.34%	92.98%	0.00%	0.00%
									max	16.63%	6.36%

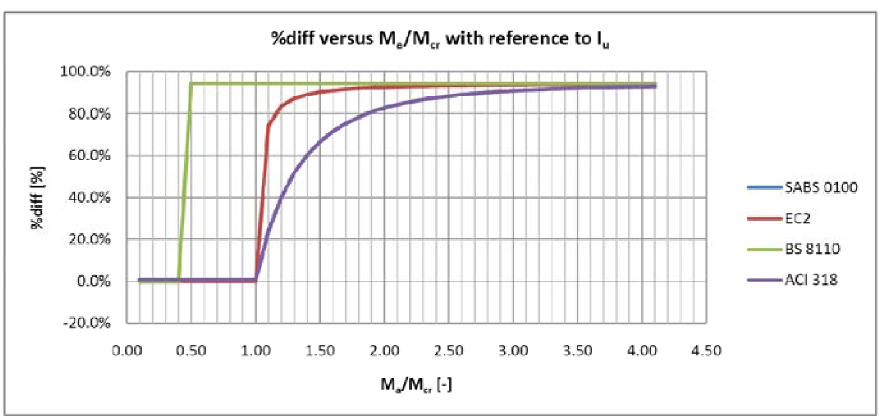

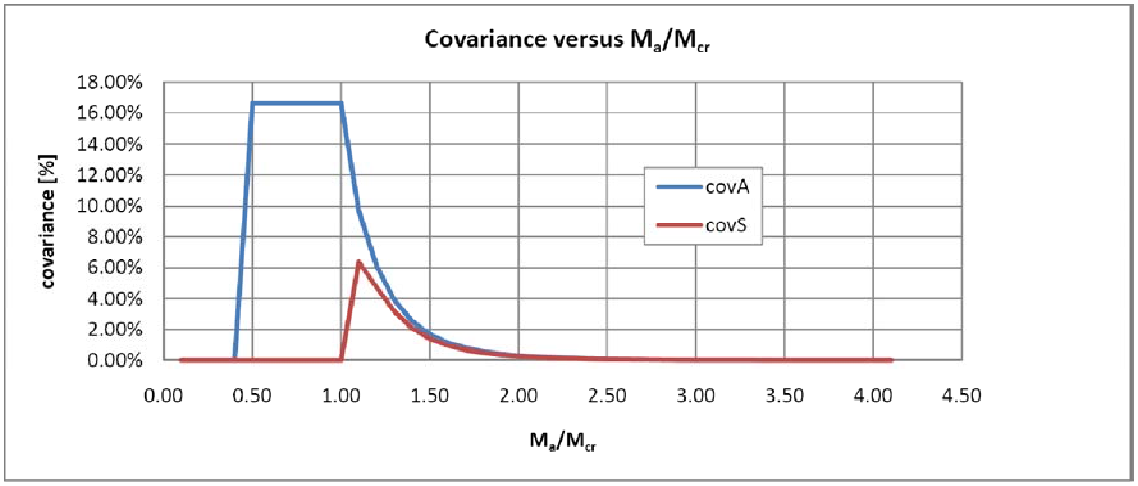

The graph above shows the M_a/M_{cr} range where there is a large difference between the Ie equations. Over this range it may become very critical what I_e equation is used to calculate deflections.

As the percentage reinforcement decreases so does the percentage covariance over the critical M_a/M_{cr} range increase.

MAX		
ρ [%]	cov_A	cov_S
1.5	8.47%	0.17%
1.10	10.21%	0.49%
0.84	11.58%	0.90%
0.52	13.69%	2.07%
0.30	15.48%	4.15%
0.18	16.63%	6.36%

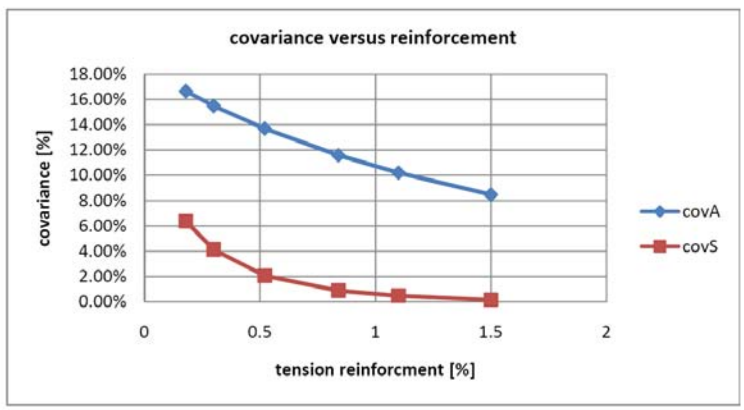

Note: The critical M_a/M_{cr} range decrease with increase reinforcement

The average covariance occurs at a larger percentage due to the influence of the BS 8110 assumptions on effective immediate curvature.

The ACI 318 and the SABS 0100-1 have the exact same expression for Ie, therefore no specific reference is made to the ACI 318. Every conclusion for the SABS 0100-1 Ie approach is similar for the ACI 318.

The specific covariance percentages show a exponential increase as the percentage reinforcement decrease.

APPENDIX F

The calculations to obtain the values of the moment of inertia are similar to those of Appendix A. The beam section is kept constant while the percentage tension reinforcement varies. More detail on the calculations is presented on the data disks.

Percentage Difference between I_g and I_u

Refer to the previous sheets for the tables below:

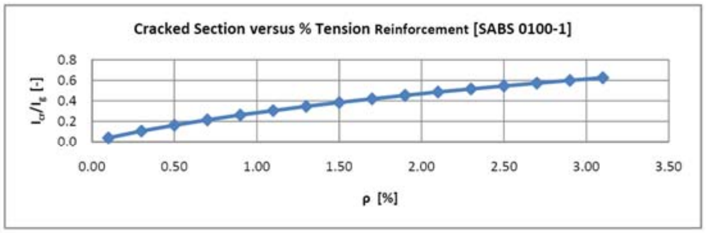

The ACI 318 produced a similar trend equation as the SABS 0100-1

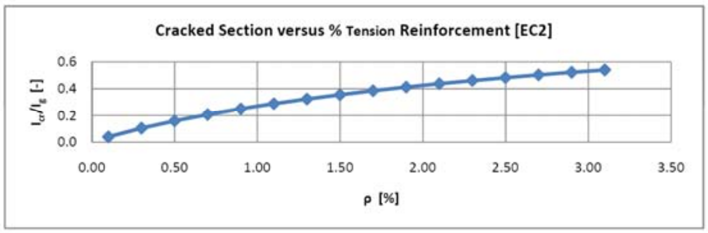

The BS 8110 produced a similar trend equation as the EC2

$I_g < I_u$

$$\%diff = \left(I_u - I_g\right)/I_u$$

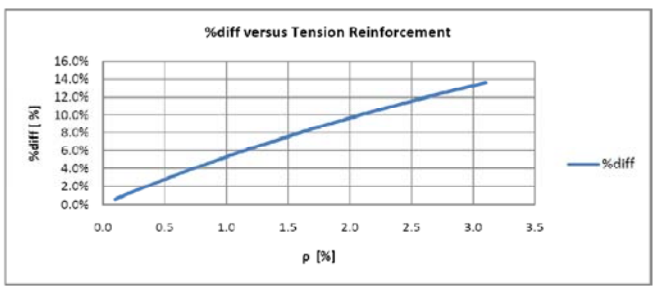

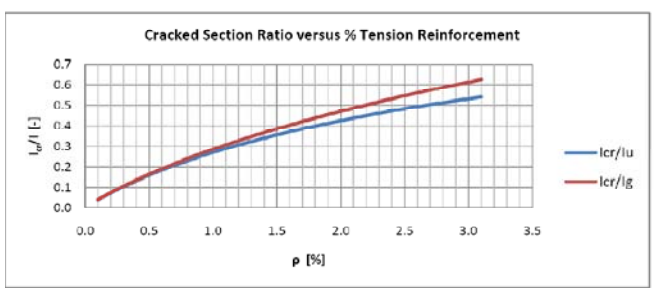

ρ	I_{cr}/I_u	I_{cr}/I_g	I_g	I_u	%diff	I_u/I_g
[%]	[-]	[-]	[mm^4]	[mm^4]	[%]	[-]
0.10	0.039	0.040	7.08E+07	7.12E+07	0.6%	1.01
0.30	0.104	0.106	7.08E+07	7.21E+07	1.7%	1.02
0.50	0.159	0.164	7.08E+07	7.29E+07	2.8%	1.03
0.70	0.207	0.216	7.08E+07	7.37E+07	3.8%	1.04
0.90	0.250	0.263	7.08E+07	7.44E+07	4.8%	1.05
1.10	0.289	0.306	7.08E+07	7.52E+07	5.8%	1.06
1.30	0.324	0.347	7.08E+07	7.59E+07	6.7%	1.07
1.50	0.356	0.385	7.08E+07	7.66E+07	7.6%	1.08
1.70	0.385	0.421	7.08E+07	7.74E+07	8.4%	1.09
1.90	0.412	0.454	7.08E+07	7.81E+07	9.3%	1.10
2.10	0.438	0.486	7.08E+07	7.87E+07	10.0%	1.11
2.30	0.461	0.517	7.08E+07	7.94E+07	10.8%	1.12
2.50	0.483	0.546	7.08E+07	8.01E+07	11.5%	1.13
2.70	0.503	0.574	7.08E+07	8.07E+07	12.3%	1.14
2.90	0.522	0.600	7.08E+07	8.14E+07	12.9%	1.15
3.10	0.540	0.625	7.08E+07	8.20E+07	13.6%	1.16

APPENDIX G

The calculations for Slab S3 are presented in this appendix. The detailed deflection calculations are presented for only one column strip. The calculations are repeated for the other column and middle strips in the slab panel. The calculations for the second loading stage are included in this appendix. The span/effective depth ratio calculations are also presented.

More information on the calculations is presented on the data disks.

Layout of the Experimental Slab and Columns: (according to article)

The figure below shows the layout of the experimental slab.

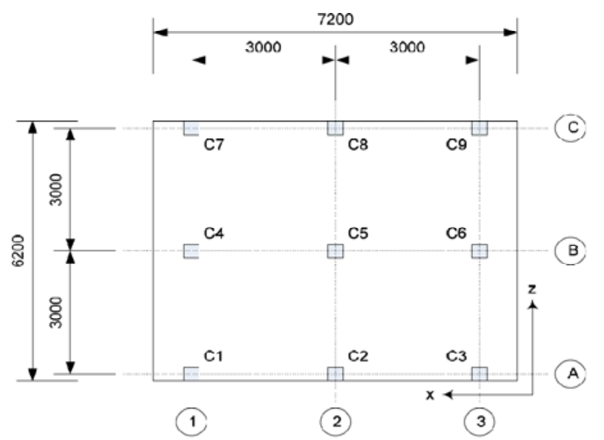

It is assummed that the deflection in the centre of the slab is the same in every panel, due to the symmetry of the slab.

The Reinforcement Layout: (accordingly to article)

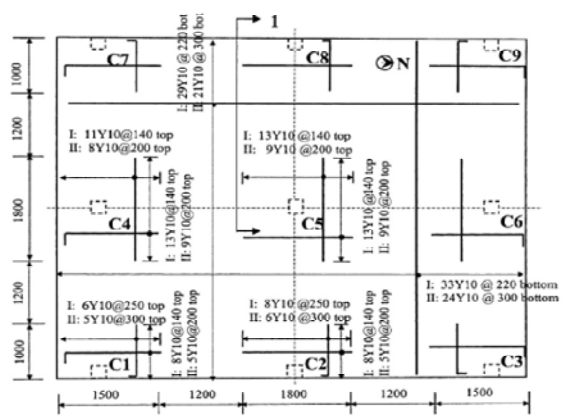

Consider Panel between Column C4, C7, C8 and C5:

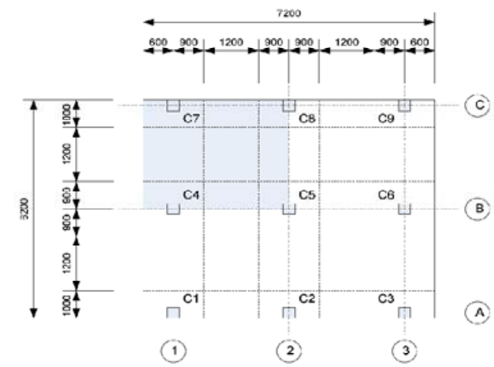

The panel is divided into column and middle strips, as observed from the article published. These strips will be taken into consideration when calculating the deflections at variuous points.

The following Load Combinations were applied to the model:

1. Dead Load Moments: Load Combination 1 (LC1)
   $Q = 1.0G_k$
2. Live Load Moments: Load Combination 2 (LC2)
   $Q = 1.0Q_k$
3. Sustained Portion of the Serviceability Limit State Moments: Load Combination 3 (LC3)
   $Q = 1.0G_k + 1.0Q_k$

Column and Middle Strip Dimensions and Reinforcement:

Column Strip C7 - C8:

b = 1000.0 mm
L = 3000.0 mm
d = 77.0 mm
d' = 13.0 mm
h = 90.0 mm

	A_s [mm^2]		A'_s [mm^2]	
Sup_{LEFT}	8Y10	628.32	5Y10	392.70
Mid	5Y10	392.70	0	0
Sup_{RIGHT}	8Y10	628.32	5Y10	392.70

Column Strip C4 - C5:

b = 1800.0 mm
L = 3000.0 mm
d = 77.0 mm
d' = 13.0 mm
h = 90.0 mm

	A_s [mm²]		A'_s [mm²]	
Sup_{LEFT}	13Y10	1021.02	9Y10	706.86
Mid	9Y10	706.86	0	0
Sup_{RIGHT}	13Y10	1021.02	9Y10	706.86

Middle Strip C4,C5 - C7,C8:

b = 1200.0 mm
L = 3000.0 mm
d = 77.0 mm
d' = 13.0 mm
h = 90.0 mm

	A_s [mm²]		A'_s [mm²]	
Sup_{LEFT}	0	0.00	6Y10	471.24
Mid	6Y10	471.24	0	0
Sup_{RIGHT}	0	0.00	6Y10	471.24

Column Strip C7 - C4:

b = 1500.0 mm
L = 3000.0 mm
d = 77.0 mm
d' = 13.0 mm
h = 90.0 mm

	A_s [mm²]		A'_s [mm²]	
Sup_{LEFT}	6Y10	628.32	7Y10	549.78
Mid	7Y10	549.78	0	0
Sup_{RIGHT}	11Y10	863.94	7Y10	549.78

Column Strip C8 - C5:

b = 1800.0 mm
L = 3000.0 mm
d = 77.0 mm
d' = 13.0 mm
h = 90.0 mm

	A_s [mm²]		A'_s [mm²]	
Sup_{LEFT}	8Y10	628.32	9Y10	706.86
Mid	9Y10	706.86	0	0
Sup_{RIGHT}	13Y10	1021.02	9Y10	706.86

Middle Strip C4,C7 - C5,C8:

b = 1200.0 mm
L = 3000.0 mm
d = 77.0 mm
d' = 13.0 mm
h = 90.0 mm

	A_s [mm²]		A'_s [mm²]	
Sup_{LEFT}	0	0.00	6Y10	471.24
Mid	6Y10	471.24	0	0
Sup_{RIGHT}	0	0.00	6Y10	471.24

Serviceability Moments for Gridline C: XX-Moments

* Properties for Uncracked Section

$$x_u = \frac{\frac{bh^2}{2} + (\alpha_e - 1)(A_s d + A'_s d')}{bh + (\alpha_e - 1)(A_s + A'_s)}$$

$$I_u = \frac{bh^3}{12} + bh\left(\frac{h}{2} - x_u\right)^2 + (\alpha_e - 1)\left[A_s(d - x_u)^2 + A'_s(x_u - d')^2\right]$$

* Cracking Moment

$$M_{cr} = \frac{f_t I_u}{h - x_u}$$

Midspan

A_s = 392.70 mm²
A'_s = 0.0 mm²

b = 1000.0 mm
h = 90.0 mm
d = 77.0 mm
d' = 13.0 mm

f_t = 1.67 MPa
M_{cr} = 2.57 kNm

E_s = 219.0 GPa
$E_{c,28}$ = 13.97 GPa

α_e = 15.67

x_u = 46.9 mm
I_u = 6.63E+07 mm⁴

Right Support

A_s = 628.32 mm²
A'_s = 392.7 mm²

b = 1000.0 mm
h = 90.0 mm
d = 77.0 mm
d' = 13.0 mm

f_t = 1.67 MPa
M_{cr} = 2.88 kNm

E_s = 219.0 GPa
$E_{c,28}$ = 13.97 GPa

α_e = 15.67

x_u = 46.1 mm
I_u = 7.60E+07 mm⁴

Left Support

A_s = 628.32 mm²
A'_s = 392.70 mm²

(similar properties) M_{cr} = 2.88 kNm

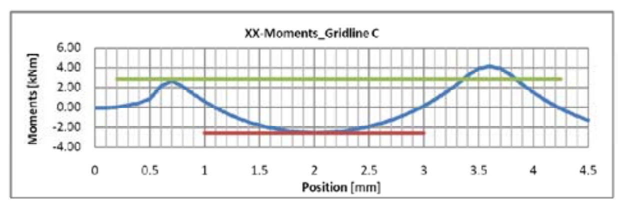

Serviceability Moments for Gridline B: XX-Moments

* Properties for Uncracked Section

$$x_u = \frac{\frac{bh^2}{2} + (\alpha_e - 1)(A_s d + A'_s d')}{bh + (\alpha_e - 1)(A_s + A'_s)}$$

* Cracking Moment

$$M_{cr} = \frac{f_t I_u}{h - x_u}$$

$$I_u = \frac{bh^3}{12} + bh\left(\frac{h}{2} - x_u\right)^2 + (\alpha_e - 1)\left[A_s(d - x_u)^2 + A'_s(x_u - d')^2\right]$$

Midspan

A_s =	706.86 mm^2	E_s =	219.0 GPa
A'_s =	0.0 mm^2	$E_{c,28}$ =	13.97 GPa
b =	1800.0 mm	α_e =	15.67
h =	90.0 mm		
d =	77.0 mm	x_u =	46.9 mm
d' =	13.0 mm	I_u =	1.19E+08 mm^4
f_t =	1.67 MPa		
M_{cr} =	4.62 kNm		

Right Support

A_s =	1021.02 mm^2	E_s =	219.0 GPa
A'_s =	706.9 mm^2	$E_{c,28}$ =	13.97 GPa
b =	1800.0 mm	α_e =	15.67
h =	90.0 mm		
d =	77.0 mm	x_u =	45.8 mm
d' =	13.0 mm	I_u =	1.35E+08 mm^4
f_t =	1.67 MPa		
M_{cr} =	5.10 kNm		

Left Support

A_s =	1021.02 mm^2
A'_s =	706.86 mm^2

(similar properties) M_{cr} = 5.10 kNm

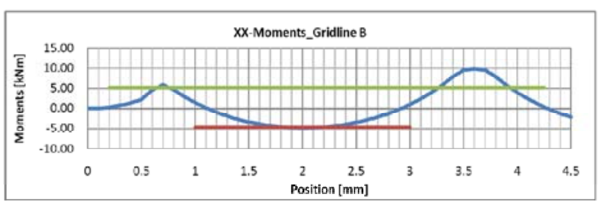

Serviceability Moments between Gridline B and C: ZZ-Moments

* Properties for Uncracked Section

$$x_u = \frac{\frac{bh^2}{2} + (\alpha_e - 1)(A_s d + A'_s d')}{bh + (\alpha_e - 1)(A_s + A'_s)}$$

* Cracking Moment

$$M_{cr} = \frac{f_t I_u}{h - x_u}$$

$$I_u = \frac{bh^3}{12} + bh\left(\frac{h}{2} - x_u\right)^2 + (\alpha_e - 1)\left[A_s(d - x_u)^2 + A'_s(x_u - d')^2\right]$$

Midspan

A_s =	471.24 mm^2	E_s =	219.0 GPa
A'_s =	0.0 mm^2	$E_{c,28}$ =	13.97 GPa
b =	1200.0 mm	α_e =	15.67
h =	90.0 mm		
d =	77.0 mm	x_u =	46.9 mm
d' =	13.0 mm	I_u =	7.96E+07 mm^4
f_t =	1.67 MPa		
M_{cr} =	3.08 kNm		

Left Support

A_s =	0.00 mm^2	E_s =	219.0 GPa
A'_s =	471.2 mm^2	$E_{c,28}$ =	13.97 GPa
b =	1200.0 mm	α_e =	15.67
h =	90.0 mm		
d =	77.0 mm	x_u =	43.1 mm
d' =	13.0 mm	I_u =	7.96E+07 mm^4
f_t =	1.67 MPa		
M_{cr} =	2.83 kNm		

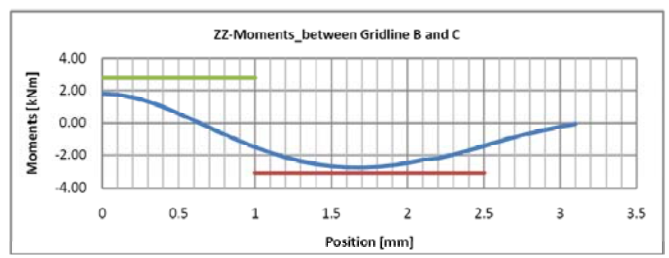

Serviceability Moments for Gridline 1: ZZ-Moments

* Properties for Uncracked Section

$$x_u = \frac{\frac{bh^2}{2} + (\alpha_e - 1)(A_s d + A'_s d')}{bh + (\alpha_e - 1)(A_s + A'_s)}$$

* Cracking Moment

$$M_{cr} = \frac{f_t I_u}{h - x_u}$$

$$I_u = \frac{bh^3}{12} + bh\left(\frac{h}{2} - x_u\right)^2 + (\alpha_e - 1)\left[A_s (d - x_u)^2 + A'_s (x_u - d')^2\right]$$

Midspan

A_s =	549.78 mm^2	E_s =	219.0 GPa
A'_s =	0.0 mm^2	$E_{c,28}$ =	13.97 GPa
b =	1500.0 mm	α_e =	15.67
h =	90.0 mm		
d =	77.0 mm	x_u =	46.8 mm
d' =	13.0 mm	I_u =	9.89E+07 mm^4
f_t =	1.67 MPa		
M_{cr} =	3.82 kNm		

Right Support

A_s =	863.94 mm^2	E_s =	219.0 GPa
A'_s =	549.8 mm^2	$E_{c,28}$ =	13.97 GPa
b =	1500.0 mm	α_e =	15.67
h =	90.0 mm		
d =	77.0 mm	x_u =	45.9 mm
d' =	13.0 mm	I_u =	1.12E+08 mm^4
f_t =	1.67 MPa		
M_{cr} =	4.25 kNm		

Left Support

A_s =	628.32 mm^2	x_u =	45.2 mm
A'_s =	549.78 mm^2	I_u =	1.09E+08 mm^4

M_{cr} = 4.05 kNm

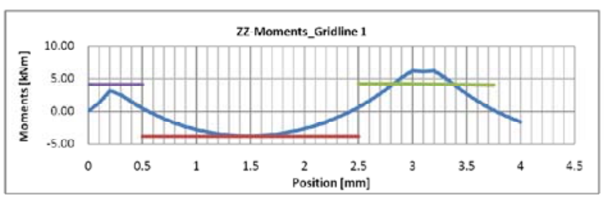

Serviceability Moments for Gridline 2: ZZ-Moments

* Properties for Uncracked Section

$$x_u = \frac{\frac{bh^2}{2} + (\alpha_e - 1)(A_s d + A'_s d')}{bh + (\alpha_e - 1)(A_s + A'_s)}$$

* Cracking Moment

$$M_{cr} = \frac{f_t I_u}{h - x_u}$$

$$I_u = \frac{bh^3}{12} + bh\left(\frac{h}{2} - x_u\right)^2 + (\alpha_e - 1)\left[A_s (d - x_u)^2 + A'_s (x_u - d')^2\right]$$

Midspan

A_s =	706.86 mm^2	E_s =	219.0 GPa
A'_s =	0.0 mm^2	$E_{c,28}$ =	13.97 GPa
b =	1800.0 mm	α_e =	15.67
h =	90.0 mm		
d =	77.0 mm	x_u =	46.9 mm
d' =	13.0 mm	I_u =	1.19E+08 mm^4
f_t =	1.67 MPa		
M_{cr} =	4.62 kNm		

Right Support

A_s =	1021.02 mm^2	E_s =	219.0 GPa
A'_s =	706.9 mm^2	$E_{c,28}$ =	13.97 GPa
b =	1800.0 mm	α_e =	15.67
h =	90.0 mm		
d =	77.0 mm	x_u =	45.8 mm
d' =	13.0 mm	I_u =	1.35E+08 mm^4
f_t =	1.67 MPa		
M_{cr} =	5.10 kNm		

Left Support

A_s =	628.32 mm^2	x_u =	44.8 mm
A'_s =	706.86 mm^2	I_u =	1.29E+08 mm^4

M_{cr} = 4.77 kNm

Serviceability Moments between Gridline 1 & 2: XX-Moments

* Properties for Uncracked Section

$$x_u = \frac{\frac{bh^2}{2} + (\alpha_e - 1)(A_s d + A'_s d')}{bh + (\alpha_e - 1)(A_s + A'_s)}$$

$$I_u = \frac{bh^3}{12} + bh\left(\frac{h}{2} - x_u\right)^2 + (\alpha_e - 1)\left[A_s (d - x_u)^2 + A'_s (x_u - d')^2\right]$$

* Cracking Moment

$$M_{cr} = \frac{f_t I_u}{h - x_u}$$

Midspan

A_s =	471.24	mm^2	E_s =	219.0	GPa
A'_s =	0.00	mm^2	$E_{c,28}$ =	13.97	GPa
b =	1200.0	mm	α_e =	15.67	
h =	90.0	mm			
d =	77.0	mm	x_u =	46.9	mm
d' =	13.0	mm	I_u =	7.96E+07	mm^4
f_t =	1.67	MPa			
M_{cr} =	3.08	kNm			

Right Support

A_s =	0.00	mm^2	E_s =	219.0	GPa
A'_s =	471.2	mm^2	$E_{c,28}$ =	13.97	GPa
b =	1200.0	mm	α_e =	15.67	
h =	90.0	mm			
d =	77.0	mm	x_u =	43.1	mm
d' =	13.0	mm	I_u =	7.96E+07	mm^4
f_t =	1.67	MPa			
M_{cr} =	2.83	kNm			

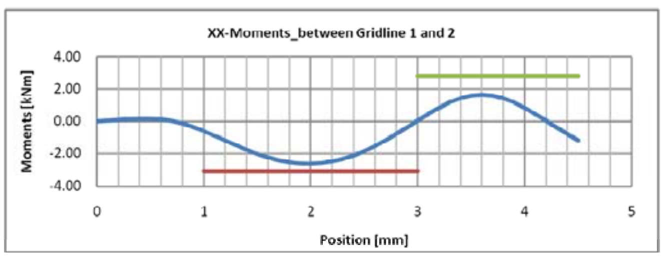

Experimental Data

SLAB 3

Time-Dependent Delfection and Deformation of Reinforced Concrete Flat Slabs - An Experimental Study
by R.I. Gilbert and X.H. Guo ACI Journal May-June 2005

Thickness = 90.0 mm
Column Support Condition = Fixed
Reinforcement Layer = I

Age at First Loading = 14 days
Test Period = 599 days

Value of f_r (EC2, table 3.1)

$$f_r = 0.3 f'^{(2/3)}_c$$

Concrete Strength

Compressive Strength	Flexural Tensile Strength	Axial Tensile Strength
$f'_{c,14}$ = 13.1 MPa	$f_{tf,14}$ = - MPa	$f_{t,14}$ = 1.67 MPa
$f'_{c,28}$ = 18.1 MPa	$f_{tf,28}$ = 2.48 MPa	$f_{t,28}$ = 2.07 MPa

Applied Load

DL_{14} = 2.16 kPa
LL_{14} = 0.00 kPa
LL_{28} = 3.10 kPa
LL_{387} = 0.00 kPa

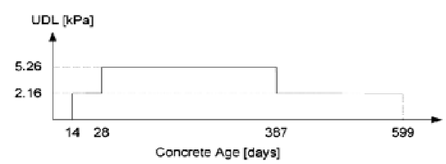

Concrete Batch 3

$E_{c,14}$ = 22.08 GPa
$E_{c,28}$ = 22.62 GPa

Data Recorded

The data recorded by Gilbert and Guo is shown in the table below.
It is assumed that at the modulus of elasticity, $E_{c,14}$ is the point where the slabs start cracking.

All fromwork props were removed at an age of bewteen 10 and 14 days.

Where data is missing or not recorded, it was interpolated between the known data points to find the missing values.

$$E_{c,t} = \frac{E_c}{1+\phi(\infty,t)}$$

the following equation was applied to calculate the modulus of elasticity as it changes with time, using E_c as $E_{c,14}$.

time [days]	Δ_{EXP} [mm]	ϕ [-]	ε_{cs} 10^{-6}[-]	$E_{eff,t}$ [GPa]	Δ_{P_U} [mm]	$\Delta_{P\_U}/\Delta_{EXP}$	
14	0.94	0.00	-6.00	22.08	0.91	0.96	Stage 1
15	1.04	0.00	4.17	22.08			
20		0.00	55.00	22.08			
28	1.52	0.58	85.00	13.97	1.43	0.94	
28	2.84	0.58	85.00	13.97	3.53	1.24	Stage 2
40		0.81	182.00	12.20			
80		1.30	448.00	9.60			
120		1.55	504.00	8.66			
159	10.4	1.79	558.60	7.90			
200		1.89	621.00	7.64			
250		1.95	625.00	7.48			
300		2.05	735.00	7.24			
309	12.3	2.07	754.80	7.20			
387	13.2	2.16	761.83	6.98	7.06	0.54	
388	11.8	2.17	761.92	6.98	2.87	0.24	Stage 3
400		2.18	763.00	6.94			
450		2.34	791.00	6.61			
599	11.9	2.82	874.44	5.78	3.46	0.29	

Δ_{EXP}	Recorded mid panel deflections from Gilber and Guo, 2005.
Δ_{P_U}	Predicted deflection not taking an uncracked section into account using a FE model. Stiffness reduced using $E_{c,t}$ as time increases for different FE models.
$\Delta_{P\_U}/\Delta_{EXP}$	Deflection Ratio. The closer the ratio tends toward 1.0, the more accurate the deflection prediction approach is.

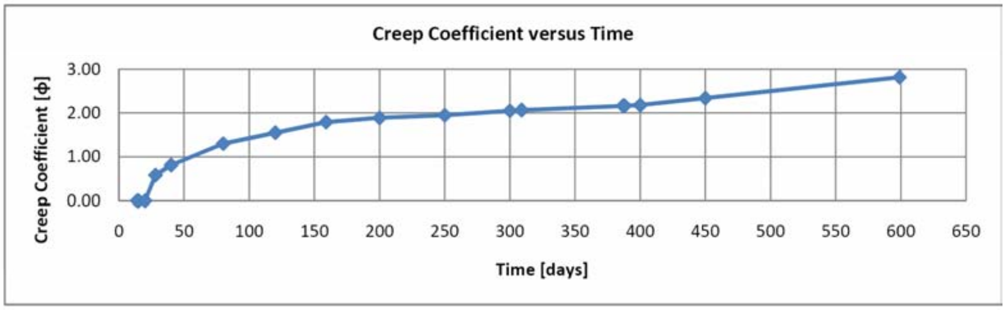

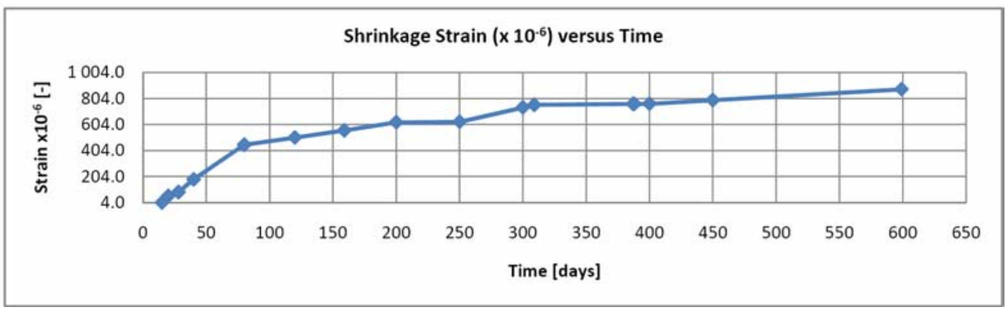

Moment Comparisons in Slab Panel

Moments depend on the applied Load:

Stages of Loading: 3

Stage 1:	DL_{14}	=	2.16 kPa
	LL_{14}	=	0.00 kPa
Stage 2:	DL_{28}	=	2.16 kPa
	LL_{28}	=	3.10 kPa
Stage 3:	DL_{387}	=	2.16 kPa
	LL_{387}	=	0.00 kPa

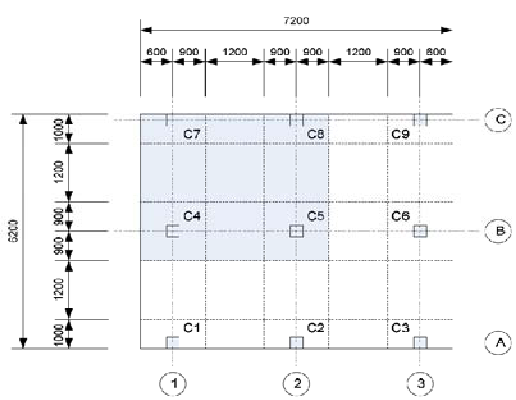

Using a Partially Cracked Section to Evaluate Time-Dependent Deflections

Data Recorded

using Effective Modulus of Elasticity

time [days]	Δ_{EXP} [mm]	ϕ [-]	ε_{cs} 10^{-6}[-]	$E_{eff,t}$ [GPa]	Δ_{P_CR} [mm]	$\Delta_{P\_CR}/\Delta_{EXP}$	
14	0.94	0.00	-6.00	22.08	0.91	0.96	Stage 1
15	1.04	0.00	4.17	22.08			
20		0.00	55.00	22.08			
28	1.52	0.58	85.00	13.97	1.43	0.94	
28	2.84	0.58	85.00	13.97	4.23	1.49	Stage 2
40		0.81	182.00	12.20			
80		1.30	448.00	9.60			
120		1.55	504.00	8.66			
159	10.4	1.79	558.60	7.90			
200		1.89	621.00	7.64			
250		1.95	625.00	7.48			
300		2.05	735.00	7.24			
309	12.3	2.07	754.80	7.20			
387	13.2	2.16	761.83	6.98	8.47	0.64	
388	11.8	2.17	761.92	6.98	3.44	0.29	Stage 3
400		2.18	763.00	6.94			
450		2.34	791.00	6.61			
599	11.9	2.82	874.44	5.78	4.14	0.35	

Calculate Cracked E (Modulus of Elasticity) to account for Partially Cracked Section

Equations used to account for a Partially Cracked Section. The effect of reinforcement is included to produce more accurate results.

x_u for the Uncracked Condition	I_u for the Uncracked Condition
$x_u = \dfrac{\frac{bh^2}{2} + (\alpha_e - 1)(A_s d + A'_s d')}{bh + (\alpha_e - 1)(A_s + A'_s)}$	$I_u = \dfrac{bh^3}{12} + bh\left(\dfrac{h}{2} - x_u\right)^2 + (\alpha_e - 1)\left[A_s(d - x_u)^2 + A'_s(x_u - d')^2\right]$

x_{cr} for the Cracked Condition	I_{cr} for the Cracked Condition
$\omega = A_s\alpha_e + A'_s(\alpha_e - 1)$ $x_{cr} = \left\{\left[\omega^2 + 2b\left(A_s d\alpha_e + A'_s d'(\alpha_e - 1)\right)\right]^{0.5} - \omega\right\}/b$	$I_{cr} = \dfrac{b{x_{cr}}^3}{3} + \alpha_e A_s(d - x_{cr})^2 + (\alpha_e - 1)A'_s(d' - x_{cr})^2$

Equations used by the **SABS 0100-1** to calculate the effective moment of inertia for a partially cracked section.

Modulus of Rupture	Mod. Ratio	Cracking Moment	Effective Moment of Inertia
$f_r = 0.3\sqrt{f_c}$	$\alpha_e = \dfrac{E_s}{E_c}$	$M_{cr} = \dfrac{f_r I_g}{y_t}$	$I_e = \left(\dfrac{M_{cr}}{M_a}\right)^3 I_g + \left[1 - \left(\dfrac{M_{cr}}{M_a}\right)^3\right] I_{cr}$

Equations used by the **EC2** to calculate the effective moment of inertia for a partially cracked section.

Tensile Concrete Strength	Mod. Ratio	Cracking Moment	Effective Moment of Inertia
$f_t = \dfrac{f_{tfl}}{(1.6 - h/1000)}$	$\alpha_e = \dfrac{E_s}{E_c}$	$M_{cr} = \dfrac{f_t I_u}{h - x_u}$	$I_e = \dfrac{I_{cr}}{1 - \left(1 - \dfrac{I_{cr}}{I_u}\right)\left(\dfrac{M_{cr}}{M_a}\right)^2}$

LOADING STAGE	STAGE 1

No moments larger than the cracking moment - thus no cracking occured.

LOADING STAGE	STAGE 2

Cracking expected along Gridline C, B, 1 and 2:

Column Strip C7 - C8

Assume $E_{cracked}$ is constant for the given stage of loading

Reinforcement at C8:

A_s = 628.3 mm^2
A'_s = 392.7 mm^2

E_s = 219.0 GPa
$E_{c,28}$ = 13.97 GPa

I_g = 6.08E+07 mm^4
y_t = 45.00 mm
f'_c = 13.10 MPa
f_c = 16.38 MPa
f_t = 1.67 MPa

b = 1000.0 mm
d = 77.0 mm
h = 90.0 mm
d' = 13.0 mm

α_e [$E_s/E_{c,t}$]	x_u [mm]	x_{cr} [mm]	I_u [mm^4]	I_{cr} [mm^4]	M_a [kNm]
15.67	46.05	28.1	7.60E+07	3.23E+07	4.18

SABS 0100		
f_r [MPa]	M_{cr} [kNm]	I_e [mm^4]
1.21	1.64	3.40E+07

EC2		
f_t [MPa]	M_{cr} [kNm]	I_e [mm^4]
1.67	2.88	4.44E+07

Length along Gridline where $M_a > M_{cr}$ 400.0 mm

%diff		
f_r	M_{cr}	I_c
27.2%	43.1%	23.4%

assume $$I_u E_{cr} = I_e E_{c,28}$$ E_{cr} = 8.16 GPa

$$G = \frac{E}{2(1+\upsilon)}$$ G = 3.40 GPa

υ = 0.2

Column Strip C4 - C5

Assume $E_{cracked}$ is constant for the given stage of loading

Reinforcement at C4:

A_s = 1021.0 mm^2
A'_s = 706.9 mm^2

E_s = 219.0 GPa
$E_{c,28}$ = 13.97 GPa

I_g = 1.09E+08 mm^4
y_t = 45.00 mm
f'_c = 13.10 MPa
f_c = 16.38 MPa
f_t = 1.67 MPa

b = 1800.0 mm
d = 77.0 mm
h = 90.0 mm
d' = 13.0 mm

α_e [$E_s/E_{c,t}$]	x_u [mm]	x_{cr} [mm]	I_u [mm^4]	I_{cr} [mm^4]	M_a [kNm]
15.67	45.79	27.0	1.35E+08	5.38E+07	5.91

SABS 0100		
f_r [MPa]	M_{cr} [kNm]	I_e [mm^4]
1.21	2.95	6.07E+07

EC2		
f_t [MPa]	M_{cr} [kNm]	I_e [mm^4]
1.67	5.10	9.74E+07

Length along Gridline where $M_a > M_{cr}$ 100.0 mm

%diff		
f_r	M_{cr}	I_c
27.2%	42.1%	37.6%

assume $$I_u E_{cr} = I_e E_{c,28}$$ E_{cr} = 10.07 GPa

$$G = \frac{E}{2(1+\upsilon)}$$ G = 4.19 GPa

υ = 0.2

Column Strip C4 - C5

Assume $E_{cracked}$ is constant for the given stage of loading

Reinforcement at C5:

A_s = 1021.0 mm^2
A'_s = 706.9 mm^2

E_s = 219.0 GPa
$E_{c,28}$ = 13.97 GPa

I_g = 1.09E+08 mm^4
y_t = 45.00 mm
f'_c = 13.10 MPa
f_c = 16.38 MPa
f_t = 1.67 MPa

b = 1800.0 mm
d = 77.0 mm
h = 90.0 mm
d' = 13.0 mm

α_e $[E_s/E_{c,t}]$	x_u [mm]	x_{cr} [mm]	I_u $[mm^4]$	I_{cr} $[mm^4]$	M_a [kNm]
15.67	45.79	27.0	1.35E+08	5.38E+07	9.89

SABS 0100		
f_r [MPa]	M_{cr} [kNm]	I_e $[mm^4]$
1.21	2.95	5.53E+07

EC2		
f_t [MPa]	M_{cr} [kNm]	I_e $[mm^4]$
1.67	5.10	6.41E+07

Length along Gridline where $M_a > M_{cr}$ 600.0 mm

%diff		
f_r	M_{cr}	I_e
27.2%	42.1%	13.7%

assume $I_u E_{cr} = I_e E_{c,28}$ E_{cr} = 6.62 GPa

$G = \dfrac{E}{2(1+\upsilon)}$ G = 2.76 GPa

υ = 0.2

Column Strip C4 - C5

Assume $E_{cracked}$ is constant for the given stage of loading

Reinforcement at mid C4 - C5:

A_s = 706.9 mm^2
A'_s = 0.0 mm^2

E_s = 219.0 GPa
$E_{c,28}$ = 13.97 GPa

I_g = 1.09E+08 mm^4
y_t = 45.00 mm
f'_c = 13.10 MPa
f_c = 16.38 MPa
f_t = 1.67 MPa

b = 1800.0 mm
d = 77.0 mm
h = 90.0 mm
d' = 13.0 mm

α_e $[E_s/E_{c,t}]$	x_u [mm]	x_{cr} [mm]	I_u $[mm^4]$	I_{cr} $[mm^4]$	M_a [kNm]
15.67	46.93	25.2	1.19E+08	3.93E+07	4.81

SABS 0100		
f_r [MPa]	M_{cr} [kNm]	I_e $[mm^4]$
1.21	2.95	5.54E+07

EC2		
f_t [MPa]	M_{cr} [kNm]	I_e $[mm^4]$
1.67	4.62	1.03E+08

Length along Gridline where $M_a > M_{cr}$ 200.0 mm

%diff		
f_r	M_{cr}	I_e
27.2%	36.1%	46.0%

assume $I_u E_{cr} = I_e E_{c,28}$ E_{cr} = 12.03 GPa

$G = \dfrac{E}{2(1+\upsilon)}$ G = 5.01 GPa

υ = 0.2

Column Strip C7 - C4

Assume $E_{cracked}$ is constant for the given stage of loading

Reinforcement at C4:

A_s = 863.9 mm^2
A'_s = 549.8 mm^2

E_s = 219.0 GPa
$E_{c,28}$ = 13.97 GPa

I_g = 9.11E+07 mm^4
y_t = 45.00 mm
f'_c = 13.10 MPa
f_c = 16.38 MPa
f_t = 1.67 MPa

b = 1500.0 mm
d = 77.0 mm
h = 90.0 mm
d' = 13.0 mm

α_e $[E_s/E_{c,t}]$	x_u [mm]	x_{cr} [mm]	I_u $[mm^4]$	I_{cr} $[mm^4]$	M_a [kNm]
15.67	45.95	27.3	1.12E+08	4.53E+07	6.19

SABS 0100		
f_r [MPa]	M_{cr} [kNm]	I_e $[mm^4]$
1.21	2.46	4.81E+07

EC2		
f_t [MPa]	M_{cr} [kNm]	I_e $[mm^4]$
1.67	4.25	6.29E+07

Length along Gridline where $M_a > M_{cr}$ 400.0 mm

%diff		
f_r	M_{cr}	I_e
27.2%	42.1%	23.5%

assume $$I_u E_{cr} = I_e E_{c,28}$$ E_{cr} = 7.83 GPa

$$G = \frac{E}{2(1+\upsilon)}$$ G = 3.26 GPa

υ = 0.2

Column Strip C8 - C5

Assume $E_{cracked}$ is constant for the given stage of loading

Reinforcement at C5:

A_s = 1021.0 mm^2
A'_s = 706.9 mm^2

E_s = 219.0 GPa
$E_{c,28}$ = 13.97 GPa

I_g = 1.09E+08 mm^4
y_t = 45.00 mm
f'_c = 13.10 MPa
f_c = 16.38 MPa
f_t = 1.67 MPa

b = 1800.0 mm
d = 77.0 mm
h = 90.0 mm
d' = 13.0 mm

α_e $[E_s/E_{c,t}]$	x_u [mm]	x_{cr} [mm]	I_u $[mm^4]$	I_{cr} $[mm^4]$	M_a [kNm]
15.67	45.79	27.0	1.35E+08	5.38E+07	10.02

SABS 0100		
f_r [MPa]	M_{cr} [kNm]	I_e $[mm^4]$
1.21	2.95	5.53E+07

EC2		
f_t [MPa]	M_{cr} [kNm]	I_e $[mm^4]$
1.67	5.10	6.38E+07

Length along Gridline where $M_a > M_{cr}$ 600.0 mm

%diff		
f_r	M_{cr}	I_e
27.2%	42.1%	13.3%

assume $$I_u E_{cr} = I_e E_{c,28}$$ E_{cr} = 6.59 GPa

$$G = \frac{E}{2(1+\upsilon)}$$ G = 2.75 GPa

υ = 0.2

Column Strip C8 - C5

Assume $E_{cracked}$ is constant for the given stage of loading

Reinforcement at mid C8 - C5:

A_s = 706.9 mm^2
A'_s = 0.0 mm^2

E_s = 219.0 GPa
$E_{c,28}$ = 13.97 GPa

I_g = 1.09E+08 mm^4
y_t = 45.00 mm
f'_c = 13.10 MPa
f_c = 16.38 MPa
f_t = 1.67 MPa

b = 1800.0 mm
d = 77.0 mm
h = 90.0 mm
d' = 13.0 mm

α_e $[E_s/E_{c,t}]$	x_u [mm]	x_{cr} [mm]	I_u $[mm^4]$	I_{cr} $[mm^4]$	M_a [kNm]
15.67	46.93	25.2	1.19E+08	3.93E+07	5.02

SABS 0100		
f_r [MPa]	M_{cr} [kNm]	I_e $[mm^4]$
1.21	2.95	5.35E+07

EC2		
f_t [MPa]	M_{cr} [kNm]	I_e $[mm^4]$
1.67	4.62	9.09E+07

Length along Gridline where $M_a > M_{cr}$ 500.0 mm

%diff		
f_r	M_{cr}	I_e
27.2%	36.1%	41.1%

assume $$I_u E_{cr} = I_e E_{c,28}$$ E_{cr} = 10.65 GPa

$$G = \frac{E}{2(1+\upsilon)}$$ G = 4.44 GPa

υ = 0.2

C8: Grid C	E_{cr} =	8.16 GPa	G =	3.40 GPa
C4: Grid B	E_{cr} =	10.07 GPa	G =	4.19 GPa
C5: Grid B	E_{cr} =	6.62 GPa	G =	2.76 GPa
mid C4 - C5: Grid B	E_{cr} =	12.03 GPa	G =	5.01 GPa
C4: Grid 1	E_{cr} =	7.83 GPa	G =	3.26 GPa
C5: Grid 2	E_{cr} =	6.59 GPa	G =	2.75 GPa
mid C8 - C5: Grid 2	E_{cr} =	10.65 GPa	G =	4.44 GPa
C4	AVG	8.95 GPa		
C5	AVG	6.61 GPa		

Ecracked reduced due to the Effects of Creep (at day 387)

Certina moments during the second loading stage are below the calculated cracking moment. A similar partially cracked slab is assumed with reduced $E_{cracked}$ values to accomodate the effect of time.

The relationship between $E_{c,28}$ and $E_{c,387}$ may be calculated with which to reduce the $E_{cracked}$ values.

$$E_{c,t} = \frac{E_c}{1+\phi(\infty,t)}$$ therefore $$\phi(\infty,t) = (E_c/E_{c,t}) - 1$$ and

$E_{c,28}$ = 13.97 GPa
$E_{c,387}$ = 6.98 GPa
Φ = 1.00

C8: Grid C	E_{cr} =	4.07 GPa	G =	1.70 GPa
C4: Grid B	E_{cr} =	5.03 GPa	G =	2.09 GPa
C5: Grid B	E_{cr} =	3.31 GPa	G =	1.38 GPa
mid C4 - C5: Grid B	E_{cr} =	6.01 GPa	G =	2.50 GPa
C4: Grid 1	E_{cr} =	3.91 GPa	G =	1.63 GPa
C5: Grid 2	E_{cr} =	3.29 GPa	G =	1.37 GPa
mid C8 - C5: Grid 2	E_{cr} =	5.32 GPa	G =	2.22 GPa
C4	AVG	4.47 GPa		
C5	AVG	3.30 GPa		

LOADING STAGE	STAGE 3

No moments larger than the cracking moment - thus no cracking occured.

To include the effects of cumulative cracking, a similar cracking pattern is assumed as in Stage 2. The values of $E_{cracked}$ are reduced to include the effects of time.

Ecracked reduced due to the Effects of Creep (at day 388)

The relationship between $E_{c,28}$ and $E_{c,387}$ may be calculated with which to reduce the $E_{cracked}$ values.

$$E_{c,t} = \frac{E_c}{1+\phi(\infty,t)} \quad \text{therefore} \quad \phi(\infty,t) = (E_c/E_{c,t}) - 1 \quad \text{and}$$

$E_{c,387}$ = 6.98 GPa

$E_{c,388}$ = 6.98 GPa

Φ = 0.00

C8: Grid C	E_{cr} =	4.07 GPa	G =	1.70 GPa
C4: Grid B	E_{cr} =	5.03 GPa	G =	2.09 GPa
C5: Grid B	E_{cr} =	3.31 GPa	G =	1.38 GPa
mid C4 - C5: Grid B	E_{cr} =	6.00 GPa	G =	2.50 GPa
C4: Grid 1	E_{cr} =	3.91 GPa	G =	1.63 GPa
C5: Grid 2	E_{cr} =	3.29 GPa	G =	1.37 GPa
mid C8 - C5: Grid 2	E_{cr} =	5.32 GPa	G =	2.22 GPa
C4	AVG	4.47 GPa		
C5	AVG	3.30 GPa		

Ecracked reduced due to the Effects of Creep (at day 599)

The relationship between $E_{c,28}$ and $E_{c,387}$ may be calculated with which to reduce the $E_{cracked}$ values.

$$E_{c,t} = \frac{E_c}{1+\phi(\infty,t)} \quad \text{therefore} \quad \phi(\infty,t) = (E_c/E_{c,t}) - 1 \quad \text{and}$$

$E_{c,388}$ = 6.98 GPa

$E_{c,599}$ = 5.78 GPa

Φ = 0.206

C8: Grid C	E_{cr} =	3.38 GPa	G =	1.41 GPa
C4: Grid B	E_{cr} =	4.17 GPa	G =	1.74 GPa
C5: Grid B	E_{cr} =	2.74 GPa	G =	1.14 GPa
mid C4 - C5: Grid B	E_{cr} =	4.98 GPa	G =	2.07 GPa
C4: Grid 1	E_{cr} =	3.24 GPa	G =	1.35 GPa
C5: Grid 2	E_{cr} =	2.73 GPa	G =	1.14 GPa
mid C8 - C5: Grid 2	E_{cr} =	4.41 GPa	G =	1.84 GPa
C4	AVG	3.71 GPa		
C5	AVG	2.74 GPa		

Result Comparison

Data — Comparison between FE and Predicted/Calculated Results

DEFLECTION

time [days]	Δ_{EXP} [mm]	Δ_{P_UNCR} [mm]	Δ_{P_CR} [mm]	Δ_{SABS} [mm]	Δ_{EC2} [mm]	Δ_{BS} [mm]	Δ_{ACI} [mm]	Δ_{ALT} [mm]	
14	0.94	0.91	0.91	1.16	1.06	1.06	1.12	1.06	Stage 1
28	1.52	1.43	1.43	2.81	4.64	4.69	1.35	3.50	
28	2.84	1.43	4.23	6.81	4.24	3.32	4.59	4.24	Stage 2
387	13.2	7.06	8.47	19.41	22.45	28.21	11.55	19.12	
388	11.8	2.87	3.44	5.53	3.45	3.01	3.74	3.35	Stage 3
599	11.9	3.46	4.14	8.26	6.50	4.28	3.20	6.70	

DEFLECTION RATIO

time [days]	$\Delta_{P\_UNCR}/\Delta_{EXP}$	$\Delta_{P\_CR}/\Delta_{EXP}$	$\Delta_{SABS}/\Delta_{EXP}$	$\Delta_{EC2}/\Delta_{EXP}$	Δ_{BS}/Δ_{EXP}	$\Delta_{ACI}/\Delta_{EXP}$	$\Delta_{ALT}/\Delta_{EXP}$	
14	0.96	0.96	1.23	1.13	1.12	1.19	1.13	Stage 1
28	0.94	0.94	1.85	3.05	3.08	0.89	2.30	
28	0.50	1.49	2.40	1.49	1.17	1.62	1.49	Stage 2
387	0.54	0.64	1.47	1.70	2.14	0.87	1.45	
388	0.24	0.29	0.47	0.29	0.26	0.32	0.28	Stage 3
599	0.29	0.35	0.69	0.55	0.36	0.27	0.56	

Design Standard Deflections Compared to Measured Deflections

ρ = 0.476%

DEFLECTION (Stage 1)

	time [days]	Δ_{EXP} [mm]	Δ_{P_UNCR} [mm]	Δ_{P_CR} [mm]	Δ_{SABS} [mm]	Δ_{EC2} [mm]	Δ_{BS} [mm]	Δ_{ACI} [mm]	Δ_{ALT} [mm]	Median	median/Δ_{EXP}
Short-Term Δ	14	0.94	0.91	0.91	1.16	1.06	1.06	1.12	1.06	1.06	1.13
Shrinkage Δ		0.00	0.00	0.00	1.46	1.93	1.87	0.80	1.87	1.87	
Long-Term Δ		0.00	0.00	0.00	1.34	2.71	2.81	0.55	1.63	1.63	
Total Δ	28	1.52	1.43	1.43	2.81	4.64	4.69	1.35	3.50	2.81	1.85

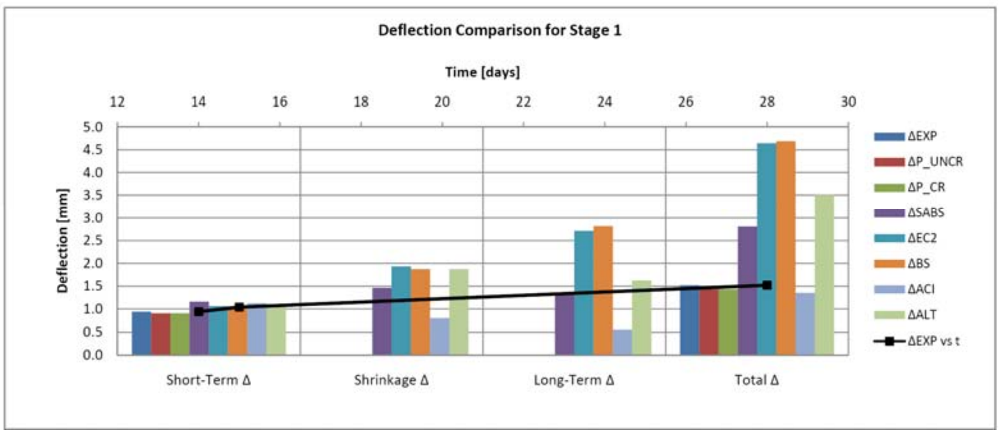

	DEFLECTION (Stage 2)										
	time [days]	Δ_{EXP} [mm]	Δ_{P_UNCR} [mm]	Δ_{P_CR} [mm]	Δ_{SABS} [mm]	Δ_{EC2} [mm]	Δ_{BS} [mm]	Δ_{ACI} [mm]	Δ_{ALT} [mm]	Median	median/Δ_{EXP}
Short-Term Δ	28	2.84	1.43	4.23	6.81	4.24	3.32	4.59	4.24	4.23	1.49
Shrinkage Δ		0.00	0.00	0.00	11.64	14.03	20.02	6.34	12.87	12.83	
Long-Term Δ		0.00	0.00	0.00	7.77	8.42	8.19	5.20	6.25	7.98	
Total Δ	387	13.20	7.06	8.47	19.41	22.45	28.21	11.55	19.12	15.48	1.17

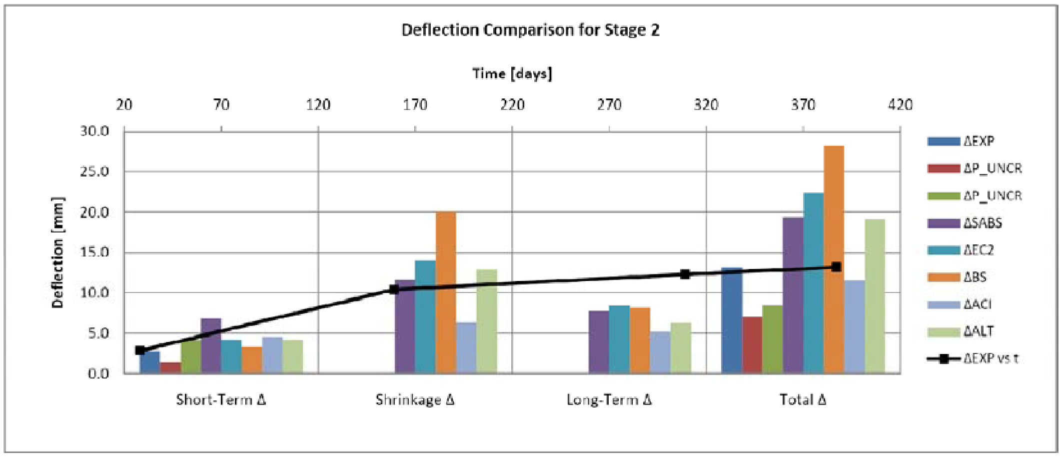

	DEFLECTION (Stage 3)										
	time [days]	Δ_{EXP} [mm]	Δ_{P_UNCR} [mm]	Δ_{P_CR} [mm]	Δ_{SABS} [mm]	Δ_{EC2} [mm]	Δ_{BS} [mm]	Δ_{ACI} [mm]	Δ_{ALT} [mm]	Median	median/Δ_{EXP}
Short-Term Δ	388	11.80	2.87	3.44	5.53	3.45	3.01	3.74	3.35	3.44	0.29
Shrinkage Δ		0.00	0.00	0.00	1.94	2.37	2.61	1.05	2.19	2.19	
Long-Term Δ		0.00	0.00	0.00	6.32	4.13	1.68	2.15	4.51	4.13	
Total Δ	599	11.90	3.46	4.14	8.26	6.50	4.28	3.20	6.70	4.28	0.36

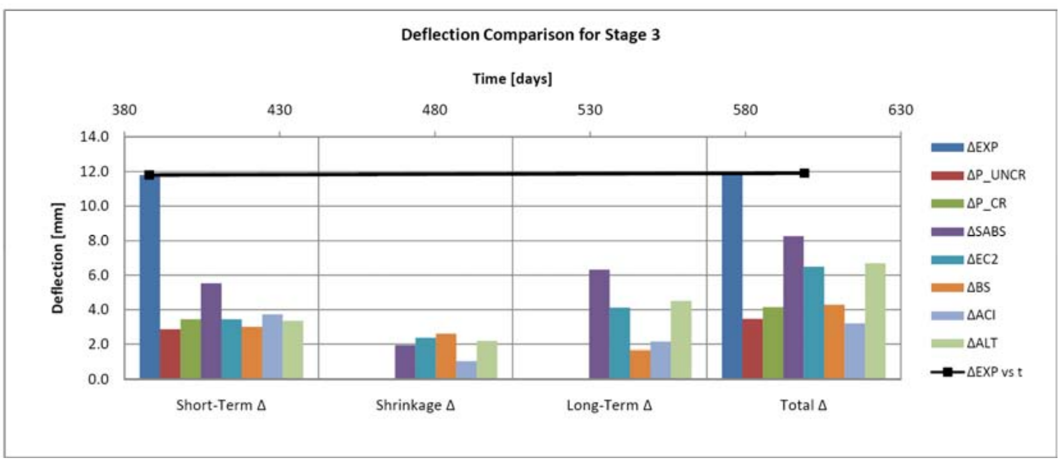

Calculation of the Time-dependent Deflection according to SABS0100-1, A.2.4

Slab Panel Parameters:

Time-Dependent Material Properties:

$f'_c = 0.8 f_c$

(Roberts and Marshall, 2008)

$f'_{c,14}$ = 13.1 MPa
$f_{c,14}$ = 16.38 MPa
$f_{dl,14}$ = - MPa
$f_{l,14}$ = 1.67 MPa

at t_0 = 28 days
t = 387 days

$E_{c,28}$ = 13.97 GPa

Φ_{28} = 0.58
Φ_{387} = 2.16

$\Delta\Phi$ = 1.58

$\varepsilon_{cs,28}$ = 8.50E-05
$\varepsilon_{cs,387}$ = 7.62E-04

$\Delta\varepsilon_{cs}$ = 6.77E-04

Immediate Deflection (A.2.4): Column Strip C7 - C8

Critical M_x Moments [kNm]				
	Stage 1		Stage 2	
	DL	LC	DL	LC
Sup_{LEFT}	1.09	1.1	1.09	2.7
Mid	-1.03	-1.0	-1.03	-2.5
Sup_{RIGHT}	1.70	1.7	1.70	4.2

Column Strip C7 - C8:

b = 1000.0 mm
L = 3000.0 mm
d = 77.0 mm
d' = 13.0 mm
h = 90.0 mm

	A_s [mm²]		A'_s [mm²]	
Sup_{LEFT}	8Y10	628.32	5Y10	392.70
Mid	5Y10	392.70	0	0.00
Sup_{RIGHT}	8Y10	628.32	5Y10	392.70

Reference

Immediate Deflection: Δ_i

* Determine K for Bending Moment Diagram

M_1 = 2.69 kNm
M_2 = 4.18 kNm
M_0 = 2.53 kNm

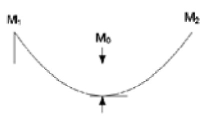

SABS 0100-1 fig A.2

$$\beta = \frac{M_1 + M_2}{M_0}$$

β = 2.72

Reference

$$K = 0.104\left(1 - \frac{\beta}{10}\right)$$

K = 0.0757

* Modulus of Rupture: (for unrestrained slabs)

A.2.4.1.1

$$f_r = 0.3\sqrt{f_c}$$

f_r = 1.21 MPa

Critical Positive Moment Section:

Cracking Moment:

$$M_{cr} = \frac{f_r I_g}{y_t}$$

I_g = 6.08E+07 mm⁴
y_t = 45.0 mm
M_{cr} = 1.6 kNm

Momenf of Inertia of Cracked Section:

$$x_{cr\_1} = \frac{\frac{1}{2} x_{cr\_2}{}^2 b + A_s d \alpha_e}{x_{cr\_2} b + A_s \alpha_e}$$

x_{cr_1} = 25.2 mm

where $\alpha_e = \frac{E_s}{E_c}$

b = 1000.0 mm
A_s = 392.7 mm²
d = 77.0 mm
E_s = 219.0 GPa
E_c = 14.0 GPa
α_e = 15.7
x_{cr_2} = 25.2 mm

$$I_{cr} = \tfrac{1}{3} b x_{cr}{}^3 + A_s (d - x_{cr})^2 \alpha_e$$

I_{cr} = 2.2E+07 mm⁴

$$I_{em} = \left(\frac{M_{cr}}{M_a}\right)^3 I_g + \left[1 - \left(\frac{M_{cr}}{M_a}\right)^3\right] I_{cr}$$

M_a = 2.5 kNm
I_{em} = 3.2E+07 mm⁴

I_{em} < I_g Section is Cracked

Left Critical Negative Moment Section:

Cracking Moment:

$$M_{cr} = \frac{f_r I_g}{y_t}$$

I_g = 6.08E+07 mm⁴
y_t = 45.0 mm
M_{cr} = 1.6 kNm

Momenf of Inertia of Cracked Section:

$$x_{cr\_1} = \frac{\frac{1}{2} x_{cr\_2}{}^2 b + A_s d \alpha_e}{x_{cr\_2} b + A_s \alpha_e}$$

x_{cr_1} = 30.3 mm

where $\alpha_e = \frac{E_s}{E_c}$

b = 1000.0 mm
A_s = 628.3 mm²
d = 77.0 mm
E_s = 219.0 GPa
E_c = 14.0 GPa

Reference
A.2.4.1.1

α_e = 15.7
x_{cr_2} = 30.3 mm

$$I_{cr} = \tfrac{1}{3}bx_{cr}^3 + A_s(d-x_{cr})^2\alpha_e$$

I_{cr} = 3.1E+07 mm^4

$$I_{e1} = \left(\frac{M_{cr}}{M_a}\right)^3 I_g + \left[1-\left(\frac{M_{cr}}{M_a}\right)^3\right] I_{cr}$$

M_a = 2.69 kNm
I_{e1} = 3.8E+07 mm^4

I_{e1} < I_g Section is Cracked

Right Critical Negative Moment Section:

Cracking Moment:

$$M_{cr} = \frac{f_r I_g}{y_t}$$

I_g = 6.08E+07 mm^4
y_t = 45.0 mm
M_{cr} = 1.6 kNm

Momenf of Inertia of Cracked Section:

$$x_{cr\_1} = \frac{\frac{1}{2}x_{cr\_2}{}^2 b + A_s d\alpha_e}{x_{cr\_2}b + A_s\alpha_e}$$

where $\alpha_e = \frac{E_s}{E_c}$

x_{cr_1} = 30.3 mm

b = 1000.0 mm
A_s = 628.3 mm^2
d = 77.0 mm
E_s = 219.0 GPa
E_c = 14.0 GPa
α_e = 15.7
x_{cr_2} = 30.3 mm

$$I_{cr} = \tfrac{1}{3}bx_{cr}^3 + A_s(d-x_{cr})^2\alpha_e$$

I_{cr} = 3.1E+07 mm^4

$$I_{e2} = \left(\frac{M_{cr}}{M_a}\right)^3 I_g + \left[1-\left(\frac{M_{cr}}{M_a}\right)^3\right] I_{cr}$$

M_a = 4.18 kNm
I_{e2} = 3.3E+07 mm^4

I_{e2} < I_g Section is Cracked

* Effective Second Moment of Inertia

$$I_{ea} = 0.5\left[\frac{I_{e1}+I_{e2}}{2} + I_{em}\right]$$

I_{e1} = 3.75E+07 mm^4
I_{e2} = 3.25E+07 mm^4
I_{em} = 3.24E+07 mm^4

I_{ea} = 3.37E+07 mm^4

Reference
A.2.4.1.1

* Immediate Deflection: Δ_{C7_C8}

$$\Delta_i = KM_a\frac{L^2}{E_c I_{ea}}$$

K = 0.076
M_a = 2.5 kNm
L = 3000.0 mm
E_c = 14.0 GPa
I_{ea} = 3.4E+07 mm^4

Δ_{C7_C8} = 3.65 mm

	Sup_{LEFT}	Mid	Sup_{RIGHT}
Status	Cracked	Cracked	Cracked
I_g/I_{cr}	1.976	2.781	1.976
M_a/M_{cr}	1.640	1.543	2.554

Long-Term Creep Deflection Δ_l

A method to determine long-term creep deflections from immediate deflections is described in SABS 0100-1, Annexure A, clause A.2.4.1.2 and A.2.5

The long-term creep deflections are calculated using the immediate deflections from clause A.2.4.1.1.

To obtain a final long-term deflection the shrinkage deflections as calculated in the above section are added to the long-term creep deflections for each respective column and middle strip.

A final midspan long-term deflection is then calculated.

Long-Term Deflection (A.2.5): C7 - C8

Reference

Long-Term Creep Deflection:

SABS 0100-1 A.2.4.1.2

$$\lambda = 1 + x_i \phi$$

Φ = 1.58

$$x_i = x_{cr} / d$$

x_{cr} = 25.24 mm (from above)
d = 77.00 mm
x_i = 0.33

λ = 1.52

* Short-term deflection due to Permanent Load

A.2.4.1.1

$$I_e = \left(\frac{M_{cr}}{M_p}\right)^3 I_g + \left[1 - \left(\frac{M_{cr}}{M_p}\right)^3\right] I_{cr}$$

M_{cr} = 1.6 kNm
I_g = 6.08E+07 mm^4

(from short-term deflection calculations)

	x_{cr} [mm]	I_{cr} [mm^4]	M_p [kNm]	I_e [mm^4]	> I_g
I_{em} [mm^4]	25.2	2.2E+07	1.03	1.80E+08	TRUE
I_{e1} [mm^4]	30.3	3.1E+07	1.09	1.32E+08	TRUE
I_{e2} [mm^4]	30.3	3.1E+07	1.70	5.77E+07	FALSE

$$I_{ea} = 0.5\left[\frac{I_{e1} + I_{e2}}{2} + I_{em}\right]$$

I_{em} = 6.08E+07 mm^4
I_{e1} = 6.08E+07 mm^4
I_{e2} = 5.77E+07 mm^4

I_{ea} = 6.00E+07 mm^4

Reference

$$\Delta_{i,p} = K M_p \frac{L^2}{E_c I_{ea}}$$

K = 0.0757
M_p = 1.026 kNm
L = 3000.0 mm
E_c = 13.97 GPa
I_{ea} = 6.00E+07 mm^4

$\Delta_{i,p}$ = 0.83 mm

* Long-term deflection due to Permanent Load

A.2.4.1.2

$$\Delta_{l,p} = \lambda \Delta_{i,p}$$

λ = 1.52
$\Delta_{i,p}$ = 0.83 mm

$\Delta_{l,p}$ = 1.27 mm

* Additional Initial Deflection

$$\Delta_{i,add} = \Delta_i - \Delta_{i,p}$$

Δ_i = 3.65 mm
$\Delta_{i,p}$ = 0.83 mm

$\Delta_{i,add}$ = 2.82 mm

* Total Long-term Deflection

$$\Delta_l = \Delta_{i,add} + \Delta_{l,p}$$

$\Delta_{l,p}$ = 1.27 mm
$\Delta_{i,add}$ = 2.82 mm

Δ_l = 4.09 mm

A.2.5

Shrinkage Deflection:

$$\Delta_{cs} = K_{sh} k_{cs} \frac{\varepsilon_{cs} L^2}{h}$$

K_{sh} = 0.086
ε_{cs} = 6.77E-04

check:

$$\rho = \frac{100 A_s}{bd} \le 3$$

A_s = 392.7 mm^2
d = 77.0 mm

ρ = 0.5100

$$\rho' = \frac{100 A'_s}{bd}$$

A'_s = 0.0 mm^2
d = 77.0 mm

ρ' = 0.0000

$$\frac{\rho'}{\rho} \le 1$$

ρ'/ρ = 0.00 OK!

check: $k_{cs} = 1 - \frac{\rho'}{\rho}\left[1 - 0.11(3 - \rho)^2\right]$

k_{cs} = 1.0

$0.3 \le k_{cs} \le 1$ OK!

Reference

$$0.3 \le k_{cs} \le 1$$

L = 3000.0 mm
h = 90.0 mm

Δ_{cs} = 5.82 mm

Total Deflection:

$$\Delta_t = \Delta_l + \Delta_{cs}$$

Δ_l = 4.09 mm
Δ_{cs} = 5.82 mm

Δ_t = 9.91 mm

SUMMARY of the calculated Deflections:

This section aims to summarize the deflections from the above calculated methods.

A	B	C	D
Short-Term Deflection from A.2.2	Long-Term Deflection from A.2.2	Creep Deflection from A.2.2.5	Total Deflection from B and C

A	B	C	D
Short-Term Deflection from A.2.2	Long-Term Deflection from A.2.2	Creep Deflection from A.2.2.5	Total Deflection from B and C

COLUMN STRIP C7 - C8			
METHOD A.2.2 and A.2.3 [mm]			
Δ_{short}	Δ_{long}	Δ_{shrink}	Δ_{total}
3.65	4.09	5.82	9.91

COLUMN STRIP C7 - C4			
METHOD A.2.2 and A.2.3 [mm]			
Δ_{short}	Δ_{long}	Δ_{shrink}	Δ_{total}
3.84	4.34	5.82	10.16

COLUMN STRIP C4 - C5			
METHOD A.2.2 and A.2.3 [mm]			
Δ_{short}	Δ_{long}	Δ_{shrink}	Δ_{total}
3.89	4.35	5.82	10.17

COLUMN STRIP C8 - C5			
METHOD A.2.2 and A.2.3 [mm]			
Δ_{short}	Δ_{long}	Δ_{shrink}	Δ_{total}
4.41	4.91	5.82	10.73

MIDDLE STRIP C7,C8 - C4,C5			
METHOD A.2.2 and A.2.3 [mm]			
Δ_{short}	Δ_{long}	Δ_{shrink}	Δ_{total}
2.97	3.46	5.82	9.29

MIDDLE STRIP C4,C7 - C5,C8			
METHOD A.2.2 and A.2.3 [mm]			
Δ_{short}	Δ_{long}	Δ_{shrink}	Δ_{total}
2.75	3.23	5.82	9.05

$$\Delta_{mid\_i} = \tfrac{1}{2}\left(\Delta_{col\_1} + \Delta_{col\_2}\right) + \Delta_{middle}$$ where i = 1 or 2

MID DEFLECTION (Average of Strips)			
METHOD A.2.2 and A.2.3 [mm]			
Δ_{short}	Δ_{long}	Δ_{shrink}	Δ_{total}
6.74	7.68	11.64	19.32

MID DEFLECTION (Average of Strips)			
METHOD A.2.2 and A.2.3 [mm]			
Δ_{short}	Δ_{long}	Δ_{shrink}	Δ_{total}
6.88	7.85	11.64	19.49

$$\Delta_{final} = \tfrac{1}{2}\left(\Delta_{mid\_1} + \Delta_{mid\_2}\right)$$

FINAL MID DEFLECTION			
METHOD A.2.2 and A.2.3 [mm]			
Δ_{short}	Δ_{long}	Δ_{shrink}	Δ_{total}
6.81	7.77	11.64	19.41

Calculation of the Short- and Long-Term Deflections according to Eurocode 2: Clause 7.4.3:

The long-term deflections will be determined using the different column strips and middle strips, also known as the Equivalent Frame Method.

Slab Panel Parameters:

Time-Dependent Material Properties:

$f'_c = 0.8f_c$
(Roberts and Marshall, 2008)

$f'_{c,14}$ = 13.1 MPa
$f_{c,14}$ = 16.38 MPa
$f_{tfl,14}$ = - MPa
$f_{t,14}$ = 1.67 MPa

at t_0 = 28 days
t = 387 days

$E_{c,28}$ = 13.97 GPa

Φ_{28} = 0.58
Φ_{387} = 2.16

$\Delta\Phi$ = 1.58

$\varepsilon_{cs,28}$ = 8.50E-05
$\varepsilon_{cs,387}$ = 7.62E-04

$\Delta\varepsilon_{cs}$ = 6.77E-04

Long-Term Deflections for Slab Panel:

Long-Term Deflection (7.4.3): Column Strip C7 - C8

Reference

* Moments used for Column Strip C7 - C8:

Position	Stage 1 DL	Stage 1 LC	Stage 2 DL	Stage 2 LC
	Critical M_x Moments [kNm]			
Sup_{LEFT}	1.09	1.09	1.09	2.69
Mid	-1.03	-1.03	-1.03	-2.53
Sup_{RIGHT}	1.70	1.70	1.70	4.18

Column Strip C7 - C8:

b = 1000.0 mm
L = 3000.0 mm
d = 77.0 mm
d' = 13.0 mm
h = 90.0 mm

	A_s [mm^2]		A'_s [mm^2]	
Sup_{LEFT}	8Y10	628.32	5Y10	392.70
Mid	5Y10	392.70	0	0.00
Sup_{RIGHT}	8Y10	628.32	5Y10	392.70

Reference

EC2

eq. 7.20

* Modulus of Elasticity: Long-Term

$$E_{eff} = \frac{E_c}{(1+\varphi(\infty, t_0))}$$

where $E_{c,14}$ = 22.08 MPa
Φ_{387} = 2.16

E_{eff} = 6.98 GPa

* Modulus of Elasticity: Reinforcement

E_s = 219.0 GPa

* Deflection Coefficient

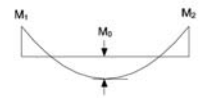

M_1 = 2.69 kNm
M_2 = 4.18 kNm
M_0 = 2.53 kNm

$$\beta = \frac{M_1 + M_2}{M_0}$$

β = 2.72

$$K = 0.104\left(1 - \frac{\beta}{10}\right)$$

K = 0.0757

Short-Term Properties:

eq. 7.21

* Effective Modulus Ratio

$$\alpha_e = \frac{E_s}{E_c}$$

E_s = 219.0 GPa
E_c = 13.97 GPa

α_e = 15.67

* Moment of Inertia for Uncracked Condition

$$x_u = \frac{\frac{bh^2}{2} + (\alpha_e - 1)(A_s d + A'_s d')}{bh + (\alpha_e - 1)(A_s + A'_s)}$$

b = 1000.0 mm
h = 90.0 mm
d = 77.0 mm
d' = 13.0 mm
A_s = 392.70 mm^2
A'_s = 0.0 mm^2

x_u = 46.93 mm

$$I_u = \frac{bh^3}{12} + bh\left(\frac{h}{2} - x_u\right)^2 + (\alpha_e - 1)\left[A_s(d - x_u)^2 + A'_s(x_u - d')^2\right]$$

I_u = 6.63E+07 mm^4

Reference

* Moment of Inertia for Cracked Condition

$$x_{cr} = \left\{\left[\omega^2 + 2b\left(A_s d\alpha_e + A'_s d'(\alpha_e - 1)\right)\right]^{0.5} - \omega\right\}/b$$

$$\omega = A_s\alpha_e + A'_s(\alpha_e - 1)$$

b = 1000.0 mm
d = 77.0 mm
d' = 13.0 mm
A_s = 392.70 mm^2
A'_s = 0.0 mm^2
α_e = 15.67

ω = 6154.06 mm^2
x_{cr} = 25.24 mm

$$I_{cr} = \frac{bx_{cr}^3}{3} + \alpha_e A_s(d - x_{cr})^2 + (\alpha_e - 1)A'_s(d' - x_{cr})^2$$

I_{cr} = 2.18E+07 mm^4 I_u/I_{cr} = 3.03

* Cracking Moment

$$M_{cr} = \frac{f_t I_u}{h - x_u}$$

f_t = 1.7 MPa
h = 90.0 mm

M_{cr} = 2.57 kNm
M_a = 2.53 kNm (from above)

M_a/M_{cr} = 0.99

M_a < M_{cr}

Section is Uncracked

* Short-Term Flexural Curvature

eq. 7.18

Section is Uncracked	Section is Cracked
ζ = 0	ζ = 1 - $(M_{cr}/M_a)^2$
$I_e = I_u$	$I_e = \dfrac{I_{cr}}{1 - \left(1 - \dfrac{I_{cr}}{I_u}\right)\left(\dfrac{M_{cr}}{M_a}\right)^2}$

I_e = 6.63E+07 mm^4

E_c = 13.97 GPa
E_{eff} = 6.98 GPa
I_{cr} = 2.18E+07 mm^4
I_u = 6.63E+07 mm^4

$$\frac{1}{r_i} = \frac{M_a}{E_c I_e}$$

$1/r_i$ = 2.73E-03 m^{-1}

* Short-Term Flexure Deflection

$$\Delta_i = KL^2\frac{1}{r_i}$$

L = 3.0 m
$1/r_i$ = 2.73E-03 m^{-1}
K = 0.0757

Δ_i = 1.86 mm

Reference

Long-Term Properties:

* Effective Modulus Ratio

eq. 7.21

$$\alpha_e = \frac{E_s}{E_{eff}}$$

E_s = 219.0 GPa
E_{eff} = 6.98 GPa

α_e = 31.38

* Moment of Inertia for Uncracked Condition

$$x_u = \frac{\frac{bh^2}{2} + (\alpha_e - 1)(A_s d + A'_s d')}{bh + (\alpha_e - 1)(A_s + A'_s)}$$

b = 1000.0 mm
h = 90.0 mm
d = 77.0 mm
d' = 13.0 mm
A_s = 392.7 mm^2
A'_s = 0.0 mm^2

x_u = 48.75 mm

$$I_u = \frac{bh^3}{12} + bh\left(\frac{h}{2} - x_u\right)^2 + (\alpha_e - 1)\left[A_s(d - x_u)^2 + A'_s(x_u - d')^2\right]$$

I_u = 7.15E+07 mm^4

* Moment of Inertia for Cracked Condition

$$x_{cr} = \left\{\left[\omega^2 + 2b\left(A_s d\alpha_e + A'_s d'(\alpha_e - 1)\right)\right]^{0.5} - \omega\right\}/b$$

$$\omega = A_s\alpha_e + A'_s(\alpha_e - 1)$$

b = 1000.0 mm
d = 77.0 mm
d' = 13.0 mm
A_s = 392.70 mm^2
A'_s = 0.0 mm^2
α_e = 31.38

ω = 12323.71 mm^2
x_{cr} = 32.95 mm

$$I_{cr} = \frac{bx_{cr}^3}{3} + \alpha_e A_s(d - x_{cr})^2 + (\alpha_e - 1)A'_s(d' - x_{cr})^2$$

I_{cr} = 3.58E+07 mm^4 I_u/I_{cr} = 2.00

* Long-Term Flexural Curvature

eq. 7.18

Section is Uncracked	Section is Cracked
ζ = 0	ζ = 1 - 0.5$(M_{cr}/M_a)^2$
$I_e = I_u$	$I_e = \dfrac{I_{cr}}{1 - \left(1 - \dfrac{I_{cr}}{I_u}\right)0.5\left(\dfrac{M_{cr}}{M_a}\right)^2}$

Reference
eq. 7.21 & 7.18

I_e = 7.15E+07 mm^4

E_c = 13.97 GPa
E_{eff} = 6.98 GPa
I_{cr} = 3.58E+07 mm^4
I_u = 7.15E+07 mm^4
ζ = 0.00
M_a = 2.53 kNm

$$\frac{1}{r_l} = \frac{M_a}{E_{eff} I_e}$$

$1/r_l$ = 5.07E-03 m^{-1}

* Long-Term Flexure Deflection

L = 3.0 m
$1/r_l$ = 5.07E-03 m^{-1}
K = 0.0757

$$\Delta_l = KL^2 \frac{1}{r_l}$$

Δ_l = 3.45 mm

* Shrinkage Curvature

ε_{cs} = 6.77E-04
d = 77.0 mm
d' = 13.0 mm
A_s = 392.7 mm^2
A'_s = 0.0 mm^2
x_u = 48.75 mm
x_{cr} = 32.95 mm
α_e = 31.38
ζ = 0.0
I_u = 7.15E+07 mm^4
I_{cr} = 3.58E+07 mm^4

$$\frac{1}{r_{cs}} = \varsigma \varepsilon_{cs} \alpha_e \frac{S_u}{I_u} + (1-\varsigma) \varepsilon_{cs} \alpha_e \frac{S_{cr}}{I_{cr}}$$

$$S_u = A_s(d - x_u) - A'_s(x_u - d')$$

S_u = 1.11E+04 mm^3

$$S_{cr} = A_s(d - x_{cr}) - A'_s(x_{cr} - d')$$

S_{cr} = 1.73E+04 mm^3

$1/r_{cs}$ = 1.03E-05 mm^{-1}

* Shrinkage Deflection

L = 3000.0 mm
$1/r_{cs}$ = 1.03E-05 mm^{-1}
K_{sh} = 0.0840 (Branson 1977)

$$\Delta_{cs} = K_{sh} L^2 \frac{1}{r_{cs}}$$

Δ_{cs} = 7.75 mm

* Total Deflection

Δ_l = 3.45 mm
Δ_{cs} = 7.75 mm

$$\Delta_t = \Delta_{cs} + \Delta_l$$

Δ_t = 11.20 mm

SUMMARY of the calculated Deflections:

This section aims to summarize the deflections from the above calculated methods.

A	B	C	D
Short-Term Deflection from eq. 7.18	Long-Term Deflection from eq. 7.18	Shrinkage Deflection from eq. 7.21	Total Deflection from B and C

COLUMN STRIP C7 - C8			
METHOD 7.4.3 [mm]			
Δ_{short}	Δ_{long}	Δ_{shrink}	Δ_{total}
1.86	3.45	7.75	11.20

COLUMN STRIP C4 - C5			
METHOD 7.4.3 [mm]			
Δ_{short}	Δ_{long}	Δ_{shrink}	Δ_{total}
2.11	5.18	4.91	10.09

MIDDLE STRIP C7,C8 - C4,C5			
METHOD 7.4.3 [mm]			
Δ_{short}	Δ_{long}	Δ_{shrink}	Δ_{total}
2.16	4.00	7.75	11.75

A	B	C	D
Short-Term Deflection from eq. 7.18	Long-Term Deflection from eq. 7.18	Shrinkage Deflection from eq. 7.21	Total Deflection from B and C

COLUMN STRIP C7 - C4			
METHOD 7.4.3 [mm]			
Δ_{short}	Δ_{long}	Δ_{shrink}	Δ_{total}
1.92	3.58	7.72	11.29

COLUMN STRIP C8 - C5			
METHOD 7.4.3 [mm]			
Δ_{short}	Δ_{long}	Δ_{shrink}	Δ_{total}
2.63	5.85	4.72	10.57

MIDDLE STRIP C4,C7 - C5,C8			
METHOD 7.4.3 [mm]			
Δ_{short}	Δ_{long}	Δ_{shrink}	Δ_{total}
2.06	3.81	7.75	11.57

$$\Delta_{mid\_i} = \tfrac{1}{2}\left(\Delta_{col\_1} + \Delta_{col\_2}\right) + \Delta_{middle}$$

where i = 1 or 2

MID DEFLECTION (Average of Strips)			
METHOD 7.4.3 [mm]			
Δ_{short}	Δ_{long}	Δ_{shrink}	Δ_{total}
4.14	8.32	14.08	22.40

MID DEFLECTION (Average of Strips)			
METHOD 7.4.3 [mm]			
Δ_{short}	Δ_{long}	Δ_{shrink}	Δ_{total}
4.33	8.53	13.97	22.50

$$\Delta_{final} = \tfrac{1}{2}\left(\Delta_{mid\_1} + \Delta_{mid\_2}\right)$$

FINAL MID DEFLECTION			
METHOD 7.4.3 [mm]			
Δ_{short}	Δ_{long}	Δ_{shrink}	Δ_{total}
4.24	8.42	14.03	22.45

Calculation of the Long-Term Deflections according to BS 8110: Part 2: Clause 3.7

Equations from BS 8110 were obtained from *KONG&EVANS, Reinforced and Prestressed Concrete, Third Edition, Chapter 5, Section5.3*

Slab Panel Parameters:

Time-Dependent Material Properties:

$f'_c = 0.8f_c$
(Roberts and Marshall, 2008)

$f'_{c,14}$ = 13.1 MPa
$f_{c,14}$ = 16.38 MPa
$f_{ut,14}$ = - MPa
$f_{t,14}$ = 1.67 MPa

at t_0 = 28 days, t = 387 days

$E_{c,28}$ = 13.97 GPa

Φ_{28} = 0.58
Φ_{387} = 2.16
$\Delta\Phi$ = 1.58

$\varepsilon_{cs,28}$ = 0.00E+00
$\varepsilon_{cs,387}$ = 8.74E-04
$\Delta\varepsilon_{cs}$ = 8.74E-04

Long-Term Deflections for Slab Panel:

Long-Term Deflection: Column Strip C7 - C8

Reference: BS 8110 3.6

* Modulus of Elasticity: Short and Long-Term

$E_{c,14}$ = 22.08 GPa

$$E_{eff} = \frac{E_c}{(1+\Phi)}$$

where Φ_{387} = 2.16

E_{eff} = 6.98 GPa
E_s = 219.0 GPa

* Sectional Properties — Column Strip C7 - C8

b = 1000.0 mm
L = 3000.0 mm
d = 77.0 mm
d' = 13.0 mm
h = 90.0 mm

	A_s [mm^2]		A'_s [mm^2]	
Sup_{LEFT}	8Y10	628.32	5Y10	392.70
Mid	5Y10	392.70	0	0.00
Sup_{RIGHT}	8Y10	628.32	5Y10	392.70

Reference

* Midspan Moments used for Column Strip C7 - C8:

M_p = 1.03 kNm (Moment due to Permanent Load)
M_a = 2.53 kNm (Moment due to Total Load)

* Reinforcement provided for Column Strip C7 - C8:

A_s = 392.7 mm^2
A'_s = 0.0 mm^2

* Percentage Reinforcement

ρ = A_s/bd = 0.00510
ρ' = A'_s/bd = 0.00000

* Sectional Properties

SHORT-TERM

Kong&Evans

$$\alpha_e = \frac{E_s}{E_c}$$

α_e = 15.67

$$x_u = \frac{\frac{bh^2}{2} + (\alpha_e)(A_s d + A'_s d')}{bh + (\alpha_e)(A_s + A'_s)}$$

x_u = 47.05 mm

b = 1000.0 mm
h = 90.0 mm
d = 77.0 mm
d' = 13.0 mm
A_s = 392.70 mm^2
A'_s = 0.00 mm^2

$$I_u = \frac{bh^3}{12} + bh\left(\frac{h}{2} - x_u\right)^2 + (\alpha_e)\left[A_s(d-x_u)^2 + A'_s(x_u - d')^2\right]$$

I_u = 6.66E+07 mm^4

eq 5.2-4

$$\frac{x_{cr}}{d} = -\alpha_e(\rho+\rho') + \sqrt{\left\{\alpha_e^2(\rho+\rho')^2 + 2\alpha_e\left(\rho + \frac{d'}{d}\rho'\right)\right\}}$$

x_{cr}/d = 0.33
x_{cr} = 25.2 mm

d = 77.0 mm
d' = 13.0 mm

eq 5.2-9

$$\frac{I_{cr}}{bd^3} = \frac{1}{3}\left(\frac{x_{cr}}{d}\right)^3 + \alpha_e\rho\left(1 - \frac{x_{cr}}{d}\right)^2 + \alpha_e\rho'\left(\frac{x_{cr}}{d} - \frac{d'}{d}\right)^2$$

I_{cr}/bd^3 = 0.0478544
I_{cr} = 2.18E+07 mm^4

Reference

LONG-TERM

$$\alpha_e = \frac{E_s}{E_{eff}}$$

α_e = 31.38

eq 5.2-4

$$\frac{x_{cr}}{d} = -\alpha_e(\rho+\rho') + \sqrt{\left\{\alpha_e^2(\rho+\rho')^2 + 2\alpha_e\left(\rho + \frac{d'}{d}\rho'\right)\right\}}$$

x_{cr}/d = 0.43 | d = 77.0 mm

x_{cr} = 33.0 mm | d' = 13.0 mm

eq 5.2-9

$$\frac{I_{cr}}{bd^3} = \frac{1}{3}\left(\frac{x_{cr}}{d}\right)^3 + \alpha_e\rho\left(1-\frac{x_{cr}}{d}\right)^2 + \alpha_e\rho\left(\frac{x_{cr}}{d}-\frac{d'}{d}\right)^2$$

I_{cr}/bd^3 = 0.0784994

I_{cr} = 3.6E+07 mm^4

* Short-Term Deflection Curves (use all short-term properties)

Short-Term Curvature due to Total Moment

$$M_{net} = M_a - \Delta M = M_a - \tfrac{1}{3}\frac{b(h-x_{cr})^3}{d-x_{cr}}f_t$$

M_a = 2.53 kNm
b = 1000.0 mm
d = 77.0 mm
h = 90.0 mm
x_{cr} = 25.2 mm
f_t = 1.0 MPa

ΔM = 1.75 kNm

M_{net} = 0.78 kNm

M_a > ΔM

$M_a > \Delta M$	$M_a \leq \Delta M$
$\frac{1}{r_i} = \frac{M_{net}}{E_c I_{cr}}$	$\frac{1}{r_i} = \frac{M_a}{E_c I_u}$

$1/r_i$ = 2.553E-06 mm^{-1}

I_u = 6.66E+07 mm^4
I_{cr} = 2.18E+07 mm^4
E_c = 13.97 GPa

* Short-Term Deflection

Short-Term Deflection

BS 8110 3.5

$$\Delta_i = KL^2\frac{1}{r_i}$$

$1/r_i$ = 2.553E-06 mm^{-1}
K = 0.0757
(from SABS_St_2)
L = 3000.0 mm

Δ_i = 1.74 mm

Reference

* Long-Term Deflection Curves

Instantaneous Curvature due to Non-Permanent Load

Kong&Evans eq 5.2-24

$$\frac{1}{r_{in}} = \frac{1}{r_{it}} - \frac{1}{r_{ip}} = \frac{M_a - M_p}{E_c I_{cr}}$$

M_a = 2.53 kNm
M_p = 1.03 kNm
E_c = 13.97 GPa
I_{cr} = 2.18E+07 mm^4

$1/r_{in}$ = 4.92E-06 mm^{-1}

Moment due to Concrete Tension (use long-term properties)

eq 5.2-19

$$\Delta M = \tfrac{1}{3}\frac{b(h-x_{cr})^3}{(d-x_{cr})}f_t$$

b = 1000.0 mm
d = 77.0 mm
h = 90.0 mm
x_{cr} = 33.0 mm
f_t = 0.55 MPa

ΔM = 0.77 kNm

Long-term Curvature

eq 5.2-23

$$\frac{1}{r_{pl}} = \frac{M_p - \Delta M}{E_{eff} I_{cr}}$$

M_p = 1.03 kNm
ΔM = 0.77 kNm
E_{eff} = 6.98 GPa
I_{cr} = 3.6E+07 mm^4

$1/r_{pl}$ = 1.0E-06 mm^{-1}

Shrinkage Curvature

eq 5.5.6

$$\frac{1}{r_{cs}} = \frac{\varepsilon_{cs}\alpha_e S_{cr}}{I_{cr}}$$

α_e = 31.38
ε_{cs} = 8.74E-04
I_{cr} = 3.6E+07 mm^4

$$S_{cr} = A_s(d-x_{cr}) - A'_s(x_{cr}-d')$$

A_s = 392.70 mm^2
A'_s = 0.00 mm^2
d = 77.0 mm
d' = 13.0 mm
x_{cr} = 33.0 mm

S_{cr} = 1.7E+04 mm^3

$1/r_{cs}$ = 1.3E-05 mm^{-1}

* Long-Term Deflections

Long-Term Deflection

$$\frac{1}{r_l} = \frac{1}{r_{pl}} + \frac{1}{r_{in}}$$

$1/r_{in}$ = 4.92E-06 mm^{-1}
$1/r_{pl}$ = 1.0E-06 mm^{-1}

$1/r_l$ = 5.9E-06 mm^{-1}

BS 8110 3.5

$$\Delta_l = KL^2\frac{1}{r_l}$$

K = 0.0757
(from SABS_St_2)
L = 3000.0 mm

Δ_l = 4.04 mm

Reference

BS 8110

3.7

<u>Shrinkage Deflection</u>

The shrinkage curvature is assumed to be constant along the member.

$1/r_{cs}$ = 1.3E-05 mm^{-1}

$$\Delta_{cs} = K_{sh} L^2 \frac{1}{r_{cs}}$$

K = 0.0840

(Branson 1977)

L = 3000.0 mm

Δ_{cs} = 10.01 mm

<u>Total Long-Term Deflection</u>

$$\Delta_t = \Delta_l + \Delta_{cs}$$

Δ_t = 14.06 mm

This section aims to summarize the deflections from the above calculated methods.

A	B	C	D
Short-Term Deflection from 3.7	Long-Term Deflection from 3.7	Shrinkage Deflection from 3.6	Total Deflection from B and C

A	B	C	D
Short-Term Deflection from 3.7	Long-Term Deflection from 3.7	Shrinkage Deflection from 3.6	Total Deflection from B and C

COLUMN STRIP C7 - C8			
METHOD 3.6 and 3.7 [mm]			
Δ_{short}	Δ_{long}	Δ_{shrink}	Δ_{total}
1.74	4.04	10.01	14.06

COLUMN STRIP C7 - C4			
METHOD 3.6 and 3.7 [mm]			
Δ_{short}	Δ_{long}	Δ_{shrink}	Δ_{total}
1.78	4.30	9.97	14.27

COLUMN STRIP C4 - C5			
METHOD 3.6 and 3.7 [mm]			
Δ_{short}	Δ_{long}	Δ_{shrink}	Δ_{total}
1.91	4.06	10.01	14.07

COLUMN STRIP C8 - C5			
METHOD 3.6 and 3.7 [mm]			
Δ_{short}	Δ_{long}	Δ_{shrink}	Δ_{total}
2.27	3.24	10.01	13.26

MIDDLE STRIP C7,C8 - C4,C5			
METHOD 3.6 and 3.7 [mm]			
Δ_{short}	Δ_{long}	Δ_{shrink}	Δ_{total}
1.56	4.46	10.01	14.47

MIDDLE STRIP C4,C7 - C5,C8			
METHOD 3.6 and 3.7 [mm]			
Δ_{short}	Δ_{long}	Δ_{shrink}	Δ_{total}
1.25	4.10	10.01	14.12

$$\Delta_{mid\_i} = \tfrac{1}{2}\left(\Delta_{col\_1} + \Delta_{col\_2}\right) + \Delta_{middle}$$

where i = 1 or 2

MID DEFLECTION (Average of Strips)			
METHOD 3.6 and 3.7 [mm]			
Δ_{short}	Δ_{long}	Δ_{shrink}	Δ_{total}
3.38	8.51	20.03	28.54

MID DEFLECTION (Average of Strips)			
METHOD 3.6 and 3.7 [mm]			
Δ_{short}	Δ_{long}	Δ_{shrink}	Δ_{total}
3.27	7.88	20.01	27.88

$$\Delta_{final} = \tfrac{1}{2}\left(\Delta_{mid\_1} + \Delta_{mid\_2}\right)$$

FINAL MID DEFLECTION			
METHOD 3.6 and 3.7 [mm]			
Δ_{short}	Δ_{long}	Δ_{shrink}	Δ_{total}
3.32	8.19	20.02	28.21

Calculation of the Short- and Long-Term Deflections according to ACI 318: Clause 9.5.2.3:

The long-term deflections will be determined using the different column strips and middle strips, also known as the Equivalent Frame Method.

Slab Panel Parameters:

Time-Dependent Material Properties:

$f'_c = 0.8f_c$
(Roberts and Marshall, 2008)

$f'_{c,14}$ = 13.1 MPa
$f_{c,14}$ = 16.38 MPa
$f_{t,14}$ = - MPa

at t_0 = 28 days
t = 387 days

$E_{c,28}$ = 13.97 GPa

Φ_{28} = 0.58
Φ_{387} = 2.16
$\Delta\Phi$ = 1.58

$\varepsilon_{cs,28}$ = 8.50E-05
$\varepsilon_{cs,387}$ = 7.62E-04
$\Delta\varepsilon_{cs}$ = 6.77E-04

Long-Term Deflections for Slab Panel:

Long-Term Deflection: Column Strip C7 - C8

Critical M_x Moments [kNm]

Position	Stage 1		Stage 2	
	DL	LC	DL	LC
Sup_{LEFT}	1.09	1.09	1.09	2.69
Mid	-1.03	-1.03	-1.03	-2.53
Sup_{RIGHT}	1.70	1.70	1.70	4.18

Column Strip C7 - C8:

b = 1000.0 mm
L = 3000.0 mm
d = 77.0 mm
d' = 13.0 mm
h = 90.0 mm

	A_s [mm²]		A'_s [mm²]	
Sup_{LEFT}	8Y10	628.32	5Y10	392.70
Mid	5Y10	392.70	0	0.00
Sup_{RIGHT}	8Y10	628.32	5Y10	392.70

Reference

* Modulus of Elasticity: Reinforcement

E_s = 219.0 GPa

Reference

* Effective Modulus Ratio

$$\alpha_e = \frac{E_s}{E_c}$$

α_e = 15.67

Branson

* Deflection Coefficient

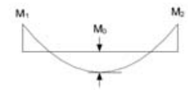

M_1 = 2.69 kNm
M_2 = 4.18 kNm
M_o = 2.53 kNm

$$\beta = \frac{M_1 + M_2}{M_o}$$

β = 2.72

$$K = 0.104\left(1 - \frac{\beta}{10}\right)$$

K = 0.0757

* Modulus of Rupture of Concrete

ACI 318 eq. 9-10

$$f_r = 0.623\sqrt{f'_c}$$

f'_c = 13.1 MPa
f_r = 2.25 MPa

* Cracking Moment:

eq. 9-9

$$M_{cr} = \frac{f_r I_g}{y_t}$$

I_g = 6.08E+07 mm⁴
f_r = 2.25 MPa
y_t = 45.0 mm

M_{cr} = 3.0 kNm

LEFT SUPPORT: Critical Moment for Support C7

* Moment of Inertia of a Cracked Section

$$x_{cr} = \left\{\left[\omega^2 + 2b\left(A_s d\alpha_e + A'_s d'(\alpha_e - 1)\right)\right]^{0.5} - \omega\right\}/b$$

$$\omega = A_s\alpha_e + A'_s(\alpha_e - 1)$$

b = 1000.0 mm
d = 77.0 mm
d' = 13.0 mm
A_s = 628.32 mm²
A'_s = 392.7 mm²
α_e = 15.67

ω = 15607.87 mm²
x_{cr} = 28.09 mm

$$I_{cr} = \frac{bx_{cr}^3}{3} + \alpha_e A_s (d - x_{cr})^2 + (\alpha_e - 1)A'_s (d' - x_{cr})^2$$

I_{cr} = 3.23E+07 mm⁴

Reference

ACI 318 eq. 9-8

* Moment of Inertia for a Partially Cracked Section

$$I_{e1} = \left(\frac{M_{cr}}{M_a}\right)^3 I_g + \left[1 - \left(\frac{M_{cr}}{M_a}\right)^3\right] I_{cr}$$

I_{cr} = 3.23E+07 mm^4
M_a = 2.69 kNm

I_{e1} = 7.37E+07 mm^4

I_{e1} > I_g then I_{e1} = 6.08E+07 mm^4

RIGHT SUPPORT: Critical Moment for Support C8

* Moment of Inertia of a Cracked Section

$$x_{cr} = \left\{\left[\omega^2 + 2b\left(A_s d\alpha_e + A'_s d'(\alpha_e - 1)\right)\right]^{0.5} - \omega\right\} / b$$

$$\omega = A_s\alpha_e + A'_s(\alpha_e - 1)$$

ω = 15607.87 mm^2
x_{cr} = 28.09 mm

b = 1000.0 mm
d = 77.0 mm
d' = 13.0 mm
A_s = 628.32 mm^2
A'_s = 392.7 mm^2
α_e = 15.67

$$I_{cr} = \frac{bx_{cr}^3}{3} + \alpha_e A_s(d - x_{cr})^2 + (\alpha_e - 1)A'_s(d' - x_{cr})^2$$

I_{cr} = 3.23E+07 mm^4

eq. 9-8

* Moment of Inertia for a Partially Cracked Section

$$I_{e2} = \left(\frac{M_{cr}}{M_a}\right)^3 I_g + \left[1 - \left(\frac{M_{cr}}{M_a}\right)^3\right] I_{cr}$$

I_{cr} = 3.23E+07 mm^4
M_a = 4.18 kNm

I_{e2} = 4.32E+07 mm^4

I_{e2} < I_g then I_{e2} = 4.32E+07 mm^4

MIDSPAN: Critical Moment for mid C7 - C8

* Moment of Inertia of a Cracked Section

$$x_{cr} = \left\{\left[\omega^2 + 2b\left(A_s d\alpha_e + A'_s d'(\alpha_e - 1)\right)\right]^{0.5} - \omega\right\} / b$$

$$\omega = A_s\alpha_e + A'_s(\alpha_e - 1)$$

ω = 6154.06 mm^2
x_{cr} = 25.24 mm

b = 1000.0 mm
d = 77.0 mm
d' = 13.0 mm
A_s = 392.70 mm^2
A'_s = 0.0 mm^2
α_e = 15.67

Reference

$$I_{cr} = \frac{bx_{cr}^3}{3} + \alpha_e A_s(d - x_{cr})^2 + (\alpha_e - 1)A'_s(d' - x_{cr})^2$$

I_{cr} = 2.18E+07 mm^4

eq. 9-8

* Moment of Inertia for a Partially Cracked Section

$$I_{em} = \left(\frac{M_{cr}}{M_a}\right)^3 I_g + \left[1 - \left(\frac{M_{cr}}{M_a}\right)^3\right] I_{cr}$$

I_{cr} = 2.18E+07 mm^4
M_a = 2.53 kNm

I_{em} = 8.97E+07 mm^4

I_{em} > I_g then I_{em} = 6.08E+07 mm^4

Branson

* Average Effective Moment of Inertia for Continuous Members

$$I_{ea} = 0.5\left[\frac{I_{e1} + I_{e2}}{2} + I_{em}\right]$$

I_{e1} = 6.08E+07 mm^4
I_{e2} = 4.32E+07 mm^4
I_{em} = 6.08E+07 mm^4

I_{ea} = 5.64E+07 mm^4

* Short-Term Deflection

$$\Delta_i = KL^2 \frac{M_a}{E_c I_{ea}}$$

Δ_i = 2.19

L = 3000.0 mm
M_a = 2.53 kNm
K = 0.0757
E_c = 13.97 GPa

* Shrinkage Deflection

Branson eq. 3-53

$$\frac{1}{r_{cs}} = 0.7\frac{\varepsilon_{cs}}{h}(\rho - \rho')^{\frac{1}{3}}\left[\frac{\rho - \rho'}{\rho}\right]^{\frac{1}{2}} \quad \text{for} \quad \rho - \rho' \leq 3.0\%$$

eq. 3-54

$$\frac{1}{r_{cs}} = 0.7\frac{\varepsilon_{cs}}{h} \quad \text{for} \quad \rho > 3.0\%$$

check: $\rho = 100A_s/bd$

ρ = 0.510 %

A_s = 392.70 mm^2
b = 1000.0 mm
d = 77.0 mm

$\rho' = 100A'_s/bd$

ρ = 0.000 %

A'_s = 0.00 mm^2
b = 1000.0 mm
d = 77.0 mm

therfore: $1/r_{cs}$ = 4.206E-06 mm^{-1}

ε_{cs} = 6.77E-04
h = 90.0 mm

Branson
eq. 3-58

$$\Delta_{cs} = K_{sh} L^2 \frac{1}{r_{cs}}$$

K_{sh} = 0.084 (Branson 1977)
L = 3000.0 mm
$1/r_{cs}$ = 4.206E-06 mm^{-1}

Δ_{cs} = 3.18 mm

* Long-Term Creep Deflection

Short-term deflection due to Permanent Load

$$I_e = \left(\frac{M_{cr}}{M_p}\right)^3 I_g + \left[1 - \left(\frac{M_{cr}}{M_p}\right)^3\right] I_{cr}$$

M_{cr} = 3.0 kNm
I_g = 6.08E+07 mm^4

(from short-term deflection calculations)

	x_{cr} [mm]	I_{cr} [mm^4]	M_p [kNm]	I_e [mm^4]	> I_g
I_{em} [mm^4]	25.2	2.2E+07	1.03	1.04E+09	TRUE
I_{e1} [mm^4]	28.1	3.2E+07	1.09	6.51E+08	TRUE
I_{e2} [mm^4]	28.1	3.2E+07	1.70	1.96E+08	TRUE

$$I_{ea} = 0.5\left[\frac{I_{e1} + I_{e2}}{2} + I_{em}\right]$$

I_{em} = 6.08E+07 mm^4
I_{e1} = 6.08E+07 mm^4
I_{e2} = 6.08E+07 mm^4

I_{ea} = 6.08E+07 mm^4

$$\Delta_{i,p} = K M_p \frac{L^2}{E_c I_{ea}}$$

K = 0.0757
M_p = 1.026 kNm
L = 3000.0 mm
E_c = 13.97 GPa
I_{ea} = 6.08E+07 mm^4

$\Delta_{i,p}$ = 0.82 mm

Long-term deflection due to Permanent Load

Branson
eq. 3-71

$$k_r = 0.85/(1 + 50/\rho')$$

A'_s = 0.00 mm^2
b = 1000.0 mm
d = 77.0 mm

k_r = 0.85

ρ' = A'_s/bd
= 0.00

eq. 3-74

$$\Delta_{l,p} = k_r \cdot \phi \cdot \Delta_{i,p}$$

Φ = 1.58
$\Delta_{i,p}$ = 0.82 mm

$\Delta_{l,p}$ = 1.11 mm

Reference

Additional Initial Deflection

$$\Delta_{i,add} = \Delta_i - \Delta_{i,p}$$

Δ_i = 2.19 mm
$\Delta_{i,p}$ = 0.82 mm

$\Delta_{i,add}$ = 1.36 mm

Total Long-term Deflection

$$\Delta_l = \Delta_{i,add} + \Delta_{l,p}$$

$\Delta_{l,p}$ = 1.11 mm
$\Delta_{i,add}$ = 1.36 mm

Δ_l = 2.47 mm

* Total Deflection

$$\Delta_t = \Delta_l + \Delta_{cs}$$

Δ_l = 2.47 mm
Δ_{cs} = 3.18 mm

Δ_t = 5.65 mm

SUMMARY of the calculated Deflections:

This section aims to summarize the deflections from the above calculated methods.

A	B	C	D
Short-Term Deflection from 9.5.2.3	Long-Term Deflection from Branson	Shrinkage Deflection from Branson	Total Deflection from B and C

A	B	C	D
Short-Term Deflection from 9.5.2.3	Long-Term Deflection from Branson	Shrinkage Deflection from Branson	Total Deflection from B and C

COLUMN STRIP C7 - C8			
METHOD 9.5.2.3 [mm]			
Δ_{short}	Δ_{long}	Δ_{shrink}	Δ_{total}
2.19	2.47	3.18	5.65

COLUMN STRIP C7 - C4			
METHOD 9.5.2.3 [mm]			
Δ_{short}	Δ_{long}	Δ_{shrink}	Δ_{total}
2.25	2.55	3.11	5.65

COLUMN STRIP C4 - C5			
METHOD 9.5.2.3 [mm]			
Δ_{short}	Δ_{long}	Δ_{shrink}	Δ_{total}
2.28	2.56	3.18	5.74

COLUMN STRIP C8 - C5			
METHOD 9.5.2.3 [mm]			
Δ_{short}	Δ_{long}	Δ_{shrink}	Δ_{total}
2.45	2.75	3.18	5.93

MIDDLE STRIP C7,C8 - C4,C5			
METHOD 9.5.2.3 [mm]			
Δ_{short}	Δ_{long}	Δ_{shrink}	Δ_{total}
2.35	2.68	3.18	5.86

MIDDLE STRIP C4,C7 - C5,C8			
METHOD 9.5.2.3 [mm]			
Δ_{short}	Δ_{long}	Δ_{shrink}	Δ_{total}
2.24	2.56	3.18	5.74

$$\Delta_{mid\_i} = \tfrac{1}{2}\left(\Delta_{col\_1} + \Delta_{col\_2}\right) + \Delta_{middle}$$

where i = 1 or 2

MID DEFLECTION (Average of Strips)			
METHOD 9.5.2.3 [mm]			
Δ_{short}	Δ_{long}	Δ_{shrink}	Δ_{total}
4.59	5.20	6.36	11.56

MID DEFLECTION (Average of Strips)			
METHOD 9.5.2.3 [mm]			
Δ_{short}	Δ_{long}	Δ_{shrink}	Δ_{total}
4.59	5.21	6.32	11.53

$$\Delta_{final} = \tfrac{1}{2}\left(\Delta_{mid\_1} + \Delta_{mid\_2}\right)$$

FINAL MID DEFLECTION			
METHOD 9.5.2.3 [mm]			
Δ_{short}	Δ_{long}	Δ_{shrink}	Δ_{total}
4.59	5.20	6.34	11.55

Calculation of the Short- and Long-Term Deflections according an Alternative Approach:

The long-term deflections will be determined using the different column strips and middle strips, also known as the Equivalent Frame Method.

Slab Panel Parameters:

Time-Dependent Material Properties:

$f'_c = 0.8f_c$
(Roberts and Marshall, 2008)

$f'_{c,14}$ = 13.1 MPa
$f_{c,14}$ = 16.38 MPa
$f_{tfl,14}$ = - MPa
$f_{t,14}$ = 1.67 MPa

at t_0 = 28 days
t = 387 days

$E_{c,28}$ = 13.97 GPa

Φ_{28} = 0.58
Φ_{387} = 2.16

$\Delta\Phi$ = 1.58

$\varepsilon_{cs,28}$ = 8.50E-05
$\varepsilon_{cs,387}$ = 7.62E-04

$\Delta\varepsilon_{cs}$ = 6.77E-04

Long-Term Deflections for Slab Panel:

Long-Term Deflection: Column Strip C7 - C8

Reference

* Moments used for Column Strip C7 - C8:

Critical M_x Moments [kNm]				
Position	Stage 1		Stage 2	
	DL	LC	DL	LC
Sup_{LEFT}	1.09	1.09	1.09	2.69
Mid	-1.03	-1.03	-1.03	-2.53
Sup_{RIGHT}	1.70	1.70	1.70	4.18

Column Strip C7 - C8:

b = 1000.0 mm
L = 3000.0 mm
d = 77.0 mm
d' = 13.0 mm
h = 90.0 mm

	A_s [mm^2]		A'_s [mm^2]	
Sup_{LEFT}	8Y10	628.32	5Y10	392.70
Mid	5Y10	392.70	0	0.00
Sup_{RIGHT}	8Y10	628.32	5Y10	392.70

Reference
EC2
eq. 7.20
eq. 7.21

* Modulus of Elasticity: Long-Term

$$E_{eff} = \frac{E_c}{(1+\varphi(\infty, t_0))}$$ where $E_{c,14}$ = 22.08 MPa, Φ_{387} = 2.16

E_{eff} = 6.98 GPa

* Modulus of Elasticity: Reinforcement

E_s = 219.0 GPa

* Deflection Coefficient

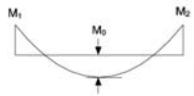

M_1 = 2.69 kNm
M_2 = 4.18 kNm
M_0 = 2.53 kNm

$$\beta = \frac{M_1 + M_2}{M_0}$$ β = 2.72

$$K = 0.104\left(1 - \frac{\beta}{10}\right)$$ K = 0.0757

Short-Term Properties:

* Effective Modulus Ratio

$$\alpha_e = \frac{E_s}{E_c}$$

E_s = 219.0 GPa
E_c = 13.97 GPa

α_e = 15.67

* Moment of Inertia for Uncracked Condition

$$x_u = \frac{\frac{bh^2}{2} + (\alpha_e - 1)(A_s d + A'_s d')}{bh + (\alpha_e - 1)(A_s + A'_s)}$$

b = 1000.0 mm
h = 90.0 mm
d = 77.0 mm
d' = 13.0 mm
A_s = 392.70 mm^2
A'_s = 0.0 mm^2

x_u = 46.93 mm

$$I_u = \frac{bh^3}{12} + bh\left(\frac{h}{2} - x_u\right)^2 + (\alpha_e - 1)\left[A_s(d - x_u)^2 + A'_s(x_u - d')^2\right]$$

I_u = 6.63E+07 mm^4

Reference
eq. 7.18

* Moment of Inertia for Cracked Condition

$$x_{cr} = \left\{\left[\omega^2 + 2b(A_s d\alpha_e + A'_s d'(\alpha_e - 1))\right]^{0.5} - \omega\right\}/b$$

$$\omega = A_s\alpha_e + A'_s(\alpha_e - 1)$$

b = 1000.0 mm
d = 77.0 mm
d' = 13.0 mm
A_s = 392.70 mm^2
A'_s = 0.0 mm^2
α_e = 15.67

ω = 6154.06 mm^2
x_{cr} = 25.24 mm

$$I_{cr} = \frac{bx_{cr}^3}{3} + \alpha_e A_s(d - x_{cr})^2 + (\alpha_e - 1)A'_s(d' - x_{cr})^2$$

I_{cr} = 2.18E+07 mm^4 I_u/I_{cr} = 3.03

* Cracking Moment

$$M_{cr} = \frac{f_t I_u}{h - x_u}$$

f_t = 1.7 MPa
h = 90.0 mm

M_{cr} = 2.57 kNm
M_a = 2.53 kNm (from above)

M_a/M_{cr} = 0.99

M_a < M_{cr}

Section is Uncracked

* Short-Term Flexural Curvature

Section is Uncracked	Section is Cracked
ζ = 0	ζ = 1 - β(M_{cr}/M_a)^2
$I_e = I_u$	$I_e = \dfrac{I_{cr}}{1 - \beta\left(1 - \frac{I_{cr}}{I_u}\right)\left(\frac{M_{cr}}{M_a}\right)^2}$

I_e = 6.63E+07 mm^4

$$\frac{1}{r_i} = \frac{M_a}{E_c I_e}$$

E_c = 13.97 GPa
β = 1.00
I_{cr} = 2.18E+07 mm^4
I_u = 6.63E+07 mm^4

$1/r_i$ = 2.73E-03 m^{-1}

* Short-Term Flexure Deflection

$$\Delta_i = KL^2\frac{1}{r_i}$$

L = 3.0 m
$1/r_i$ = 2.73E-03 m^{-1}
K = 0.0757

Δ_i = 1.86 mm

Reference	

Long-Term Properties:

* Effective Modulus Ratio

eq. 7.21

$$\alpha_e = \frac{E_s}{E_{eff}}$$

E_s = 219.0 GPa
E_{eff} = 6.98 GPa

α_e = 31.38

* Moment of Inertia for Uncracked Condition

$$x_u = \frac{\frac{bh^2}{2} + (\alpha_e - 1)(A_s d + A'_s d')}{bh + (\alpha_e - 1)(A_s + A'_s)}$$

b = 1000.0 mm
h = 90.0 mm
d = 77.0 mm
d' = 13.0 mm
A_s = 392.7 mm^2
A'_s = 0.0 mm^2

x_u = 48.75 mm

$$I_u = \frac{bh^3}{12} + bh\left(\frac{h}{2} - x_u\right)^2 + (\alpha_e - 1)\left[A_s(d - x_u)^2 + A'_s(x_u - d')^2\right]$$

I_u = 7.15E+07 mm^4

* Moment of Inertia for Cracked Condition

$$x_{cr} = \left\{\left[\omega^2 + 2b(A_s d\alpha_e + A'_s d'(\alpha_e - 1))\right]^{0.5} - \omega\right\}/b$$

$$\omega = A_s\alpha_e + A'_s(\alpha_e - 1)$$

b = 1000.0 mm
d = 77.0 mm
d' = 13.0 mm
A_s = 392.70 mm^2
A'_s = 0.0 mm^2
α_e = 31.38

ω = 12323.71 mm^2
x_{cr} = 32.95 mm

$$I_{cr} = \frac{bx_{cr}^3}{3} + \alpha_e A_s(d - x_{cr})^2 + (\alpha_e - 1)A'_s(d' - x_{cr})^2$$

I_{cr} = 3.58E+07 mm^4

I_u/I_{cr} = 2.00

Reference	

* Cracking Moment (from above)

Section is Uncracked	Section is Cracked
$M_{cr} = M'_{cr}$	$M_{cr} = M'_{cr}$

$$f_{res} = E_s\varepsilon_{cs}S_u(h - x_u)/I_u + A_s E_s\varepsilon_{cs}/\left[A_c(1 + \alpha_e(A_s/A_c))\right]$$

E_s = 219.0 GPa
ε_{cs} = 6.77E-04
A_s = 392.70 mm^2
A_c = 90000.0 mm^2
d = 77.0 mm
A'_s = 0.00 mm^2

h = 90.0 mm
x_u = 48.75 mm
I_u = 7.15E+07 mm^4
α_e = 31.38
d' = 13.0 mm

$$S_u = A_s(d - x_u) - A'_s(x_u - d')$$

S_u = 11095.479 mm^3

f_{res} = 1.517 MPa
f_t = 1.7 MPa

M_{cr} = 2.57 kNm

$$M'_{cr} = \left(1 - \frac{f_{res}}{f_t}\right)M_{cr}$$

M'_{cr} = 0.23 kNm

therefore M_{cr} = 0.23 kNm

* Long-Term Flexural Curvature due to Permanent Load

eq. 7.18

Section is Uncracked	Section is Cracked
ζ = 0	ζ = 1 - β(M_{cr}/M_a)^2
$I_e = I_u$	$I_e = \dfrac{I_{cr}}{1 - \beta\left(1 - \frac{I_{cr}}{I_u}\right)\left(\frac{M_{cr}}{M_a}\right)^2}$

I_e = 7.15E+07 mm^4

$$\frac{1}{r_l} = \frac{M_p}{E_{eff} I_e}$$

β = 0.5
E_{eff} = 6.98 GPa
I_{cr} = 3.58E+07 mm^4
I_u = 7.15E+07 mm^4
ζ = 0.00
M_p = 1.03 kNm

$1/r_l$ = 2.06E-03 m^{-1}

* Long-Term Flexure Deflection due Permanent Load

$$\Delta_{l,p} = KL^2\frac{1}{r_l}$$

L = 3.0 m
$1/r_l$ = 2.06E-03 m^{-1}
K = 0.0757

$\Delta_{l,p}$ = 1.40 mm

Reference

* Additional Initial Deflection

$$\Delta_{i,add} = K(M_a - M_p)\frac{L^2}{E_c I_e}$$

K = 0.0757
M_a = 2.53 kNm
M_p = 1.03 kNm
L = 3000.0 mm
E_c = 13.97 GPa
I_e = 6.6E+07 mm^4

$\Delta_{i,add}$ = 1.11 mm

* Total Long-term Deflection

$$\Delta_l = \Delta_{i,add} + \Delta_{l,p}$$

$\Delta_{l,p}$ = 1.40 mm
$\Delta_{i,add}$ = 1.11 mm

Δ_l = 2.51 mm

* Shrinkage Curvature

$$\frac{1}{r_{cs}} = \varsigma\varepsilon_{cs}\alpha_e\frac{S_u}{I_u} + (1-\varsigma)\varepsilon_{cs}\alpha_e\frac{S_{cr}}{I_{cr}}$$

$$S_u = A_s(d - x_u) - A'_s(x_u - d')$$

S_u = 1.11E+04 mm^3

$$S_{cr} = A_s(d - x_{cr}) - A'_s(x_{cr} - d')$$

S_{cr} = 1.73E+04 mm^3

$1/r_{cs}$ = 1.03E-05 mm^{-1}

ε_{cs} = 6.77E-04
d = 77.0 mm
d' = 13.0 mm
A_s = 392.7 mm^2
A'_s = 0.0 mm^2
x_u = 48.75 mm
x_{cr} = 32.95 mm
α_e = 31.38
ζ = 0.0
I_u = 7.15E+07 mm^4
I_{cr} = 3.58E+07 mm^4

* Shrinkage Deflection

$$\Delta_{cs} = K_{sh}L^2\frac{1}{r_{cs}}$$

Δ_{cs} = 7.75 mm

L = 3000.0 mm
$1/r_{cs}$ = 1.03E-05 mm^{-1}
K_{sh} = 0.0840 (Branson 1977)

* Long-Term Deflection

$$\Delta_t = \Delta_{cs} + \Delta_l$$

Δ_l = 2.51 mm
Δ_{cs} = 7.75 mm

Δ_t = 10.26 mm

SUMMARY of the calculated Deflections:

This section aims to summarize the deflections from the above calculated methods.

A	B	C	D
Short-Term Deflection from Chapter 3	Long-Term Deflection from Chapter 3	Shrinkage Deflection from Chapter 3	Total Deflection from B and C

A	B	C	D
Short-Term Deflection from Chapter 3	Long-Term Deflection from Chapter 3	Shrinkage Deflection from Chapter 3	Total Deflection from B and C

COLUMN STRIP C7 - C8			
Alternative METHOD [mm]			
Δ_{short}	Δ_{long}	Δ_{shrink}	Δ_{total}
1.86	2.51	7.75	10.26

COLUMN STRIP C7 - C4			
Alternative METHOD [mm]			
Δ_{short}	Δ_{long}	Δ_{shrink}	Δ_{total}
1.92	2.59	7.72	10.31

COLUMN STRIP C4 - C5			
Alternative METHOD [mm]			
Δ_{short}	Δ_{long}	Δ_{shrink}	Δ_{total}
2.11	3.98	2.51	6.49

COLUMN STRIP C8 - C5			
Alternative METHOD [mm]			
Δ_{short}	Δ_{long}	Δ_{shrink}	Δ_{total}
2.63	4.57	2.51	7.08

MIDDLE STRIP C7,C8 - C4,C5			
Alternative METHOD [mm]			
Δ_{short}	Δ_{long}	Δ_{shrink}	Δ_{total}
2.16	2.91	7.75	10.66

MIDDLE STRIP C4,C7 - C5,C8			
Alternative METHOD [mm]			
Δ_{short}	Δ_{long}	Δ_{shrink}	Δ_{total}
2.06	2.77	7.75	10.52

$$\Delta_{mid\_i} = \tfrac{1}{2}(\Delta_{col\_1} + \Delta_{col\_2}) + \Delta_{middle}$$

where i = 1 or 2

MID DEFLECTION (Average of Strips)			
Alternative METHOD [mm]			
Δ_{short}	Δ_{long}	Δ_{shrink}	Δ_{total}
4.14	6.15	12.88	19.03

MID DEFLECTION (Average of Strips)			
Alternative METHOD [mm]			
Δ_{short}	Δ_{long}	Δ_{shrink}	Δ_{total}
4.33	6.35	12.86	19.21

$$\Delta_{final} = \tfrac{1}{2}(\Delta_{mid\_1} + \Delta_{mid\_2})$$

FINAL MID DEFLECTION			
Alternative METHOD [mm]			
Δ_{short}	Δ_{long}	Δ_{shrink}	Δ_{total}
4.24	6.25	12.87	19.12

Obtain the Allowable L/d ratio according to SABS 0100-1, clause 4.3.6

Slab Panel Parameters:

Material Properties:

f'_c = 13.1 MPa
f_c = 16.38 MPa
f_t = 1.67 MPa
E_c = 22.08 MPa
f_y = 650.0 MPa

Middle Strip: Middle Strip C7,C8 - C4,C5

b = 1200.0 mm
L = 3000.0 mm
d = 77.0 mm
d' = 13.0 mm
h = 90.0 mm

Provided Reinforcement:

Middle Strip C7,C8 - C4,C5

A_s = 471.24 mm^2
A'_s = 0.00 mm^2

Allowable Span/Depth Ratio compared to the Actual Span/Depth Ratio: Middle Strip C7,C8 - C4,C5

Step 1: Basic span/depth ratio for rectangular beams

Support Condition	Rectangular Section
One end continuous	24

L > 10.0 m ? FALSE

Condition			
TRUE	k_1	=	10/L
FALSE	k_1	=	1.0

k_1 = 1.0

Step 2: Modification of span/depth ratio due to tension reinforcement

Design Service Stress:

assume the normal partial load combination factors apply

γ_1 = 1.0
γ_2 = 1.0
γ_3 = 1.0
γ_4 = 1.0

assume no moment redistribution occurs

β_b = 1.0

$$f_s = 0.87 f_y \cdot \frac{\gamma_1 + \gamma_2}{\gamma_3 + \gamma_4} \cdot \frac{A_{s,req}}{A_{s,prov}} \cdot \frac{1}{\beta_b}$$

f_y = 650.0 MPa

Calculate the Design Ultimate Bending Moment (clause 4.3.3.4):

assume only tension reinforcement is required, therefore $K \leq K'$

$$K = \frac{M}{bd^2 f_c}$$

b = 1200.0 mm
f_c = 16.38 MPa
d = 77.00 mm

M_{ULS} = 2.7 kNm (moments spreadsheet)

K = 0.0236

$$z = d\left\{0.5 + \sqrt{0.25 - \frac{K}{0.9}}\right\} \leq 0.95d$$

z = 0.9731 d > 0.95d

assume z = 0.95d = 73.15 mm

therefore

$$A_s = \frac{M}{0.87 f_y z}$$

f_y = 650.0 MPa
d = 77.0 mm

$A_{s,req}$ = 96.00 mm²

therefore f_s = 115.20 MPa

$A_{s,prov}$ = 471.24 mm²

Modification Factor k_2:

$$k_2 = 0.55 + \frac{(477 - f_s)}{120\left(0.9 + \frac{M}{bd^2}\right)} \leq 2.0$$

b = 1200.0 mm
d = 77.0 mm
f_s = 115.2 MPa

k_2	2.89
> 2.0	2.00

Step 3: Modification of span/depth ratio due to compression reinforcement

no compression reinforcement provided
therefore k_3 = 1.00

Step 4: Deflection due to creep and shrinkage

assume normal creep and shrinkage occurs and is accounted for from step 1 to 3
therefore k_4 = 1.00

Step 5: Span/depth ratio for flanged beams

beam is rectangular and not flanged, step 5 is not applicable
therefore k_5 = 1.00

Compare Actual and Allowable L/d Ratios

$$\left(L/d\right)_{ACTUAL} \leq \left(L/d\right)_{ALLOWABLE} = \left(L/d\right)_{BASIS} \cdot k_1 \cdot k_2 \cdot k_3 \cdot k_4 \cdot k_5$$

L = 3000.0 mm
d = 77.0 mm

$(L/d)_{ACTUAL}$ = 38.96

$(L/d)_{BASIS}$ = 24.0

k_1	1.0
k_2	2.00
k_3	1.0
k_4	1.0
k_5	1.0
flat slab ?	0.9
$(L/d)_{ALLOWABLE}$	43.20

Serviceable ?	OK

Obtain the Allowable L/d ratio according to EC2, clause 7.4.2

Slab Panel Parameters:

Material Properties:

f'_c = 13.1 MPa
f_c = 16.38 MPa
f_t = 1.67 MPa
E_c = 22.08 MPa
f_y = 650.0 MPa > 500 MPa

$A_{s,req}$ = 94.46 mm^2
$A_{s,prov}$ = 471.24 mm^2

Middle Strip: Middle Strip C7,C8 - C4,C5

$$310/\sigma_s = 500/(f_y \cdot A_{s,req}/A_{s,prov})$$ (EC2 , clause 7.4.2)

b = 1200.0 mm
L = 3000.0 mm
d = 77.0 mm
d' = 13.0 mm
h = 90.0 mm

σ_s = 80.8 MPa
$310/\sigma_s$ = 3.84

Provided Reinforcement:

Middle Strip C7,C8 - C4,C5

A_s = 471.24 mm^2
A'_s = 0.00 mm^2

Allowable Span/Depth Ratio compared to the Actual Span/Depth Ratio:

Determine which L/d Equation is applicable:

1 $$\frac{L}{d} = K\left[11 + 1.5\sqrt{f_c'} \cdot \frac{\rho_o}{\rho} + 3.2\sqrt{f_c'} \cdot \left(\frac{\rho_o}{\rho} - 1\right)^{3/2}\right]$$ if $\rho \leq \rho_o$

2 $$\frac{L}{d} = K\left[11 + 1.5\sqrt{f_c'} \cdot \frac{\rho_o}{\rho - \rho'} + \frac{1}{12}\sqrt{f_c'} \cdot \sqrt{\frac{\rho'}{\rho_o}}\right]$$ if $\rho > \rho_o$

where $$\rho_o = 10^{-3}\sqrt{f_c'}$$

ρ_o = 0.004

A_s [mm^2]	471.2
A'_s [mm^2]	0.0
$\rho = A_s/bd$ [-]	0.005
$\rho' = A'_s/bd$ [-]	0
eq. ?	2

f'_c = 13.1 MPa

b = 1200.0 mm
d = 77.0 mm

Flanged Sections:

if b_f/b_w > 3.0 then k_1 = 0.8

b_f/b_w = 0.00 therefore k_1 = 1.00

Beam and Slab Elements:

if L > 7000.0 which support partitions liable to be damaged by excessive deflection then k_2 = 7000 / L_{eff}

L < 7000.0 therefore k_2 = 1.00

Flat Slabs:

if greater span > 8500.0 which support partitions liable to be damaged by excessive deflections then k_3 = 8500 / L_{eff}

greater span < 8500.0 therefore k_3 = 1.00

Basic Span/Depth Ratio:

Structural System	K	Concrete Highly Stressed ρ = 1.5%	Concrete Lightly Stressed ρ = 0.5%
Simply supported beam, one- or two-way spanning simply supported slab	1.0	14	20
End span of continuouse beam or one-way continuous slab or two-way spanning slab continuous over one long side	1.3	18	26
Interior span of beam or one-way or two-way spanning slab	1.5	20	30
Slab supported on columns without beams (flat slab)(based on longer span)	1.2	17	24
Cantilever	0.4	6	8

Compare Actual and Allowable L/d Ratios

$$\left(L/d\right)_{ACTUAL} \leq \left(L/d\right)_{ALLOWABLE}$$

L = 3000.0 mm (L/d)$_{ACTUAL}$ = 38.96

d = 77.0 mm

eq. 1
$$\left(L/d\right)_{ALLOWABLE} = K\left[11 + 1.5\sqrt{f_c'}\cdot\frac{\rho_o}{\rho} + 3.2\sqrt{f_c'}\cdot\left(\frac{\rho_o}{\rho}-1\right)^{3/2}\right]\cdot k_1\cdot k_2\cdot k_3$$

eq. 2
$$\left(L/d\right)_{ALLOWABLE} = K\left[11 + 1.5\sqrt{f_c'}\cdot\frac{\rho_o}{\rho-\rho'} + \frac{1}{12}\sqrt{f_c'}\cdot\sqrt{\frac{\rho'}{\rho_o}}\right]\cdot k_1\cdot k_2\cdot k_3$$

f'_c = 13.1 MPa

ρ_o = 0.004

ρ = A_s/bd [-]	0.005
ρ' = A'_s/bd [-]	0.00
eq. ?	2

k_1	1.0
k_2	1.0
k_3	1.0

K	1.2
310/σ_s	3.8

(L/d)$_{ALLOWABLE}$	68.40

Serviceable ?	OK

Obtain the Allowable L/d ratio according to BS 8110, clause 3.4.6

Slab Panel Parameters:

Material Properties:

f'_c = 13.1 MPa
f_c = 16.38 MPa
f_t = 1.67 MPa
E_c = 22.08 MPa
f_y = 650.0 MPa

Middle Strip: Middle Strip C7,C8 - C4,C5

b = 1200.0 mm
L = 3000.0 mm
d = 77.0 mm
d' = 13.0 mm
h = 90.0 mm

Provided Reinforcement:

Middle Strip C7,C8 - C4,C5

A_s = 471.24 mm^2
A'_s = 0.00 mm^2

Allowable Span/Depth Ratio compared to the Actual Span/Depth Ratio:

Step 1: Basic span/depth ratio for rectangular beams

Support Condition	Rectangular Section	Flanged Section $b_w/b \le 0.3$
Continuous	26	20.8

L > 10.0 m ? FALSE

Condition			
TRUE	k_1	=	10/L
FALSE	k_1	=	1.0

k_1 = 1.0

Step 2: Modification of span/depth ratio due to tension reinforcement

Design Service Stress:

assume the normal partial load combination factors apply

γ_1 = 1.0
γ_2 = 1.0
γ_3 = 1.0
γ_4 = 1.0

assume no moment redistribution occurs

β_b = 1.0

$$f_s = \frac{5f_y}{8} \cdot \frac{A_{s,req}}{A_{s,prov}} \cdot \frac{1}{\beta_b}$$

f_y = 650.0 MPa

Calculate the Design Ultimate Bending Moment (clause 4.3.3.4):

assume only tension reinforcement is required, therefore $K \le K'$

$$K = \frac{M}{bd^2 f_c}$$

b = 1200.0 mm
f_c = 16.38 MPa
d = 77.00 mm

M_{ULS} = 2.7 kNm (moments spreadsheet)

K = 0.0236

$$z = d\left\{0.5 + \sqrt{0.25 - \frac{K}{0.9}}\right\} \le 0.95d$$

z = 0.973 d > 0.95d

assume z = 0.95d = 73.15 mm

therefore

$$A_s = \frac{M}{0.87 f_y z}$$

f_y = 650.0 MPa
d = 77.0 mm

$A_{s,req}$ = 96.000 mm^2

therefore f_s = 82.7604 MPa $A_{s,prov}$ = 471.24 mm^2

Modification Factor k_2:

$$k_2 = 0.55 + \frac{(477 - f_s)}{120\left(0.9 + \frac{M}{bd^2}\right)} \le 2.0$$

b = 1200.0 mm
d = 77.0 mm
f_s = 82.8 MPa

k_2	3.10
> 2.0	2.00

Step 4: Deflection due to creep and shrinkage

assume normal creep and shrinkage occurs and is accounted for from step 1 to 3

therefore k_4 = 1.00

Step 5: Span/depth ratio for flanged beams

beam is rectangular and not flanged, step 5 is not applicable

therefore k_5 = 1.00

Compare Actual and Allowable L/d Ratios

$$\left(\tfrac{L}{d}\right)_{ACTUAL} \le \left(\tfrac{L}{d}\right)_{ALLOWABLE} = \left(\tfrac{L}{d}\right)_{BASIS} \cdot k_1 \cdot k_2 \cdot k_3 \cdot k_4 \cdot k_5$$

L = 3000.0 mm $(L/d)_{ACTUAL}$ = 38.96
d = 77.0 mm

$(L/d)_{BASIS}$ = 26

k_1	1.0
k_2	2.0
k_3	1.0
k_4	1.0
k_5	1.0
Flat Slab ?	0.9
$(L/d)_{ALLOWABLE}$	52.00

Serviceable ?	OK

Obtain the Allowable L/d ratio according to ACI 318, Chapter 9, Clause 9.5

Slab Panel Parameters:

Material Properties:

f'_c = 13.1 MPa
f_c = 16.38 MPa
f_t = 1.67 MPa
E_c = 22.08 MPa
f_y = 650.0 MPa

Middle Strip: Middle Strip C7,C8 - C4,C5

b = 1200.0 mm (200 x 200 columns)
L = 3000.0 mm
d = 77.0 mm
d' = 13.0 mm
h = 90.0 mm

Provided Reinforcement:

Middle Strip C7,C8 - C4,C5

A_s = 471.24 mm^2
A'_s = 0.00 mm^2

Allowable Span/Depth Ratio compared to the Actual Span/Depth Ratio:

One-way Construction (Nonprestressed): (clause 9.5.2)

L/h Ratios for Nonprestresses Beams ot One-way Slabs				
	Simply-Supported	One End Continuous	Both Ends Continuous	Cantilever
Member	Members not supporting or attached to partitions or other construction likely to be damaged by large deflections.			
Solid one-way slabs	20	24	28	10
Beams or ribbed one-way slabs	16	18.5	21	8

Two-way Construction (Nonprestressed): (clause 9.5.3)

L_n/h Ratios for Nonprestressed Slabs without Interior Beam						
Yield Stength	Without Drop Panels			With Drop Panels		
	Exterior Panels		Interior Panels	Exterior Panels		Interior Panels
f_y [MPa]	Without Edge Beams	With Edge Beams		Without Edge Beams	With Edge Beams	
300.0	33	36	36	36	40	40
420.0	30	33	33	33	36	36
520.0	28	31	31	31	34	34
650.0	25.4	28.4	28.4	28.4	31.4	31.4

(last row of values are interpolated values)

For slabs without interior beams spanning between the supports and having ratio of long to short span not greater than 2, the minimum thickness shall be in accordance with the provision as stated above for two-way construction.

Consider the L_n/h ratio for Two-way Construction

Compare Actual and Allowable L/d Ratios

$$\left(\frac{L_n}{h}\right)_{ACTUAL} \leq \left(\frac{L_n}{h}\right)_{ALLOWABLE}$$

L_n = 2800.0 mm

h = 90.0 mm

$(L_n/h)_{ACTUAL}$ = 31.11

$(L_n/h)_{ALLOWABLE}$ = 25.4

$(L_n/h)_{ALLOWABLE}$	25.40
Serviceable ?	NO

APPENDIX H

The calculations to obtain the predicted deflections for the parking deck case study are similar to the calculations presented in Appendix F. The column and middles strip properties are presented for the slab panel under consideration. The data presented in this appendix may be applied to the calculation procedures from Appendix F to obtain the predicted deflections.

Layout of the Experimental Slab and Columns:

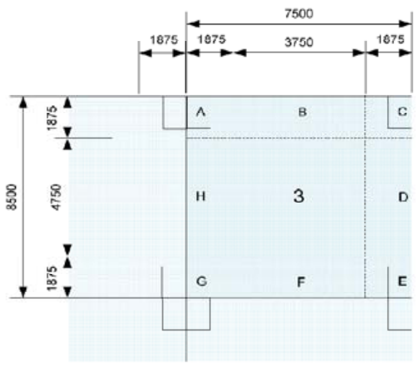

Figure 3: Flat Slab Panel 3

The panel is divided into column and middle strips, as observed from the article published. These strips will be taken into consideration when calculating the deflections at variuous points.

The following Load Combinations were applied to the model:

1. Ultimate Limit State Moments: Load Combination 1 (LC1)
   $Q = 1.2G_k + 1.6Q_k$
2. Serviceability Limit State Moments: Load Combination 2 (LC2)
   $Q = 1.1G_k + 1.0Q_k$
3. Sustained Portion of the Serviceability Limit State Moments: Load Combination 3 (LC3)
   $Q = 1.1G_k + 0.6Q_k$
4. Dead Load Moments: Load Combination 4 (LC4)
   $Q = 1.0G_k$

Column and Middle Strip Dimensions and Reinforcement:

Column Strip A - G:

b = 3750.0 mm
L = 8500.0 mm
d = 225.0 mm
d' = 25.0 mm
h = 250.0 mm

	A_s [mm^2]		A'_s [mm^2]	
Sup_{LEFT}	20Y12	2261.95	22Y12	2488.14
Mid	22Y12	2488.14	14Y10	1099.56
Sup_{RIGHT}	25Y16, 1Y12	5139.65	22Y12	2488.14

Column Strip C - E:

b = 1875.0 mm
L = 8500.0 mm
d = 225.0 mm
d' = 25.0 mm
h = 250.0 mm

	A_s [mm^2]		A'_s [mm^2]	
Sup_{LEFT}	10Y12	1130.97	11Y12	1244.07
Mid	11Y12	1244.07	0	0
Sup_{RIGHT}	21Y12	2375.04	11Y12	1244.07

Middle Strip H - D:

b = 4750.0 mm
L = 7500.0 mm
d = 225.0 mm
d' = 25.0 mm
h = 250.0 mm

	A_s [mm^2]		A'_s [mm^2]	
Sup_{LEFT}	18Y12	2035.75	26Y12	2940.53
Mid	26Y12	2940.53	0	0
Sup_{RIGHT}	0	0.00	26Y12	2940.53

APPENDIX I

The calculations to obtain the predicted deflections for the office case study are similar to the calculations presented in Appendix F. The column and middles strip properties are presented for the slab panel under consideration for the office block case study. The variables presented in this appendix may be applied to the calculation procedures from Appendix F to obtain the predicted deflections.

Layout of the Experimental Slab and Columns:

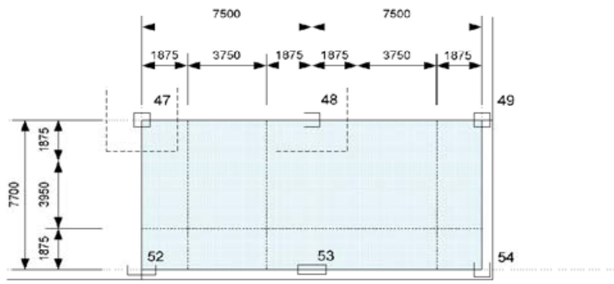

Apply the calculation proceure as stipulated in Annexure A SABS 0100-1.
All relevant parameters/notation should refer to the longer span.

The panel is divided into column and middle strips, using Figure 16 (a) from SABS 0100-1. These strips will be taken into consideration when calculating the deflections at variuous points.

The following Load Combinations were applied to the model:

1. Dead Load Moments: Load Combination 1 (LC1)
   $Q = 1.0G_k$
2. Live Load Moments: Load Combination 2 (LC2)
   $Q = 1.0Q_k$
3. Sustained Portion of the Serviceability Limit State Moments: Load Combination 3 (LC3)
   $Q = 1.1G_k + 0.3Q_k$
4. Serviceability Limit State Moments: Load Combination 4 (LC4)
   $Q = 1.1G_k + 1.0Q_k$
5. Ultimate Limit State Moments: Load Combination 5 (LC5)
   $Q = 1.2G_k + 1.6Q_k$

Column and Middle Strip Dimensions and Reinforcement:

Column Strip 47 - 48:

b = 3750.0 mm
L = 7500.0 mm
d = 207.0 mm
d' = 23.0 mm
h = 230.0 mm

	A_s [mm^2]		A'_s [mm^2]	
Sup_{LEFT}	17Y16	3418.05	0	0.00
Mid	9Y16, 9Y16	3619.11	0	0.00
Sup_{RIGHT}	9Y16, 8Y20	4322.83	0	0.00

Middle Strip 52,53 - 47,48:

b = 3750.0 mm
L = 7700.0 mm
d = 207.0 mm
d' = 23.0 mm
h = 230.0 mm

	A_s [mm^2]		A'_s [mm^2]	
Sup_{LEFT}	20Y12	2261.95	19Y16	3820.18
Mid	19Y16	3820.18	0	0
Sup_{RIGHT}	8Y10	628.32	19Y16	3820.18

Column Strip 48 - 49:

b = 3750.0 mm
L = 7500.0 mm
d = 207.0 mm
d' = 23.0 mm
h = 230.0 mm

	A_s [mm^2]		A'_s [mm^2]	
Sup_{LEFT}	9Y16, 8Y20	4322.83	0	0.00
Mid	13Y16, 8Y16	4222.30	0	0.00
Sup_{RIGHT}	16Y16, 3Y10	3452.61	13Y16, 8Y16	4222.30

Middle Strip 53,54 - 48,49:

b = 3750.0 mm
L = 7700.0 mm
d = 207.0 mm
d' = 23.0 mm
h = 230.0 mm

	A_s [mm^2]		A'_s [mm^2]	
Sup_{LEFT}	19Y12	2148.85	19Y16	3820.18
Mid	19Y16	3820.18	0	0
Sup_{RIGHT}	8Y10	628.32	19Y16	3820.18

APPENDIX J

The calculation for the short-term moment-deflection behaviour is presented for the first slab specimens, Slabs 1a-c, as specified by Maritz (2009). The calculations for the other slab specimens may be acquired from the data disks.

MARITZ SLAB: 0.39% - Slab 1a-c

Calculation of the Immediate Deflection according to SABS 0100-1, clause A.2.4

Slab Panel Parameters:

Material Properties:	f'_c =	32.08 MPa
	f_c =	40.10 MPa
	f_t =	- MPa
	E_c =	26.08 GPa
Wide Beam:	b =	600.0 mm
	L =	2400.0 mm
	d =	75.0 mm
	d' =	25.0 mm
	h =	100.0 mm

Modulus of Rupture: (for unrestrained slabs)

$$f_r = 0.65\sqrt{f_c}$$ f_r = 4.12 MPa

Cracking Moment:

$$M_{cr} = \frac{f_r I_g}{y_t}$$

I_g = 5.0E+07 mm^4
y_t = 50.0 mm
M_{cr} = 4.12 kNm

M_a = 4.62 kNm

M_{cr} =	4.12 kNm
M_a/M_{cr} =	1.12

Momenf of Inertia of Cracked Section: Equations used

x_{cr} for the Cracked Condition	I_{cr} for the Cracked Condition	Modular Ratio
$x_{cr\_1} = \frac{\frac{1}{2}x_{cr\_2}{}^2 b + A_s d\alpha_e}{x_{cr\_2} b + A_s\alpha_e}$ where $x_{cr\_1} = x_{cr\_2}$	$I_{cr} = \frac{1}{3}bx_{cr}{}^3 + A_s(d-x_{cr})^2\alpha_e$	$\alpha_e = \frac{E_s}{E_c}$

ρ	[%]	0.39
x_{cr_1}	[mm]	18.5
b	[mm]	600.0
A_s	[mm^2]	236.0
d	[mm]	75.0
E_s	[GPa]	200.0
E_c	[GPa]	26.1
α_e	[-]	7.7
x_{cr_2}	[mm]	18.5
I_{cr}	[mm^4]	7.0E+06

I_e for Partially Cracked Condition	Immediate Curvature $1/r_i$	Deflection [mm]
$I_e = \left(\frac{M_{cr}}{M_a}\right)^3 I_g + \left[1-\left(\frac{M_{cr}}{M_a}\right)^3\right] I_{cr} \le I_g$	$\frac{1}{r_i} = \frac{M_a}{E_c I_e}$	$\Delta_i = KL^2\frac{1}{r_i}$

Deflection Coefficient, K (Annexure A, table A.2)

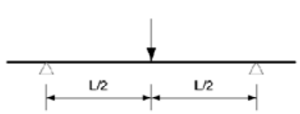

Loading on Beam

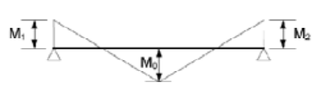

Bending Moment Diagram

$$\beta = \frac{M_1 + M_2}{M_0}$$ β = 1.205 (from Maritz, 2009)

$$K = 0.083\left(1-\frac{\beta}{4}\right)$$ K = 0.0580

ρ [%]		0.39		
M_{cr}/M_a	M_a/M_{cr}	I_e	$1/r_i$	Δ_i
[-]	[-]	[mm^4]	[10^{-6} mm^{-1}]	[mm]
10.00	0.10	5.0E+07	0.3	0.1
5.00	0.20	5.0E+07	0.6	0.2
3.33	0.30	5.0E+07	0.9	0.3
2.50	0.40	5.0E+07	1.3	0.4
2.00	0.50	5.0E+07	1.6	0.5
1.67	0.60	5.0E+07	1.9	0.6
1.43	0.70	5.0E+07	2.2	0.7
1.25	0.80	5.0E+07	2.5	0.8
1.11	0.90	5.0E+07	2.8	0.9
1.00	1.00	5.0E+07	3.2	1.1
0.91	1.10	3.9E+07	4.4	1.5
0.83	1.20	3.2E+07	5.9	2.0
0.77	1.30	2.7E+07	7.7	2.6
0.71	1.40	2.3E+07	9.7	3.3
0.67	1.50	2.0E+07	12.0	4.0
0.63	1.60	1.8E+07	14.4	4.8
0.59	1.70	1.6E+07	17.0	5.7
0.56	1.80	1.4E+07	19.7	6.6
0.53	1.90	1.3E+07	22.5	7.5
0.50	2.00	1.2E+07	25.4	8.5
0.48	2.10	1.2E+07	28.4	9.5
0.45	2.20	1.1E+07	31.3	10.5
0.43	2.30	1.1E+07	34.3	11.5
0.42	2.40	1.0E+07	37.3	12.5
0.40	2.50	9.8E+06	40.3	13.5
0.38	2.60	9.5E+06	43.3	14.4
0.37	2.70	9.2E+06	46.2	15.4
0.36	2.80	9.0E+06	49.1	16.4
0.34	2.90	8.8E+06	52.0	17.4
0.33	3.00	8.6E+06	54.8	18.3

Uncracked Condition				
M_{cr}/M_a	M_a/M_{cr}	I_g	$1/r_i$	Δ_i
[-]	[-]	[mm^4]	[10^{-6} mm^{-1}]	[mm]
10.00	0.10	5.0E+07	0.3	0.1
5.00	0.20	5.0E+07	0.6	0.2
3.33	0.30	5.0E+07	0.9	0.3
2.50	0.40	5.0E+07	1.3	0.4
2.00	0.50	5.0E+07	1.6	0.5
1.67	0.60	5.0E+07	1.9	0.6
1.43	0.70	5.0E+07	2.2	0.7
1.25	0.80	5.0E+07	2.5	0.8
1.11	0.90	5.0E+07	2.8	0.9
1.00	1.00	5.0E+07	3.2	1.1
0.91	1.10	5.0E+07	3.5	1.2
0.83	1.20	5.0E+07	3.8	1.3
0.77	1.30	5.0E+07	4.1	1.4
0.71	1.40	5.0E+07	4.4	1.5
0.67	1.50	5.0E+07	4.7	1.6
0.63	1.60	5.0E+07	5.1	1.7
0.59	1.70	5.0E+07	5.4	1.8
0.56	1.80	5.0E+07	5.7	1.9
0.53	1.90	5.0E+07	6.0	2.0
0.50	2.00	5.0E+07	6.3	2.1
0.48	2.10	5.0E+07	6.6	2.2
0.45	2.20	5.0E+07	6.9	2.3
0.43	2.30	5.0E+07	7.3	2.4
0.42	2.40	5.0E+07	7.6	2.5
0.40	2.50	5.0E+07	7.9	2.6
0.38	2.60	5.0E+07	8.2	2.7
0.37	2.70	5.0E+07	8.5	2.8
0.36	2.80	5.0E+07	8.8	3.0
0.34	2.90	5.0E+07	9.2	3.1
0.33	3.00	5.0E+07	9.5	3.2

MARITZ SLAB: 0.39% - Slab 1a-c

Calculation of the Immediate Deflection according to Eurocode 2, Section 7.4

Slab Panel Parameters:

Material Properties:

f'_c = 32.08 MPa
f_c = 40.10 MPa
f_t = 3.03 MPa
E_c = 26.08 GPa

Wide Beam:

b = 600.0 mm
L = 2400.0 mm
d = 75.0 mm
d' = 25.0 mm
h = 100.0 mm

Momenf of Inertia for a Partailly Cracked Section: Equation used

x_u for the Uncracked Condition	I_u for the Uncracked Condition	Modular Ratio
$x_u = \dfrac{\frac{bh^2}{2} + (\alpha_e - 1)(A_s d + A'_s d')}{bh + (\alpha_e - 1)(A_s + A'_s)}$	$I_u = \dfrac{bh^3}{12} + bh\left(\dfrac{h}{2} - x_u\right)^2 + (\alpha_e - 1)\left[A_s(d - x_u)^2 + A'_s(x_u - d')^2\right]$	$\alpha_e = \dfrac{E_s}{E_c}$

x_{cr} for the Cracked Condition	I_{cr} for the Cracked Condition	Cracking Moment
$\omega = A_s\alpha_e + A'_s(\alpha_e - 1)$ $x_{cr} = \left\{\left[\omega^2 + 2b\left(A_s d\alpha_e + A'_s d'(\alpha_e - 1)\right)\right]^{0.5} - \omega\right\}/b$	$I_{cr} = \dfrac{bx_{cr}^3}{3} + \alpha_e A_s(d - x_{cr})^2 + (\alpha_e - 1)A'_s(d' - x_{cr})^2$	$M_{cr} = \dfrac{f_t I_u}{h - x_u}$

ρ	[%]	0.39
b	[mm]	600.0
h	[mm]	100.0
A_s	[mm²]	236.0
d	[mm]	75.0
E_s	[GPa]	200.0
E_c	[GPa]	26.1
α_e	[-]	7.7
x_u	[mm]	50.6
I_u	[mm⁴]	5.1E+07
ω	[mm²]	1809.8
x_{cr}	[mm]	18.5
I_{cr}	[mm⁴]	7.0E+06
M_{cr}	[kNm]	3.1

M_a = 4.62 kNm

M_{cr} = 3.13 kNm
M_a/M_{cr} = 1.48

I_e for Partially Cracked Condition	Immediate Curvature $1/r_i$	Deflection [mm]
$I_e = \dfrac{I_{cr}}{1-\left(1-\dfrac{I_{cr}}{I_u}\right)\left(\dfrac{M_{cr}}{M_a}\right)^2}$	$\dfrac{1}{r_i} = \dfrac{M_a}{E_c I_e}$	$\Delta_i = KL^2 \dfrac{1}{r_i}$

Deflection Coefficient, K (Annexure A, table A.2)

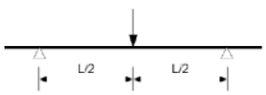

Loading on Beam

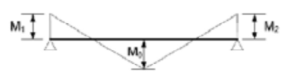

Bending Moment Diagram

$$\beta = \frac{M_1 + M_2}{M_o}$$

β = 1.205
(from Maritz, 2009)

$$K = 0.083\left(1 - \frac{\beta}{4}\right)$$

K = 0.0580

Cracked Condition

ρ [%]		0.39		
M_{cr}/M_a	M_a/M_{cr}	I_e	$1/r_i$	Δ_i
[-]	[-]	[mm⁴]	[10⁻⁶ mm⁻¹]	[mm]
10.00	0.10	5.1E+07	0.2	0.08
5.00	0.20	5.1E+07	0.5	0.16
3.33	0.30	5.1E+07	0.7	0.24
2.50	0.40	5.1E+07	0.9	0.31
2.00	0.50	5.1E+07	1.2	0.39
1.67	0.60	5.1E+07	1.4	0.47
1.43	0.70	5.1E+07	1.6	0.55
1.25	0.80	5.1E+07	1.9	0.63
1.11	0.90	5.1E+07	2.1	0.71
1.00	1.00	5.1E+07	2.4	0.79
0.91	1.10	2.4E+07	5.4	1.80
0.83	1.20	1.8E+07	8.2	2.74
0.77	1.30	1.4E+07	10.8	3.62
0.71	1.40	1.3E+07	13.4	4.46
0.67	1.50	1.1E+07	15.8	5.26
0.63	1.60	1.1E+07	18.1	6.04
0.59	1.70	1.0E+07	20.3	6.78
0.56	1.80	9.6E+06	22.5	7.51
0.53	1.90	9.3E+06	24.6	8.23
0.50	2.00	9.0E+06	26.7	8.92
0.48	2.10	8.8E+06	28.8	9.61
0.45	2.20	8.6E+06	30.8	10.28
0.43	2.30	8.4E+06	32.8	10.95
0.42	2.40	8.3E+06	34.7	11.61
0.40	2.50	8.2E+06	36.7	12.26
0.38	2.60	8.1E+06	38.6	12.90
0.37	2.70	8.0E+06	40.5	13.54
0.36	2.80	7.9E+06	42.4	14.17
0.34	2.90	7.8E+06	44.3	14.80
0.33	3.00	7.8E+06	46.2	15.43

Uncracked Condition			
M_a/M_{cr}	I_u	$1/r_i$	Δ_i
[-]	[mm⁴]	[10⁻⁶ mm⁻¹]	[mm]
0.10	5.1E+07	0.2	0.1
0.20	5.1E+07	0.5	0.2
0.30	5.1E+07	0.7	0.2
0.40	5.1E+07	0.9	0.3
0.50	5.1E+07	1.2	0.4
0.60	5.1E+07	1.4	0.5
0.70	5.1E+07	1.6	0.6
0.80	5.1E+07	1.9	0.6
0.90	5.1E+07	2.1	0.7
1.00	5.1E+07	2.4	0.8
1.10	5.1E+07	2.6	0.9
1.20	5.1E+07	2.8	0.9
1.30	5.1E+07	3.1	1.0
1.40	5.1E+07	3.3	1.1
1.50	5.1E+07	3.5	1.2
1.60	5.1E+07	3.8	1.3
1.70	5.1E+07	4.0	1.3
1.80	5.1E+07	4.2	1.4
1.90	5.1E+07	4.5	1.5
2.00	5.1E+07	4.7	1.6
2.10	5.1E+07	4.9	1.7
2.20	5.1E+07	5.2	1.7
2.30	5.1E+07	5.4	1.8
2.40	5.1E+07	5.6	1.9
2.50	5.1E+07	5.9	2.0
2.60	5.1E+07	6.1	2.0
2.70	5.1E+07	6.4	2.1
2.80	5.1E+07	6.6	2.2
2.90	5.1E+07	6.8	2.3
3.00	5.1E+07	7.1	2.4

I_{cr}	$1/r_i$	Δ_i
[mm⁴]	[10⁻⁶ mm⁻¹]	[mm]
7.0E+06	0.0	0.0
7.0E+06	1.7	0.6
7.E+06	3.4	1.1
7.E+06	5.1	1.7
7.E+06	6.8	2.3
7.E+06	8.5	2.8
7.E+06	10.2	3.4
7.E+06	11.9	4.0
7.E+06	13.6	4.5
7.E+06	15.3	5.1
7.E+06	17.0	5.7
7.E+06	18.7	6.3
7.E+06	20.4	6.8
7.E+06	22.1	7.4
7.E+06	23.8	8.0
7.E+06	25.5	8.5
7.E+06	27.2	9.1
7.E+06	28.9	9.7
7.E+06	30.6	10.2
7.E+06	32.3	10.8
7.E+06	34.0	11.4
7.E+06	35.7	11.9
7.E+06	37.4	12.5
7.E+06	39.1	13.1
7.E+06	40.9	13.6
7.E+06	42.6	14.2
7.E+06	44.3	14.8
7.E+06	46.0	15.4
7.E+06	47.7	15.9
7.E+06	49.4	16.5
7.E+06	51.1	17.1

MARITZ SLAB: 0.39% - Slab 1a-c

Calculation of the Immediate Deflection according to BS 8110, 3.6

Slab Panel Parameters:

Material Properties:

f'_c = 32.08 MPa
f_c = 40.10 MPa
f_t = - MPa
E_c = 26.08 GPa

Wide Beam:

b = 600.0 mm
L = 2400.0 mm
d = 75.0 mm
d' = 25.0 mm
h = 100.0 mm

Cracking Moment: M_{cr} = 3.13 kNm (from EC2 data)

M_a = 4.62 kNm
M_a/M_{cr} = 1.48

Momenf of Inertia of Cracked Section: Equations used

x_u for the Uncracked Condition	I_u for the Uncracked Condition	Modular Ratio
$x_u = \dfrac{\frac{bh^2}{2} + (\alpha_e)(A_s d + A'_s d')}{bh + (\alpha_e)(A_s + A'_s)}$	$I_u = \dfrac{bh^3}{12} + bh\left(\dfrac{h}{2} - x_u\right)^2 + (\alpha_e)\left[A_s(d - x_u)^2 + A'_s(x_u - d')^2\right]$	$\alpha_e = \dfrac{E_s}{E_c}$

x_{cr} for the Cracked Condition	I_{cr} for the Cracked Condition
$\dfrac{x_{cr}}{d} = -\alpha_e(\rho + \rho') + \sqrt{\left\{\alpha_e^2(\rho + \rho')^2 + 2\alpha_e\left(\rho + \dfrac{d'}{d}\rho'\right)\right\}}$	$\dfrac{I_{cr}}{bd^3} = \dfrac{1}{3}\left(\dfrac{x_{cr}}{d}\right)^3 + \alpha_e\rho\left(1 - \dfrac{x_{cr}}{d}\right)^2 + \alpha_e\rho'\left(\dfrac{x_{cr}}{d} - \dfrac{d'}{d}\right)^2$

ρ	[%]	0.39
b	[mm]	600.0
d	[mm]	75.0
A_s	[mm²]	236.0
ρ	[-]	0.0039
E_s	[GPa]	200.0
E_c	[GPa]	26.1
α_e	[-]	7.7
x_u	[mm]	50.7
I_u	[mm⁴]	5.1E+07
x_{cr}/d	[-]	0.216
x_{cr}	[mm]	16.2
I_{cr}/bd^3	[-]	0.0217
I_{cr}	[mm⁴]	5.5E+06
ΔM	[kNm]	2.00

Immediate Curvature $1/r_i$ for Uncracked Section	Net Applied Moment for Partially Cracked Section	Immediate Curvature $1/r_i$ for Partially Cracked Section
$\dfrac{1}{r_i} = \dfrac{M_a}{E_c I_u}$	$M_{net} = M_a - \Delta M = M_a - \frac{1}{3}\dfrac{b(h - x_{cr})^3}{d - x_{cr}} f_t$	$\dfrac{1}{r_i} = \dfrac{M_{net}}{E_c I_{cr}}$

Deflection Coefficient, K (Annexure A, table A.2)

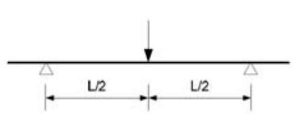

Loading on Beam

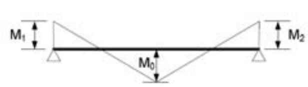

Bending Moment Diagram

$$\beta = \frac{M_1 + M_2}{M_0}$$

β = 1.205 (from Maritz, 2009)

$$K = 0.083\left(1 - \frac{\beta}{4}\right)$$

K = 0.0580

Moment of Inertia of Cracked Section: Equations used

x_{cr} for the Cracked Condition	I_{cr} for the Cracked Condition	Modular Ratio
$\omega = A_s\alpha_e + A'_s(\alpha_e - 1)$ $x_{cr} = \left\{\left[\omega^2 + 2b\left(A_s d\alpha_e + A'_s d'(\alpha_e - 1)\right)\right]^{0.5} - \omega\right\}/b$	$I_{cr} = \frac{bx_{cr}^3}{3} + \alpha_e A_s(d - x_{cr})^2 + (\alpha_e - 1)A'_s(d' - x_{cr})^2$	$\alpha_e = \frac{E_s}{E_c}$

ρ	[%]	0.39
b	[mm]	600.0
A_s	[mm^2]	236.0
d	[mm]	75.0
E_s	[GPa]	200.0
E_c	[GPa]	26.1
α_e	[-]	7.7
ω	[mm^2]	1809.8
x_{cr}	[mm]	18.5
I_{cr}	[mm^4]	7.0E+06

I_e for Partially Cracked Condition	Immediate Curvature $1/r_i$	Deflection [mm]
$I_e = \left(\frac{M_{cr}}{M_a}\right)^3 I_g + \left[1 - \left(\frac{M_{cr}}{M_a}\right)^3\right] I_{cr} \leq I_g$	$\frac{1}{r_i} = \frac{M_a}{E_c I_e}$	$\Delta_i = KL^2 \frac{1}{r_i}$

Deflection Coefficient, K (Annexure A, table A.2)

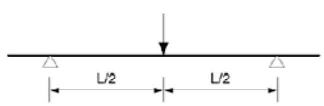

Loading on Beam

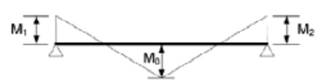

Bending Moment Diagram

$$\beta = \frac{M_1 + M_2}{M_0}$$

β = 1.205 (from Maritz, 2009)

$$K = 0.083\left(1 - \frac{\beta}{4}\right)$$

K = 0.0580

ρ [%]		0.39		
M_{cr}/M_a	M_a/M_{cr}	I_e	$1/r_i$	Δ_i
[-]	[-]	[mm^4]	[10^{-6} mm^{-1}]	[mm]
10.00	0.10	5.1E+07	0.23	0.08
5.00	0.20	5.1E+07	0.47	0.16
3.33	0.30	5.1E+07	0.70	0.24
2.50	0.40	5.1E+07	0.94	0.31
2.00	0.50	5.1E+07	1.17	0.39
1.67	0.60	5.1E+07	1.41	0.47
1.43	0.70	5.1E+07	1.64	0.55
1.25	0.80	5.5E+06	3.49	1.17
1.11	0.90	5.5E+06	5.67	1.89
1.00	1.00	5.5E+06	7.85	2.62
0.91	1.10	5.5E+06	10.03	3.35
0.83	1.20	5.5E+06	12.21	4.08
0.77	1.30	5.5E+06	14.38	4.81
0.71	1.40	5.5E+06	16.56	5.53
0.67	1.50	5.5E+06	18.74	6.26
0.63	1.60	5.5E+06	20.92	6.99
0.59	1.70	5.5E+06	23.10	7.72
0.56	1.80	5.5E+06	25.28	8.44
0.53	1.90	5.5E+06	27.46	9.17
0.50	2.00	5.5E+06	29.63	9.90
0.48	2.10	5.5E+06	31.81	10.63
0.45	2.20	5.5E+06	33.99	11.36
0.43	2.30	5.5E+06	36.17	12.08
0.42	2.40	5.5E+06	38.35	12.81
0.40	2.50	5.5E+06	40.53	13.54
0.38	2.60	5.5E+06	42.71	14.27
0.37	2.70	5.5E+06	44.88	14.99
0.36	2.80	5.5E+06	47.06	15.72
0.34	2.90	5.5E+06	49.24	16.45
0.33	3.00	5.5E+06	51.42	17.18

Uncracked Condition				
M_{cr}/M_a	M_a/M_{cr}	I_u	$1/r_i$	Δ_i
[-]	[-]	[mm^4]	[10^{-6} mm^{-1}]	[mm]
10.00	0.10	5.1E+07	0.2	0.1
5.00	0.20	5.1E+07	0.5	0.2
3.33	0.30	5.1E+07	0.7	0.2
2.50	0.40	5.1E+07	0.9	0.3
2.00	0.50	5.1E+07	1.2	0.4
1.67	0.60	5.1E+07	1.4	0.5
1.43	0.70	5.1E+07	1.6	0.5
1.25	0.80	5.1E+07	1.9	0.6
1.11	0.90	5.1E+07	2.1	0.7
1.00	1.00	5.1E+07	2.3	0.8
0.91	1.10	5.1E+07	2.6	0.9
0.83	1.20	5.1E+07	2.8	0.9
0.77	1.30	5.1E+07	3.1	1.0
0.71	1.40	5.1E+07	3.3	1.1
0.67	1.50	5.1E+07	3.5	1.2
0.63	1.60	5.1E+07	3.8	1.3
0.59	1.70	5.1E+07	4.0	1.3
0.56	1.80	5.1E+07	4.2	1.4
0.53	1.90	5.1E+07	4.5	1.5
0.50	2.00	5.1E+07	4.7	1.6
0.48	2.10	5.1E+07	4.9	1.6
0.45	2.20	5.1E+07	5.2	1.7
0.43	2.30	5.1E+07	5.4	1.8
0.42	2.40	5.1E+07	5.6	1.9
0.40	2.50	5.1E+07	5.9	2.0
0.38	2.60	5.1E+07	6.1	2.0
0.37	2.70	5.1E+07	6.3	2.1
0.36	2.80	5.1E+07	6.6	2.2
0.34	2.90	5.1E+07	6.8	2.3
0.33	3.00	5.1E+07	7.0	2.4

Deflection [mm]
$\Delta_i = KL^2 \frac{1}{r_i}$

MARITZ SLAB: 0.39% - Slab 1a-c

Calculation of the Immediate Deflection according to ACI 318, Chapter 9.

Slab Panel Parameters:

<u>Material Properties:</u>

f'_c =	32.08	MPa
f_c =	40.10	MPa
f_t =	-	MPa
E_c =	26.08	GPa

<u>Wide Beam:</u>

b =	600.0	mm
L =	2400.0	mm
d =	75.0	mm
d' =	25.0	mm
h =	100.0	mm

<u>Modulus of Rupture:</u> (for unrestrained slabs)

$$f_r = 0.623\sqrt{f'_c}$$

f'_c =	32.1	MPa
f_r =	3.53	MPa

<u>Cracking Moment:</u>

$$M_{cr} = \frac{f_r I_g}{y_t}$$

I_g =	5.0E+07	mm^4
y_t =	50.0	mm
M_{cr} =	3.53	kNm

M_a = 4.62 kNm

M_{cr} =	3.53	kNm
M_a/M_{cr} =	1.31	

<u>Momenf of Inertia of Cracked Section:</u> Equations used

x_{cr} for the Cracked Condition	I_{cr} for the Cracked Condition	Modular Ratio
$\omega = A_s\alpha_e + A'_s(\alpha_e - 1)$ $x_{cr} = \left\{\left[\omega^2 + 2b\left(A_s d\alpha_e + A'_s d'(\alpha_e - 1)\right)\right]^{0.5} - \omega\right\}/b$	$I_{cr} = \frac{bx_{cr}^3}{3} + \alpha_e A_s(d - x_{cr})^2 + (\alpha_e - 1)A'_s(d' - x_{cr})^2$	$\alpha_e = \frac{E_s}{E_c}$

ρ	[%]	0.39
b	[mm]	600.0
A_s	[mm^2]	236.0
d	[mm]	75.0
E_s	[GPa]	200.0
E_c	[GPa]	26.1
α_e	[-]	7.7
ω	[mm^3]	1809.8
x_{cr}	[mm]	18.5
I_{cr}	[mm^4]	7.0E+06

I_e for Partially Cracked Condition	Immediate Curvature $1/r_i$	Deflection [mm]
$I_e = \left(\frac{M_{cr}}{M_a}\right)^3 I_g + \left[1 - \left(\frac{M_{cr}}{M_a}\right)^3\right] I_{cr} \leq I_g$	$\frac{1}{r_i} = \frac{M_a}{E_c I_e}$	$\Delta_i = KL^2\frac{1}{r_i}$

Deflection Coefficient, K (Annexure A, table A.2)

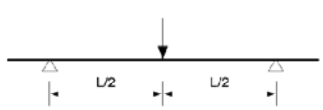

Loading on Beam

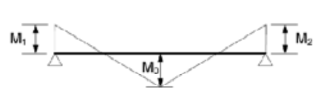

Bending Moment Diagram

$$\beta = \frac{M_1 + M_2}{M_0}$$

β = 1.205 (from Maritz, 2009)

$$K = 0.083\left(1 - \frac{\beta}{4}\right)$$

K = 0.0580

ρ [%]		0.39		
M_{cr}/M_a	M_a/M_{cr}	I_e	$1/r_i$	Δ
[-]	[-]	[mm⁴]	[10^{-6} mm^{-1}]	[mm]
10.00	0.10	5.0E+07	0.3	0.1
5.00	0.20	5.0E+07	0.5	0.2
3.33	0.30	5.0E+07	0.8	0.3
2.50	0.40	5.0E+07	1.1	0.4
2.00	0.50	5.0E+07	1.4	0.5
1.67	0.60	5.0E+07	1.6	0.5
1.43	0.70	5.0E+07	1.9	0.6
1.25	0.80	5.0E+07	2.2	0.7
1.11	0.90	5.0E+07	2.4	0.8
1.00	1.00	5.0E+07	2.7	0.9
0.91	1.10	3.9E+07	3.8	1.3
0.83	1.20	3.2E+07	5.1	1.7
0.77	1.30	2.7E+07	6.6	2.2
0.71	1.40	2.3E+07	8.3	2.8
0.67	1.50	2.0E+07	10.3	3.4
0.63	1.60	1.8E+07	12.3	4.1
0.59	1.70	1.6E+07	14.6	4.9
0.56	1.80	1.4E+07	16.9	5.6
0.53	1.90	1.3E+07	19.3	6.5
0.50	2.00	1.2E+07	21.8	7.3
0.48	2.10	1.2E+07	24.3	8.1
0.45	2.20	1.1E+07	26.9	9.0
0.43	2.30	1.1E+07	29.4	9.8
0.42	2.40	1.0E+07	32.0	10.7
0.40	2.50	9.8E+06	34.5	11.5
0.38	2.60	9.5E+06	37.1	12.4
0.37	2.70	9.2E+06	39.6	13.2
0.36	2.80	9.0E+06	42.1	14.1
0.34	2.90	8.8E+06	44.6	14.9
0.33	3.00	8.6E+06	47.0	15.7

Uncracked Condition				
M_{cr}/M_a	M_a/M_{cr}	I_g	$1/r_i$	$Δ_i$
[-]	[-]	[mm⁴]	[10^{-6} mm^{-1}]	[mm]
10.00	0.10	5.0E+07	0.3	0.1
5.00	0.20	5.0E+07	0.5	0.2
3.33	0.30	5.0E+07	0.8	0.3
2.50	0.40	5.0E+07	1.1	0.4
2.00	0.50	5.0E+07	1.4	0.5
1.67	0.60	5.0E+07	1.6	0.5
1.43	0.70	5.0E+07	1.9	0.6
1.25	0.80	5.0E+07	2.2	0.7
1.11	0.90	5.0E+07	2.4	0.8
1.00	1.00	5.0E+07	2.7	0.9
0.91	1.10	5.0E+07	3.0	1.0
0.83	1.20	5.0E+07	3.2	1.1
0.77	1.30	5.0E+07	3.5	1.2
0.71	1.40	5.0E+07	3.8	1.3
0.67	1.50	5.0E+07	4.1	1.4
0.63	1.60	5.0E+07	4.3	1.4
0.59	1.70	5.0E+07	4.6	1.5
0.56	1.80	5.0E+07	4.9	1.6
0.53	1.90	5.0E+07	5.1	1.7
0.50	2.00	5.0E+07	5.4	1.8
0.48	2.10	5.0E+07	5.7	1.9
0.45	2.20	5.0E+07	6.0	2.0
0.43	2.30	5.0E+07	6.2	2.1
0.42	2.40	5.0E+07	6.5	2.2
0.40	2.50	5.0E+07	6.8	2.3
0.38	2.60	5.0E+07	7.0	2.4
0.37	2.70	5.0E+07	7.3	2.4
0.36	2.80	5.0E+07	7.6	2.5
0.34	2.90	5.0E+07	7.8	2.6
0.33	3.00	5.0E+07	8.1	2.7

Predicted Results from Design Codes

		SABS 0100		EC2		BS 8110		ACI 318		Uncracked Section		Uncracked Section	
ρ [%]		0.39		0.39		0.39		0.39		I_g (SABS)		I_u (EC2)	
M_{cr}/M_a	M_a/M_{cr}	I_e	Δ	I_e	$Δ_i$	I_e	$Δ_i$	I_e	$Δ_i$	I_e	$Δ_i$	I_e	$Δ_i$
[-]	[-]	[mm⁴]	[mm]	[mm⁴]	[mm]	[mm⁴]	[mm]	[mm⁴]	[mm]	[mm⁴]	[mm]	[mm⁴]	[mm]
0.00	0.00	5.0E+07	0.00	5.1E+07	0.00	5.1E+07	0.00	5.0E+07	0.00	5.0E-07	0.00	5.1E+07	0.00
10.00	0.10	5.0E+07	0.11	5.1E+07	0.08	5.1E+07	0.08	5.0E+07	0.1	5.0E-07	0.1	5.1E+07	0.1
5.00	0.20	5.0E+07	0.21	5.1E+07	0.16	5.1E+07	0.16	5.0E+07	0.2	5.0E-07	0.2	5.1E+07	0.2
3.33	0.30	5.0E+07	0.32	5.1E+07	0.24	5.1E+07	0.24	5.0E+07	0.3	5.0E-07	0.3	5.1E+07	0.2
2.50	0.40	5.0E+07	0.42	5.1E+07	0.31	5.1E+07	0.31	5.0E+07	0.4	5.0E-07	0.4	5.1E+07	0.3
2.00	0.50	5.0E+07	0.53	5.1E+07	0.39	5.1E+07	0.39	5.0E+07	0.5	5.0E-07	0.5	5.1E+07	0.4
1.67	0.60	5.0E+07	0.63	5.1E+07	0.47	5.1E+07	0.47	5.0E+07	0.5	5.0E-07	0.6	5.1E+07	0.5
1.43	0.70	5.0E+07	0.74	5.1E+07	0.55	5.1E+07	0.55	5.0E+07	0.6	5.0E-07	0.7	5.1E+07	0.6
1.25	0.80	5.0E+07	0.84	5.1E+07	0.63	5.5E+06	1.17	5.0E+07	0.7	5.0E-07	0.8	5.1E+07	0.6
1.11	0.90	5.0E+07	0.95	5.1E+07	0.71	5.5E+06	1.89	5.0E+07	0.8	5.0E-07	0.9	5.1E+07	0.7
1.00	1.00	5.0E+07	1.05	5.1E+07	0.79	5.5E+06	2.62	5.0E+07	0.9	5.0E-07	1.1	5.1E+07	0.8
0.91	1.10	3.9E+07	1.48	2.4E+07	1.80	5.5E+06	3.35	3.9E+07	1.3	5.0E-07	1.2	5.1E+07	0.9
0.83	1.20	3.2E+07	1.98	1.8E+07	2.74	5.5E+06	4.08	3.2E+07	1.7	5.0E-07	1.3	5.1E+07	0.9
0.77	1.30	2.7E+07	2.58	1.4E+07	3.62	5.5E+06	4.81	2.7E+07	2.2	5.0E-07	1.4	5.1E+07	1.0
0.71	1.40	2.3E+07	3.25	1.3E+07	4.46	5.5E+06	5.53	2.3E+07	2.8	5.0E-07	1.5	5.1E+07	1.1
0.67	1.50	2.0E+07	4.00	1.1E+07	5.26	5.5E+06	6.26	2.0E+07	3.4	5.0E-07	1.6	5.1E+07	1.2
0.63	1.60	1.8E+07	4.81	1.1E+07	6.04	5.5E+06	6.99	1.8E+07	4.1	5.0E-07	1.7	5.1E+07	1.3
0.59	1.70	1.6E+07	5.68	1.0E+07	6.78	5.5E+06	7.72	1.6E+07	4.9	5.0E-07	1.8	5.1E+07	1.3
0.56	1.80	1.4E+07	6.59	9.6E+06	7.51	5.5E+06	8.44	1.4E+07	5.6	5.0E-07	1.9	5.1E+07	1.4
0.53	1.90	1.3E+07	7.53	9.3E+06	8.23	5.5E+06	9.17	1.3E+07	6.5	5.0E-07	2.0	5.1E+07	1.5
0.50	2.00	1.2E+07	8.49	9.0E+06	8.92	5.5E+06	9.90	1.2E+07	7.3	5.0E-07	2.1	5.1E+07	1.6
0.48	2.10	1.2E+07	9.48	8.8E+06	9.61	5.5E+06	10.63	1.2E+07	8.1	5.0E-07	2.2	5.1E+07	1.7
0.45	2.20	1.1E+07	10.47	8.6E+06	10.28	5.5E+06	11.36	1.1E+07	9.0	5.0E-07	2.3	5.1E+07	1.7
0.43	2.30	1.1E+07	11.47	8.4E+06	10.95	5.5E+06	12.08	1.1E+07	9.8	5.0E-07	2.4	5.1E+07	1.8
0.42	2.40	1.0E+07	12.47	8.3E+06	11.61	5.5E+06	12.81	1.0E+07	10.7	5.0E-07	2.5	5.1E+07	1.9
0.40	2.50	9.8E+06	13.46	8.2E+06	12.26	5.5E+06	13.54	9.8E+06	11.5	5.0E-07	2.6	5.1E+07	2.0
0.38	2.60	9.5E+06	14.45	8.1E+06	12.90	5.5E+06	14.27	9.5E+06	12.4	5.0E-07	2.7	5.1E+07	2.0
0.37	2.70	9.2E+06	15.43	8.0E+06	13.54	5.5E+06	14.99	9.2E+06	13.2	5.0E-07	2.8	5.1E+07	2.1

0.36	2.80	9.0E+06	16.40	7.9E+06	14.17	5.5E+06	15.72	9.0E+06	14.1	5.0E-07	3.0	5.1E+07	2.2
0.34	2.90	8.8E+06	17.36	7.8E+06	14.80	5.5E+06	16.45	8.8E+06	14.9	5.0E-07	3.1	5.1E+07	2.3
0.33	3.00	8.6E+06	18.32	7.8E+06	15.43	5.5E+06	17.18	8.6E+06	15.7	5.0E-07	3.2	0.0E+00	2.4

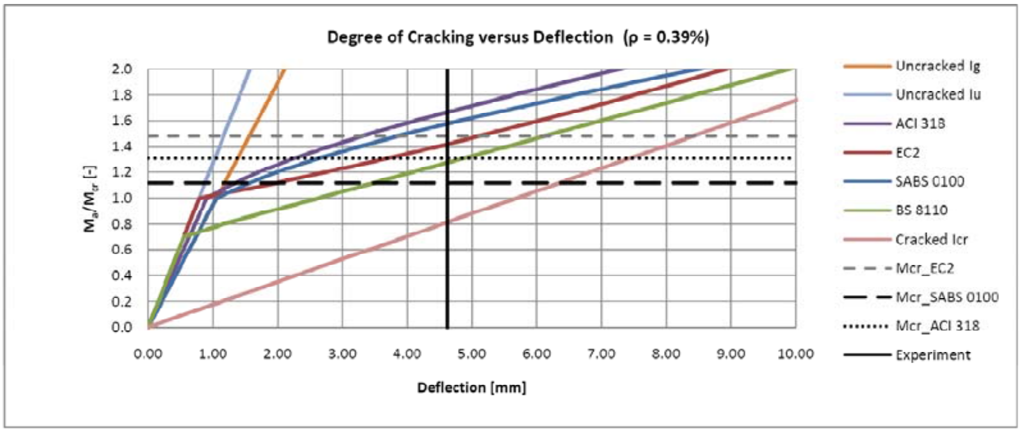

Δ_{EXP} = 4.52 mm

	EC2	SABS 0100	ACI 318	BS 8110
M_a/M_{cr}	1.48	1.12	1.31	1.48
Δ_i [mm]	5.10	1.58	2.27	6.12
Δ_i/Δ_{EXP}	1.10	0.34	0.49	1.32